

Black Hole - String Transition and Rolling D-brane

Yu Nakayama¹

*Department of Physics, Faculty of Science, University of Tokyo
Hongo 7-3-1, Bunkyo-ku, Tokyo 113-0033, Japan*

¹E-mail: nakayama@hep-th.phys.s.u-tokyo.ac.jp

Abstract

We investigate the black hole - string transition in the two-dimensional Lorentzian black hole system from the exact boundary states that describe the rolling D-brane falling down into the two-dimensional black hole. The black hole - string phase transition is one of the fundamental properties of the non-supersymmetric black holes in string theory, and we will reveal the nature of the phase transition from the exactly solvable world-sheet conformal field theory viewpoint. Since the two-dimensional Lorentzian black hole system ($SL(2; \mathbb{R})_k/U(1)$ coset model at level k) typically appears as near-horizon geometries of various singularities such as NS5-branes in string theory, our results can be regarded as the probe of such singularities from the non-supersymmetric probe rolling D-brane. The exact construction of boundary states for the rolling D0-brane falling down into the two-dimensional D-brane enables us to probe the phase transition at $k = 1$ directly in the physical amplitudes. During the study, we uncover three fundamental questions in string theory as a consistent theory of quantum gravity: small charge limit v.s. large charge limit of non-supersymmetric quantum black holes, analyticity v.s. non-analyticity in physical amplitudes and physical observables, and unitarity v.s. open closed duality in time-dependent string backgrounds. This work is based on the PhD thesis submitted to Department of Physics, Faculty of Science, University of Tokyo, which was defended on January 2007.

Contents

1	Introduction	4
2	Two-dimensional Black Hole: Space-Time Viewpoint	7
2.1	(Black) NS5-brane background	7
2.2	Noncritical superstring and LST	11
2.2.1	noncompact Calabi-Yau and wrapped NS5-branes	11
2.2.2	singular limit and LST	15
2.2.3	obstruction for conical metrics	18
2.3	Classical two-dimensional black hole	20
2.4	Wick rotation: thermodynamic properties	22
3	Two-dimensional Black Hole: CFT Viewpoint	25
3.1	Classical geometries for $SL(2; \mathbb{R})/U(1)$ coset	25
3.2	Euclidean spectrum	29
3.2.1	algebraic coset	30
3.2.2	spectrum from partition function	31
3.2.3	minisuperspace analysis	34
3.3	Lorentzian spectrum	39
3.3.1	classical string in two-dimensional black hole	39
3.3.2	folded strings	41
3.3.3	spectrum from partition function?	44
3.3.4	minisuperspace approximation	46
3.4	Duality and winding tachyon condensation	51
4	Black Hole - String Transition	55
4.1	In general dimensions	55
4.2	Two-dimensional black hole case	58
4.3	Other solvable backgrounds	61
5	Tachyon Radion Correspondence	64
5.1	Rolling tachyon	64
5.1.1	overview	64
5.2	Radiation from rolling tachyon boundary states	66
5.2.1	closed string emission	68
5.2.2	open string channel viewpoint	69
5.2.3	Lorentzian cylinder amplitude	70
5.2.4	D-brane decay in two-dimensional string theory	72
5.2.5	ZZ brane decay in various dimensions	73
5.2.6	electric field and long string formation	75
5.3	Classical correspondence	76
5.4	Quantum correspondence	78
5.5	Cosmological implications	79

6	D-branes in Two-dimensional Black Hole	83
6.1	Classical D-branes	83
6.1.1	DBI analysis	83
6.1.2	group theoretical viewpoint	85
6.1.3	mini-superspace boundary wavefunction	87
6.1.4	embedding into NS5-branes	91
6.2	Exact boundary states	92
6.2.1	Ishibashi states	92
6.2.2	exact boundary wavefunction	94
6.2.3	Cardy condition and modular bootstrap	95
7	Rolling D-brane in Two-dimensional Black Hole	100
7.1	Classical D-branes	100
7.1.1	DBI analysis	100
7.1.2	group theoretical viewpoint	102
7.2	Boundary states from Wick rotation	103
7.2.1	analytic continuation of boundary states	103
7.2.2	boundary state of D0-brane absorbed to future horizon	106
7.2.3	boundary state of D0-brane emitted from past horizon	107
7.2.4	boundary state of time-symmetric D0-brane	108
7.3	Rolling D-brane gathers moss	110
8	Black Hole - String Transition from Probe Rolling D-brane	112
8.1	Radiation out of rolling D-brane from closed string viewpoint	112
8.1.1	radiation distribution in superstring theory	115
8.1.2	radiation distribution in bosonic string theory	119
8.1.3	radiation distribution for emitted or time-symmetric boundary states	121
8.1.4	revisit to the radiation distribution from thermal sting propagator	121
8.2	Radiation out of rolling D-brane from open string viewpoint	123
8.2.1	open string channel viewpoint	123
8.2.2	Lorentzian cylinder amplitude	128
8.2.3	analytic continuation	129
8.2.4	optical theorem at work	131
8.2.5	imaginary D-instantons: decaying versus rolling	132
8.2.6	comparisons	134
8.3	Black hole - string transition	134
8.3.1	probing black hole - string transition via D-brane	135
8.3.2	holographic viewpoint	136
8.4	Boundary states and radiation in Ramond-Ramond sector	138
8.5	Back to extremal NS5-brane background	140
8.6	More on physical interpretations : Hartle-Hawking states	142
9	Conclusion and Discussions	147

A	Appendices I: Conventions and Useful Formulae	151
A.1	conventions	151
A.2	$SL(2; \mathbb{R})$ current algebra	153
A.3	Coordinate on $SL(2; \mathbb{R})$	155
A.4	Frequently used formulae	156
A.5	Proof of (6.30) and (6.40)	156
B	Appendix II: Miscellaneous Topics	159
B.1	Partition functions	159
B.2	T-duality and Buscher's rule	161
B.3	$\mathcal{N} = 2$ superconformal algebra and spectral flow	161
B.4	Lichnerowicz obstruction and a -theorem	162
B.5	Boundary wavefunction from direct integration	163

1 Introduction

From the Heaven

A luminous star, of the same density as the Earth, and whose diameter should be two hundred and fifty times larger than that of the Sun, would not, in consequence of its attraction, allow any of its rays to arrive at us; it is therefore possible that the largest luminous bodies in the universe may, through this cause, be invisible (Laplace: 1798). It was Laplace who first predicted the existence of the black hole from the Newtonian mechanics. More than a hundred years later, in 1915 when he was serving in Russia for World War I, Schwarzschild discovered the exact static black hole solution in Einstein's general relativity. Ever since, the black hole has continued to attract our broad attention in theoretical physics.

Black holes are fascinating and indeed mysterious. It is remarkable that some properties of the black hole are quite reminiscent of those of the thermodynamics: it has a definite temperature, energy and entropy, and moreover it satisfies the thermodynamical laws. To understand this coincidence, it had been long suggested that the quantum gravity would explain the microscopic statistical origins of the thermodynamic properties of the black hole. Furthermore black holes challenge the validity of the quantum mechanics. The Hawking radiation, predicted from the quantum mechanics, leads to evaporation of the black hole, which ironically results in the failure of the unitary evolution of the quantum system. These mysterious natures of the black holes have continued to enchant generations of theoretical physicists.

Over this past two decades, theoretical physicists have gained more and more confidence in string theory as a candidate for the final theory of everything. The theory of everything, from its tacit implication, should include a consistent theory of quantum gravity with sufficient predictive power. The best arena to test the quantum gravity is quantum black hole systems, where the semiclassical analysis leads to the puzzling issues raised above. Whether the string theory resolves these issues or not is a big challenge to string theorists.

One of the greatest achievements of the string theory so far is to yield a microscopic explanation of the entropy for (near) BPS black holes with large charges. The string theory, along with various dualities, has enabled us to “count” microscopic states forming such black holes. The counting successfully agrees with the classical Bekenstein-Hawking entropy formula of the corresponding macroscopic black hole.

The situations, however, still remain unclear when one studies non-BPS black holes with small charge. The large quantum corrections, both in string coupling constant and large curvature effects, prevent us from the quantitative enumeration of quantum states corresponding to the black hole. Qualitatively, it has been suggested that the so-called black hole - string phase transition occurs when we consider such a small charge black hole. One of the motivations of this thesis is to understand the black hole - string phase transition in exactly solvable string theory backgrounds.

In this thesis, we study the exact dynamics of rolling D-brane in the two-dimensional black hole system. The two-dimensional black hole system not only gives a toy model for the exactly solvable black hole systems in string theory, but also it can be embedded in the full superstring theory as a solution corresponding to black NS5-branes. Although our model is rather specific, we will uncover many important and universal features of quantum gravity such as the black hole - string transition. In particular We would like ask three fundamental

questions about the nature of the quantum gravity, or string theory as a candidate for the theory of everything.

The first problem we would like to ask in this thesis is the small charge limit of the non-supersymmetric black hole and its relation to the black hole - string transition. By studying the black hole - string transition in the two-dimensional black hole, we would like to explicitly show the phase transition between the large charge limit and the small charge limit of the non-BPS black hole systems. The origin of the phase transition is the existence of two characteristic temperatures in the string theory: the one is the Hawking temperature associated with the Hawking radiation from the black hole, and the other is the Hagedorn temperature of the underlying string theory. The relation between the two temperatures is of utmost importance in understanding the black hole - string phase transition, and we will show that the phase transition occurs exactly when these two temperatures coincide in the two-dimensional black hole system by examining the properties of the exact probe rolling D-brane boundary states.

A related issue is whether the genuine two-dimensional non-critical string theory (i.e. the target space is two-dimensional) admits a black hole solution. The question has remained long unanswered. Actually, the two-dimensional black hole in the two-dimensional non-critical string theory is located well below the black hole - string phase transition point, suggesting the difficulty of physical interpretations as a black hole. Our study will also support this argument in a negative way.

The second problem we would like to investigate in this thesis is the relation between the analyticity and non-analyticity in amplitudes and physical quantities. It is well-known that in the supersymmetric situations, holomorphy (analyticity) plays a crucial role in determining exact BPS properties of the theory. On the other hand, to discuss phase transitions such as the black hole - string transition, the non-analyticity of the physical quantities is essential. Throughout this thesis, the interplay between the analyticity and non-analyticity appears intermittently. Especially, we highlight the universality of the decaying D-brane and the subtleties associated with Wick rotation in curved spaces in this context.

The third problem we would like to study is the consistency between the unitarity and the open-closed duality. The unitarity is one of the crucial ingredients of the quantum theory. In the first quantized string theory, however, the unitarity in time-dependent background is not always manifest, especially in the Euclidean world-sheet formulation. The simplest consequence of the unitarity is the optical theorem. In the time-dependent physics associated with the D-brane decay, however, it is not apparently obvious whether the analytic continuation involved is consistent with the requirement from the unitarity. Indeed, the abuse of the careless Wick rotation between the Lorentzian world-sheet theory and the Euclidean world-sheet theory, would result in inconsistent results, violating the optical theorem, which will be only fixed after the careful studies of the neglected pole contributions that appear through the process of Wick rotation. The rolling D-brane in the two-dimensional black hole system is an excellent arena to check the validities of proposed prescription for the Wick rotations given in the literatures.

Down to Earth

So far, we have stated the celestial motivations of the thesis. What about the terrestrial motivations? In other words, which practical physics can we learn from the study of the rolling D-brane in two-dimensional black holes?

The dynamics of the rolling D-brane in the two-dimensional black holes closely resembles that of the rolling tachyon associated with the D-brane decay in flat space. Indeed, our study suggests that this tachyon - radion correspondence shows rather universal features of closed string radiation rate from the decaying D-brane. The string (particle) production from the time-dependent system such as the dynamical D-brane system itself is an interesting arena of theoretical physics, but it also has potential applications to the quantum cosmology based on the superstring theory.

In the recent observational cosmology, the existence of the inflationary epoch of our universe has been confirmed with increasingly great accuracy. It is, therefore, a great challenge for the string theory to provide a natural setup for the inflation. One viable scenario for the string inflation is the so-called brane inflation, where the potential between the D-brane and anti D-brane provides the inflaton field. Recent studies show that the brane inflation could be embedded in the flux compactification of the type II string theory with all moduli fixed.

The end-point of the brane inflation is the pair annihilation between the D-brane and the anti D-brane. This is the point where the effective field theory approximation for the brane inflation breaks down and the stringy effects dominate. The reheating of the universe associated with the inflation decay is astonishingly different in the brane inflation scenario from the conventional field theory scenario. To understand the reheating process with the open string tachyon condensation, the universality of the radiation rate of the D-brane decay we will discuss in this thesis is crucial.

We will also see that large closed string loops will form during the D-brane decay and they will dominate the radiated energy once the fundamental string charge is induced. The subsequent evolution of such macroscopic strings will be of great importance to understand and estimate the relic cosmic strings in our universe, which might be observed in near future by experiment, directly proving the string theory.

In this way, the study of the D-brane decay has potential applications to quantum cosmology. We believe that our results, especially the universal properties of the decaying D-branes will become fundamental backgrounds for the realistic brane inflation models with successful reheating.

Organization of the Thesis

The organization of this paper is as follows. In section 2, we review the two-dimensional black hole from the space-time viewpoint. In section 3, we review the two-dimensional black hole from the conformal field theory viewpoint. In section 4, we introduce the concept of the black hole - string transition. In section 5, we study the rolling tachyon dynamics and introduce the tachyon - radion correspondence conjecture. In section 6, we study the D-branes in two-dimensional black hole system in the Euclidean signature. In section 7, we construct the exact boundary states for the rolling D-brane in two-dimensional black hole in the Lorentzian signature. In section 8, we study the closed string radiation rate from the rolling D-brane and probe the black hole - string transition. In section 9, we present some discussions and the conclusion of the paper.

In appendices we collect useful facts used in the main part of the thesis. In appendix A, we fix our conventions and collect useful formulae. In appendix B, we present miscellaneous topics, whose detailed discussions are omitted in the main stream of the thesis.

A part of the thesis is based on the published papers. In particular, a large portion of the discussions in section 7 and 8 is based on [1, 2].

2 Two-dimensional Black Hole: Space-Time Viewpoint

In this section, we review the two-dimensional black hole from the space-time viewpoint. We will see that the string theory is replete with exactly solvable solutions containing the two-dimensional black hole systems. By studying such backgrounds, we can understand the α' exact physics of the string theory near singularities.

The organization of this section is as follows. In section 2.1, we introduce the black NS5-brane background as a most typical string solution based on the two-dimensional black hole system. In section 2.2, we generalize the construction to study string theory near various singularities. In section 2.3, we review the basic aspect of the classical two-dimensional black hole system. In particular we focus on the thermodynamic properties in section 2.4.

2.1 (Black) NS5-brane background

As is often said, the string theory is not a theory of strings only. It turns out to contain other higher dimensional nonperturbative objects such as D-branes and NS-branes. Stable D-branes are charged under the Ramond-Ramond fields, and defined as objects on which perturbative strings can end. On the other hand, NS-branes are charged under the Kalb-Ramond $B_{\mu\nu}$ field, and do not possess a perturbative definition. They can be constructed as solitonic solutions of the equation of motions of the effective supergravity in ten-dimension.

Historically, all these important ingredients of the string theory are discovered as exact (BPS) solitonic solutions of the effective supergravity in ten-dimension. The tension of the D-branes is proportional to $1/g_s$ while the tension of the NS-branes is proportional to $1/g_s^2$, where g_s denotes the string coupling constant. Hence, in the perturbative limit (i.e. $g_s \rightarrow 0$), all these objects are infinitely massive compared with the perturbative string spectrum and could be neglected as excitations. Rather we regard the existence of such solitonic objects as super-selection sectors of the perturbative string theory.

The moduli spaces of the string theory is connected by various dualities. In particular, one of the most important recent achievements is the advent of the gauge - gravity correspondence. Before this new development, it had been believed that the local quantum field theory cannot realize the gravitational theory (Weinberg-Witten theorem [3]). However, the holographic realization of the gauge theory avoid this no-go theorem in a remarkable manner, and it has enabled us to study the strongly coupled gauge theory from the weakly coupled gravity. Explicit realization in the string theory involves the low-energy decoupling limit (Maldacena limit [4]) of the localized excitations: the most famous example is the low-energy field theory limit of open-string theory living on the D3-brane in flat ten-dimensional space, which yields the duality between type IIB string theory on $AdS_5 \times S^5$ and the $\mathcal{N} = 4$ supersymmetric Yang-Mills theory on $\mathbb{R}^{1,3}$ (or $\mathbb{R}^1 \times S^3$) [4, 5].

The decoupling limit of the localized degrees of freedom and the gauge - gravity correspondence are not only important for the understanding of the strongly coupled gauge theories, but also essential to understand the quantum gravitational nature of the string theory. What is the microscopic origin of the black hole entropy? What is the fundamental degrees of freedom for the quantum gravity? How does (or does not) string theory solve the information paradox? These questions have been partially answered from the gauge - gravity correspondence of D-branes. The decoupling limit is essentially the near horizon limit of the

corresponding supergravity background, and the properties of black hole can be understood through the gauge - gravity correspondence in this way.

For NS5-brane, situations are more involved. Compared with D-branes, the NS5-brane is more geometrical in its origin. Indeed, as we will see in section 2.2, it is T-dual to the singular geometry, and it appears not obvious what is the localized degrees of freedom in the decoupling limit. On the other hand, the closed string background for the near horizon limit of the NS5-brane is exactly quantized, so we are able to understand the gauge - gravity correspondence beyond the supergravity approximation.

Our starting point is the supergravity solution for the extremal NS5-brane: the solution contains nontrivial dilaton and the metric²

$$ds^2 \equiv G_{\mu\nu} dx^\mu dx^\nu = -dt^2 + \left(1 + \frac{k\alpha'}{r^2}\right) (dr^2 + r^2 d\Omega_3^2) + d\mathbf{y}_{\mathbb{R}^5}^2, \quad e^{2\Phi(r)} = g_s^2 \left(1 + \frac{k\alpha'}{r^2}\right), \quad (2.1)$$

along with k -units of NS-NS H_3 -flux penetrating through \mathbb{S}^3 :

$$H_{mnp} = -\epsilon_{mnp}{}^q \partial_q \Phi(r), \quad (2.2)$$

where x^m ($m = 6, \dots, 9$) are transverse to the 5-brane. Thus, k refers to the number of NS5-branes at $r = 0$, \mathbf{y} are the spatial coordinates of the planar NS5-brane worldvolume, and g_s is the string coupling constant at infinity. The background preserves 16 supercharges of the type II (A or B) supergravity.

Following the argument of decoupling limit given above, we take the near horizon limit of the geometry (2.1) by zooming in the $r^2 \ll \alpha'$ region. Neglecting the constant term (i.e. 1) in the harmonic function $\left(1 + \frac{k\alpha'}{r^2}\right)$, we obtain the near horizon limit of the extremal NS5-brane background [6, 7, 8, 9, 10]

$$ds^2 = -dt^2 + k\alpha' d\rho^2 + k\alpha' d\Omega_3^2 + d\mathbf{y}_{\mathbb{R}^5}^2, \quad \Phi = -\rho + \text{constant}, \quad (2.3)$$

where $r = \sqrt{k\alpha'} \exp \rho$. This near horizon background remarkably admits an exact conformal field theory description involving a linear dilaton theory and $SU(2)_k$ super Wess-Zumino-Novikov-Witten (WZNW) model:³

$$\left[\mathbb{R}_t \times \mathbb{R}_{\rho, \sqrt{\frac{2}{k}}} \times SU(2)_k \right]_{\perp} \times \left[\mathbb{R}^5 \right]_{\parallel}. \quad (2.4)$$

The first part describes the five-dimensional curved space-time transverse to the NS5-brane while the second part describes the flat spatial directions parallel to the NS5-brane. The criticality condition for superstring theories is satisfied for any k because

$$\left(1 + \frac{6}{k} + \frac{1}{2}\right) + 3 \times \left(\frac{k-2}{k} + \frac{1}{2}\right) + 6 \times \left(1 + \frac{1}{2}\right) = 15. \quad (2.5)$$

²Throughout this thesis, we use the string frame for supergravity solutions.

³Here, k is the level of total current of super $SU(2)$ WZNW models and $\sqrt{\frac{2}{k}}$ is the amount of background charge for the linear dilaton system.

Although the background is exactly solvable, the string background is singular due to the existence of the linear dilaton direction ρ . In the large negative ρ , the string coupling constant effectively diverges and the string perturbation theory is ill-defined. Physically, there exists a core of NS5-branes at $r = 0$, and the dynamical degrees of freedom on the NS5-brane cannot be neglected.

There are several ways to regularize this linear dilaton singularity so that the string world-sheet perturbation theory makes sense with sufficient predictive power. One way to do this is to introduce the non-extremality to the geometry. Let us consider the non-extremal or black NS5-brane solution in the ten-dimensional type II supergravity:

$$ds^2 = - \left(1 - \frac{r_0^2}{r^2}\right) dt^2 + \left(1 + \frac{k\alpha'}{r^2}\right) \left(\frac{dr^2}{1 - \frac{r_0^2}{r^2}} + r^2 d\Omega_3^2\right) + d\mathbf{y}_{\mathbb{R}^5}^2, \quad e^{2\Phi(r)} = g_s^2 \left(1 + \frac{k\alpha'}{r^2}\right) \quad (2.6)$$

along with k -units of NS-NS H_3 -flux penetrating through \mathbb{S}^3 again. Here $r = r_0$ is the location of the event horizon of the black NS5-brane.

One type of near-horizon limit is $r_0 \rightarrow 0$ and $g_s \rightarrow 0$ independently, leading to the ‘throat geometry’ of extremal NS5-branes that reduce to (2.3). Another type of near-horizon limit is $r_0 \rightarrow 0$ and $g_s \rightarrow 0$ while keeping the energy density above the extremal configuration $\mu \equiv r_0^2/g_s^2\alpha'$ fixed. It yields ‘throat geometry’ of the near-extremal NS5-branes (2.6) [11, 12]:

$$ds^2 = - \tanh^2 \rho dt^2 + k\alpha' d\rho^2 + k\alpha' d\Omega_3^2 + d\mathbf{y}_{\mathbb{R}^5}^2, \quad e^{2\Phi} = \frac{k}{\mu \cosh^2 \rho}, \quad (2.7)$$

where $r = r_0 \cosh \rho$. For (t, ρ) -subspace, the metric and the dilaton coincide with those of the two-dimensional black hole with a Lorentzian signature. This Lorentzian black hole can be described by Kazama-Suzuki supercoset conformal field theory $SL(2; \mathbb{R})_k/U(1)$ (where $U(1)$ subgroup is chosen to be the non-compact component (i.e. space-like direction)) of central charge $c = 3(1 + 2/k)$. Likewise, taking account of the NS-NS H_3 -flux penetrating through \mathbb{S}^3 which is omitted in (2.7), the angular part \mathbb{S}^3 can be described by the (super) $SU(2)$ -WZNW model as we have seen in the extremal case. In this way, the string background of the nonextremal NS5-brane is reduced to a solvable superconformal field theory system:⁴

$$\left[\frac{SL(2; \mathbb{R})_k}{U(1)} \times SU(2)_k\right]_{\perp} \times \left[\mathbb{R}^5\right]_{\parallel}. \quad (2.8)$$

Here, the first part describes the five-dimensional curved space-time (including the time direction) transverse to the NS5-brane, while the second part describes the flat spatial directions parallel to the NS5-brane. The criticality condition is satisfied for any k as in (2.5).

As we will review in the next section, the classical geometry of the two-dimensional black hole itself is not singularity free. This is because although in the Schwarzschild-like coordinate used in (2.7) there is no singularity at all, the event horizon exists at $\rho = 0$, and we can extend the coordinate inside the horizon. In the maximally extended geometry, we observe a curvature and dilaton singularity as is the case with the usual Schwarzschild black hole. It is

⁴Here again, k denotes the level of total current of super WZNW models. Namely, $k + 2$, $k - 2$ are the levels of bosonic $SL(2)$ and $SU(2)$ currents.

interesting, however, despite the appearance of the singularity, the exact SCFT formulation (2.8) appears perfectly well-defined, at least formally.

Another way to regularize the linear dilaton singularity, while keeping the space-time supersymmetry in contrast with the above non-extremal resolution, is to separate the position of the NS5-branes in a ring-like manner and study the smeared solution [13] (see also [14, 15]). The background is described by the coset model

$$\frac{\left[\frac{SL(2;\mathbb{R})_k}{U(1)} \times \frac{SU(2)_k}{U(1)} \right]_{\perp}}{\mathbb{Z}_k} \times \left[\mathbb{R}^{1,5} \right]_{\parallel} . \quad (2.9)$$

Here \mathbb{Z}_k orbifold serves as a GSO projection⁵ that restricts the spectrum to the sector with integral $U(1)_R$ charge so that the space-time supercharge is well-defined. Intuitively, we have extracted a particular $U(1)$ direction from the $SU(2)$ WZNW model and combined it with the linear dilaton direction to construct the Euclidean $\frac{SL(2;\mathbb{R})_k}{U(1)}$ coset model by a marginal deformation.⁶ The linear dilaton direction together with the $U(1)$ direction is deformed to the $\frac{SL(2;\mathbb{R})_k}{U(1)}$ coset model that does not possess a dilaton singularity.

To see the geometrical meaning of this deformation, we write the coset part $\left[\frac{SL(2;\mathbb{R})_k}{U(1)} \times \frac{SU(2)_k}{U(1)} \right]_{\perp}$ as

$$ds^2 = \alpha' k (d\theta^2 + \tan^2 \theta d\tilde{\phi}_2^2 + d\rho^2 + \tanh^2 \rho d\tilde{\phi}_1^2) , \quad e^{2\Phi} = \frac{1}{\cos^2 \theta \cosh^2 \rho} . \quad (2.10)$$

It is interesting to note that this geometry does *not* admit any Killing spinor needed for an apparent supersymmetry: the supersymmetry will be recovered after taking the \mathbb{Z}_k orbifold [14] (see also [17, 18, 19] for earlier discussions). The \mathbb{Z}_k orbifold is defined as $(\tilde{\phi}_1, \tilde{\phi}_2) \sim (\tilde{\phi}_1 + 2\pi/k, \tilde{\phi}_2 + 2\pi/k)$. We define new coordinates

$$\tilde{\phi}_1 = \phi_1 + \phi_2/k , \quad \tilde{\phi}_2 = \phi_2/k \quad (2.11)$$

so that the \mathbb{Z}_k orbifold simply acts as $(\phi_1, \phi_2) \sim (\phi_1, \phi_2 + 2\pi)$. In the new coordinates, the metric reads

$$ds^2 = \alpha' k (d\theta^2 + d\rho^2 \tanh^2 \rho d\phi_1^2) + 2\alpha' \tanh^2 \rho d\phi_1 d\phi_2 + \frac{\alpha'}{k} (\tan^2 \theta + \tanh^2 \rho) d\phi_2^2 . \quad (2.12)$$

Since ϕ_2 direction has a usual 2π periodicity, one can perform the T-duality along the ϕ_2 direction. Applying Buscher's rule (see appendix B.2), we obtain

$$\begin{aligned} ds^2 &= \alpha' k \left(d\theta^2 + d\rho^2 + \frac{\tan^2 \theta \tanh^2 \rho}{\tan^2 \theta + \tanh^2 \rho} d\phi_1^2 + \frac{1}{\tan^2 \theta + \tanh^2 \rho} d\hat{\phi}_2^2 \right) \\ B &= \frac{\alpha' k \tanh^2 \rho}{\tan^2 \theta + \tanh^2 \rho} d\phi_1 \wedge d\hat{\phi}_2 , \quad e^{2\Phi} = \frac{1}{\cos^2 \theta \cosh^2 \rho (\tan^2 \theta + \tanh^2 \rho)} . \end{aligned} \quad (2.13)$$

⁵With the abuse of convention, the Gliozzi-Scherk-Olive (GSO) projection has a two-fold meaning in this thesis (and in many literatures). The one is the summation over the spin structure [16], and the other is the restriction to the integral $U(1)_R$ charge sector for the internal SCFT. Both are imperative to preserve the target-space supersymmetry.

⁶ $U(1)$ subgroup here is chosen to be the compact direction.

In the asymptotic region $\rho \rightarrow \infty$, we recover the NS5-brane solution (2.3), and we can also see that the NS5-branes are now localized along the ring $\theta = \rho = 0$, where the dilaton diverges (see figure 1 for a description of our coordinate system). In other words, the NS5-branes are located along the ring in the (x^8, x^9) plane.⁷ In this sense, the geometry still appears singular, but as we will discuss later, this is just an artefact of loose applications of T-duality: the trumpet singularity in (2.13) will be resolved by the “winding tachyon condensation”. Another quick way to see the absence of singularity is to revisit our starting point (2.10): it does not possess any dilaton singularity. It is also clear that the coset (2.9) is manifestly singularity free as an SCFT up to a harmless orbifold structure.

Although we will not explicitly do it here, we can begin with the appropriate (smeared) harmonic function ansatz for the ring-likely distributed NS5-branes and reproduce the metric (2.13) purely from the supergravity solution by taking a suitable near horizon limit [13]. In this approach, the space-time supersymmetry is manifest.

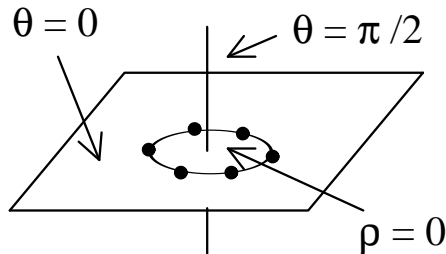


Figure 1: NS5-branes are localized along the ring in the (x_8, x_9) plane with $\theta = \rho = 0$.

2.2 Noncritical superstring and LST

In section 2.1, we discussed the relation between the two-dimensional black hole systems and the near horizon NS5-brane configurations. It is possible to generalize this construction to describe the singular limit of the geometry from exactly solvable conformal field theories. The construction is similar to the Gepner construction for compact Calabi-Yau spaces [20, 21], and it can be named “non-compact Gepner construction” [22, 23, 24, 25, 26, 27]. In this subsection, we would like to review this construction. Thanks to this generalized “non-compact Gepner construction”, most of the results we will present in later sections can be applied to various singular Calabi-Yau spaces.

2.2.1 noncompact Calabi-Yau and wrapped NS5-branes

Our starting points to construct exactly solvable world-sheet conformal field theories for singular Calabi-Yau spaces from two-dimensional black hole and minimal models are the following two claims.

⁷Our parametrization is $x^6 = \rho_0 \sinh \rho \sin \theta \cos \phi_1$, $x^7 = \rho_0 \sinh \rho \sin \theta \sin \phi_1$, $x^8 = \rho_0 \cosh \rho \cos \theta \cos \hat{\phi}_2$, $x^9 = \rho_0 \cosh \rho \cos \theta \sin \hat{\phi}_2$.

Calabi-Yau / Landau-Ginzburg correspondence [28, 29, 30, 31]

Let us consider the algebraic varieties defined by

$$\sum_{i=1}^{n+2} x_i^{r_i} = 0 \quad (2.14)$$

in the weighted projective space $\mathbb{WCP}_{n+1} \left(\frac{1}{r_1}, \dots, \frac{1}{r_{n+2}} \right)$. The Calabi-Yau condition reads $\sum_{i=1}^{n+2} \frac{1}{r_i} = 1$. The Calabi-Yau / Landau-Ginzburg correspondence says that the (quantum) sigma model defined on the n -dimensional algebraic varieties (2.14) is (weakly) equivalent⁸ to the $\mathcal{N} = 2$ supersymmetric Landau-Ginzburg orbifold theory with the superpotential

$$W(X_i) = \sum_{i=1}^{n+2} X_i^{r_i} . \quad (2.15)$$

The orbifold projection serves as a GSO projection demanding the integrality of the $U(1)_R$ -charge of the total model. The Calabi-Yau condition can be understood as the criticality condition for the SCFT with the central charge $\hat{c} = c/3 = n$.

When all r_i are positive, the resulting model is nothing but the Gepner construction for compact Calabi-Yau spaces (see also [33, 31]). When some of r_i are negative, the Calabi-Yau manifold is non-compact and the definition of the Landau-Ginzburg orbifold needs extra care as we will do it momentarily.

Landau-Ginzburg / minimal model correspondence [29]

The $\mathcal{N} = 2$ supersymmetric Landau-Ginzburg model with the superpotential $W(X) = X^k$ is equivalent to the $\mathcal{N} = 2$ $(k - 2)$ -th minimal model with the central charge $\hat{c} = c/3 = 1 - \frac{2}{k}$. The minimal model has an algebraic formulation, but an alternative construction is based on the Kazama-Suzuki coset $SU(2)_k/U(1)$ associated with the level k $SU(2)$ current algebra.⁹ Kazama-Suzuki construction guarantees that the coset CFT associated with the $\mathcal{N} = 1$ current algebra actually possesses $\mathcal{N} = 2$ superconformal symmetry when the target space is a special Kahler manifold (the hermitian symmetric manifold) [34, 35]. In our simplest case, it is indeed the case and the theory is equivalent to the $\mathcal{N} = 2$ minimal model.¹⁰

We can formally generalize the above discussion to define the $\mathcal{N} = 2$ supersymmetric Landau-Ginzburg model with the negative power superpotential $W(X) = X^{-k}$. The analytic continuation of the central charge for the positive power superpotential yields $\hat{c} = c/3 = 1 + \frac{2}{k}$. The Kazama-Suzuki coset construction has a natural generalization in this case as well. Instead of considering $SU(2)_k/U(1)$ supercoset model, we consider $SL(2; \mathbb{R})_k/U(1)$ supercoset model whose central charge is also given by $\hat{c} = c/3 = 1 + \frac{2}{k}$. This CFT will be reviewed in section 3. Since the Lagrangian formulation based on the Landau-Ginzburg model with the negative power superpotential does not seem to be well-defined while the $SL(2; \mathbb{R})_k/U(1)$

⁸The precise meaning of the weak equivalence can be found e.g. in [32].

⁹We always stick to the convention where k denotes the *total* level of the current algebra: the bosonic $SU(2)$ current algebra has the level $\kappa = k - 2$ and the bosonic $SL(2; \mathbb{R})$ current algebra has the level $\kappa = k + 2$.

¹⁰Actually, if the denominator H in the coset G/H is a Cartan subgroup of G , the coset admits the $\mathcal{N} = 2$ superconformal symmetry even if it is a non-symmetric space [36].

coset does, the precise claim of the non-compact Gepner construction is that the Landau-Ginzburg orbifold appearing in (2.15) should be understood as the $SL(2; \mathbb{R})_k/U(1)$ coset model.

At this point, it would be interesting to mention that the formal Landau-Ginzburg description suggests a duality between the $\mathcal{N} = 2$ Liouville theory and the $SL(2; \mathbb{R})_k/U(1)$ coset model. We begin with the topological path integral for the partition function on the sphere:

$$\begin{aligned} Z &= \int dX d\bar{X} \frac{1}{g_s^2} e^{-W(X) - \bar{W}(\bar{X})} \\ &= \int dX d\bar{X} \frac{1}{g_s^2} e^{-X^{-k} - \bar{X}^{-k}}. \end{aligned} \quad (2.16)$$

Introducing the $\mathcal{N} = 2$ Liouville coordinate $X^{-k} = e^{\frac{1}{\mathcal{Q}}\Phi}$ with $\mathcal{Q}^2 = \frac{2}{k}$, we can rewrite the path integral (2.16) as

$$Z = \int d\Phi d\bar{\Phi} \frac{1}{g_s^2} \exp\left(-\mathcal{Q}\text{Re}\Phi - e^{\frac{1}{\mathcal{Q}}\Phi} - e^{\frac{1}{\mathcal{Q}}\bar{\Phi}}\right). \quad (2.17)$$

The important step is to regard the measure factor $\exp(-\mathcal{Q}\text{Re}\Phi)$ as a space-dependent coupling constant, namely, linear dilaton background with the slope \mathcal{Q} . The remaining action shows the structure of the $\mathcal{N} = 2$ Liouville superpotential $W(\Phi) = e^{\frac{1}{\mathcal{Q}}\Phi}$. This heuristic equivalence between the $SL(2; \mathbb{R})/U(1)$ coset model and the $\mathcal{N} = 2$ Liouville theory at the topological level will be made more precise in later section 3.4.

Now combining these two facts, we can construct the equivalent description for (non-compact) Calabi-Yau spaces by considering tensor products of $SL(2; \mathbb{R})/U(1)$ coset models ($\mathcal{N} = 2$ Liouville theory) and $SU(2)/U(1)$ coset models ($\mathcal{N} = 2$ minimal models) with appropriate GSO projections. We call such a construction a generalized (non-compact) Gepner construction.

Let us discuss some simple examples.

1) A_{k-1} type ALE spaces

We take $n = 2$, and set $-r_1 = r_2 = k$, $r_3 = r_4 = 2$. From the projective invariance, we can set $x_1 = -\mu$ without loss of generality.¹¹ The resulting algebraic variety is given by

$$x_2^k + x_3^2 + x_4^2 = \mu^k \quad (2.18)$$

in \mathbb{C}^3 , which is nothing but the A_{k-1} type ALE space with a deformation parametrized by μ . On the other hand, the noncompact Gepner construction yields

$$\frac{\left[\frac{SL(2; \mathbb{R})_k}{U(1)} \times \frac{SU(2)_k}{U(1)} \right]}{\mathbb{Z}_k} \quad (2.19)$$

because the massive theory with the quadratic superpotential $W(X) = X^2$ will decouple under the renormalization group flow. We now recognize that the resulting theory is same

¹¹Note that we are considering a noncompact space, so the domain of the projective coordinate x_1 is in $\mathbb{C}^* \equiv \mathbb{C} - \{0\}$.

as the near horizon limit of the k NS5-brane solutions discussed in section 2.1. This shows an equivalence between the near horizon limit of k NS5-brane solutions and the A_k type ALE spaces. They are indeed related with each other via the T-duality. The deformation parameter μ in the ALE space corresponds to the separation of NS5-branes. We can easily generalize the construction for other ALE spaces with ADE singularities.

2) Generalized conifolds

We next consider the case of Calabi-Yau three-fold ($n = 3$). We take $r_2, r_3, r_4, r_5 > 0$ and set $r_1 = 1 - \frac{1}{\sum_{i=2}^5 r_i^{-1}} < 0$. After fixing the projective invariance by eliminating x_1 , the resultant Calabi-Yau space is the so-called generalized (deformed) conifold

$$x_2^{r_2} + x_3^{r_3} + x_4^{r_4} + x_5^{r_5} = \mu \quad (2.20)$$

in \mathbb{C}^4 . Mathematically, we can regard it as a complex structure deformation of the Brieskorn-Pham type singularity (see section 2.2.3). The Gepner construction leads to the orbifolded tensor products of $\mathcal{N} = 2$ minimal models with one $SL(2; \mathbb{R})_{-r_1}/U(1)$ coset model. The simplest example is the case with $r_1 = -1$ and $r_2 = r_3 = r_4 = r_5 = 2$. The geometry is the deformed conifold:

$$x_2^2 + x_3^2 + x_4^2 + x_5^2 = \mu . \quad (2.21)$$

The noncompact Gepner construction is given by $SL(2; \mathbb{R})_1/U(1)$ coset model with the level 1 parent current algebra. This is the famous Ghoshal-Vafa duality [22].

3) ALE(A_{k-1}) fibration over weighted projective spaces

We finally consider the model with two negative charges: $n = 3$, $r_1 = -k(1 + \frac{k_1}{k_2})$, $r_2 = -k(1 + \frac{k_2}{k_1})$, $r_3 = k$, and $r_4 = r_5 = 2$. The Landau-Ginzburg superpotential is given by

$$W(X_i) = X_1^{-k(1+\frac{k_1}{k_2})} + X_2^{-k(1+\frac{k_2}{k_1})} + X_3^k . \quad (2.22)$$

By introducing new variables: $Z = \log X_1 + \log X_2$, $Y = k k_1 \log X_1 - k k_2 \log X_2$ and $X^k = e^{kZ} X_3^k$, we can rewrite the Landau-Ginzburg superpotential as

$$W = e^{-kZ} (X^k + e^{Y/k_1} + e^{-Y/k_2}) , \quad (2.23)$$

with the linear dilaton $\Phi = -\text{Re}Z$. After integrating over Z , the topological path integral is localized along the locus¹²

$$e^{y/k_1} + e^{-y/k_2} + x^k + w_1^2 + w_2^2 = 0 , \quad (2.24)$$

which shows a structure of ALE(A_{k-1}) fibration over $\mathbb{WCP}^1(k_1, k_2)$. The simplest example with $k_1 = k_2$, we obtain the ALE(A_{k-1}) fibration over \mathbb{CP}_1 . The geometry of the two $SL(2; \mathbb{R})/U(1)$ coset and one $SU(2)/U(1)$ coset can be analysed in a similar way as we did in section 2.1, and the result is given by the wrapped NS5-brane solution around \mathbb{CP}_1 , where we have chosen $k_1 = k_2 = 1$ for simplicity (see [26] for details). This is expected from the fact that the A_{k-1} singularity is T-dual to flat k NS5-branes and we could perform the fiber-wise T-duality for the ALE(A_{k-1}) fibration over \mathbb{CP}_1 .

¹²We have added the superpotential term $W_1^2 + W_2^2$ by hand to match the dimensionality.

The partition functions and elliptic genera of these noncompact Gepner models have been studied in [37, 27, 38]. In this section we restricted ourselves to the Landau-Ginzburg construction where the theory is defined as (an orbifold of) the direct product of the Landau-Ginzburg models with monomial superpotentials. Geometrically, they corresponded to the (deformations of) the Brieskorn-Pham type singularities. It is possible to construct more general Landau-Ginzburg orbifolds with generic polynomial superpotentials. The generalized models have a potential applications to the singular locus of the $\mathcal{N} = 2$ supersymmetric Yang-Mills theories (Argyres-Douglas point) and their deformations. The exact quantization of the world-sheet theory beyond the topological subsector, however, is a difficult task and we would not pursue these generalizations any further in this thesis.

2.2.2 singular limit and LST

In section 2.1, we have discussed that the coinciding k NS5-branes superstring solution corresponds to the linear dilaton background while the supersymmetric deformation (separation of NS5-branes in a ring-like manner) corresponds to the $SL(2; \mathbb{R})/U(1)$ coset background (i.e. two-dimensional Euclidean black hole). Here we would like to take the similar singular limit in more general noncritical superstring backgrounds discussed in section 2.2.1.¹³

It is particularly easy to see the singular limit if we start with the $\mathcal{N} = 2$ Liouville description: it has a superpotential

$$W(\Phi) = \mu e^{\frac{1}{\mathfrak{Q}}\Phi} , \quad (2.25)$$

and the parameter μ directly corresponds to the deformation parameter appearing e.g. in (2.18),(2.20). Thus the singular limit $\mu \rightarrow 0$ is equivalent to switching off the Liouville potential so that we are left with the linear dilaton theory. The duality between the $\mathcal{N} = 2$ Liouville theory and $SL(2; \mathbb{R})/U(1)$ coset theory then confirms the statement that the singular limits of the non-compact Gepner models correspond to replacing $SL(2; \mathbb{R})/U(1)$ coset part by the $\mathcal{N} = 2$ supersymmetric linear dilaton theory with the same central charge and the same asymptotic dilaton gradient.

Let us formulate the proposal discussed above in a more precise way [24]. We begin with the type II string theory on a singular Calabi-Yau varieties X^{2n} with the complex dimension n defined as the vicinity of a hypersurface singularity

$$F(z_1, \dots, z_{n+1}) = 0 \quad (2.26)$$

in \mathbb{C}^{n+1} , where F is a quasi-homogeneous polynomial on \mathbb{C}^{n+1} . This means that F has degree 1 under the \mathbb{C}^* action:

$$z_i \rightarrow \lambda^{r_i} z_i . \quad (2.27)$$

Now we can define a locally holomorphic n -form Ω as

$$\Omega = \frac{dz_1 \wedge \dots \wedge dz_n}{\partial F / \partial z_{n+1}} \quad (2.28)$$

¹³What we mean by “noncritical” here is that the SCFTs involved does not necessarily possess an apparent 10-dimensional background as is the case with the Gepner construction for compact Calabi-Yau spaces. In a more specific narrower sense, we sometimes call a theory “noncritical” when it possesses a Liouville direction.

on the patch $\partial F/\partial z_{n+1} \neq 0$. It can be extended to other patches where $\partial F/\partial z_i \neq 0$ with the similar expressions and glued together to form a globally well-defined holomorphic n -form with the charge $r_\Omega = \sum_i r_i - 1$ under the \mathbb{C}^* action (2.27). Such constructed varieties X^{2n} are Gorenstein¹⁴ equipped with a natural \mathbb{C}^* action (2.27) by construction.

We consider the type II string theory on the singular Calabi-Yau varieties $\mathbb{R}^{d-1,1} \times X^{2n}$ in the vicinity of the isolated singular point y_0 in the decoupling limit $g_s \rightarrow 0$. The proposed dual theory is the type II string theory on $\mathbb{R}^{d-1,1} \times \mathbb{R}_\phi \times \mathcal{N}$. Here \mathcal{N} is the infrared limit of the sigma model on the manifold $\mathcal{N} = X^{2n}/\mathbb{R}_+$, where the division by \mathbb{R}_+ is an action on z_i as (2.27) with $\lambda \in \mathbb{R}_+$. The infrared limit¹⁵ of the sigma model on \mathcal{N} is given by a Landau-Ginzburg model with superpotential $F(Z_i)$ and an additional \mathbb{S}^1 circle.¹⁶ Here \mathbb{S}^1 direction corresponds to the $U(1)_R$ symmetry associated with the residual $U(1)$ action (2.27) with $|\lambda| = 1$. The quotient space $\mathcal{N}/U(1)$ is equivalent to the Landau-Ginzburg model with superpotential $W = F(Z_i)$ from the standard Landau-Ginzburg / non-linear sigma model correspondence. The linear dilaton slope is determined by the total criticality condition of the string theory.

This construction is equivalent to the one discussed above by turning off the $\mathcal{N} = 2$ Liouville superpotential or $SL(2; \mathbb{R})/U(1)$ deformation. For later purposes, it is worthwhile studying the normalizability of such deformations. Consider the variation of the complex structure of X^{2n} :

$$F(z_i) + \sum_a t_a A_a(z_i) = 0 . \quad (2.29)$$

Here t_a are complex deformation parameters, and $A_a(z_i)$ are complex structure deformations of the defining equation (2.26). The Kahler potential of the Weil-Petersson metric for such complex structure deformations is given by the formula [39]

$$K = -\log \int_{X^{2n}} \Omega \wedge \bar{\Omega} . \quad (2.30)$$

To discuss the normalizability of the perturbation associated with A_a , we have to evaluate

$$\frac{\partial^2}{\partial t_a \partial \bar{t}_a} \Omega \wedge \bar{\Omega} . \quad (2.31)$$

This can be done by the simple scaling argument [40]: if A_a scales under (2.27) as λ^{r_a} , t_a should scale as λ^{1-r_a} , so (2.31) scales with a weight

$$\omega_a = 2 \left(\sum_i r_i + r_a - 2 \right) . \quad (2.32)$$

The modes satisfying $r_a > 1 - r_\Omega$ are non-normalizable deformations as $|z_i| \rightarrow \infty$ while the modes satisfying $r_a < 1 - r_\Omega$ are normalizable deformations.

¹⁴Gorenstein means that $X^{2n} - \{0\}$ admit a nowhere vanishing holomorphic n -form.

¹⁵We assume $r_\Omega > 0$ so that \mathcal{N} is Fano meaning that the curvature of the Einstein metric on it is positive.

¹⁶As a CFT, they are not a simple direct product but an orbifold. We need to impose the GSO projection to preserve the target-space supersymmetry.

The non-normalizable deformations should be regarded as boundary conditions we have to impose at infinity to define a theory. Different boundary conditions would give rise to different theories. On the other hand, the normalizable deformations should be regarded as fluctuating fields after the quantization. Their values can be varied within a given theory. As we will discuss later in section 3.1, the normalizability of the deformations from the space-time viewpoint presented here is deeply connected with the normalizability of the corresponding operators in the world-sheet $\mathcal{N} = 2$ linear dilaton theory. Indeed, one can regard this agreement as a nontrivial support for the duality proposed in [24] and reviewed here.

As an example, let us consider a class of generalized conifolds defined by the hypersurface

$$F(z_i) = H(z_1, z_2) + z_3^2 + z_4^2 \quad (2.33)$$

in \mathbb{C}^4 . It can be regarded as an NS5-brane wrapped around the Riemann surface $H(z_1, z_2) = 0$ along the line of arguments reviewed at the end of section 2.2.1. We begin with the A_{n-1} type Brieskorn-Pham singularity with $H(z_1, z_2) = z_1^n + z_2^2$, and consider the perturbations of the form z_1^a ($a = 0, 1, \dots, n-2$). $U(1)_R$ -charges are given by $r_\Omega = \frac{1}{n} + \frac{1}{2}$ and $r_a = \frac{a}{n}$. From the condition $r_a > 1 - r_\Omega$, we conclude that the deformations with

$$a > \frac{n}{2} - 1 \quad (2.34)$$

are non-normalizable [40, 24]. We can also understand the normalizability of these deformations from the dual $\mathcal{N} = 2$ supersymmetric four-dimensional field theory viewpoints by studying the Seiberg-Witten theory near the Argyres-Douglas points [41, 42, 43].

To conclude this section, we would like to revisit the question: what is the decoupling limit of the theory defined on the singularities (2.26)? We have reviewed the proposed *dual* string theory defined as (deformations of) the $\mathcal{N} = 2$ linear dilaton theory coupled with the Landau-Ginzburg model. We here summarize the low-energy decoupled physics from the original NS5-brane construction in flat ten-dimensional Minkowski space. The decoupled theory has a conventional name “little string theory (LST)” [44].¹⁷

- As a decoupled six-dimensional theory, it has $\mathcal{N} = (2, 0)$ (type IIA) or $\mathcal{N} = (1, 1)$ (type IIB) supersymmetry. The theory is non-local.
- They are classified by the ADE classification.
- IR limit is the six-dimensional super Yang-Mills theory in type IIB and the six-dimensional interacting (2,0) SCFT in type IIA [46].
- BPS excitation includes a string with tension l_s (little string) and the theory shows a Hagedorn-like thermodynamics with the Hagedorn temperature $\beta_{\text{Hg}} \sim 2\pi\sqrt{2k}$ (see section 2.4). Most of these high-energy states are nonperturbative in nature.

After compactification (by wrapping NS5-branes on projective spaces for instance), we have four- (or two-) dimensional effective theory, which includes Seiberg-Witten theory near the Argyres-Douglas singularities, corresponding to the Calabi-Yau 3-fold singularities.

¹⁷See [45] for an earlier review.

The properties of these theories, known as the LST, are less known than the field theory living on D-branes. However, the closed string dual theory is exactly quantizeable in many cases unlike the R-R background in the near horizon limit of the D-branes. The study of α' exact information is an interesting subject of its own, besides the application to the dual theories, and we will pursue this direction in the following sections.

2.2.3 obstruction for conical metrics

So far, we have assumed the existence of the Calabi-Yau varieties defined on the hypersurface singularity (2.26). In the compact Calabi-Yau case such as the curve defined in (2.14), Calabi-Yau theorem guarantees the existence of the unique Ricci-flat Kahler metric once the Calabi-Yau condition is satisfied. The existence of the Calabi-Yau metric on the hypersurface singularities (2.26), however, is an open problem (see [47] for a review).

From the \mathbb{C}^* action (2.27) on the complex variables z_i , it is natural to assume the conical metric

$$ds_{X^{2n}}^2 = dr^2 + r^2 ds_L^2, \quad (2.35)$$

where $r \leq 0$ denotes the radial direction \mathbb{R}_+ and ds_L^2 is the Sasaki-Einstein metric of the link L associated with the non-compact Calabi-Yau variety $X^{2n}/\{0\} = \mathbb{R}_+ \times L$. The Sasaki condition is equivalent to the statement that the total metric is Kahler, and the Einstein condition is equivalent to the statement that the total metric is Ricci flat.

It turns out to be extremely difficult to give necessary and sufficient conditions for the existence of such conical metric (or alternatively existence of the Sasaki-Einstein metric on the link L) while infinitely many examples of explicit metrics have been constructed quite recently [48, 49, 50].

For definiteness we restrict ourselves to the Brieskorn-Pham type singularities defined by the particular polynomial

$$F(z_i) = \sum_{i=1}^{n+1} z_i^{a_i}. \quad (2.36)$$

The corresponding hypersurface singularities X^{2n} are always isolated and Gorenstein. However from the following physical reasoning, we believe that not every singularity possesses a conical metric.

Assuming the existence of such a conical metric, we can compute the volume of such a hypothetical Sasaki-Einstein link L by the formula [51]

$$\text{Vol}(L) = \frac{r_\Omega^n}{n^n \prod_{i=1}^{n+1} r_i} \text{Vol}(\mathbb{S}^{2n-1}), \quad (2.37)$$

where $\text{Vol}(\mathbb{S}^{2n-2}) = \frac{2\pi^n}{(n-1)!}$.¹⁸ Via the AdS-CFT correspondence, the central charge a of the dual SCFT living on D3-branes placed at the tip of the cone is related to the volume of the

¹⁸We have assumed that the Reeb-vector (conformal $U(1)_R$ -symmetry) is given by the natural \mathbb{C}^* action (2.27). If this is not the case, we have to determine the “correct” Reeb-vector by using the Z -minimization [52, 53] (a -maximization [54]) principle.

Sasaki-Einstein link L [55] as

$$a \propto \frac{1}{\text{Vol}(L)}. \quad (2.38)$$

On the other hand, the conjectured a -theorem states that a is a decreasing function during a renormalization group flow from UV to IR. Geometrically speaking, the relevant deformations to (2.36) should increase the volume.¹⁹ However, this statement is clearly violated in some explicit examples such as the series $F = z_1^k + z_2^2 + z_3^2 + z_4^2$ with $k > 4$, where $\text{Vol}(k+1) > \text{Vol}(k)$ contradicting with the a -theorem.

Recently, [57] has given two mathematical obstructions for the existence of conical Calabi-Yau metric for such varieties.

The Bishop obstruction

For the existence of the conical Calabi-Yau metric (2.35), $\text{Vol}(L) < \text{Vol}(\mathbb{S}^{2n-1})$ is necessary. From the dual gauge theory viewpoint, the condition corresponds to the fact that by appropriate Higgsing that decreases a , we can reach $\mathcal{N} = 4$ SYM theory.

The Lichnerowicz obstruction

When X^{2n} admits a holomorphic function with $U(1)_R$ -charge $\lambda < 1$, the conical Calabi-Yau metric does not exist. For the Brieskorn-Pham type singularities, it is equivalent to the statement $r_\Omega \leq nr_a$ for any deformation. From the dual gauge theory viewpoint, the condition corresponds to the unitarity bound of dual operators for the deformations. It can be shown that the Lichnerowicz obstruction also eliminate a possible violation of a -theorem for the Brieskorn-Pham type singularities (see appendix B.4).

As an example let us consider the Calabi-Yau four-fold defined by

$$F = z_1^k + z_2^2 + z_3^2 + z_4^2 + z_5^2 = 0. \quad (2.39)$$

The conical Calabi-Yau metric only exists for $k = 2$, and other varieties are obstructed from the Lichnerowicz bound. Thus the $AdS_3 \times L_7$ compactification of M-theory is only possible for $k = 2$. This should be so because otherwise the a -theorem would be violated or the weaker energy-condition would be spoiled.

On the other hand, one can consider the two-dimensional string compactification on such a hypothetical conical Calabi-Yau manifold (2.39) and add N_f fundamental strings on the noncompact $\mathbb{R}^{1,1}$ directions at the tip of the cone. Due to the gravitational backreaction, we can see the near horizon geometry would be $AdS_3 \times \mathcal{N}$ with the constant string coupling $g_s^2 \sim \frac{1}{N_f}$, where \mathcal{N} has been introduced in section 2.2.2 denoting the infrared limit of the sigma model on the hypothetical Sasaki-Einstein link L associated with (2.39). As discussed in this section, the Sasaki-Einstein link L is obstructed, but the string theory on $AdS_3 \times \mathbb{S}^1 \times (LG(F) \sim \mathcal{N}/U(1))$ has a well-defined perturbative description based on the $SL(2; \mathbb{R})$ current algebra with level k times Landau-Ginzburg orbifold defined by $F(Z_i)$ (or $\mathcal{N} = 2$ minimal model) [5].²⁰ Interestingly, unlike the a -theorem associated with the M-theory compactification on $AdS_3 \times \mathcal{N}$, the c -theorem for the dual CFT of $AdS_3 \times \mathbb{S}^1 \times (LG(F) \sim$

¹⁹From the pure gravity viewpoint, this is a consequence of the weaker energy condition [56].

²⁰This does not mean the existence of such Sasaki-Einstein metric because we are sitting at the Gepner-point of the sigma model, where the geometrical description is questionable due to large α' corrections.

$\mathcal{N}/U(1)$) is always satisfied because the dual CFT central charge, which is determined from the curvature of the $AdS_3 \sim SL(2; \mathbb{R})$, is given by $c = 6kQ_1$.²¹

In a similar fashion, the near horizon geometry of every Brieskorn-Pham singularities admit the noncritical string construction based on the non-compact Gepner models as we have presented in this section irrespective of the above-mentioned obstructions. It would be interesting to understand the obstructions of the existence of conical metrics for such singularities from the noncritical string theory viewpoint. For instance, we can translate the Lichnerowicz obstruction as the claim that every relevant deformations up to $z_i^{a_i-3}$ should be normalizable.

2.3 Classical two-dimensional black hole

In section 2.1, we have introduced the two-dimensional black hole geometry as a near horizon limit of the black NS5-brane solutions in the type II superstring theory:

$$ds^2 = k\alpha'(-\tanh^2 \rho dt^2 + d\rho^2), \quad (2.40)$$

with nontrivial dilaton gradient $e^{2\Phi} = \frac{k}{\mu \cosh^2 \rho}$.²² It has been claimed in the literature that the background is α' exact perturbatively in the type II superstring theory while the bosonic two-dimensional black hole might receive perturbative world-sheet $\alpha' \sim \frac{1}{k}$ corrections [58]. We will discuss physical importance of the nonperturbative corrections later in section 3.4.

In this subsection, we review the classical geometry of the two-dimensional black hole. First of all, the metric (2.4) has an event horizon at $\rho = 0$, but the (t, ρ) coordinate does not cover the whole causal region of the black hole. One can maximally extend the geometry (2.4) by introducing the Kruscal coordinate

$$u = \sinh \rho e^t, \quad v = -\sinh \rho e^{-t}, \quad ds^2 = -2k \frac{dudv}{1-uv}, \quad e^{2\Phi} = \frac{k}{\mu(1-uv)}. \quad (2.41)$$

Note that in two-dimension, it is always possible to introduce the conformal coordinate (u, v) locally with the conformally flat metric $ds^2 = f(u, v)dudv$. In this coordinate, the event horizon is located at $uv = 0$, and inside the horizon, we encounter singularity at $uv = 1$, where the curvature and the dilaton diverges. The Kruscal diagram can be found in figure 2. Causal region of the Lorentzian black hole background has four boundaries: past and future horizons \mathcal{H}^\pm , and past and future asymptotic infinities \mathcal{I}^\pm .

We can also study the global structure of the metric by using the Penrose coordinates, and one can write down the Penrose diagram (see figure 3) of the two-dimensional black hole system, which looks exactly same as that for the four-dimensional Schwarzschild black hole system (upon neglecting S^2 angular directions). This is one of the motivations to study the two-dimensional black hole system as an exactly solvable toy model for four-dimensional Schwarzschild black hole.

²¹For instance, $k = \frac{n}{n+1}$ for A_{n-1} type Calabi-Yau four-folds.

²²We have rescaled the normalization of t for simplicity of notation. We will sometimes do this in the following without notice, for it would be convenient to stick to 2π periodicity in the Euclidean time direction after the Wick rotation.

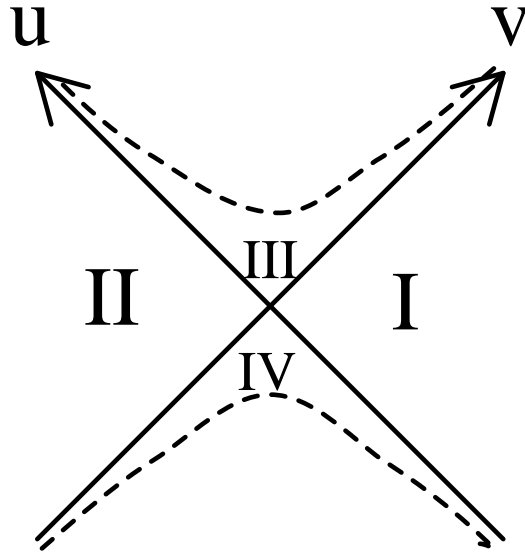


Figure 2: Kruskal diagram for the two-dimensional black hole system.

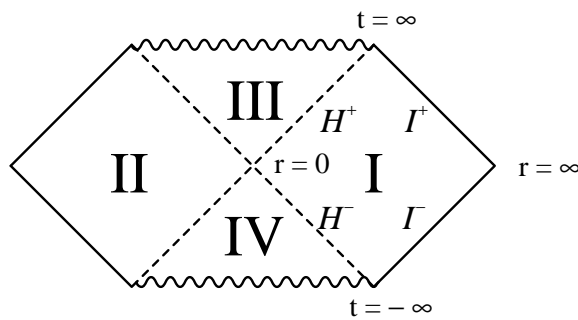


Figure 3: Penrose diagram for the two-dimensional black hole.

The geodesic motion of a particle with the minimal coupling interaction to the geometry

$$S = \int ds = \int d\tau \sqrt{\frac{\dot{u}\dot{v}}{1-uv}}, \quad (2.42)$$

where dot denotes the derivative with respect to τ , is given by

$$\begin{cases} \ddot{u}(1-uv) = -v\dot{u}^2 \\ \ddot{v}(1-uv) = -u\dot{v}^2 \end{cases}. \quad (2.43)$$

Later, we will compare this with the string motion and D-particle motion, both of which show quite distinct properties.

Finally, we would like to study the “mass” of the two-dimensional black hole. For this purposes, it is convenient to use the Schwarzschild(-like) coordinate (2.6):

$$ds^2 = -\left(1 - \frac{2M}{r}\right) dt^2 + \frac{k}{1 - \frac{2M}{r}} \frac{dr^2}{r^2}, \quad e^{2\phi} = r, \quad (2.44)$$

where $r_0 = 2M$ is the location of the horizon. From the expression, it is clear that we can easily shift the value of M multiplicatively $M \rightarrow aM$ by the scaling of r as $r \rightarrow r/a$. Therefore the physical meaning of the “mass” of the two-dimensional black hole is solely determined by the value of the string coupling constant (dilaton) at the horizon $r = 2M$. It corresponds to the fact that the mass parameter M is related to the world-sheet $\mathcal{N} = 2$ Liouville cosmological constant μ in the dual $\mathcal{N} = 2$ Liouville theory, where μ can be shifted by the shift of the Liouville coordinate (see section 3.4 for more about the duality).

Because of this property, the Hawking temperature of the two-dimensional black hole is independent of M unlike the case with higher-dimensional black-holes. Similarly many features of the string theory in the two-dimensional black hole background such as scattering amplitudes also show rather trivial dependence on M .²³ It is related to the Knizhnik-Polyakov-Zamolodchikov (KPZ) scaling law of the dual Liouville theory [59].

2.4 Wick rotation: thermodynamic properties

In this section, we would like to study thermodynamic properties of the two-dimensional black hole (and hence LST on the black NS5-branes). It is a well-known but profound fact that the black hole system shows a thermodynamic properties [60, 61]:

- Surface gravity κ (temperature T) is constant over horizon of stationary black hole (the zeroth law: $T = \frac{\kappa}{2\pi}$)
- $dM = \frac{1}{8\pi}\kappa dA + \Omega dQ$ (the first law: $S = \frac{A}{4}$)
- $\delta A \geq 0$ in any physical process (the second law)
- It is impossible to achieve $\kappa = 0$ by any physical process (the third law)

²³It is customary to set $M = 1$ as we will do in most part of the thesis.

Here M is the mass of the black hole, $A = 4S$ is the area of the event horizon (= entropy), Q is the charge, and Ω is its chemical potential. One of the biggest motivations to study the quantum gravity such as the string theory is to understand the black hole thermodynamics from the microscopic viewpoint.

Let us begin with the temperature of the two-dimensional black hole. One convenient way to compute the Hawking temperature of black hole systems [62] is to use the Euclidean path integral formalism [63]. In our case, we can study the Wick rotation (i.e. $t \rightarrow i\tau_E$) of the Lorentzian two-dimensional black hole :

$$ds_E^2 = \tanh^2 \rho d\tau_E^2 + k\alpha' d\rho^2 . \quad (2.45)$$

To avoid a conical singularity at the origin $\rho = 0$, we have to set the periodicity of the Euclidean time direction by $\beta_{\text{Hw}} = 2\pi\sqrt{k\alpha'}$: $\tau_E \sim \tau_E + \beta_{\text{Hw}}$. In the Euclidean path integral formulation, we regard this periodicity as the inverse of the Hawking temperature of the black hole: $T_{\text{Hw}} = \frac{1}{\beta_{\text{Hw}}} = \frac{1}{2\pi\sqrt{k\alpha'}}$ because in the Matsubara formalism, the periodicity of the Euclidean time corresponds to the inverse temperature. Note that in the large k semi-classical limit, we have vanishing Hawking temperature so that the back-reaction associated with the Hawking radiation is negligible and the black hole geometry is infinitely long-lived (i.e. eternal). As we mentioned in section 2.3, it is also interesting to note that the Hawking temperature does not depend on the mass m of the two-dimensional black hole. In the context of the dual LST defined in section 2.3, we will regard this temperature as the (non-perturbative) Hagedorn temperature of the LST.

There are several derivations of the Hawking temperature other than the Euclidean path integral method. Recently [64, 65] proposed a new derivation based on the gravitational anomaly in the vicinity of the event horizon.²⁴ We briefly review their derivation focusing on the two-dimensional case (see [67, 68, 69, 70] for related works).

Let us take the very near-horizon limit (Rindler-limit)²⁵ of the two-dimensional black hole:

$$ds^2 = -\frac{2(r-r_0)}{\sqrt{k\alpha'}} dt^2 + \frac{\sqrt{k\alpha'}}{2(r-r_0)} dr^2 , \quad \Phi = \text{const} . \quad (2.46)$$

Now let us suppose we neglect the classically irrelevant in-falling modes of any scalar field propagating in the vicinity of the horizon $r = r_0$. The massless scalar fields with this boundary condition are effectively chiral, so it will show a gravitational anomaly:

$$\nabla_\mu T^\mu_\nu = \frac{1}{\sqrt{-g}} \partial_\mu N^\mu_\nu \quad (2.47)$$

²⁴See also [66] for a derivation based on the trace anomaly.

²⁵Although there is nothing wrong with taking the Rindler-limit in the general relativity, the limit is a little bit subtle in the string theory because the string theory introduces a “minimal size” (string scale) to the geometry. In our example, the central charge of the original two-dimensional black-hole and its very near horizon limit is different, so we need an extra compensation of the central charge in order to preserve the criticality condition. Since we are only interested in the classical thermodynamics, we will neglect this subtlety for a time being. See also the discussion of stretched horizon of the two-dimensional black holes in section 4.

with the explicit component expression

$$N_t^t = N_r^r = 0, \quad N_t^r = \frac{1}{192\pi} \frac{4}{k\alpha'}, \quad N_r^t = -\frac{1}{192\pi(r-r_0)^2}. \quad (2.48)$$

Especially, it shows a pure flux contribution

$$\Phi = N_t^r|_{r=r_0} = \frac{1}{192\pi} \frac{4}{k\alpha'}. \quad (2.49)$$

To cancel the gravitational anomaly, we need a quantum contribution that can be attributed to the Hawking radiation from the black hole. The black body radiation with the temperature T_{Hw} gives rise to the flux

$$\Phi = \frac{\pi}{12} T_{\text{Hw}}^2, \quad (2.50)$$

and the comparison between (2.49) and (2.50) establishes the Hawking temperature $T_{\text{Hw}} = \frac{1}{2\pi\sqrt{k\alpha'}}$. We will later see similar effects related with the choice of boundary conditions of wavefunction at the horizon when we study D-brane motions in the two-dimensional black hole geometries.

Let us move on to the other thermodynamic quantities. Since the temperature does not depend on the mass of the two-dimensional black hole, we see that the black hole entropy is given by

$$S(m) = \beta_{\text{Hw}} m = 2\pi\sqrt{\alpha' k} m. \quad (2.51)$$

In higher dimensions, we could identify the entropy of the black hole as the area of the event horizon (i.e. the Bekenstein formula $S = \frac{A}{4\pi}$), but in the two-dimensional space-time, the event horizon is just a point and we cannot apply the Bekenstein formula. Instead, we have defined the entropy through the thermodynamic relation $\beta = \frac{\partial S}{\partial m}$. This formula predicts the high energy density of states in the LST. Assuming the microscopic explanation of the black hole entropy (2.51) from the LST, the density of states of LST should be given by

$$\rho(E) \sim e^{2\pi\sqrt{\alpha' k} E}, \quad (2.52)$$

in the high energy limit $E \rightarrow \infty$.

3 Two-dimensional Black Hole: CFT Viewpoint

In this section, we review the two-dimensional black hole from the exactly solvable CFT viewpoint. We begin with the Euclidean version of the two-dimensional black hole and then we move on to the Lorentzian two-dimensional black hole from an appropriate Wick rotation. This is because the Euclidean version is much better understood than the Lorentzian counterpart.

The organization of this section is as follows. In section 3.1, We begin with the classical geometries for the $SL(2; \mathbb{R})/U(1)$ coset model that yields an exact CFT model for the two-dimensional black hole system. In section 3.2, we review the Euclidean spectrum of the $SL(2; \mathbb{R})/U(1)$ coset model. In section 3.3, we deal with the Lorentzian case in detail. In section 3.4, we comment the duality between $SL(2; \mathbb{R})/U(1)$ coset model and the $\mathcal{N} = 2$ Liouville theory and discuss implications of the associated winding tachyon condensation.

3.1 Classical geometries for $SL(2; \mathbb{R})/U(1)$ coset

From the world-sheet viewpoint, the reason why we are interested in the two-dimensional black hole system is that we can quantize the string theory on it by using the $SL(2; \mathbb{R})/U(1)$ coset CFT. In this subsection, we would like to overview the correspondence between the $SL(2; \mathbb{R})/U(1)$ coset model and the two-dimensional black hole system from the gauged Wess-Zumino-Novikov-Witten (WZNW) model construction [71, 72, 73].

It is possible to define the coset CFT such as $SL(2; \mathbb{R})/U(1)$ model purely from the algebraic viewpoint (at least at the level of the left-right chiral $SL(2; \mathbb{R})/U(1)$ representations: the most difficult point is to construct the modular invariant combinations), but we would like to begin with the Lagrangian construction based on [71]. This is because the construction directly gives the geometric interpretation of the model as the non-linear sigma model on the two-dimensional black hole in the semi-classical limit ($k \rightarrow \infty$). The path integral formulation based on the Lagrangian can also be used to derive the (formally) modular invariant partition function of the Euclidean two-dimensional black hole [74] (see appendix B.1).

The ungauged WZNW model for a general Lie group G has the following action:

$$S_{WZNW}(g) = \frac{\kappa}{8\pi} \int_{\Sigma} d^2x \sqrt{|\gamma|} \gamma^{ij} \text{tr}(g^{-1} \partial_i g g^{-1} \partial_j g) + i\kappa \Gamma(g) . \quad (3.1)$$

The Wess-Zumino term $\Gamma(g)$ is given by

$$\Gamma(g) = \frac{1}{12\pi} \int_B \text{tr}(g^{-1} dg \wedge g^{-1} dg \wedge g^{-1} dg) , \quad (3.2)$$

where B is a three-dimensional manifold whose boundary is Σ . κ denotes the level of the current algebra realized by the WZNW model. When the Lie group G is compact, the level κ should be quantized so that the Wess-Zumino term contributes to the path-integral uniquely with an arbitrary choice of B . In our case, however, since the Lie group is non-compact and $H^3(SL(2; \mathbb{R}), \mathbb{R}) = 0$, the quantization condition of the level κ is not necessary.

Let G be $SL(2; \mathbb{R})$ for our discussion in the following. The action (3.1) possesses a global $SL(2; \mathbb{R}) \times SL(2; \mathbb{R})$ symmetry $g \rightarrow agb^{-1}$, with $a, b \in SL(2; \mathbb{R})$. Quantum mechanically, it will be elevated to a current algebra with the level κ : the chiral current

$$j^A(z) = \kappa \text{Tr}(T^A \partial g g^{-1}) , \quad (3.3)$$

with $T^3 = \frac{1}{2}\sigma_2$, $T^\pm = \pm \frac{1}{2}(\sigma_3 \pm i\sigma_1)$, satisfies the OPE of the affine $\widehat{SL(2; \mathbb{R})}_\kappa$ current algebra

$$\begin{cases} j^3(z)j^3(0) \sim -\frac{\kappa}{2z^2} \\ j^3(z)j^\pm(0) \sim \pm \frac{1}{z}j^\pm(0) \\ j^+(z)j^-(0) \sim \frac{\kappa}{z^2} - \frac{2}{z}j^3(0) \end{cases} . \quad (3.4)$$

The bosonic $SL(2; \mathbb{R})$ WZNW model has the central charge $c = \frac{3\kappa}{\kappa-2}$. We will gauge the anomaly free subgroup of the global symmetry of the $SL(2; \mathbb{R})$ WZNW model to obtain the Lagrangian formulation for the coset CFT.

Let us first begin with the Euclidean coset. The $SL(2; \mathbb{R})$ WZNW model has a negative-signature direction in $J^3 \sim i\sigma_2$ and the target space is a Lorentzian manifold. We gauge the (compact) $U(1)$ subgroup generated by

$$\delta g = \epsilon(i\sigma_2 \cdot g + g \cdot (i\sigma_2)) , \quad (3.5)$$

or by setting

$$a = b^{-1} = h = \begin{pmatrix} \cos \epsilon & \sin \epsilon \\ -\sin \epsilon & \cos \epsilon \end{pmatrix} . \quad (3.6)$$

To promote the global axial symmetry $g \rightarrow hgh$ to the gauge symmetry, we have to introduce the gauge connection A_i that transforms as $\delta A_i = -\partial_i \epsilon$ under the gauge transformation (3.6) with a space varying gauge parameter $\epsilon(x_i)$. The covariantized action reads

$$\begin{aligned} S_{\text{gauged}} &= S_{\text{WZNW}}(g) + \\ &+ \frac{\kappa}{2\pi} \int d^2z \bar{A} \text{Tr}(i\sigma_2 g^{-1} \partial g) + A \text{Tr}(i\sigma_2 \bar{\partial} g^{-1}) + A \bar{A} (-2 + \text{Tr}(i\sigma_2 g i\sigma_2 g^{-1})) \end{aligned} \quad (3.7)$$

We call this gauged WZNW model as $SL(2; \mathbb{R})^{(A)}/U(1)$ axial coset. To obtain the classical geometry of the $SL(2; \mathbb{R})^{(A)}/U(1)$ coset CFT, we will integrate out the gauge field by fixing the gauge ²⁶

$$g = \cosh r + \sinh r \begin{pmatrix} \cos \theta & \sin \theta \\ \sin \theta & -\cos \theta \end{pmatrix} . \quad (3.8)$$

The resulting sigma model for the gauge fixed coordinate (r, θ) is given by the action

$$S = \frac{\kappa}{2\pi} \int d^2z (\partial r \bar{\partial} r + \tanh^2 r \partial \theta \bar{\partial} \theta) , \quad (3.9)$$

²⁶In terms of the Euler angle parametrization (see appendix A.3), $g = e^{i\sigma_2 \frac{t-\phi}{2}} e^{r\sigma_1} e^{i\sigma_2 \frac{t+\phi}{2}}$ and we set $t = 0$, where $\phi = \theta - \frac{\pi}{2}$. It is clear that this gauge fixing is always possible and unique.

with the dilaton gradient $e^{2\Phi} = \frac{k}{\mu \cosh^2 r}$, which originates from the one-loop determinant factor for the gauge field A_i . The geometry one can read from the sigma model action is the Euclidean two-dimensional black hole we have introduced in section 2.

In the bosonic coset model, we expect a perturbative (and nonperturbative) α' corrections for this gauge fixing procedure and the corrected sigma model was proposed in [75]. In the supersymmetric Kazama-Suzuki coset, it is believed that there is no perturbative α' corrections to the metric. Nonperturbative corrections which will be reviewed in section 3.4, however, are present and they are one of the key elements to understand the “black hole - string transition”.

The Lorentzian coset is obtained by gauging the non-compact subgroup

$$\delta g = \epsilon (\sigma_3 g + g \sigma_3) . \quad (3.10)$$

We fix the gauge by setting

$$g = \begin{pmatrix} a & u \\ -v & a \end{pmatrix} \quad (3.11)$$

with the determinant constraint $uv = 1 - a^2$. The gauge fixing condition is valid for $1 - uv > 0$ and we can see that u and v are gauge invariant coordinates. With this gauge fixing condition,²⁷ the target space is spanned by the (u, v) plane. After integrating out the gauge field A_i , the resulting sigma model is given by

$$S = -\frac{\kappa}{4\pi} \int d^2x \sqrt{|\gamma|} \frac{\gamma^{ij} \partial_i u \partial_j v}{1 - uv} , \quad (3.12)$$

which reproduces the classical two-dimensional black hole system discussed in section 2. Here we have used the Lorentzian signature world-sheet so that the sigma model with a Lorentzian signature target space is well-defined.

In this thesis, we mainly focus on the supersymmetric generalization of the two-dimensional black hole based on the supersymmetric $SL(2; \mathbb{R})_k/U(1)$ coset model. The starting point is the bosonic $SL(2; \mathbb{R})_\kappa/U(1)$ coset mode with the level $\kappa = k + 2$ bosonic current algebra. In addition to the bosonic action (3.7), we introduce the fermionic part:

$$S_f = \frac{1}{2\pi} \int d^2z \left(\psi^+ (\bar{\partial} - \bar{A}) \psi^- + \psi^- (\bar{\partial} + \bar{A}) \psi^+ + \tilde{\psi}^+ (\partial - A) \tilde{\psi}^- + \tilde{\psi}^- (\partial + A) \tilde{\psi}^+ \right) , \quad (3.13)$$

with the OPE $\psi^+(z)\psi^-(0) \sim 1/z$, $\psi^\pm(z)\psi^\pm(0) \sim 0$. Let us concentrate on the Euclidean case for definiteness. From the Kazama-Suzuki construction, we can realize the $\mathcal{N} = 2$ superconformal symmetry on the supersymmetric $SL(2; \mathbb{R})/U(1)$ coset model. The explicit realization is given by

$$\begin{aligned} T(z) &= \frac{1}{k} (j^1 j^1 + j^2 j^2) - \frac{1}{2} (\psi^+ \partial \psi^- - \partial \psi^+ \psi^-) \\ G^\pm(z) &= \frac{1}{\sqrt{k}} \psi^\pm j^\mp \\ J(z) &= \psi^+ \psi^- + \frac{2}{k} (j^3 + \psi^+ \psi^-) , \end{aligned} \quad (3.14)$$

²⁷Strictly speaking, the coset is a double cover of the (u, v) plane, where the two-sheets are distinguished by the signature of a . We will neglect this small subtlety throughout the thesis.

whose central charge is given by $c = 3(1 + \frac{2}{k})$. The gauging current is defined by $J^3 = j^3 + \psi^+ \psi^-$, which commutes with all the elements of the $\mathcal{N} = 2$ superalgebra. The fermionic part of the Lorentzian case is obtained from the analytic continuation by formally replacing $\psi^+ = \frac{1}{\sqrt{2}}(\psi^1 + i\psi^2) \rightarrow \frac{1}{\sqrt{2}}(\psi^1 + \psi^3)$ and $\psi^- = \frac{1}{\sqrt{2}}(\psi^1 - i\psi^2) \rightarrow \frac{1}{\sqrt{2}}(\psi^1 - \psi^3)$.

From the path integral viewpoint, instead of treating the (Euclidean) $SL(2; \mathbb{R})^{(A)}/U(1)$ coset, it is more convenient to study the equivalent description based on the $\mathbb{H}_3^+/\mathbb{R}$ coset model. The $\mathbb{H}_3^+ = SL(2; \mathbb{C})/SU(2)$ model is defined by the sigma model on the upper sheet

$$g = \begin{pmatrix} a & u \\ \bar{u} & b \end{pmatrix} = \begin{pmatrix} e^\phi & e^{\phi\bar{\gamma}} \\ e^{\phi\gamma} & e^{\phi\gamma\bar{\gamma}} + e^{-\phi} \end{pmatrix}, \quad (3.15)$$

where we have introduced a real field ϕ and a complex field γ with its complex conjugation $\bar{\gamma}$. The sigma model has the action

$$S = -\frac{\kappa}{2\pi} \int d^2z (\partial\phi\bar{\partial}\phi + e^{2\phi}\partial\gamma\bar{\partial}\bar{\gamma}). \quad (3.16)$$

The model has a positive definite action and the path integral is well-defined (unlike the ungauged $SL(2; \mathbb{R})$ WZNW model).²⁸ The two-dimensional Euclidean black hole is obtained by axially gauging the noncompact $U(1)$ direction σ_2 (e.g. one can choose a gauge $a = b$ and obtain the metric $ds^2 = \kappa \frac{dud\bar{u}}{1+|u|^2}$). This construction has the advantage that the parent sigma model has a definite Euclidean path integral while the $SL(2; \mathbb{R})/U(1)$ coset does not because the parent WZNW model has a Lorentzian signature.

So far, we have studied the axial coset of the $SL(2; \mathbb{R})$ WZNW model, but it is possible to gauge the vector symmetry

$$\delta g = \epsilon(i\sigma_2 \cdot g - g \cdot (i\sigma_2)). \quad (3.17)$$

This symmetry has a fixed point, and the corresponding effective action

$$S = \frac{\kappa}{2\pi} \int d^2z \left(\partial\rho\bar{\partial}\rho + \frac{1}{\tanh^2\rho} \partial\tilde{\theta}\bar{\partial}\tilde{\theta} \right), \quad (3.18)$$

which is also known as the trumpet model, has a singularity at $\rho = 0$. However, from the algebraic coset viewpoint, there is no singularity at all. We have just replaced right moving \bar{J}_3 current of the $SL(2; \mathbb{R})$ WZNW model with $-\bar{J}_3$.

In order to specify the model, we have to determine the periodicity of the variable $\tilde{\theta}$ in the effective action (3.18). The angular variable θ in the cigar geometry has a natural periodicity 2π coming from the $SL(2; \mathbb{R})$ WZNW model. In the trumpet case, there is no a priori natural periodicity of $\tilde{\theta}$ because it is non-contractible loop in $SL(2; \mathbb{R})$ and any periodicity is allowed if we study the universal cover of the $SL(2; \mathbb{R})$. In terms of the Euler angle parametrization (see appendix A.3), $g = e^{i\sigma_2 \frac{t-\phi}{2}} e^{r\sigma_1} e^{i\sigma_2 \frac{t+\phi}{2}}$ and we set $\phi = 0$. In this sense, the natural periodicity for $t = \tilde{\theta}$ is 2π . We *define* that the $SL(2; \mathbb{R})^{(V)}/U(1)$ vector coset model has 2π periodicity in $\tilde{\theta}$.

From the algebraic construction, the vector coset merely changes the sign convention of the right-moving current \bar{J}_3 , which reminds us of the T-duality or mirror symmetry. Along this line of reasoning, an alternatively good definition of the vector coset is to take $2\pi/k$ periodicity in $\tilde{\theta}$.²⁹ This is indeed motivated by Bucsher's T-duality rule: if we perform

²⁸However, the model has an imaginary H_3 flux, so the physical interpretation is unclear.

²⁹This convention is the one given in [75].

the T-duality to our original cigar model (3.9) with 2π periodicity in θ , we obtain the trumpet model with $2\pi/k$ periodicity. We call this model as “ \mathbb{Z}_k orbifold of the vector coset $SL(2; \mathbb{R})^{(V)}/U(1)$ ”. The \mathbb{Z}_k orbifold of the $SL(2; \mathbb{R})^{(V)}/U(1)$ or \mathbb{Z}_k orbifold of the trumpet model is same as the cigar model as a CFT (up to a GSO projection in the supersymmetric case).³⁰

Since the vector coset model with the trumpet geometry is related to the T-duality of the cigar geometry, there should be no singularity at all in the vector coset model as a CFT. What happens to the apparent singularity of the classical geometry? We will come back to this problem in section 3.4.

The equivalence between the axial coset and the (\mathbb{Z}_k orbifold of) vector coset leads to a remarkable observation made in [75] — the duality between the singularity and the horizon. If we gauge the vector symmetry for the Lorentzian coset, we end up with the same Lorentzian two-dimensional black hole.³¹ However, the analytic continuation of the trumpet geometry (vector coset) has a natural interpretation as the region inside the singularity:

$$ds^2 = \alpha' k \left(-\frac{1}{\tanh^2 \rho} dt^2 + d\rho^2 \right). \quad (3.19)$$

In this way, the axial-vector duality suggests the duality of the region parametrized uv and $1 - uv$ while keeping t . In particular, it exchanges the region outside the horizon and the one inside the singularity. This duality would shed a new light on the physics of the black hole and especially, relation between the T-duality and “winding tachyon” in the Lorentzian two-dimensional black hole. It is, however, fair to say that the precise physical meaning of the duality is far from being well-understood in the Lorentzian signature.

To close this section, we discuss the pure two-dimensional background by setting $k = 1/2$ or $\kappa = 9/4$. Then the model is a critical string theory by itself and one can regard it as a pure two-dimensional background [71]. In the Euclidean signature, there is a proposed dual matrix model [76] and the theory is supposedly exactly solvable. In the context of more general dilaton gravity in the two-dimensional space-time, the classical solutions are investigated in [77].

3.2 Euclidean spectrum

Let us study the spectrum of the Euclidean $SL(2; \mathbb{R})/U(1)$ coset model.

³⁰Let us mention the similar structure in the $SU(2)$ case. It is known that the axial coset $SU(2)^{(A)}/U(1)$ is the \mathbb{Z}_k orbifold of the vector coset $SU(2)^{(V)}/U(1)$. However, in this case, \mathbb{Z}_k orbifold of the vector coset $SU(2)^{(V)}/U(1)$ is the same model as the original $SU(2)^{(V)}/U(1)$. Therefore, we can also say that the T-dual of the $SU(2)^{(A)}/U(1)$ coset is the $SU(2)^{(V)}/U(1)$. In the $SL(2; \mathbb{R})$ case, although the asymptotic spectrum of the \mathbb{Z}_k orbifold of the $SL(2; \mathbb{R})^{(V)}/U(1)$ coincides with that of the $SL(2; \mathbb{R})^{(V)}/U(1)$, the (un-regularized) partition function is different from each other. Here we implicitly assumed that k is an integer, but the situation is more involved when k is not an integer because the meaning of the \mathbb{Z}_k orbifold is obscure. Note that we have defined the \mathbb{Z}_k orbifold of the $SL(2; \mathbb{R})^{(V)}/U(1)$ as the T-dual of the $SL(2; \mathbb{R})^{(A)}/U(1)$, which perfectly makes sense even for irrational k .

³¹This is up to global duplications. For instance, if one considers an axial coset of the universal cover of the $SL(2; \mathbb{R})/U(1)$ coset, we have an infinite copies of the Lorentzian two-dimensional black holes.

3.2.1 algebraic coset

We begin with the algebraic structure of the coset model from the noncompact para-fermion construction.

Let $\Phi_{jm}(z)$ be holomorphic part of the primary fields of $SL(2; \mathbb{R})$ WZNW model with bosonic level κ . It has a (bosonic) left-moving j_0^3 eigenvalue m :

$$j^3(z)\Phi_{jm}(0) = m\frac{\Phi_{jm}}{z} . \quad (3.20)$$

It is also a holomorphic part of the primary for the supersymmetric $SL(2; \mathbb{R})$ WZNW model with the same eigenvalue for J_0^3 . Here, the supersymmetric current J^3 is defined by

$$J^3 = j^3 - \psi^- \psi^+ . \quad (3.21)$$

For later convenience, we introduce the bosonized current³²

$$\begin{aligned} \partial H &= i\psi^- \psi^+ \\ J^3 &= -\sqrt{\frac{\kappa}{2}} \partial X_3 \\ j^3 &= J^3 + i\partial H = -\sqrt{\frac{\kappa}{2}} \partial x_3 . \end{aligned} \quad (3.22)$$

Using X_3 , or x_3 , we can decompose Φ_{jm} as

$$\Phi_{jm} = U_{jm} e^{m\sqrt{\frac{2}{\kappa}} X_3} = V_{jm} e^{m\sqrt{\frac{2}{\kappa}} x_3} . \quad (3.23)$$

The para-fermion fields U_{jm} and V_{jm} have the conformal dimension

$$\begin{aligned} \Delta(U_{jm}) &= \frac{-j(j+1) + m^2}{\kappa} \\ \Delta(V_{jm}) &= -\frac{j(j+1)}{\kappa - 2} + \frac{m^2}{\kappa} , \end{aligned} \quad (3.24)$$

and they are (holomorphic) primaries of the supersymmetric Euclidean coset $SL(2; \mathbb{R})/U(1)$ and the bosonic coset respectively.

For the supersymmetric case, we should also decompose the $U(1)$ fermion current as

$$e^{inH} = e^{n\sqrt{\frac{2}{\kappa}} X_3} e^{i\sqrt{\frac{c}{3}} X_R} , \quad (3.25)$$

where the bosonized $U(1)_R$ -current (of the $\mathcal{N} = 2$ SUSY algebra: see appendix B.3) is defined by

$$J = i\sqrt{\frac{c}{3}} \partial X_R , \quad (3.26)$$

³²Note that the gauging current must be time-like in the Euclidean coset.

where

$$iH = \sqrt{\frac{2}{k}}X_3 + i\sqrt{1 + \frac{2}{k}}X_R . \quad (3.27)$$

Under the decomposition (3.23) and (3.25), (holomorphic) primary fields of the supersymmetric $SL(2; \mathbb{R})/U(1)$ coset takes the form

$$V_{jm}^n = V_{jm} e^{i(\frac{2m}{k+2}+n)\sqrt{\frac{c}{3}}X_R} , \quad (3.28)$$

which has the conformal dimension

$$\Delta(V_{jm}^n) = -\frac{j(j+1) + (m+n)^2}{k} + \frac{n^2}{2} , \quad (3.29)$$

and the $U(1)_R$ charge

$$R(V_{jm}^n) = \frac{2m}{k} + \frac{nc}{3} . \quad (3.30)$$

The (half) integer n is the amount of the spectral flow of the $\mathcal{N} = 2$ superconformal algebra. The structure of the descendants, depending on quantum numbers (j, m, n) , are completely fixed from that of the $SL(2; \mathbb{R})$ (see appendix A.2), or alternatively from the representation of the $\mathcal{N} = 2$ superconformal algebra.

3.2.2 spectrum from partition function

To obtain the full spectrum of the CFT from the holomorphic data discussed in section 3.2.1, we need to combine left-moving parts and right-moving parts in a consistent way. For example, in the compact $SU(2)$ WZNW model, the complete classification of the modular invariant partition function (and hence the spectrum) is given by the so-called ADE classification. In the non-compact case, we have not yet achieved such a systematic classification. Physically, however, we are primarily interested in the two-dimensional black hole interpretation of the $SL(2; \mathbb{R})/U(1)$ coset model, so we will only consider the simplest realization from the gauged WZNW model as we have focused in section 3.1.

We begin with the partition function for the bosonic Euclidean two-dimensional black hole [74]

$$Z_{\mathbb{H}_+^{3(A)}/\mathbb{R}} = \int_{\Sigma} \frac{du^2}{\tau_2} \frac{e^{\frac{u_2^2}{\tau_2}}}{\sqrt{\tau_2} |\theta_1(\tau, u)|^2} \sqrt{\tau_2} |\eta(\tau)|^2 \sum_{m, \omega \in \mathbb{Z}} e^{-\frac{\pi k}{\tau_2} |\omega\tau - m + u|^2} . \quad (3.31)$$

See appendix B.1 for a summary of various partition functions. Unfortunately, the partition function is divergent, and the leading divergence comes from the integration near $u_1 = u_2 = 0$. The diverging factor could be attributed to the volume divergence in the radial ρ direction of the cigar model. Thus, at the leading order, we have

$$Z_{\mathbb{H}_+^{3(A)}/\mathbb{R}} \sim \frac{1}{2\pi} (\log \epsilon) Z_{\text{free}}(\tau) Z_{\sqrt{\kappa}}(\tau) + \text{finite part} , \quad (3.32)$$

which gives the asymptotic degrees of freedom realized by a free non-compact boson (with the linear dilaton):

$$Z_{\text{free}}(\tau) = \frac{1}{\sqrt{\tau_2} |\eta(\tau)|^2}, \quad (3.33)$$

and a compact boson with radius $R^2 = \kappa$.

$$Z_{\sqrt{\kappa}} = \frac{\sqrt{\kappa}}{\sqrt{\tau_2} |\eta(\tau)|^2} \sum_{m, \omega \in \mathbb{Z}} e^{-\frac{\pi \kappa}{\tau_2} |\omega \tau - m|^2}. \quad (3.34)$$

The appearance of the compact boson is due to the summation over the lattice (n, ω) , which arises from the zeros of $\theta_1(\tau, u)$ in (3.31).

A more precise (but formal) manipulation [74] leads to the following decomposition of the partition function:

$$Z_{\mathbb{H}^3/\mathbb{R}} = \int_{-(\kappa-1)/2}^{-1/2} dj \text{Tr}_{\hat{D}_j^+ \otimes \hat{D}_j^+} q^{L_0} q^{\bar{L}_0} + \sum_{\omega, n} \int_0^\infty dp 2\rho(p) \text{Tr}_{\hat{C}_{-\frac{1}{2}+ip} \otimes \hat{C}_{-\frac{1}{2}+ip}} q^{L_0} q^{\bar{L}_0} + \dots, \quad (3.35)$$

where the Hilbert space $\hat{D}_j^+ \otimes \hat{D}_j^+$ is the discrete representations of the $SL(2; \mathbb{R})$ with the constraints $J_0^3 - \bar{J}_0^3 = n$, $J_0^3 + \bar{J}_0^3 = \kappa\omega$ and no contribution from the $J_{n<0}^3$ oscillators. The same restriction is imposed on the continuous representations $\hat{C}_{-\frac{1}{2}+ip} \otimes \hat{C}_{-\frac{1}{2}+ip}$. The density of states for the continuous representations is given by

$$\rho(p) = \frac{1}{2\pi} 2 \log \epsilon + \frac{1}{2\pi i} \frac{\partial}{\partial p} \log \frac{\Gamma(-ip + \frac{1}{2} - m) \Gamma(-ip + \frac{1}{2} + \bar{m})}{\Gamma(+ip + \frac{1}{2} + \bar{m}) \Gamma(+ip + \frac{1}{2} - m)}, \quad (3.36)$$

where $m = \frac{1}{2}(n + \kappa\omega)$, $\bar{m} = -\frac{1}{2}(n - \kappa\omega)$ are the eigenvalues of J_0^3 and \bar{J}_0^3 . The density of states appearing here is consistent with the reflection amplitude (or sphere two-point function) of the two-dimensional black hole as we will review in section 3.2.3. The leading diverging part proportional to $\log \epsilon$ agrees with (3.32).

There are, however, several subtleties associated with the decomposition (3.35). First of all, the expression (3.35) is *not* modular invariant although our starting point (3.31) is formally invariant. The failure is due to the nontrivial p dependent density of states (3.36) and the contribution from the discrete series. In other words, the regularization rule for the character decomposition (3.35) does not preserve the modular invariance. The only one can say is that the leading part, (or the partition function per unit volume as $\epsilon \rightarrow 0$) is modular invariant (3.32). Another subtlety is related to the omitted terms in (3.35). The regularization procedure proposed in [74] (see also [78] for related models) actually leaves us with finite terms that could not be written as the character appearing in (3.35) [14]. Again this depends on the regularization scheme and one natural (but not unique) solution is to omit this part as we will implicitly assume in the following.

Despite all these subtleties, the decomposition (3.35) seems to capture important physics of the two-dimensional black hole. In particular, it predicts the existence of the discrete

spectrum localized near the tip of the cigar. Indeed the range of the discrete representations $\frac{-\kappa+1}{2} < j < -\frac{1}{2}$ will be independently checked by the Cardy analysis of the boundary states for $SL(2; \mathbb{R})/U(1)$ coset model as we will see in section 6.2.3. Also, the minisuperspace analysis for the two-dimensional black hole reproduces the zero-slope limit of the results given here including the density of states (3.36). We will review the mini-superspace analysis in section 3.2.3.

Before moving on to the mini-superspace analysis, we will briefly present a generalization to the supersymmetric $SL(2; \mathbb{R})/U(1)$ coset model. The partition function is given by

$$Z^{(NS)}(\tau) = \int_{\Sigma} \frac{du^2}{\tau_2} \frac{|\theta_3(\tau, u)|^2}{\sqrt{\tau_2} |\theta_1(\tau, u)|^2} \sqrt{\tau_2} |\eta(\tau)|^2 \sum_{m, \omega \in \mathbb{Z}} e^{-\frac{\pi k}{\tau_2} |\omega\tau - m + u|^2} \quad (3.37)$$

and the decomposition to the character is obtained as

$$\int_{-(k+1)/2}^{-1/2} dj \text{Tr}_{\hat{D}_j^+ \otimes \hat{D}_j^+} q^{L_0} q^{\bar{L}_0} + \sum_{\omega, n \in \mathbb{Z}} \int_0^{\infty} dp 2\rho(p) \text{Tr}_{\hat{C}_{-\frac{1}{2}+ip} \otimes \hat{C}_{-\frac{1}{2}+ip}} q^{L_0} q^{\bar{L}_0} + \dots, \quad (3.38)$$

In this case, the trace should be taken over the (NS-NS) Hilbert space of the supersymmetric coset instead of the bosonic one. Explicitly

$$\text{Tr}_{\hat{C}_{-\frac{1}{2}+ip} \otimes \hat{C}_{-\frac{1}{2}+ip}} q^{L_0} q^{\bar{L}_0} = q^{\frac{p^2+m^2}{k}} \bar{q}^{\frac{p^2+\bar{m}^2}{k}} \frac{|\theta_3(\tau)|^2}{|\eta(\tau)|^6}, \quad (3.39)$$

and

$$\begin{aligned} \int_{-(k+1)/2}^{-1/2} dj \text{Tr}_{\hat{D}_j^+ \otimes \hat{D}_j^+} q^{L_0} q^{\bar{L}_0} &= \sum_{\omega, n \in \mathbb{Z}} \sum_{j \in \mathcal{J}_{\omega, n}} \chi_{\text{dis}, 1+j+\frac{k}{2}, m+\frac{k}{2}}(\tau) \chi_{\text{dis}, 1+j+\frac{k}{2}, \bar{m}+\frac{k}{2}}(\bar{\tau}) \\ \mathcal{J}_{\omega, n} &= \left[-\frac{k+1}{2}, -\frac{1}{2} \right) \cap \left(\frac{k\omega - n}{2} + \mathbb{Z} \right) \\ \chi_{\text{dis}, j, j+n}(\tau) &= \frac{q^{\frac{(j+n)^2}{k} - \frac{1}{4k}} \theta_3(\tau, 0)}{1 + q^{n+1/2}} \frac{\theta_3(\tau, 0)}{\eta(\tau)^3}. \end{aligned} \quad (3.40)$$

The partition functions of the other sectors are readily obtained by performing the spectral flow symmetry of the $\mathcal{N} = 2$ SCA. We note that in order to obtain a superstring compactification with other sectors (such as $\mathcal{N} = 2$ minimal models), we have to project down to the sectors with integral $U(1)_R$ -charge so that the space-time supersymmetry is well-defined (GSO projection).

We can read some important physics from the spectrum of the Euclidean two-dimensional black hole:

- The continuous representations have a mass gap, which is consistent with the (asymptotic) linear dilaton background. Due to the mass gap, would-be graviton is massive, which is again consistent with the statement that the LST is non-gravitational theory.
- The discrete representations correspond to local dynamical degrees of freedom that has a winding quantum number being localized near the tip of the cigar. From the space-time point of view, they are normalizable deformation of the background localized in

the vicinity of the singularity. The improved unitarity bound perfectly agrees with the geometrical normalizability condition discussed in section 2.2.2.

The improved unitarity bound has an important application to obtain the normalizable deformations of the LST. As promised, we will derive the geometrical bound (2.34) from the improved unitarity bound of the $SL(2; \mathbb{R})/U(1)$ coset model. The dual string theory for the generalized conifold

$$z_1^n + z_2^2 + z_3^2 + z_4^2 = 0 \quad (3.41)$$

is given by the $(n-2)$ -th $\mathcal{N} = 2$ minimal model coupled with $SL(2; R)/U(1)$ coset with the level $k = \frac{2n}{n+2}$.

The vertex operators corresponding to massless deformations of the geometry can be obtained by combining (anti-)chiral primary operators of the $\mathcal{N} = 2$ minimal model and the $SL(2; \mathbb{R})/U(1)$ coset model restricted to $h = \bar{h} = \frac{1}{2}$. Labeling the chiral primaries of the minimal model by l ($0 \leq l \leq n-2$) with the $U(1)_R$ charge $Q_R = \frac{l}{n}$, we obtain the conformal condition:

$$\frac{l}{n} + \frac{2m}{k} = 1 . \quad (3.42)$$

On the other hand, the improved unitarity constraint is

$$1 \leq 2m \leq 1 + k , \quad (3.43)$$

which gives the constraint

$$l = 0, 1, \dots, \left[\frac{n-2}{2} \right] . \quad (3.44)$$

The bound is in perfect agreement with (2.34).

3.2.3 minisuperspace analysis

For a complementary method to read the spectrum of the sigma model is to use the point particle approximation known as the mini-superspace approximation.

Let us consider the Euclidean two-dimensional black hole background, known as ‘cigar geometry’:

$$ds^2 \equiv G_{ij} dx^i dx^j = 2k(d\rho^2 + \tanh^2 \rho d\theta^2) \quad \text{and} \quad e^\Phi = \frac{e^{\Phi_0}}{\cosh \rho} . \quad (3.45)$$

Recall that k sets characteristic curvature radius in unit of the string scale and hence string world-sheet effects, while e^{Φ_0} sets the maximum value of the string coupling at the tip $\rho = 0$ of the cigar geometry. We shall assume the limit $k \gg 1$ and $e^{-\Phi_0} \gg 1$: this limit suppresses both string world-sheet and space-time quantum effects and facilitates to truncate closed string spectrum to zero-modes, viz. to mini-superspace approximation.

In the mini-superspace approach, difference between bosonic strings (with no world-sheet supersymmetry) and fermionic strings (with $\mathcal{N} = 2$ world-sheet supersymmetry) becomes

unimportant. The closed string Hamiltonian $L_0 + \bar{L}_0$ is reduced in the mini-superspace approximation to the target space Laplacian Δ_0 , where:

$$\Delta_0 = \frac{1}{e^{-2\Phi}\sqrt{G}}\partial_i \left(e^{-2\Phi}\sqrt{G}G^{ij}\partial_j \right) \equiv -\frac{1}{2k}[\partial_\rho^2 + 2\coth 2\rho\partial_\rho + \coth^2 \rho\partial_\theta^2] . \quad (3.46)$$

The Hamiltonian is defined with respect to the volume element:

$$d\text{Vol} = e^{-2\Phi}\sqrt{G}d\rho d\theta := 2k \sinh \rho \cosh \rho d\rho d\theta \equiv k \sinh 2\rho d\rho d\theta , \quad (3.47)$$

inherited from the Haar measure on the $SL(2; \mathbb{R})$ group manifold. In the volume element, the dilaton factor $e^{-2\Phi}$ is taken into account, as the inner product for closed string states is defined by the world-sheet two-point correlators on the sphere. The normalized eigenfunctions are obtained straightforwardly [75, 79]. They are:

$$\begin{aligned} \phi_n^j(\rho, \theta) &= -\frac{\Gamma^2(-j + \frac{|n|}{2})}{\Gamma(|n| + 1)\Gamma(-2j - 1)}e^{in\theta} \times \\ &\times \left[\sinh^{|n|} \rho \cdot F\left(j + 1 + \frac{|n|}{2}, -j + \frac{|n|}{2}; |n| + 1; -\sinh^2 \rho\right) \right] , \end{aligned} \quad (3.48)$$

where $F(\alpha, \beta; \gamma; z)$ is the Gaussian hypergeometric function. These eigenfunctions correspond to the primary state vertex operators of conformal weights

$$h = \bar{h} = -\frac{j(j+1)}{k-2} + \frac{n^2}{4k} \quad \text{or} \quad h = \bar{h} = -\frac{j(j+1)}{k} + \frac{n^2}{4k} \quad (3.49)$$

for bosonic³³ and fermionic strings, respectively. We shall focus on the continuous series, parametrise the radial quantum number j as $j = -\frac{1}{2} + i\frac{p}{2}$ ($p \in \mathbb{R}$), and label the eigenfunctions as $\phi_n^p(\rho, \theta)$ instead of $\phi_n^j(\rho, \theta)$. We adopt the convention that, in the asymptotic region $\rho \sim \infty$, the vertex operators with $p > 0$ corresponds to the incoming waves and those with $p < 0$ corresponds to the outgoing waves. The eigenfunctions (3.48) are then normalized as

$$\left(\phi_n^p, \phi_{n'}^{p'} \right) = \delta_{n,n'} \left[2\pi\delta(p-p') + \mathcal{R}_0(p', n) 2\pi\delta(p+p') \right] , \quad (3.50)$$

where the inner product is defined with respect to the volume element (3.47). Here, $\mathcal{R}_0(p, n)$ refers to the reflection amplitude of the mini-superspace analysis:

$$\mathcal{R}_0(p, n) = \frac{\Gamma(+ip)\Gamma^2(\frac{1}{2} - \frac{ip}{2} + \frac{n}{2})}{\Gamma(-ip)\Gamma^2(\frac{1}{2} + \frac{ip}{2} + \frac{n}{2})} . \quad (3.51)$$

That is, from the definition (3.48), the reflection amplitude is seen to obey the mini-superspace reflection relation:

$$\phi_n^{-p}(\rho, \theta) = \mathcal{R}_0(-p, |n|) \phi_n^{+p}(\rho, \theta) . \quad (3.52)$$

³³The eigenvalue is actually proportional to $-\frac{j(j+1)}{k} + \frac{n^2}{4k}$. We will return to this small mismatch at the end of this subsection.

We shall refer $\mathcal{R}_0(p, n)$ as ‘mini-superspace’ reflection amplitude, valid strictly within mini-superspace approximation at $k \rightarrow \infty$, and anticipate string world-sheet effects at finite k . Notice that no winding states wrapping around θ -direction are present since by definition the mini-superspace approximation retains states with zero winding only.

Utilizing the analytic continuation formula of the hypergeometric functions:

$$F(\alpha, \beta; \gamma; z) = \frac{\Gamma(\gamma)\Gamma(\beta - \alpha)}{\Gamma(\beta)\Gamma(\gamma - \alpha)}(-z)^{-\alpha} F(\alpha, \alpha + 1 - \gamma; \alpha + 1 - \beta; 1/z) + \frac{\Gamma(\gamma)\Gamma(\alpha - \beta)}{\Gamma(\alpha)\Gamma(\gamma - \beta)}(-z)^{-\beta} F(\beta, \beta + 1 - \gamma; \beta + 1 - \alpha; 1/z), \quad (3.53)$$

the eigenfunction (3.48) can be decomposed into

$$\phi_n^p(\rho, \theta) = \phi_{L,n}^p(\rho, \theta) + \mathcal{R}_0(p, |n|)\phi_{R,n}^p(\rho, \theta), \quad (3.54)$$

where

$$\begin{aligned} \phi_{L,n}^p(\rho, \theta) &\equiv e^{in\theta}(\sinh \rho)^{-1-ip} F\left(\frac{1}{2} + \frac{ip+n}{2}, \frac{1}{2} + \frac{ip-n}{2}; 1+ip; -\frac{1}{\sinh^2 \rho}\right), \\ &\sim e^{-\rho} e^{-ip\rho+in\theta} \quad \text{at} \quad \rho \rightarrow +\infty \end{aligned} \quad (3.55)$$

and

$$\begin{aligned} \phi_{R,n}^p(\rho, \theta) &\equiv e^{in\theta}(\sinh \rho)^{-1+ip} F\left(\frac{1}{2} - \frac{ip+n}{2}, \frac{1}{2} - \frac{ip-n}{2}; 1-ip; -\frac{1}{\sinh^2 \rho}\right) \\ &\sim e^{-\rho} e^{ip\rho+in\theta} \quad \text{at} \quad \rho \rightarrow +\infty \end{aligned} \quad (3.56)$$

refer to the left- and the right-movers, respectively, at $\rho \rightarrow +\infty$, and $\mathcal{R}_0(p, |n|)$ is defined in (3.51). Obviously, they are related to each other under the reflection of radial momentum: $\phi_{R,n}^{+p} = \phi_{L,n}^{-p}$, which is also evident from (3.54) and (3.51). These mini-superspace wave functions (3.54) constitute the starting point of constructing boundary states of D-brane in the Euclidean two-dimensional black hole background.

We close the mini-superspace analysis with remarks concerning Wick rotation of the results to the Lorentzian background and string world-sheet effects present at finite k .

1. The decomposition of ϕ_n^p into $\phi_{L,n}^p$ and $\phi_{R,n}^p$ cannot globally defined over the entire cigar geometry. They are ill-defined around the tip $\rho = 0$, and the reflection relation (3.52) implies that ϕ_n^{-p} is not independent of ϕ_n^{+p} . Therefore, of the continuous series, only the eigenfunctions ϕ_n^p with $p > 0$, $n \in \mathbb{Z}$ span the physical Hilbert space of the closed strings on the Euclidean two-dimensional black hole. On the other hand, the situation will become further complicated once Wick rotated to the Lorentzian two-dimensional black hole.
2. Notice that ϕ_n^p is not analytic with respect to the angular quantum number n as it depends on its absolute value, $|n|$. This leads to the ambiguity for Wick rotation from Euclidean to Lorentzian background, under which roughly speaking in is replaced by energy ω . As for the mini-superspace reflection amplitude $\mathcal{R}_0(p, n)$, since $\mathcal{R}_0(p, -n) = \mathcal{R}_0(p, n)$ holds for all $n \in \mathbb{Z}$, it is unnecessary to take absolute value $|n|$ in (3.52), (3.54). When taking Wick rotation, we will start from the expression $\mathcal{R}_0(p, |n|)$. In other words, we analytically continue $\mathcal{R}_0(p, n)$ if $n > 0$ and $\mathcal{R}_0(p, -n)$ if $n < 0$.

3. It is evident that $|\mathcal{R}_0(p, n)| = 1$, viz, the mini-superspace reflection amplitude is purely a phase shift in the Euclidean black hole background. It is of utmost importance that, in the Lorentzian black hole background, n is analytically continued to pure imaginary value, and the modulus of the reflection amplitude becomes less than unity.
4. For the fermionic Euclidean $SL(2; \mathbb{R})/U(1)$ conformal field theory, exact result for the reflection amplitude (i.e. taking account of all string world-sheet effects) is known [80, 81, 82, 83]. In our notations, it is

$$\mathcal{R}(j, m, \bar{m}) = \nu(k)^{-2j-1} \frac{\Gamma(1 + \frac{2j+1}{k})}{\Gamma(1 - \frac{2j+1}{k})} \frac{\Gamma(2j+1)\Gamma(-j+m)\Gamma(-j-\bar{m})}{\Gamma(-2j-1)\Gamma(j+1+m)\Gamma(j+1-\bar{m})}, \quad (3.57)$$

where

$$\nu(k) \equiv \frac{1}{\pi} \frac{\Gamma(1 - \frac{1}{k})}{\Gamma(1 + \frac{1}{k})}, \quad m = \frac{k\omega + n}{2}, \quad \bar{m} = \frac{k\omega - n}{2}. \quad (3.58)$$

Denoting by $\Phi_{j,m,\bar{m}}$ the vertex operator with conformal weights $h = \frac{m^2 - j(j+1)}{k}$, $\bar{h} = \frac{\bar{m}^2 - j(j+1)}{k}$, the exact reflection relation reads

$$\Phi_{-(j+1);m,\bar{m}} = \mathcal{R}(-(j+1), m, \bar{m})\Phi_{j,m,\bar{m}}, \quad (3.59)$$

The mini-superspace reflection amplitude $\mathcal{R}_0(p, n)$ is then related to the exact one $\mathcal{R}(j, m, \bar{m})$ by taking the $k \rightarrow \infty$ limit as mentioned above (up to overall constant):

$$\mathcal{R}_0(p, n) = \lim_{k \rightarrow +\infty} \mathcal{R}(j = -\frac{1}{2} + \frac{ip}{2}, m = \frac{n}{2}, \bar{m} = -\frac{n}{2}). \quad (3.60)$$

Although the mini-superspace approximation can only describe the momentum mode of the full spectrum, it is possible to study the winding mode by using the T-duality even if we restrict ourselves to the mini-superspace approximation. In the remaining part of this subsection, we will study the mini-superspace spectrum for the T-dualized trumpet geometry (i.e. \mathbb{Z}_k orbifold of the vector coset $SL(2; \mathbb{R})^{(V)}/U(1)$). T-dualized classical geometry is given by the trumpet geometry

$$ds^2 = 2 \left(kd\rho^2 + \frac{d\tilde{\theta}^2}{k \tanh^2 \rho} \right), \quad e^\Phi = \frac{\mu}{\sinh \rho}. \quad (3.61)$$

Note that we have a curvature and dilaton singularity at $\rho = 0$. For later purposes, let us discuss the minisuperspace analysis for the bulk spectrum. The minisuperspace spectrum is determined by the eigenfunctions of the string Laplacian

$$\begin{aligned} \Delta &= -\frac{1}{e^{-2\Phi} \sqrt{\det G}} \partial_i e^{-2\Phi} \sqrt{\det G} G^{ij} \partial_j \\ &= -\frac{2}{k} \left[\partial_\rho^2 + (\coth \rho + \tanh \rho) \partial_\rho + k^2 \tanh^2 \rho \partial_{\tilde{\theta}}^2 \right] \end{aligned} \quad (3.62)$$

The (delta-function normalizable) eigenfunctions are given by

$$\begin{aligned} \phi_{p,w}(\rho, \tilde{\theta}) = & C_1 e^{iw\tilde{\theta}} (\cosh \rho)^{-1-ip} F\left(\frac{1}{2} - \frac{k w}{2} + \frac{i p}{2}, \frac{1}{2} + \frac{k w}{2} + \frac{i p}{2}; 1 + i p; \frac{1}{\cosh^2 \rho}\right) \\ & + C_2 e^{iw\tilde{\theta}} (\cosh \rho)^{-1+ip} F\left(\frac{1}{2} - \frac{k w}{2} - \frac{i p}{2}, \frac{1}{2} + \frac{k w}{2} - \frac{i p}{2}; 1 - i p; \frac{1}{\cosh^2 \rho}\right). \end{aligned} \quad (3.63)$$

It is not apriori clear which boundary condition one should impose because the trumpet geometry has a singularity at $\rho = 0$. Our natural guess would be to impose $\phi_{p,w}(\rho = 0, \tilde{\theta}) \equiv 0$. With our convenient normalization $C_1 = 1$, this boundary condition amounts to

$$C_2 = \mathcal{R}_0(p, \omega) = \frac{\Gamma(ip)\Gamma(\frac{1}{2} - \frac{ip}{2} + \frac{k w}{2})\Gamma(\frac{1}{2} - \frac{ip}{2} - \frac{k w}{2})}{\Gamma(-ip)\Gamma(\frac{1}{2} + \frac{ip}{2} + \frac{k w}{2})\Gamma(\frac{1}{2} + \frac{ip}{2} - \frac{k w}{2})}, \quad (3.64)$$

which is consistent with the semiclassical limit of the exact reflection amplitude that is descended from the $SL(2; \mathbb{R})$ WZNW model (or \mathbb{H}_3^+ model). Here we have used the formulae in the appendix A to evaluate the behavior of the hypergeometric function near the singularity.

Before we close our study of the mini-superspace Euclidean two-dimensional black hole system, we introduce the so-called ‘‘exact string background’’ for the bosonic two-dimensional black hole. As we have seen, for the bosonic string case, the spectrum shows $1/k$ corrections as

$$h = \bar{h} = -\frac{j(j+1)}{k-2} + \frac{n^2}{4k}, \quad (3.65)$$

compared with the mini-superspace results

$$h_0 = \bar{h}_0 = -\frac{j(j+1)}{k} + \frac{n^2}{4k}. \quad (3.66)$$

To cure this small mismatch, [75] introduced the following improved Laplacian

$$\Delta'_0 = -\frac{1}{k-2} \left(\frac{\partial^2}{4\partial\rho^2} + \coth 2\rho \frac{\partial}{2\partial\rho} + (\coth^2 \rho - \frac{2}{k}) \frac{\partial^2}{\partial\theta^2} \right), \quad (3.67)$$

to reproduce the exact $1/k$ corrected spectrum (3.65). The corresponding metric is

$$ds^2 = 2(k-2) \left(d\rho^2 + \frac{d\theta^2}{(\coth^2 \rho - \frac{k}{2})} \right) \quad (3.68)$$

with the dilaton

$$e^{2\Phi} = \mu \sinh 2\rho \sqrt{\coth^2 \rho - \frac{2}{k}}. \quad (3.69)$$

In the literature, it has been shown that this background is a solution of the bosonic string equation of motion in a particular renormalization scheme [58]. However, from the modern viewpoint, the reflection amplitude obtained from (3.67) is the same as the one from (3.46), and does not capture the nonperturbative $1/k$ corrections that appear in the exact result (3.57). We will study the origin of the non-perturbative corrections to the mini-superspace reflection amplitude in section 3.4.

3.3 Lorentzian spectrum

3.3.1 classical string in two-dimensional black hole

We would like to study the classical string solution in the two-dimensional black hole geometry. For this purposes, we can directly solve the string equation of motion (and Virasoro constraint) on the classical background, or we can study the gauged WZNW model before integrating out the gauge constraint [84].

If one takes the axial gauge $A = 0$ in the classical gauged WZNW action (3.7), the solution can be constructed as follows.³⁴ The classical solution of the parent WZNW model is written as

$$g(\sigma_+, \sigma_-) = g_L(\sigma_+)g_R(\sigma_-)^{-1} , \quad (3.70)$$

where we parametrize $g_L(\sigma_+), g_R(\sigma_-)^{-1} \in SL(2; \mathbb{R})$ as

$$g_L = \begin{pmatrix} a_L & u_L \\ -v_L & b_L \end{pmatrix} , \quad g_R^{-1} = \begin{pmatrix} b_R & -u_R \\ v_R & a_R \end{pmatrix} , \quad (3.71)$$

$$g = \begin{pmatrix} u_L v_R + a_L b_R & -a_L u_R + u_L a_R \\ b_L v_R - v_L b_R & v_L u_R + b_L a_R \end{pmatrix} , \quad (3.72)$$

with the determinant constraint $u_L v_L + a_L b_L = u_R v_R + a_R b_R = 1$.

Now the current constraint $J_2 = \bar{J}_2 = 0$ reduces to

$$\text{Tr}(\sigma_3 \partial_+ g_L g_L^{-1}) = v_L \partial_+ u_L + b_L \partial_+ a_L = -u_L \partial_+ v_L - a_L \partial_+ b_L = 0 , \quad (3.73)$$

and the Virasoro constraint becomes³⁵

$$(a_L \partial_+ u_L - u_L \partial_+ a_L)(b_L \partial_+ v_L - v_L \partial_+ b_L) = 0 . \quad (3.74)$$

The right moving part satisfies the similar equations.

Due to the determinant constraint, two equations in (3.73) are not independent, so we expect an appearance of one arbitrary function in the full solutions. Indeed, (3.73) and (3.74) suggests that either $\partial_+ u_L = \partial_+ a_L = 0$, or $\partial_+ v_L = \partial_+ b_L = 0$ should be satisfied. Then the general solutions can be expressed as

$$g_L = \begin{pmatrix} a_L & u_L \\ -v_L(\sigma^+) & \frac{1}{a_L} - \frac{u_L}{a_L} v_L(\sigma^+) \end{pmatrix} \text{ or } \begin{pmatrix} \frac{1}{b_L} - \frac{v_L}{b_L} u_L(\sigma^+) & u_L(\sigma^+) \\ -v_L & b_L \end{pmatrix} \\ g_R^{-1} = \begin{pmatrix} \frac{1}{a_R} - \frac{u_R}{a_R} v_R(\sigma^-) & -u_R \\ v_R(\sigma^-) & a_R \end{pmatrix} \text{ or } \begin{pmatrix} b_R & -u_L(\sigma^-) \\ v_R & \frac{1}{b_R} - \frac{v_R}{b_R} u_R(\sigma^-) \end{pmatrix} . \quad (3.75)$$

³⁴Since we are studying the Lorentzian target space, we use the Lorentzian signature world-sheet.

³⁵It is interesting to study general solutions of the coset CFT without imposing the Virasoro constraint. We will later come back to this point.

Combining the left moving part and the right moving part, we totally obtain four possible solutions:

$$\begin{aligned}
g_A(\sigma_+, \sigma_-) &= \begin{pmatrix} \frac{1}{b}(1 - u(\sigma^+)v(\sigma^-)) & u(\sigma^+) \\ -v(\sigma^-) & b \end{pmatrix} \\
g_B(\sigma_+, \sigma_-) &= \begin{pmatrix} a & \bar{u}(\sigma^-) \\ -\bar{v}(\sigma^+) & \frac{1}{a}(1 - \bar{u}(\sigma^-)\bar{v}(\sigma^+)) \end{pmatrix} \\
g_C(\sigma_+, \sigma_-) &= \begin{pmatrix} a(\sigma^-) & c_1 \\ \frac{1}{c_1}(-1 + a(\sigma^-)b(\sigma^+)) & b(\sigma^+) \end{pmatrix} \\
g_D(\sigma_+, \sigma_-) &= \begin{pmatrix} \bar{a}(\sigma^+) & \frac{1}{c_2}(1 - \bar{a}(\sigma^+)\bar{b}(\sigma^-)) \\ -c_2 & \bar{b}(\sigma^-) \end{pmatrix}, \tag{3.76}
\end{aligned}$$

where $u(\sigma^+), v(\sigma^-), \bar{u}(\sigma^-), \bar{v}(\sigma^+), a(\sigma^-), b(\sigma^+), \bar{a}(\sigma^+), \bar{b}(\sigma^-)$ are arbitrary real functions, and (b, a, c_1, c_2) are real integration constants. We can read off the gauge invariant motion of strings from u and v components:

$$\begin{aligned}
A : \quad & u = u(\sigma^+), & v &= v(\sigma^-) \\
B : \quad & u = \bar{u}(\sigma^-), & v &= \bar{v}(\sigma^+) \\
C : \quad & u = c_1, & v &= \frac{1}{c_1}(1 - a(\sigma^-)b(\sigma^+)) \\
D : \quad & u = \frac{1}{c_2}(1 - \bar{a}(\sigma^+)\bar{b}(\sigma^-)), & v &= c_2. \tag{3.77}
\end{aligned}$$

It is interesting to note that the solution A and B are actually solutions of the string equation of motion of any two-dimensional target space metric written in the conformal (Kruscal) coordinate: $ds^2 = f(u, v)dudv$.

We still have a gauge degree of freedom associated with the conformal transformation: $\sigma^+ \rightarrow f(\sigma^+)$ and $\sigma^- \rightarrow \bar{f}(\sigma^-)$. By using this gauge symmetry, we can *locally* gauge away the arbitrary functions in (3.77) to make them reduce to the point particle (collapsed) string solution. For example, in the solution A (similarly for B), we can expand

$$u = u_0 + p_u(\tau + \sigma) + \sum_{n \neq 0} \alpha_n e^{-in(\tau + \sigma)}. \tag{3.78}$$

As is the case with the flat space, we can gauge away the oscillatory part, and due to the periodicity of σ for closed strings, we have to set $p_u = 0$ unless the target space has a periodic directions. In the solution C (similarly for D), we can locally set $v = v(\tau)$ independent of σ by using the conformal transformation. The resultant string motion is nothing but the geodesics for the massless point particle in the two-dimensional black hole.

Thus the classical solution of the string equation collapses to a massless point particle in the two-dimensional black hole background, and it seems to be consistent with the vertex operator analysis, where the only tachyon fields are dynamical classically. However, if one allows a folded string solution, we can construct more general string solutions as we will review in the following section 3.3.2. This can be done by patching different solutions of (3.77) within the same world-sheet.

3.3.2 folded strings

For an illustrative purpose, let us begin with the folded string solution [85, 86] in two-dimensional flat space (T, X) . We can fix the world-sheet conformal invariance by choosing the gauge $\tau = T$.³⁶ The classical equation of motion is given by $\partial_+ \partial_- X = 0$ with the Virasoro constraint³⁷

$$-2 + (\partial_+ X)^2 = 0, \quad -2 + (\partial_- X)^2 = 0, \quad (3.79)$$

which amounts to $\partial_+ X = \pm\sqrt{2}$. If we restrict ourselves to the solutions with continuous first derivative, they reduce to massless particles. To obtain the folded string solution, we can set $X = X_+(\sigma^+) + X_-(\sigma^-)$, where X_+ and X_- are periodic functions with the same period and with derivatives $\pm\sqrt{2}$. In other words, we partition the world-sheet and assign different solutions that satisfy $\partial_+ X = \pm\sqrt{2}$ and patch-work together so that the full solution is periodic in σ direction. A simple solution with the static center of motion is given by

$$X = \sqrt{2}(|\sigma^+|_{\text{per}} + |\sigma^-|_{\text{per}}), \quad (3.80)$$

where the periodic absolute value function $|\sigma^+|_{\text{per}}$ is given by $|\sigma^+|_{\text{per}} = |\sigma^+|$ for $-\pi < \sigma^+ \leq \pi$ and periodically extended outside this interval. More complicated solutions are possible, and one simple way to obtain them is to perform the target space Lorentz boost to the solution (3.80). The resultant string solutions describes the folded string with the motion of the center of mass. Note that the Lorentz boost breaks our original gauge choice.

Next, we will consider the linear dilaton background $\Phi = QX$. The equation of motion does not change, but the Virasoro constraint is modified as

$$-2 + (\partial_+ X)^2 - Q\partial_+^2 X = 0, \quad -2 + (\partial_- X)^2 - Q\partial_-^2 X = 0. \quad (3.81)$$

The point is that due to the existence of the second derivatives in the Virasoro constraint, the solutions such as (3.80) are no more allowed. The most general solutions are given by

$$X = X_0 - Q \log \left(\cosh \frac{\sqrt{2}\tau}{Q} + \cosh \frac{\sqrt{2}\sigma}{Q} \right). \quad (3.82)$$

Except for the special limit where the string collapse to a point particle, the solution is not periodic in σ direction. Thus only the long string stretched to the infinity is the allowed folded string solution. This agrees with the fact that there are no closed string states in the linear dilaton theory other than the massless tachyon. The inclusion of the Liouville potential does not alter the qualitative feature of the classical string solutions.

Let us now move on to the folded string solutions in the two-dimensional black hole. First, we partition the string world-sheet as in figure 4. We know that the solution should be

³⁶This static gauge choice is not always possible especially in the curved space-time background.

³⁷If one embeds the two-dimensional Minkowski space in higher dimensional space-time, the Virasoro constraint can be relaxed. For instance, if one introduces a contribution from the other zero modes than (T, X) the resultant two-dimensional motion becomes massive rather than massless.

locally given by (3.77). We fix the world-sheet conformal invariance by giving the boundary condition:

$$\begin{aligned} A : & \quad u = u_0 + p^+ \sigma_{\text{per}}^+ , & \quad v = v_0 + p^- \sigma_{\text{per}}^- , \\ B : & \quad u = u_0 + p^+ \sigma_{\text{per}}^- , & \quad v = v_0 + p^- \sigma_{\text{per}}^+ , \end{aligned} \quad (3.83)$$

where $\sigma_{\text{per}}^+ = \sigma^+ - m\pi$ for $\frac{\pi}{2} \leq \sigma^+ < \frac{3\pi}{2}$ and periodically identified outside this range. If we had considered a flat Minkowski space $ds^2 = dudv$, the solution in the region C and D would be independent of σ :

$$\begin{aligned} C_{\text{flat}} : & \quad u = u_0 + \frac{\pi p^+}{2} , & \quad v = v_0 + \frac{\pi p^-}{2} + p^- (\sigma_{\text{per}}^+ + \sigma_{\text{per}}^-) \\ D_{\text{flat}} : & \quad u = u_0 + \frac{\pi p^+}{2} + p^+ (\sigma_{\text{per}}^- + \sigma_{\text{per}}^-) , & \quad v = v_0 + \frac{\pi p^-}{2} . \end{aligned} \quad (3.84)$$

so that we have a fold as in (3.80). In the two-dimensional black-hole case, the solution in C and D region is given by

$$\begin{aligned} C_{2\text{DBH}} : & \quad u = u_0 + \frac{\pi p^+}{2} , \\ & \quad v = \frac{1}{u_0 + \frac{\pi p^+}{2}} \left(1 - \frac{[1 - (u_0 + \frac{\pi p^+}{2})(v_0 + p^- \sigma_{\text{per}}^+)] \times [1 - (u_0 + \frac{\pi p^+}{2})(v_0 + p^- \sigma_{\text{per}}^-)]}{[1 - (u_0 + \frac{\pi p^+}{2})(v_0 - \frac{\pi p^-}{2})]} \right) , \\ D_{2\text{DBH}} : & \quad u = \frac{1}{v_0 + \frac{\pi p^-}{2}} \left(1 - \frac{[1 - (v_0 + \frac{\pi p^-}{2})(u_0 + p^+ \sigma_{\text{per}}^+)] \times [1 - (v_0 + \frac{\pi p^-}{2})(u_0 + p^+ \sigma_{\text{per}}^-)]}{[1 - (v_0 + \frac{\pi p^-}{2})(u_0 - \frac{\pi p^+}{2})]} \right) \\ & \quad v = v_0 + \frac{\pi p^-}{2} . \end{aligned} \quad (3.85)$$

We could continue this analysis, but important point is that in the region A' and B' the solution turns out to be linear in σ^+ and σ^- again just as in (3.83). Thus the structure repeats itself and the simple recursion formula to derive the full solution exists (see [84]). Physically, the pulsating string falls into the black-hole as a massive particle. The folds move with the speed of light because u or v is constant.

The folded string solution in the two-dimensional Liouville background was identified as the *open string* attached to the FZZT brane [87, 88] in a certain limit [86]. The scattering amplitude computed from the CFT analysis completely matches with the matrix model computation in the non-singlet sector [89, 90]. In this sense, it makes sense to regard the non-singlet sector (or winding sector) in the matrix model corresponds to the folded string solution in the Lorentzian target space theory in the Liouville background.

Therefore, one might expect that the folded string solution in the two-dimensional black hole background should play an important role in constructing the dual matrix model for the two-dimensional black hole with the Lorentzian target space signature. At present, we do not have a conclusive argument for or against this direction, but we present some remarks here:

- It is important to note that the folded string solution in the Liouville background is in the open string sector and not in the closed string sector. This should be contrasted with the winding sector in the Euclidean two-dimensional black hole (and its hypothetical analytic continuation to the Lorentzian signature black hole).

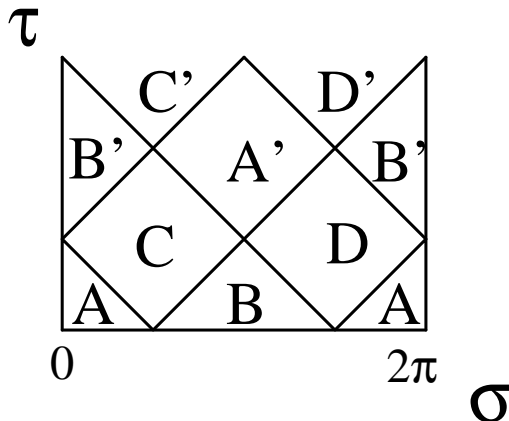


Figure 4: In order to obtain folded string solution, we partition the world-sheet and assign different solutions on each patch.

- To obtain the long stretched string solution, the existence of the linear dilaton in the Virasoro constraint has been crucial. In our semiclassical analysis for the two-dimensional black hole, the existence of the nontrivial dilaton was neglected. This is the reason why we obtained a folded string solution that is asymptotically identical to the flat space solution (3.80). Since in the linear dilaton case, such a solution was excluded, we might expect that only the long string solution would survive in the full quantization.³⁸
- In order to have a support for such long string solutions, we need a D-brane localized at asymptotic infinity. However, the two-dimensional Lorentzian black hole does *not* admit such a D-brane solution from the classical DBI action analysis (see section 7.1).

We leave the role of the folded strings in the full quantization of the Lorentzian two-dimensional black hole system for future studies. In most of the following sections, we will concentrate on the mini-superspace approximation (point-particle approximation).

Before closing our discussion on the classical string solutions in the two-dimensional black hole, we would like to present the most general solutions of the classical sigma model without imposing the Virasoro constraint for completeness [91]. First we introduce arbitrary three-component vectors lying on the hyperboloids

$$\begin{aligned}\vec{A} \cdot \vec{A} &= -(A_0)^2 + (A_1)^2 + (A_2)^2 = 1 \\ \vec{B} \cdot \vec{B} &= -(B_0)^2 + (B_1)^2 + (B_2)^2 = 1 .\end{aligned}\tag{3.86}$$

³⁸Just adding the dilaton term in the classical energy-momentum tensor is not consistent in the classical treatment because the one-loop correction to the equation of motion together with the classical contribution from the dilaton guarantee the one-loop holomorphic structure of the energy-momentum tensor.

Then the most general solutions of the sigma model (in the Schwarzschild-like coordinate) are given by

$$\begin{aligned}\cosh^2 \rho(\sigma, \tau) &= \frac{1}{2} \left(1 + \vec{A}(\sigma^+) \cdot \vec{B}(\sigma^-) \right) \\ t(\sigma, \tau) &= \frac{1}{2} \int_a^{\sigma^+} \left(\frac{\epsilon_{abc} A'_a A_b B_c}{\vec{A} \cdot \vec{B} - 1} \right) (x_+, b) dx_+ \\ &\quad - \frac{1}{2} \int_b^{\sigma^-} \left(\frac{\epsilon_{abc} B'_a A_b B_c}{\vec{A} \cdot \vec{B} - 1} \right) (\sigma_+, x_-) dx_- + c\end{aligned}\tag{3.87}$$

The energy momentum tensor takes the form

$$T_{++} = -\frac{A'(\sigma^+)^2}{8}, \quad T_{--} = -\frac{B'(\sigma^-)^2}{8}.\tag{3.88}$$

If one imposes the Virasoro constraint, the solutions reduce to (3.77).

3.3.3 spectrum from partition function?

The partition function for the Lorentzian two-dimensional black hole should be able to determine its spectrum in principle. However, in practice the subtleties associated with the non-compactness of the target space and the Lorentzian signature make the partition function ill-defined and prevent us from reading the spectrum.

At the classical level, the Lorentzian two-dimensional black hole is obtained by the Wick rotation $\theta \rightarrow it$ in the cigar geometry. The vertex operator (corresponding to the massive character) should be Wick rotated as well

$$\begin{aligned}\Delta(j, m = -\bar{m} = \frac{n}{2}) &= -\frac{j(j+1)}{k-2} + \frac{n^2}{4k} \\ \rightarrow \Delta(j, \omega) &= -\frac{j(j+1)}{k-2} - \frac{\omega^2}{4k}\end{aligned}\tag{3.89}$$

based on the naive Wick rotation $n \rightarrow i\omega$. Since the time-direction t is non-compact, ω should be continuous unlike the Euclidean two-dimensional black hole case, where n is quantized. For the same reason, the Lorentzian black hole does not have a winding states along the t direction.³⁹ From the mini-superspace analysis we will review in 3.3.4, the classical spectrum is obtained from this naive analytic continuation (with some care about the boundary conditions).

We would like to make an attempt to read the spectrum from the Lorentzian partition function with some hindsight from the mini-superspace analysis. The proposed partition function (with a suitable analytic continuation) for the Lorentzian $SL(2; \mathbb{R})/U(1)$ coset is

$$Z_{SL(2; \mathbb{R})/U(1)} = \int_{\mathbb{R}^2} \frac{dv^2}{\tau_2} \frac{e^{\frac{v_1^2}{\tau_2} - \frac{\pi k}{\tau_2} |v|^2}}{\sqrt{\tau_2} |\theta_1(\tau, iv)|^2} \sqrt{\tau_2} |\eta(\tau)|^2.\tag{3.90}$$

³⁹Since the discrete states that descend from the $SL(2; \mathbb{R})$ primaries have a winding quantum number in the Euclidean black hole, the corresponding states do not seem to exist in the Lorentzian black hole, but this is a controversial issue.

Here we study the bosonic case first for simplicity. Since we are integrating over the whole complex plane spanned by v , this partition function is formally same as that for the Euclidean axial coset (3.31). The conclusion that the spectrum of the Euclidean coset and the Lorentzian coset, nevertheless, has the same spectrum seems too quick given the fact that the mini-superspace approximation gives a totally different answer.

In the Euclidean case, the divergence near $iv = u = n + \omega\tau$ gives a bulk contribution of the noncompact boson (with a linear dilaton) coupled to a compact boson with radius $R^2 = k$, where the summation over n and ω shows the existence of the compact direction. In the Lorentzian case, we propose that the the torus modulus τ should be Lorentzian, namely τ and $\bar{\tau}$ and real and mutually independent.

On the Lorentzian torus, the divergence of the partition function (3.90) only appears at $v = 0$, leading to the contribution of the noncompact boson (with a linear dilaton) coupled to a non-compact boson:⁴⁰

$$Z \sim \log \epsilon Z_{free}^2 + \text{finite terms} . \quad (3.91)$$

The leading order partition function seems to agree with the mini-superspace analysis.⁴¹

More precise discussions are needed to determine the finite part of the partition function. The situation is more involved than in the Euclidean case, and so far no conclusive agreements are available. One interesting related question is how the target-space supersymmetry is broken in the (world-sheet supersymmetric) Lorentzian two-dimensional black hole background. If we restrict ourselves to the leading order partition function, we can certainly define a GSO projection, and the partition function (at the leading order) vanishes because asymptotically the theory is essentially free and the spectrum coincides with the supersymmetric linear dilaton theory, and the target-space supersymmetry operator can be constructed. Therefore, the target-space supersymmetry should be broken near the horizon, where the curvature effects will be present.

To study this problem, let us consider the type II GSO projected partition function for the two-dimensional Lorentzian black hole (coupled to free transverse sectors that is represented by free CFTs for simplicity). Our original partition function for the Lorentzian $SL(2; \mathbb{R})/U(1)$ Kazama-Suzuki coset is the diagonal modular invariant one:

$$Z^{(NS)}(\tau) = \int_{\mathbb{R}^2} \frac{dv^2}{\tau_2} \frac{|\theta_3(\tau, iv)|^2}{\sqrt{\tau_2} |\theta_1(\tau, iv)|^2} \sqrt{\tau_2} |\eta(\tau)|^2 e^{-\frac{\pi k}{\tau_2} |v|^2} \quad (3.92)$$

for NS-NS sectors (other sectors can be obtain by replacing $\theta_3(\tau, u)$ with $\theta_a(\tau, u)$ ($a = 0, 1, 2$) from the spectral flow). A natural candidate for the type II partition function is

$$Z(\tau) = \int_{\mathbb{R}^2} \frac{dv^2}{\tau_2} \frac{|\theta_3(\tau, iv)\theta_3^3 - \theta_2(\tau, iv)\theta_2^3 \pm \theta_1(\tau, iv)\theta_1^3 - \theta_0(\tau, iv)\theta_0^3|^2}{\sqrt{\tau_2} |\theta_1(\tau, iv)|^2} \sqrt{\tau_2} |\eta(\tau)|^{-14} e^{-\frac{\pi k}{\tau_2} |v|^2} , \quad (3.93)$$

⁴⁰On the Lorentzian torus, the Euclidean coset partition function still has an infinitely many origin of divergence at $u = n + \omega\tau$, which gives a compact boson.

⁴¹One should note that the partition function on the Lorentzian torus needs a careful $i\epsilon$ prescription. This is an interesting but subtle subject, and we will not delve into the details here.

where $\theta_a^3 = \theta_a(\tau, 0)^3$ have been introduced from the free CFT contributions. The expression is almost supersymmetric: for example, if we first take the leading diverging part at $v = 0$, then the fermionic oscillator part gives zero after summing over the spin structure due to the abstruse identity of Jacobi.

A remaining uncancelled part, which describes the breaking of the target-space supersymmetry, is of particular interest. By using the Riemann quartic identity (A.5), we can rewrite (3.93) as

$$Z(\tau) = \int_{\mathbb{R}^2} \frac{dv^2}{\tau_2} \frac{|\theta_1(\tau, i\frac{v}{2})|^8}{\sqrt{\tau_2} |\theta_1(\tau, iv)|^2} \sqrt{\tau_2} |\eta(\tau)|^{-14} e^{-\frac{\pi k}{\tau_2} |v|^2} . \quad (3.94)$$

Now one can see that the leading order divergence near the origin ($v = 0$) is indeed removed, which suggests that the bulk part of the spectrum is supersymmetric.⁴²

It is still difficult to evaluate (3.3.3) to uncover the non-supersymmetric spectrum of the two-dimensional Lorentzian black hole partially because the formal q expansion of (3.3.3) gives a divergent series. Let us suppose that the major part of the v integral comes near the origin $v = 0$ since in the large k limit, the Gaussian factor would provide a strong convergence factor for the integral (with no good justification because of the oscillatory nature of the θ functions on the Lorentzian torus). The subsequent integration over v would lead to

$$Z(\tau) \sim |\eta(\tau)|^4 . \quad (3.95)$$

The partition function looks like a free 0-dimensional bosonic string (probably localized near the horizon). The support of the (non-supersymmetric) bosonic degrees of freedom should be localized because we do not have a diverging volume factor.

It seems likely that the supersymmetry is broken only locally in the vicinity of the horizon. One naively guess that this should correspond to the Lorentzian version of the winding condensation near the tip of the cigar in the Euclidean two-dimensional black hole as we will see in section 3.4. A further study of this subject is of great interest and the more precise definition of the (almost) supersymmetric partition function and its evaluation is highly desirable.

3.3.4 minisuperspace approximation

Since it is difficult to read the spectrum of the Lorentzian two-dimensional black hole directly from the partition function, it is very important to study the classical spectrum based on the mini-superspace approximation. The Wick rotation of the mini-superspace eigenfunctions in the Euclidean cigar geometry (3.48) is not so trivial. Fortunately, the Lorentzian eigenfunctions are already classified thoroughly in [75]. The complete basis for waves outside the black hole horizon are spanned by the following four types of eigenfunctions⁴³ of the Lorentzian

⁴²Unfortunately, for complex τ , the partition function still shows a volume divergence at $iv = n + \omega\tau$ with a pair of *odd* integers (n, ω) , where the GSO projection acts *oppositely*. We do not fully understand the origin of this failure of bulk cancellation. Since these divergences seem unphysical in the Lorentzian partition function if we stick to the Lorentzian torus, we do not see their physical relevance.

⁴³Here we adopt slightly different normalization from [75].

Klein-Gordon operator. For those with the eigenvalue $\frac{p^2}{4k} - \frac{\omega^2}{4k} + \frac{1}{4k}$ of the Klein-Gordon operator, the four eigenfunctions are

$$U_\omega^p(\rho, t) = -\frac{\Gamma^2(\nu_+)}{\Gamma(1-i\omega)\Gamma(-ip)} e^{-i\omega t} (\sinh \rho)^{-i\omega} F(\nu_+, \nu_-^*; 1-i\omega; -\sinh^2 \rho) \\ \sim e^{-i\omega t - i\omega \ln \rho} \quad \text{as } \rho \rightarrow 0, \quad (3.96)$$

$$V_\omega^p(\rho, t) = -\frac{\Gamma^2(\nu_+^*)}{\Gamma(1+i\omega)\Gamma(ip)} e^{-i\omega t} (\sinh \rho)^{i\omega} F(\nu_+^*, \nu_-; 1+i\omega; -\sinh^2 \rho) \\ \sim e^{-i\omega t + i\omega \ln \rho} \quad \text{as } \rho \rightarrow 0, \quad (3.97)$$

$$L_\omega^p(\rho, t) = e^{-i\omega t} (\sinh \rho)^{-1-ip} F(\nu_+^*, \nu_-^*; 1+ip; -\frac{1}{\sinh^2 \rho}) \\ \sim e^{-\rho} e^{-ip\rho - i\omega t} \quad \text{as } \rho \rightarrow \infty, \quad (3.98)$$

$$R_\omega^p(\rho, t) = e^{-i\omega t} (\sinh \rho)^{-1+ip} F(\nu_+, \nu_-; 1-ip; -\frac{1}{\sinh^2 \rho}) \\ \sim e^{-\rho} e^{+ip\rho - i\omega t} \quad \text{as } \rho \rightarrow \infty \quad (3.99)$$

with the notations

$$\nu_\pm = \frac{1}{2} - i \left(\frac{p}{2} \pm \frac{\omega}{2} \right).$$

These eigenfunctions are defined by the following analytic continuations of the mini-superspace Euclidean eigenfunctions:

$$U_\omega^p(\rho, t) = \begin{cases} \phi_{n=+i\omega}^p(\rho, \theta = +it) & (\omega > 0, n < 0) \\ \phi_{n=-i\omega}^p(\rho, \theta = -it) & (\omega < 0, n > 0) \end{cases} \\ V_\omega^p(\rho, t) = \begin{cases} \phi_{n=-i\omega}^{-p}(\rho, \theta = -it) & (\omega > 0, n < 0) \\ \phi_{n=+i\omega}^{-p}(\rho, \theta = +it) & (\omega < 0, n > 0) \end{cases} \\ L_\omega^p(\rho, t) = \phi_{L, n=i\omega}^p(\rho, \theta = +it) \\ R_\omega^p(\rho, t) = \phi_{R, n=i\omega}^p(\rho, \theta = +it), \quad (3.100)$$

where the $n < 0$ and $n > 0$ ranges are mapped to $\omega > 0$ and $\omega < 0$, respectively.

As discussed in [75], only two out of the four eigenfunctions are linearly independent. In particular,

$$V_\omega^p(\rho, t) = U_\omega^{p*}(\rho, -t) \quad \text{and} \quad R_\omega^p(\rho, t) = L_\omega^{p*}(\rho, -t).$$

The reason why we introduce the above four eigenfunctions is because they encode four possible boundary conditions (We here assume $p > 0$) in the Lorentzian black hole background. Recall that, for the region outside the horizon of the eternal black hole, the boundaries consist of four segments: ‘future (past) horizon’ $t = +\infty, \rho = 0$ ($t = -\infty, \rho = 0$) by \mathcal{H}^+ (\mathcal{H}^-), and the ‘future (past) infinity’ $t = +\infty, \rho = +\infty$ ($t = -\infty, \rho = +\infty$) by \mathcal{I}^+ (\mathcal{I}^-). The four eigenfunctions U, V, L, R are the ones obeying boundary conditions:

$$U_\omega^p = 0 \text{ at } \mathcal{H}^-, \quad V_\omega^p = 0 \text{ at } \mathcal{H}^+, \\ L_\omega^p = 0 \text{ (} R_\omega^p = 0 \text{) at } \mathcal{I}^+, \quad R_\omega^p = 0 \text{ (} L_\omega^p = 0 \text{) at } \mathcal{I}^- \quad (3.101)$$

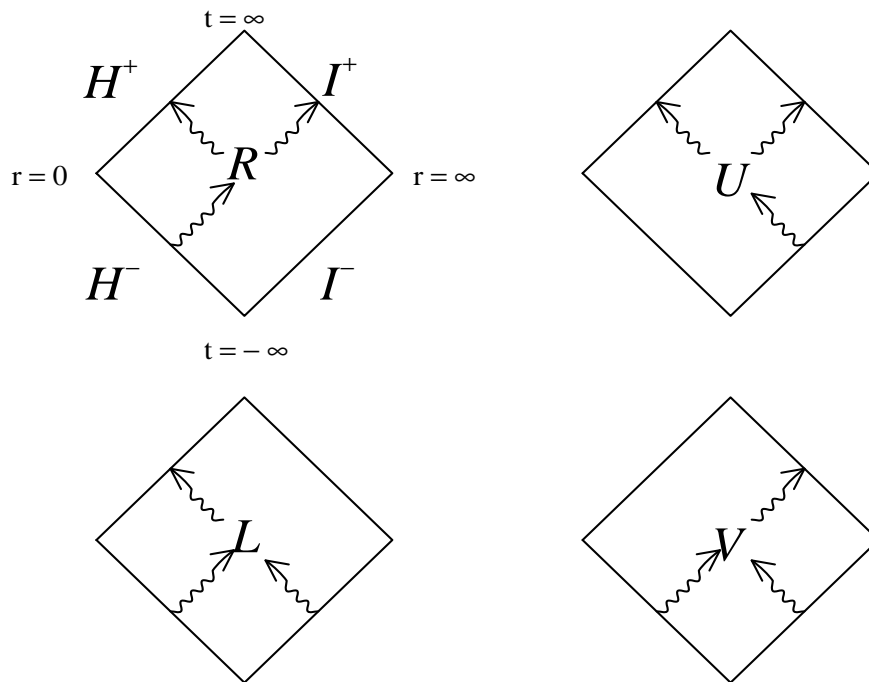


Figure 5: The boundary conditions of the Lorentzian eigenfunctions ($\omega > 0$ sector). For $\omega < 0$, the figures for L and R should be interchanged.

for $\omega > 0$ ($\omega < 0$). See Figure 5.

By Wick rotating the mini-superspace reflection relations (3.52), we obtain linear relations among the Lorentzian eigenfunctions:

$$U_\omega^p = L_\omega^p + \mathcal{R}_0(p, \omega)R_\omega^p \quad \text{and} \quad V_\omega^p = R_\omega^p + \mathcal{R}_0^*(p, \omega)L_\omega^p . \quad (3.102)$$

Equivalently,

$$\begin{aligned} L_\omega^p &= \frac{1}{1 - |\mathcal{R}_0(p, \omega)|^2} \{U_\omega^p - \mathcal{R}_0(p, \omega)V_\omega^p\} \\ \text{and} \quad R_\omega^p &= \frac{1}{1 - |\mathcal{R}_0(p, \omega)|^2} \{V_\omega^p - \mathcal{R}_0^*(p, \omega)U_\omega^p\} . \end{aligned} \quad (3.103)$$

Here, the mini-superspace reflection amplitude $\mathcal{R}_0(p, \omega)$ in Lorentzian theory is given by

$$\mathcal{R}_0(p, \omega) = \frac{\Gamma(+ip)\Gamma^2(\nu_+)}{\Gamma(-ip)\Gamma^2(\nu_-^*)} \equiv -\frac{B(\nu_+, \nu_-)}{B(\nu_+^*, \nu_-^*)} \cdot \frac{\cosh \pi \left(\frac{p-\omega}{2}\right)}{\cosh \pi \left(\frac{p+\omega}{2}\right)} . \quad (3.104)$$

Notice that, in sharp contrast to the Euclidean black hole, the reflection amplitude is less than unity due to the second factor:

$$|\mathcal{R}_0(p, \omega)|^2 = \frac{\cosh^2 \pi \left(\frac{p-\omega}{2}\right)}{\cosh^2 \pi \left(\frac{p+\omega}{2}\right)} \leq 1 . \quad (3.105)$$

The inequality is saturated at $p = \omega = 0$. The inequality (3.105) shall play a prominent role for understanding string dynamics in the Lorentzian black hole background. The mini-superspace reflection relations for U_ω^p, V_ω^p are also expressible in a form similar to the Euclidean ones. Recalling that $\mathcal{R}_0(-p, \omega)\mathcal{R}_0(+p, \omega) = 1$,

$$U_\omega^{-p}(\rho, t) = \mathcal{R}_0(-p, \omega)U_\omega^p(\rho, t) \quad \text{and} \quad V_\omega^{-p}(\rho, t) = \mathcal{R}_0^*(-p, \omega)V_\omega^p(\rho, t) , \quad (3.106)$$

while L_ω^p and R_ω^p are simply related by reflection:

$$L_\omega^{-p}(\rho, t) = R_\omega^{+p}(\rho, t) . \quad (3.107)$$

Moreover, U_ω^p and V_ω^p are linearly independent except for the special kinematic regime, $\omega = 0$. Notice also, in the relation (3.105), the reflection amplitude involves the mini-superspace contribution only, not the full-fledged stringy one.

Before proceeding further, we shall here collect explicitly relations among inner products of Lorentzian primary fields, where the inner product is defined with respect to the Lorentzian measure $dv_L = k \sinh 2\rho d\rho dt$. Taking quantum numbers p, ω fixed and dropping off delta function factors $2\pi\delta(p - p'), 2\pi\delta(\omega - \omega')$ for notational simplicity, we have

$$\begin{aligned} (U_\omega^p, U_\omega^p) &= (V_\omega^p, V_\omega^p) = N_0(p, \omega) , & N_0(p, \omega) &\equiv \frac{1 + |\mathcal{R}_0(p, \omega)|^2}{2} \\ (U_\omega^p, V_\omega^p) &= \mathcal{R}_0^*(p, \omega) , \\ (L_\omega^p, L_\omega^p) &= (R_\omega^p, R_\omega^p) = \frac{1}{2} , & (L_\omega^p, R_\omega^p) &= 0 , \\ (U_\omega^p, L_\omega^p) &= (V_\omega^p, R_\omega^p) = \frac{1}{2} , & (R_\omega^p, U_\omega^p) &= (V_\omega^p, L_\omega^p) = \frac{\mathcal{R}_0(p, \omega)}{2} . \end{aligned} \quad (3.108)$$

The inner products involving L_ω^p and R_ω^p are readily evaluated since dominant contributions are supported in the asymptotic region $\rho \gg 0$, yielding the volume factor $2\pi\delta(0)$. The remaining inner products can be extracted from the linear relations (3.102), (3.103).⁴⁴ We also fixed the overall normalization factors from consistency with the Euclidean inner product (3.50) under the $\omega \rightarrow 0$ limit. Notice also that

$$N_0(-p, \omega) = |\mathcal{R}_0(-p, \omega)|^2 N_0(+p, \omega) , \quad (3.109)$$

as is consistent with the mini-superspace reflection relation (3.106).

It is easy to construct the exact string vertex operators or primary states corresponding to the mini-superspace eigenfunctions U, V, L, R . To be specific, we shall consider primarily the fermionic $SL_k(2, \mathbb{R})/U(1)$ supercoset conformal field theory.⁴⁵ The primary states $|U_\omega^p\rangle, |V_\omega^p\rangle$ are the ones of conformal weights $h = \bar{h} = \frac{p^2}{4k} - \frac{\omega^2}{4k} + \frac{1}{4k}$ and obey the exact reflection relations

$$|U_\omega^{-p}\rangle = \mathcal{R}(-p, \omega)|U_\omega^p\rangle , \quad |V_\omega^{-p}\rangle = \mathcal{R}^*(-p, \omega)|V_\omega^p\rangle , \quad (3.110)$$

and the exact reflection amplitude is given by

$$\mathcal{R}(p, \omega) \equiv \mathcal{R}_0(p, \omega) \frac{\Gamma\left(1 + \frac{ip}{k}\right)}{\Gamma\left(1 - \frac{ip}{k}\right)} . \quad (3.111)$$

Notice that the string world-sheet effect entering through the $1/k$ -correction is a pure phase. Thus, the exact reflection probability $|\mathcal{R}(p, \omega)|^2$ remains unmodified from the mini-superspace approximation result $|\mathcal{R}_0(p, \omega)|^2$ given in (3.105). We shall normalize the primary states $|U_\omega^p\rangle, |V_\omega^p\rangle$ ($p > 0$) as

$$\begin{aligned} \langle U_\omega^p | U_{\omega'}^{p'} \rangle &= \langle V_\omega^p | V_{\omega'}^{p'} \rangle = N(p, \omega) 2\pi\delta(p - p') 2\pi\delta(\omega - \omega') , \\ \langle V_\omega^p | U_{\omega'}^{p'} \rangle &= \mathcal{R}^*(p, \omega) 2\pi\delta(p - p') 2\pi\delta(\omega - \omega') , \end{aligned} \quad (3.112)$$

where the new normalization factor $N(p, \omega)$ is simply defined by replacing \mathcal{R}_0 with \mathcal{R} in $N_0(p, \omega)$. The primary states $|L_\omega^p\rangle, |R_\omega^p\rangle$ are also definable by using the linear relations (3.102) or (3.103) but now with \mathcal{R}_0 replaced by \mathcal{R} . Notice that $|U_\omega^p\rangle, |V_\omega^p\rangle$ are the ones analytically continuable to the Euclidean primary states $|\phi_n^{\pm p}\rangle$, so often referred as the ‘Hartle-Hawking vacua’. On the other hand, the states $|L_\omega^p\rangle, |R_\omega^p\rangle$ does not have Euclidean counterparts. Recall that, over the Euclidean black hole background, $\phi_{L,n}^p, \phi_{R,n}^p$ behave badly in the vicinity of $\rho = 0$ and hence ill-defined.

We also find it useful to introduce the dual basis $\langle \widehat{U}_\omega^p |, \langle \widehat{V}_\omega^p |$ ($p, p' > 0$) with inner products

$$\langle \widehat{U}_\omega^p | U_{\omega'}^{p'} \rangle = \langle \widehat{V}_\omega^p | V_{\omega'}^{p'} \rangle = 2\pi\delta(p - p') 2\pi\delta(\omega - \omega') , \quad \langle \widehat{U}_\omega^p | V_{\omega'}^{p'} \rangle = \langle \widehat{V}_\omega^p | U_{\omega'}^{p'} \rangle = 0 . \quad (3.113)$$

⁴⁴We checked these inner products numerically using MATHEMATICA.

⁴⁵For the bosonic $SL(2; \mathbb{R})_\kappa/U(1)$ coset conformal field theory, we instead have $h = \bar{h} = \frac{p^2}{4(\kappa-2)} - \frac{\omega^2}{4\kappa} + \frac{1}{4(\kappa-2)}$, and $\mathcal{R}(p, \omega) \equiv \mathcal{R}_0(p, \omega) \frac{\Gamma(1 + \frac{ip}{\kappa-2})}{\Gamma(1 - \frac{ip}{\kappa-2})}$.

Explicitly, they are given by

$$\begin{aligned}\widehat{\langle U_\omega^p |} &= \frac{2}{1 - |\mathcal{R}(p, \omega)|^2} \{ \langle L_\omega^p | - \mathcal{R}^*(p, \omega) \langle R_\omega^p | \} , \\ \widehat{\langle V_\omega^p |} &= \frac{2}{1 - |\mathcal{R}(p, \omega)|^2} \{ \langle R_\omega^p | - \mathcal{R}(p, \omega) \langle L_\omega^p | \} .\end{aligned}\quad (3.114)$$

As such, these dual basis obey the following exact reflection relations:

$$\widehat{\langle U_\omega^{-p} |} = \mathcal{R}(p, \omega) \widehat{\langle U_\omega^p |} \quad \text{and} \quad \widehat{\langle V_\omega^{-p} |} = \mathcal{R}(p, \omega)^* \widehat{\langle V_\omega^p |} .\quad (3.115)$$

A remark is in order. The dual basis $\widehat{\langle U_\omega^p |}$, $\widehat{\langle V_\omega^p |}$ are *not* Wick rotatable to the Euclidean dual basis $\langle \phi_n^{+p} |$, $\langle \phi_n^{-p} |$, since $|\mathcal{R}(p, \omega)| = 1$ for $\omega \in i\mathbb{R}$. The correct procedure would be that we first define Wick rotations for the ‘ket’ states, and then define their dual states within the Lorentzian Hilbert space. Nevertheless, one-point correlators in the Lorentzian theory, from which a set of physical observables can be computed, ought to be always analytically continuable to the one-point correlators in the Euclidean theory. Roughly speaking, ambiguities inherent to the Wick rotation of dual states drop out upon taking inner product.

3.4 Duality and winding tachyon condensation

One of the salient features of the (Euclidean) $SL(2; \mathbb{R})/U(1)$ coset model is the so-called Fateev-Zamolodchikov-Zamolodchikov (FZZ) duality [92]. Mathematically speaking, this duality has enabled us to compute exact two-, and three-point functions of the $SL(2; \mathbb{R})/U(1)$ coset model and revealed their pole structures. Physically speaking, on the other hand, it has established a duality between the winding tachyon condensation and the singularity resolution of the geometry, and uncovered, from an exact CFT perspective, the importance of the winding tachyon condensation near the classical singularities.

Let us formulate the FZZ duality in the $\mathcal{N} = 2$ supersymmetric case. The FZZ duality states:

FZZ duality ($\mathcal{N} = 2$) supersymmetric $SL(2; \mathbb{R})/U(1)$ coset model with level k is equivalent (up to chirality) to the $\mathcal{N} = 2$ Liouville field theory (see e.g. [93] for reference):

$$\begin{aligned}L &= \int d^4\theta \Phi^\dagger \Phi + \int d^2\theta W(\Phi) + h.c. \\ W(\Phi) &= \mu e^{\frac{1}{Q}\Phi} ,\end{aligned}\quad (3.116)$$

where $Q^2 = \frac{2}{k}$.

The appearance of the chirality flip suggests the T-dual nature of the duality. Indeed, the FZZ duality can be proved in a more general context of the mirror symmetry. Physically, the appearance of the $\mathcal{N} = 2$ Liouville potential in the T-dualized set up can be anticipated as follows. As we studied in section 3.1, the T-dual of the $SL(2; \mathbb{R})^{(A)}/U(1)$ axial coset model, whose classical geometry is the cigar, is classically described by the trumpet geometry. However, the trumpet geometry has a singularity coming from the fixed point of the (T-dualized) $U(1)$ angular direction. To avoid the existence of a naked singularity of the space-

time, the (T-dualized) winding tachyon will condensate. From the world-sheet viewpoint, the (winding) tachyon condensation is nothing but the $\mathcal{N} = 2$ Liouville superpotential.⁴⁶

The operator correspondence of the FZZ duality is almost clear. In the asymptotic region, one can write the vertex operators of primary states in the $SL(2; \mathbb{R})^{(A)}/U(1)$ coset model by using those of the linear dilaton times $U(1)$ angular direction. We then perform the T-duality, to write them down as asymptotic vertex operators of primary states in the $\mathcal{N} = 2$ Liouville theory. The descendant structure is completely fixed by the $\mathcal{N} = 2$ superconformal algebra.

There are several “proofs” of the FZZ duality available in the literature. In the original work, FZZ has given a direct computation of the two- and three-point functions of the both models (including winding violating correlation functions) and has shown the equivalence between the two models when the computation based on the screening operator is available. In [94], the duality has been established rigorously at the level of the topological field theory from the viewpoint of the mirror symmetry (T-duality of the linear sigma model that flows to $SL(2; \mathbb{R})/U(1)$ coset in the infrared). As is the case with the usual mirror symmetry, it is natural to expect that the full conformal field theory is dual with each other, and indeed there is much supporting evidence for that. In another interesting derivation of the FZZ duality [95], the domain wall dynamics of a certain 2 + 1 dimensional gauge theory has been studied, resulting in two complementary descriptions — $SL(2; \mathbb{R})/U(1)$ coset model on one hand and $\mathcal{N} = 2$ Liouville theory on the other hand.

We will not review the derivation of the FZZ duality (see any of the references above, or consult [93] for a brief summary of the related discussions). Instead, we will see some physical consequences of the duality in the remaining part of this section. Let us begin with the comparison between the classical two-point function of the $SL(2; \mathbb{R})/U(1)$ coset CFT from the minisuperspace approximation and the exact one. The mini-superspace result (see (3.51) and (3.64)) is

$$\mathcal{R}_0(j, m, \bar{m}) = \frac{\Gamma(2j+1)\Gamma(-j+m)\Gamma(-j-\bar{m})}{\Gamma(-2j-1)\Gamma(j+1+m)\Gamma(j+1-\bar{m})}, \quad (3.117)$$

where

$$m = \frac{k w + n}{2}, \quad \bar{m} = \frac{k w - n}{2}, \quad (3.118)$$

while the exact result is

$$\begin{aligned} \mathcal{R}(j, m, \bar{m}) &= \nu(k)^{-2j-1} \frac{\Gamma(1 + \frac{2j+1}{k})}{\Gamma(1 - \frac{2j+1}{k})} \frac{\Gamma(2j+1)\Gamma(-j+m)\Gamma(-j-\bar{m})}{\Gamma(-2j-1)\Gamma(j+1+m)\Gamma(j+1-\bar{m})}, \\ \nu(k) &\equiv \frac{1}{\pi} \frac{\Gamma(1 - \frac{1}{k})}{\Gamma(1 + \frac{1}{k})}, \end{aligned} \quad (3.119)$$

The effects of the winding tachyon condensation can be seen in the $1/k$ suppressed factor in the exact formula as $\frac{\Gamma(1 + \frac{2j+1}{k})}{\Gamma(1 - \frac{2j+1}{k})}$. As is well-known in Liouville field theory, the poles in

⁴⁶To avoid a possible confusion, we note that the original winding tachyon condensation becomes non-winding tachyon with θ momentum after taking the T-duality.

the correlation function appear when the screening interaction coming from the $\mathcal{N} = 2$ superpotential $W = \mu e^{\frac{1}{\mathcal{Q}}\Phi}$ satisfies the screening condition for the Liouville momenta ϕ . Indeed, the perturbative Liouville insertion predicts poles in the two-point functions exactly as indicated by the factor $\frac{\Gamma(1+\frac{2j+1}{k})}{\Gamma(1-\frac{2j+1}{k})}$.

Another important aspect of the FZZ duality is that it has provided a perspective on the winding number non-conservation process. In the $SL(2; \mathbb{R})^{(A)}/U(1)$ axial coset model, one can define an asymptotic winding quantum number by ω . However, since the cigar geometry has a trivial fundamental group, the winding number is not a conserved quantity. In the free field construction of the $SL(2; \mathbb{R})^{(A)}/U(1)$ coset model (such as the one based on the Wakimoto construction of the $SL(2; \mathbb{R})$ current algebra), it is difficult to compute the winding number violating correlation functions. Indeed this was the first motivation of FZZ to propose the dual description.⁴⁷

Situations are worse in the naive T-dualized trumpet geometry. In the trumpet metric, it appears that we have a $U(1)$ isometry along $\tilde{\theta}$ that is the dual coordinate for θ , suggesting that the momentum quantum number as well as the winding quantum number are well-defined conserved quantities. The breaking of the winding number (or momentum mode in the T-dual picture) is quite obscure: the origin of the winding non-conservation, i.e. the fixed point of the $U(1)$ action, has now become the singularity of the target space.⁴⁸

The resolution of this puzzle is given by the FZZ duality. In the T-dualized picture, the singularity is removed by the tachyon condensation, or $\mathcal{N} = 2$ Liouville superpotential. At the same time, the $\mathcal{N} = 2$ superpotential explicitly breaks the translation invariance along the θ direction, which gives the origin of the momentum non-conservation in the T-dual picture. Actually, the explicit breaking of the momentum conservation is quite useful to compute the winding number violating process in $SL(2; \mathbb{R})/U(1)$ coset model: by a direct insertion of the $\mathcal{N} = 2$ Liouville superpotential, the winding number violating process can be computed perturbatively.

We end this section with three remarks

- Supersymmetric $SL(2; \mathbb{R})/U(1)$ coset model has a conserved $U(1)_R$ current. By taking quotient of the theory with this $U(1)_R$ current, we obtain the duality between the bosonic $SL(2; \mathbb{R})/U(1)$ coset model and the sine-Liouville theory [96]. The sine-Liouville theory has the potential

$$V(\phi, Y) = \mu(S^+ + S^-)$$

$$S^\pm = e^{-\frac{1}{\mathcal{Q}}(\phi \pm \sqrt{1+\mathcal{Q}^2}iY)} \equiv e^{-\sqrt{\frac{\kappa-2}{2}}\phi \mp \sqrt{\frac{\kappa}{2}}iY}, \quad (\mathcal{Q} = \sqrt{2/(\kappa-2)}). \quad (3.120)$$

We note that the potential preserves the W_∞ symmetry as a side remark, which makes the model integrable [97, 98]. In their original work (FZZ), they proposed the duality between the bosonic $SL(2; \mathbb{R})/U(1)$ coset model and the bosonic sine-Liouville theory.

⁴⁷At the same time, FZZ has also given an ingenious way to compute the winding violating correlation function within the $SL(2; \mathbb{R})/U(1)$ coset model by introducing the dual operators.

⁴⁸It is well-known that when we gauge the axial symmetry, the vector current has an anomaly and vice versa, and this is indeed the origin of this apparent paradox. In the same token, the $U(1)$ isometry of the vector coset is broken down to \mathbb{Z}_k . We should be, therefore, careful when we talk about the ‘‘T-duality’’ of the trumpet.

- There is a small controversial issue in the interpretation of the FZZ duality. Our standpoint has been that the dual description of the cigar geometry is given by the $\mathcal{N} = 2$ Liouville theory, and the $\mathcal{N} = 2$ Liouville superpotential does not appear in the original cigar geometry explicitly (otherwise the source of the winding number non-conservation is two-fold). The other common interpretation of the FZZ duality is that the winding tachyon condensation ($\mathcal{N} = 2$ Liouville superpotential written in the dual coordinate) also appears in the original cigar geometry. This interpretation is natural in the sense that it gives a natural explanation about the coexistence of the poles coming from the geometry part and the Liouville insertion part. Whichever interpretation one may take, we believe that what we call the supersymmetric $SL(2; \mathbb{R})/U(1)$ theory and the $\mathcal{N} = 2$ Liouville theory is identical, and the structure constant, e.g. the two-point function is uniquely given by formulae like (3.119).
- So far, we have focused on the Euclidean $SL(2; \mathbb{R})/U(1)$ coset model. However, things are unclear in the Lorentzian $SL(2; \mathbb{R})/U(1)$ coset model, where the dual $\mathcal{N} = 2$ Liouville theory is unavailable. A naive analytic continuation of the $\mathcal{N} = 2$ superpotential gives a wrong Liouville wall, which is localized near the weakly coupled region [99]. Furthermore, the Lorentzian coset does not have a winding mode, so the interpretation of the winding tachyon condensation is not evident. Nevertheless, we believe that the exact structure constants are given by the analytic continuation of the exact results for the Euclidean coset since the analytic continuation correctly reproduces the mini-superspace part. The clear explanation of the origin of the extra poles in the Lorentzian coset is still an open question.⁴⁹

⁴⁹The origin might be given by the degrees of freedom near the horizon on which we mentioned in section 3.2.3. A related interpretation based on the idea of stretched horizon has been given in [100].

4 Black Hole - String Transition

In this section, we review “black hole - string transition”. The transition is believed to be a fundamental property of the quantum black hole in the non-BPS regime. We will also see that the transition is related to the thermal winding tachyon condensation.

The organization of the section is as follows. In section 4.1, we formulate the “black hole - string transition” in general dimensions. In section 4.2, we specialize in the two-dimensional case, where α' exact treatment is possible. In section 4.3, we briefly summarize the current status of the black hole - string transition in other solvable backgrounds.

4.1 In general dimensions

One of the most profound results in (semi-)classical gravity is the thermodynamics of the black hole. Thus one of the most significant benchmarks of any theory of quantum gravity is to provide a satisfactory understanding of the thermodynamics of the black hole. Especially, understanding of the black hole entropy from the microscopic viewpoint has been one of the greatest achievements of the string theory as a quantum theory of gravity [101].

Let us consider the Schwarzschild black hole in the string theory as a simplest example of the non-extremal black hole system.⁵⁰ The Schwarzschild black hole in any dimension is completely determined by the parameter r_h that determines the horizon size. When $r_h \gg l_s$, the classical supergravity description is good (at least outside of the horizon), and we can trust the effective supergravity action to discuss the properties of the black hole.

If one gradually decreases the horizon size r_h , the effects of higher derivative corrections coming from the underlying quantum gravity will become important. Within the superstring theory, some higher derivative corrections are known, and it has been shown that these corrections will beautifully explain the apparent mismatch between the macroscopic derivation of the small charge BPS black hole entropy and the microscopic derivation from the string theory (see e.g. [102]). In the non-extremal cases we are discussing now, we have not yet completely grasped the structure of the higher derivative corrections and the quantitative match of the black hole entropy, but the guiding principle is summarized by the so-called “black hole - string transition” or “black hole - string crossover” introduced in [103, 104, 105, 106, 107].

When $r_h \leq l_s$, the geometrical description of the black hole breaks down and it should be replaced with the microscopic description based on the quantum strings. This is natural because the string theory has a natural cutoff given by the string length l_s as a length scale, and the objects smaller than l_s do not possess an ordinary geometrical meaning. The principle of the “black hole - string transition” is that the black hole can be understood either as the higher excitation of the strings or as the classical solution of the (higher derivative) gravities. Especially, the crossover is parametrically smooth as a function of the coupling constant g_s and l_s .

⁵⁰The exact quantization of the string in the Schwarzschild black hole is not known. However, since one can make the curvature of the Schwarzschild black hole arbitrarily small outside the horizon, it is natural to assume the existence of string solutions asymptotically given by the Schwarzschild black hole. The existence of the $SL(2; \mathbb{R})/U(1)$ two-dimensional black hole strongly supports this assumption.

In the Schwarzschild black hole example, we can roughly estimate the transition point and the “black hole - string crossover” as follows. Let us assume the four dimensional Schwarzschild black hole for definiteness. The four-dimensional Newton constant G is given by $G \sim g_s^2 l_s^2$, so the Schwarzschild radius of the string is estimated as $r_0 = m_{\text{str}} G \sim m_{\text{str}} g_s^2 l_s^2$ with the mass of excited string $m_{\text{str}}^2 \sim \frac{n}{l_s^2}$, where n denotes the oscillator level. At the black hole - string transition point $r_0 \sim l_s$, we have

$$\frac{l_s^2}{G} \sim \frac{1}{g_s^2} \sim \sqrt{n} . \quad (4.1)$$

Thus, the classical Bekenstein entropy is given by $S_{\text{Bek}} \sim \frac{r_0^2}{G} \sim \frac{l_s^2}{G} \sim \sqrt{n}$, which indeed agrees with the entropy of the perturbative string expected from the Cardy formula up to a numerical factor. Alternatively speaking, one can say that the requirement of the smooth overlap of the entropy demands that $r_0 \sim l_s$ should be the “black hole - string transition” point.

Another important concept associated with the α' corrections to the geometry is the stretched horizon [108, 105, 100]. We can formulate the stretched horizon based on the local temperature of the geometry. As is the case with the two-dimensional black hole, any neutral black hole has an intrinsic temperature determined by the periodicity of the Euclidean time (Hawking temperature). From the Lorentzian viewpoint, the temperature is defined by the observer at spacial infinity. From an observer at a fixed proper distance R from the horizon, the Hawking radiation is observed with much higher temperature

$$T_u(R) = \frac{T_{\text{Hw}}}{\sqrt{g_{00}(R)}} , \quad (4.2)$$

due to the gravitational red-shift. On the other hand, the string theory has the “highest temperature” determined by the Hagedorn temperature. Since the number of perturbative string states grows exponentially as a function of energy (mass):

$$Z(\beta) = \text{Tr} e^{-\beta E} \sim \int dM \rho(M) e^{-\beta M} . \quad (4.3)$$

with the density of states given by $\rho(M) \sim e^{\beta_{\text{Hg}} M}$, the partition function of the perturbative string theory is ill-defined beyond the Hagedorn temperature $\beta < \beta_{\text{Hg}}$. There we expect that the string interactions are much more important and the strings will disentangle.

Now let us return to the Hawking radiation. From (4.2), one can see that the (red-shifted) temperature becomes infinite at the classical horizon. Actually, before reaching the event horizon we will encounter the radius when the local temperature exceeds the Hagedorn temperature. The local Hagedorn transition blurs the local geometry near the black hole horizon. This is what we call the stretched horizon. Note that we can make the curvature at the horizon arbitrarily small, and in this regime, the size of the stretched horizon is of order one in the string unit.

It is interesting to consider some extreme limits of the above discussions. The first example is the large T_{Hw} limit: what happens if the Hawking temperature in the asymptotic infinity is larger than T_{Hg} ? We expect that the stretched horizon completely blur the black

hole geometry. Indeed in the leading order estimation of the four-dimensional Schwarzschild black hole, we have $\beta_{\text{Hw}} = r_0$ and $\beta_{\text{Hg}} = \text{const}$, and such scenario occurs when $r_0 \sim l_s$. It is interesting to note that the condition roughly coincides with that for the “black hole - string transition”. In section 4.2, we will see this coincidence is exact (after taking α' corrections into account) in the two-dimensional black hole that is an exactly solvable string background.

Another limit is the (extremal) charged black hole solution. In the charged black hole examples, the above discussion based on the Hagedorn temperature and the Hawking temperature should be generalized. This is because, as pointed out in [106], we can arbitrarily lower the Hawking temperature while keeping possible α' corrections large. In other words, one can make the transition temperature arbitrarily lower than the Hagedorn temperature. The most extreme case is the (BPS) extremal black hole, where the Hawking temperature is zero. The generalization proposed in [109] states that the “black hole - string transition” occurs when the Hawking temperature coincides with the temperature of the free-string with the same mass *and* charge. We will briefly review their discussions later in section 4.3.

It is also instructive to recapitulate the problem from the Euclidean approach. In the flat Minkowski space, the Hagedorn divergence of the partition function can be attributed to the thermal winding tachyon condensation [110, 111, 112, 113, 114]. We begin with the more precise version of (4.3).

$$\begin{aligned} \beta F &= \text{Tr}_{\text{phys}} \log(1 - e^{-\beta E}) \\ &= \int_{-\infty}^{\infty} d\tau_2 \int_{-1/2}^{1/2} d\tau_1 \frac{1}{\tau_2} \text{Tr}_{\text{CFT}} q^{L_0} q^{\bar{L}_0} . \end{aligned} \quad (4.4)$$

In the second line, we have introduced the Schwinger parameter τ_2 and the level matching condition by

$$\int_{-1/2}^{1/2} d\tau_1 e^{2\pi i \tau_1 (L_0 - \bar{L}_0)} . \quad (4.5)$$

The trace is taken over the original space-like CFT with an additional free S_1 CFT whose radius is β *restricted to the momentum mode*. The Hagedorn divergence appears in the ultraviolet region $\tau_2 \rightarrow 0$. Now let us use the Polchinski’s trick [110] to rewrite the thermal partition function (4.4) as the string 1-loop partition function

$$\beta F = \int_{\mathcal{F}} \frac{d\tau^2}{\tau_2} \text{Tr}_{\text{CFT} \times S^1} q^{L_0} q^{\bar{L}_0} , \quad (4.6)$$

where \mathcal{F} is the fundamental domain of the torus, and the trace is taken over the original CFT with the free S^1 CFT *including winding modes*. The Hagedorn divergence is now translated to the IR instability $\tau_2 \rightarrow \infty$. Apart from the ground state tachyon that should be GSO-projected out in the supersymmetric theory, a possible instability comes from the thermal winding tachyon whose mass is given by

$$m(\beta)^2 = -1 + \beta^2 . \quad (4.7)$$

When $m(\beta)^2 < 0$, the Hagedorn instability occurs. In this way, we can understand the Hagedorn divergence as the appearance of the winding tachyon in the Euclideanized thermal string theory.

The argument above suggests that when the thermal direction shrinks enough to admit “winding tachyon” in the Euclidean spectrum, the Hagedorn phase transition occurs. Assuming a semiclassical quantization of string in the Schwarzschild black hole, a similar situation occurs in the thermal string theory in the Euclidean Schwarzschild black hole background. The thermal winding tachyon has an effective mass

$$m^2(r) = -1 + r_0^2 \left(1 - \frac{r_0}{r}\right) . \quad (4.8)$$

At the point where $m^2(r)$ becomes negative, the black hole develops a stretched horizon, and when $m^2(\infty) < 0$, we expect the “black hole - string” phase transition. We will see later that the winding tachyon is crucial in the two-dimensional black hole and its exact “black hole - string phase transition”.

Recently Horowitz [115] studied the real-time winding tachyon condensation in the black hole system. If one considers a compactified black string solution, the extra dimension can show a winding tachyon condensation as the direction shrinks toward the black hole singularity. After the winding tachyon condensation, the black hole evaporates as a bubble of nothing. This process is proposed to be a new interesting end point of the Hawking black hole evaporation (see [116, 117, 118, 119] for related studies). The winding tachyon condensation could also give a solution of the cosmological singularity problems as studied in [120, 121].

4.2 Two-dimensional black hole case

To discuss the “black hole - string transition” introduced in section 4.1 in a more quantitative manner, it is imperative to study the exact string background rather than the approximate Schwarzschild black hole solution. Especially, the arguments related to the (thermal) winding tachyon condensation is rather speculative, and a demonstration based on the exactly solvable string background would be highly desirable. As we have seen in section 2, the simplest exactly solvable (non-BPS) black hole background is the two-dimensional black hole. In this subsection, we specialize in the “black hole - string transition” in the two-dimensional black hole.⁵¹

Let us consider the supersymmetric $SL(2; \mathbb{R})/U(1)$ coset model. As we discussed in section 2.4, the two-dimensional black hole has the Hawking temperature

$$T_{\text{Hw}} = \frac{1}{\beta_{\text{Hw}}} = \frac{1}{2\pi\sqrt{\alpha'k}} . \quad (4.9)$$

Since the two-dimensional black hole is asymptotically a linear dilaton theory, the Hagedorn

⁵¹Of course, what we mean by the “two-dimensional black hole” includes the embedding into the superstring theory such as the black NS5-brane background, so our results have a direct application to the ten-dimensional critical string theories.

temperature shows a $1/k$ corrected shift compared with the flat Minkowski theory⁵²:

$$T_{\text{Hg}} = \frac{1}{\beta_{\text{Hg}}} = \frac{1}{4\pi\sqrt{1 - \frac{1}{2k}}} . \quad (4.10)$$

To derive this formula, one should first note that the $SL(2; \mathbb{R})/U(1)$ coset model has a mismatch between the genuine central charge $c^{SL(2; \mathbb{R})/U(1)} = 3 + \frac{6}{k}$ and the effective central charge $c_{\text{eff}}^{SL(2; \mathbb{R})/U(1)} = 3$ due to the asymptotic linear dilaton.⁵³ Therefore, the total theory has a deficit effective central charge $c_{\text{eff}}^{\text{total}} = 12 - \frac{6}{k}$ after the subtraction of the ghost contribution. Now we recall the Cardy formula:

$$\rho(M) \sim \exp \left(2\pi\sqrt{\frac{c_{\text{eff}}}{12}}M + 2\pi\sqrt{\frac{\bar{c}_{\text{eff}}}{12}}M \right) , \quad (4.11)$$

which immediately gives the Hagedorn temperature (4.10).

For later references, we present here a similar formula for the bosonic two-dimensional black hole. The Hawking temperature and the Hagedorn temperature is given by

$$T_{\text{Hw}} = \frac{1}{\beta_{\text{Hw}}} = \frac{1}{2\pi\sqrt{\alpha'\kappa}} . \quad (4.12)$$

and

$$T_{\text{Hg}} = \frac{1}{\beta_{\text{Hg}}} = \frac{1}{4\pi\sqrt{2 - \frac{1}{2(\kappa-2)}}} . \quad (4.13)$$

There is no apparent reason to exclude possible α' corrections to the Hawking temperature in the bosonic string theory, but the exact string quantization reveals that the formula (4.12) is the correct one.⁵⁴ We will return to this problem when we discuss the exact boundary states of the probe rolling D-brane in section 8. On the other hand, the Hagedorn temperature here is obtained from the exact string quantization and trustful.

From the general discussions in section 4.1, we expect “black hole - string” at $k = 1$ (or $\kappa = 3$ for the bosonic case) when the Hawking temperature and the Hagedorn temperature coincide. At this point, the stretched horizon becomes so large that it will swallow the complete space-time. This “black hole - string transition” in the two dimension black hole is induced by the strong α' corrections: when k is large (recall $1/k$ correction corresponds to α' correction) the Hawking temperature is much larger than the Hagedorn temperature,

⁵²When we mention the Hagedorn temperature of the two-dimensional black hole, we always assume that the criticality condition of the string theory is satisfied by adding *non-dilatonic* CFTs. The NS5-brane background is a typical example.

⁵³We can also see this directly from the one-loop partition function and the spectrum. See section 3 and appendix A.

⁵⁴In general, the Hawking temperature is classically determined solely from the information near the event horizon (the Rindler limit), where the curvature and the α' corrections could become large. The effects of such α' corrections and possible renormalization of the Hawking temperature are interesting subjects to study.

and the geometry is not disturbed by the back-reaction of the Hawking radiation. When k becomes smaller, $1/k$ corrections will become more and more important, and at the phase transition point, i.e. at $k = 1$, physics changes drastically. One of the main focus of this thesis is to study this transition from the rolling D-brane probe.

At this point, we would like to point out that the “black hole - string” phase transition of the two-dimensional black hole does not involve the string coupling g_s in the discussion. This is one of the features of the two-dimensional black hole that we can clearly separate the (typically more difficult) problem of the genus expansion from the more tractable α' corrections in order to understand the “black hole - string transition”.

What is the origin of the strong $1/k$ correction? As we have mentioned earlier in section 3.1, the metric for the supersymmetric two-dimensional black hole does not receive perturbative $1/k$ corrections. The origin of the (nonperturbative) $1/k$ corrections that trigger the “black hole - string transition” is most clearly seen in the Wick rotated Euclidean two-dimensional black hole for which the dual description is available.

In the dual description, the two-dimensional black hole is described by the $\mathcal{N} = 2$ Liouville theory. The $\mathcal{N} = 2$ superpotential

$$W(\Phi) = \mu \int d^2\theta e^{\frac{1}{Q}\Phi} \quad (4.14)$$

can be seen as the localized (winding) tachyon condensation.⁵⁵ The condensation is a localized mode because the Liouville momentum j corresponding to the superpotential (4.2) is not given by the continuous series $j = -\frac{1}{2} + ip$, but lies in the discrete series.

The crucial observation has been already made early in [122] in the context of the non-critical superstring theory. The spirit is close to the discussions given in section 2.3 and 3.4. The superpotential is a normalizable perturbation if $\frac{1}{Q} > \frac{Q}{2}$ (i.e. $k > 1$) and it is a non-normalizable deformation otherwise. In the language of the noncritical string theory, the $\mathcal{N} = 2$ super Liouville potential satisfies the Seiberg bound [123] only when $\frac{1}{Q} < \frac{Q}{2}$ holds. This directly means that the $\mathcal{N} = 2$ Liouville description is good for $k < 1$ and the two-dimensional black hole description is good for $k > 1$. The transition point is exactly at $k = 1$.⁵⁶

We can repeat the same analysis for the bosonic $SL(2; \mathbb{R})/U(1)$ coset. The duality between the bosonic $SL(2; \mathbb{R})/U(1)$ and the sine-Liouville theory, together with the Seiberg bound, leads to the conclusion that $\kappa = 3$ is the phase transition point. The potential is

⁵⁵The duality between the $SL(2; \mathbb{R})^{(A)}/U(1)$ coset and the $\mathcal{N} = 2$ Liouville theory is a kind of T-duality as we discussed in section 3.4. Thus the condensation of the momentum mode in $\mathcal{N} = 2$ Liouville theory can be regarded as the condensation of the winding mode in the original $SL(2; \mathbb{R})^{(A)}/U(1)$ coset model.

⁵⁶Another interesting observation related to the $k = 1$ transition is the following. If we consider a two-dimensional $U(1)$ gauge theory in the ultraviolet that flows to $SL(2; \mathbb{R})/U(1)$ coset theory in the infrared (as was introduced in [94] to prove the mirror duality to the $\mathcal{N} = 2$ Liouville theory), the central charge of the $U(1)$ gauge theory is given by 9. Since the IR $SL(2; \mathbb{R})/U(1)$ coset theory has a central charge $c = 3(1 + \frac{2}{k})$, there is an apparent contradiction to Zamolodchikov’s c -theorem if the level $k < 1$ is considered. However, we should note that $SL(2; \mathbb{R})/U(1)$ coset theory is dilatonic so that the effective central charge is always given by 3.

given by

$$V = \mu(S^+ + S^-), \quad S^\pm = e^{-\frac{1}{\mathcal{Q}}(\phi \pm \sqrt{1+\mathcal{Q}^2}iY)} \equiv e^{-\sqrt{\frac{\kappa-2}{2}}\phi \mp \sqrt{\frac{\kappa}{2}}iY}, \quad (\mathcal{Q} = \sqrt{2/(\kappa-2)}), \quad (4.15)$$

and the normalizability changes precisely at $\kappa = 3$. Assuming that this occurs when the Hawking temperature and the Hagedorn temperature coincides, we have verified that the Hawking temperature of the bosonic two-dimensional black hole is not renormalized. We will see another support from the probe rolling D-brane later in section 8.

We could argue this transition without using the dual Liouville picture [96]. The black hole perturbation descends from the $SL(2; \mathbb{R})$ states

$$J_{-1}^+ \bar{J}_{-1}^+ |j = -1; m = \bar{m} = -1\rangle. \quad (4.16)$$

The normalizability of such states (see section 3.2.2) demand

$$-\frac{1+k}{2} < j < -\frac{1}{2} \quad (4.17)$$

with $j = -1$, which suggests the same phase transition point $k = 1$ (or $\kappa = 3$).

The situation in the Lorentzian two-dimensional black hole is less clear. We cannot perform the Wick rotation to the winding tachyon potential (4.2) naively because the time is continuous and there is no apparent winding mode in the Lorentzian two-dimensional black hole. The same thing can be said in the Hagedorn instability of the free string theory in the flat Minkowski space: the existence of the thermal winding tachyon in the Wick rotated theory does not mean the tachyonic instability in the real time physics. Rather it should be understood as the phase transition associated with the thermal dissolution of strings. At the temperature beyond the Hagedorn point, there would be no distinction between the gas of strings and the black hole.

4.3 Other solvable backgrounds

There are many other exactly solvable string theory backgrounds that exhibit the ‘‘string black hole transition’’. Most of the examples are more or less related to the $SL(2; \mathbb{R})$ WZNW model. In this subsection, we will briefly review the transition in such backgrounds.

The black hole - string transition across $k = 1$ also has a natural interpretation in terms of the holographic principle, as recently discussed in [124]. Adding Q_1 fundamental strings to k NS5-branes (more generally Calabi-Yau singularities) as we reviewed in section 2.4, one obtains the familiar bulk geometry of the AdS_3/CFT_2 -duality. In this context, the density of states of the dual conformal field theory is given by the naive Cardy formula $S = 2\pi\sqrt{\frac{cL_0}{6}} + 2\pi\sqrt{\frac{\bar{c}\bar{L}_0}{6}}$ with $c = 6kQ_1$ for $k > 1$, but not for $k < 1$. Rather, the central charge that should be used in the Cardy formula is replaced by an effective one $c_{\text{eff}} = 6Q_1(2 - \frac{1}{k})$ [122].

The origin of the difference between the c_{eff} and c is again the normalizability of a certain operator. The $SL(2; \mathbb{C})$ vacuum of the dual CFT corresponds to the states

$$J_{-1}^+ \bar{J}_{-1}^+ |j = -1; m = \bar{m} = -1\rangle \quad (4.18)$$

in the world-sheet $SL(2; \mathbb{R})$ WZNW model, and as we have seen several times, for $k > 1$, the operator is normalizable, and $c_{\text{eff}} = c$. On the other hand, for $k < 1$, the operator is non-normalizable, and we expect $c_{\text{eff}} < c$. A short computation based on the string description gives $c_{\text{eff}} = 6Q_1(2 - \frac{1}{k})$.

We note that for $k > 1$, the BTZ black hole excitation is normalizable and the partition function and the entropy is dominated by the Bekenstein-Hawking entropy of the BTZ black hole while for $k < 1$, the BTZ black hole excitation is non-normalizable and the entropy is solely explained by the string excitations. This argument is completely in agreement with the “black hole - string transition” picture at $k = 1$.

Another interesting generalization is the two-dimensional charged black hole. We consider the asymmetric coset

$$\frac{SL(2; \mathbb{R})_k \times U(1)_L}{U(1)}, \quad (4.19)$$

where the $U(1)$ gauging acts on one of the (space-like) left-moving current in $SL(2; \mathbb{R})$ and a linear combination of the right-moving current of $SL(2; \mathbb{R})$ and $U(1)_L$. After the Kaluza-Klein reduction, the geometry of (4.19) is described by the metric ($Q^2 = \frac{2}{k}$)

$$ds^2 = d\phi^2 - \left(\frac{\tanh \frac{Q}{2} \phi}{1 - a^2 \tanh^2 \frac{Q}{2} \phi} \right)^2 d\theta^2, \quad (4.20)$$

the dilaton

$$\Phi = \Phi_0 - \frac{1}{2} \log \left(1 + (1 - a^2) \sinh^2 \frac{Q}{2} \phi \right), \quad (4.21)$$

and the gauge field

$$A = \frac{a \tanh^2 \frac{Q}{2} \phi}{1 - a^2 \tanh^2 \frac{Q}{2} \phi} d\theta. \quad (4.22)$$

Here a^2 is related to the mass m and the charge q of the black hole as

$$a^2 = \frac{m - \sqrt{m^2 - q^2}}{m + \sqrt{m^2 - q^2}}. \quad (4.23)$$

At $a = 0$, the model reduces to the undeformed $SL(2; \mathbb{R})/U(1)$ black hole (and a compact boson).

The Hawking temperature of the black hole (e.g. from the Euclidean geometry) is given by

$$\beta_{\text{Hw}} = \frac{4\pi}{Q} \frac{1}{1 - a^2}. \quad (4.24)$$

On the other hand, the Hagedorn temperature is given by

$$T_{\text{Hg}} = \frac{1}{\beta_{\text{Hg}}} = \frac{1}{4\pi \sqrt{1 - \frac{1}{2k}}}, \quad (4.25)$$

irrespective of the deformation parameter a .

From the world-sheet perspective, the “black hole - string transition” of the charged two-dimensional black hole inherits from the $SL(2; \mathbb{R})$ WZNW model and the transition point should be $k = 1$. This is different from the naive guess based on the relation $\beta_{\text{Hw}} = \beta_{\text{Hg}}$. A resolution proposed in [109] is that the more precise definition of the transition temperature is when the Hawking temperature coincides with the temperature of the string that has the same mass and charge of the black hole.

In this example, the entropy of the string with charge q is given by⁵⁷

$$S = 2\pi \sqrt{1 - \frac{Q^2}{4}} \left(m + \sqrt{m^2 - q^2} \right) \quad (4.26)$$

resulting in the corresponding string temperature

$$\beta_{\text{str}} = \left. \frac{\partial S}{\partial m} \right|_q = \sqrt{1 - \frac{Q^2}{4}} \frac{4\pi}{1 - a^2} . \quad (4.27)$$

It is easy to see that the condition $\beta_{\text{str}} = \beta_{\text{Hw}}$ exactly reproduces the CFT computation, i.e. $k = 1$.

⁵⁷The shift is due to q -amount of right-moving $U(1)$ charge: we are summing over the string states with fixed $U(1)$ charge q instead of summing over all states.

5 Tachyon Radion Correspondence

In this section, we review the tachyon radion correspondence, which is one of the greatest motivations to study the rolling D-brane in the two-dimensional black hole system. The correspondence says that the dynamics of the open-string tachyon condensation may be geometrically realized by the rolling D-brane system.

The organization of the section is as follows. In section 5.1, we overview the rolling tachyon problem. In section 5.2, we study the closed string emission rate from the rolling tachyon boundary states and their variations.⁵⁸ In section 5.3, we study the correspondence at the classical level. In section 5.4, we summarize our results on the quantum correspondence. In section 5.5 some cosmological implications are studied.

5.1 Rolling tachyon

5.1.1 overview

In the days of early developments of string theory, tachyon used to be thought of as a nuisance in constructing realistic models for particle physics of our world. In recent years, open-string tachyons have obtained civil rights and have played more and more important roles in acquiring our knowledge on the nonperturbative D-brane physics with (spontaneously) broken SUSY. In addition, they have been even providing phenomenological applications such as brane inflation. More recently, the closed string tachyons (especially localized winding tachyon) have attracted much attention in relation to the topological change [125, 126] and the resolution of singularities [120].

One of the important steps in understanding the physics of unstable D-branes is Sen's conjecture with subsequent advancement (see [127] for a review), which states that the decaying process of the unstable D-branes can be regarded as the open string tachyon condensation. In particular, the energy difference between the false (perturbative) tachyonic vacuum and the true vacuum of the open string tachyon potential should explain the tension of the decaying D-brane exactly. Furthermore, the cohomology of the open string theory at the true vacuum must vanish. In the context of the open string field theory, these conjectures have been analytically proved in [128, 129].

More interesting aspects of the tachyon dynamics is to study its time evolution [130, 131, 132]. Based on the effective field theory analysis (which has been confirmed by the exact boundary states analysis later), it was found that the late time evolution of the open-string tachyon gives rise to the so-called “tachyon matter”, which is a pressureless fluid. Such a “rolling tachyon” evolution has provided us with novel understanding of the tachyon condensation and time-dependent physics in string theory. The feasibility to construct the exact boundary states enables us to study the highly non-supersymmetric time evolution in a quantitative way.

Let us begin with the effective DBI type action for the rolling tachyon

$$S = - \int dt V(T) \sqrt{1 - \dot{T}^2} . \quad (5.1)$$

⁵⁸This part of the thesis is based on [2].

Since we will focus on the homogeneous decay, we have assumed the D0-brane action without loss of generality. The effective potential $V(T)$ takes the form

$$V(T) = M_0 \frac{1}{\cosh \frac{T}{2x}} , \quad (5.2)$$

where the D0-brane tension $M_0 \propto \frac{1}{g_s}$. For the non-BPS D-branes in supersymmetric theory, $x = 1$, and for the unstable D-branes in bosonic string theory, $x = 1/2$. The solution of the equation of motion is given by

$$\sinh \frac{T}{2x} = a \cosh \frac{t}{2x} , \quad (5.3)$$

leading to the classical energy momentum tensor:

$$T_{\mu\nu} = \frac{V(T) \partial_\mu T \partial_\nu T}{\sqrt{1 + \eta^{\mu\nu} \partial_\mu T \partial_\nu T}} - V(T) \eta_{\mu\nu} \sqrt{1 + \eta^{\mu\nu} \partial_\mu T \partial_\nu T} . \quad (5.4)$$

We are interested in the late time behavior of the energy momentum tensor, which is explicitly given by

$$\begin{aligned} T_{00} &\sim E \\ T_{ij} &\sim -E \exp(-t/x) \delta_{ij} , \end{aligned} \quad (5.5)$$

where $E = M_0 / \sqrt{1 + a^2}$. As we mentioned before, we have obtained the pressureless dust as a final product of the D0-brane decay.

The energy momentum tensor yields the coupling of the rolling D-brane to the gravity. In order to study the coupling to higher string modes, we need the exact boundary state that describes the rolling D-brane. In the boundary conformal field theory approach, we introduce the boundary interaction⁵⁹

$$\delta S_{\text{full}} = \tilde{\lambda} \int ds \cosh X^0(s) , \quad (5.6)$$

for the ‘‘full S-brane’’ model, and

$$\delta S_{\text{half}} = \lambda \int ds e^{X^0(s)} , \quad (5.7)$$

for the ‘‘half S-brane’’ model. Here X^0 denotes the target-space time coordinate and the integration is taken over the boundary of the world-sheet parametrized by s .

There are several different ways to obtain the boundary states. Originally Sen [130] proposed to obtain the boundary states for (5.6) by starting with the (compactified) space-like model (boundary sine-Gordon model) and performing the Wick rotation. In the ‘‘half S-brane model’’, Gutperle and Strominger [133] proposed to use the Wick rotation of the Liouville theory in the zero linear dilaton limit (time-like Liouville theory).

⁵⁹We focus on the bosonic case for simplicity. The generalization to the non-BPS D-branes in superstring theory is straightforward.

In the coordinate space, the behavior of the boundary states from different prescription shows a different behavior (mainly in the region $X^0 < 0$), but in the momentum (energy) space, they are related with each other in the zero mode sector. To see this, let us expand the rolling tachyon boundary states as

$$\begin{aligned} |B\rangle &= i \int_C dt \rho(t) |0\rangle + \sigma(t) \alpha_{-1}^0 \bar{\alpha}_{-1}^0 |0\rangle + \dots \\ &= i \int d\omega \tilde{\rho}(\omega) |\omega\rangle + \tilde{\sigma}(\omega) \alpha_{-1}^0 \bar{\alpha}_{-1}^0 |\omega\rangle + \dots \end{aligned} \quad (5.8)$$

Since we are dealing with the time-dependent theory based on the analytic continuation, the contour choice will affect the physics. The zero mode density $\rho(\omega)$ has been computed as

$$\begin{aligned} i \int_{C_{real}} dt \rho_{full}(t) e^{i\omega t} &= \left(e^{-i\omega \log \hat{\lambda}} - e^{i\omega \log \hat{\lambda}} \right) \frac{\pi}{\sinh \pi\omega} \\ i \int_{C_{real}} dt \rho_{half}(t) e^{i\omega t} &= e^{-i\omega \log \hat{\lambda}} \frac{\pi}{\sinh \pi\omega} \\ i \int_{C_{HH}} dt \rho_{full}(t) e^{i\omega t} &= e^{-i\omega \log \hat{\lambda}} \frac{\pi}{\sinh \pi\omega} \end{aligned} \quad (5.9)$$

Note that the Hartle-Hawking contour C_{HH} integral of the full S-brane solution coincides with the real contour C_{real} integral of the half S-brane solution (see figure 6). This is intuitively expected because the half S-brane solution describes the later half dynamics of the rolling D-brane (decaying brane) and the Hartle-Hawking contour effectively sets the initial condition at $t = 0$ to give a decaying D-brane. We also note that the boundary time-like Liouville field approach directly gives the same zero mode boundary wavefunction for the half S-brane solution. Thus we can conclude that various approaches yield essentially the identical results for the zero mode boundary wavefunction (i.e. coupling to the scalar tachyon mode).

Nevertheless, there are differences in the nonzero mode sectors between the boundary sine-Gordon approach and the boundary time-like Liouville approach. The origin of the difference is that the descendants for the boundary sine-Gordon model is based on the $SU(2)$ current algebra (at the self dual radius) and those for the boundary Liouville theory is based on the Virasoro algebra. For on-shell amplitudes (and energy-momentum tensor) we can gauge away these differences as we will do in section 5.2 to compute the closed string emission rate. However, at least in the two-dimensional noncritical string example, it has been stressed in [134] that such off-shell boundary states will be important to generate infinitely many conserved charges in addition to the energy momentum tensor. We will revisit the problem later in the discussion of the rolling D-brane, so we will not delve into the details any further at this point and concentrate on the physics associated with the zero mode.

5.2 Radiation from rolling tachyon boundary states

In this subsection, we would like to study the closed string emission rate from the rolling tachyon by using the exact boundary states. We will present rather a technical aspects of the computation for two reasons. One is that we are going to compare the results of the

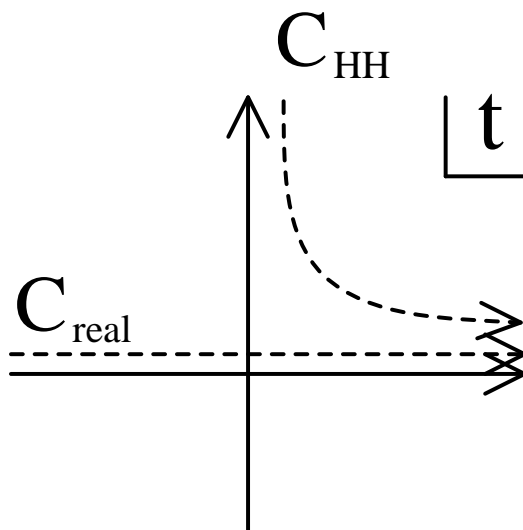


Figure 6: Different contour integration gives different boundary states.

rolling tachyon and rolling D-brane in later sections in detail. The other is to understand the nontrivial relation between the unitarity (optical theorem) and the open - closed duality, which we revisit in the more nontrivial rolling D-brane case in section 8.2.

Before entering into the computation, we summarize the main physics involved.

- At the one-loop level computation, all the energy of the D0-brane is converted into closed string radiation: the radiation rate shows a power-like divergence.
- Most of the energy is converted into highly massive strings whose mass is effectively cut off by $M \sim 1/g_s$.
- The emitted strings are highly non-relativistic.
- If one considers the Dp -brane as we increase p , the divergence becomes milder, but the spectral density is still power-like and the higher moment diverges.
- The inclusion of the *space-like* linear dilaton makes the divergence disappear due to the exponential suppression for the growth of density of states.
- On the contrary, the *time-like* linear dilaton (along the rolling tachyon direction) does not affect the divergence. This suggests a first hint of the universality of the decay of unstable D-branes.

Now we will begin our study on the closed string emission rate from the unstable D-brane. For a slight generalization of section 5.1, we consider the unstable D-brane in the linear dilaton background. For the boundary states, we will use the one obtained from the time-like Liouville theory because with a time-like linear dilaton, the corresponding boundary

states from the boundary sine-Gordon theory is unavailable. For zero time-like linear dilaton limit, however, the two computation agrees as expected.

The dilaton gradient is set by:

$$\Phi = \frac{1}{\sqrt{\alpha'}}(Q X^0 + \mathbf{V} \cdot \mathbf{X}), \quad \text{where} \quad Q \equiv \beta - \frac{1}{\beta} \quad (\beta \geq 1). \quad (5.10)$$

This puts the critical dimension D for the bosonic string theory to be

$$26 = D - 6Q^2 + 6\mathbf{V}^2, \quad \text{so} \quad c_{\text{eff}} = 6Q_\beta^2 - 6\mathbf{V}^2, \quad (5.11)$$

where $Q_\beta \equiv (\beta + 1/\beta)$. The effective central charge c_{eff} sets the growth of density of closed string states [122]:

$$\rho^{(c)}(M) \sim e^{4\pi\sqrt{\frac{c_{\text{eff}}}{24}\alpha'M^2}} \quad (5.12)$$

up to subleading pre-exponential factor of M . It grows slower than the density of states for flat space-time (obtainable by setting $Q = \mathbf{V} = 0$).

5.2.1 closed string emission

Let us consider the decay of an unstable D-brane in the linear dilaton background. The radiative transition of a Dp -brane to a single closed string state of mass M (set by the integer-valued oscillator level $N = \tilde{N}$), whose on-shell energy-momentum (ω, \mathbf{k}) is given by

$$\left(\omega_E - \frac{iQ}{\sqrt{\alpha'}}\right)^2 - \left(\mathbf{k}_E + \frac{i\mathbf{V}}{\sqrt{\alpha'}}\right)^2 = (\omega^2 - \mathbf{k}^2) = M^2 \quad \text{where} \quad \frac{1}{4}\alpha'M^2 = N - \frac{c_{\text{eff}}}{24}, \quad (5.13)$$

where (ω_E, \mathbf{k}_E) and (ω, \mathbf{k}) are energy-momenta in the Einstein and the string frame, respectively. In string loop perturbation theory, the transition amplitude is computed by the disk one-point function $\langle \exp((-i\omega + \frac{Q}{\sqrt{\alpha'}})X^0) \exp((i\mathbf{k} + \frac{\mathbf{V}}{\sqrt{\alpha'}}) \cdot \mathbf{X}) \rangle_{\text{disk}}$ with the Dp -brane boundary condition,⁶⁰ where the vertex operator is separated into temporal and spatial parts as indicated. The two parts are factorized in the gauge that no oscillator in temporal direction is allowed. Consequently, the transition probability $\mathcal{P}(\omega)$ of the radiative process is governed entirely by the temporal part (see (3.29) in [135]):

$$\begin{aligned} \mathcal{P}(\omega) &= \left| \left\langle e^{(-i\omega + \frac{Q}{\sqrt{\alpha'}})X^0} e^{(i\mathbf{k} + \frac{\mathbf{V}}{\sqrt{\alpha'}}) \cdot \mathbf{X}} \right\rangle_{\text{disk}} \right|^2 = \left| \frac{1}{\beta} \Gamma(1 + i\omega\sqrt{\alpha'}\beta) \Gamma(-i\omega\sqrt{\alpha'}/\beta) \right|^2 \\ &= \frac{\pi^2/\beta^2}{\sinh(\pi\omega\sqrt{\alpha'}\beta) \sinh(\pi\omega\sqrt{\alpha'}/\beta)}. \end{aligned} \quad (5.14)$$

Then, at leading order in string perturbation theory, the total number of emitted closed strings from the decay of a Dp -brane ($p \geq 1$) extended along \mathbf{V} -direction is computed as

$$\bar{\mathcal{N}} = N_p^2 V_p \sum_M \sqrt{\rho^{(c)}(M)} \int_{-\infty}^{\infty} \frac{d^{D-1-p}\mathbf{k}}{(2\pi)^{D-1-p}} \frac{1}{2\omega} \mathcal{P}(\omega), \quad (5.15)$$

⁶⁰We only consider the case when the D-brane has Neumann boundary condition in the space-like linear dilaton direction.

where the overall coefficient abbreviates $N_p = \pi^{\frac{D-4}{4}} (2\pi)^{\frac{D-2}{4}-p}$ and V_p is the D p -brane volume. In (5.2.1), the sum is over all final closed string states of mass M and of oscillator excitations symmetric between left- and right-moving sectors. Such oscillator excitations are equivalent in combinatorics to open string excitation, so the density of the final states is given by square-root of (5.12).

Attributed to the Hagedorn growth of the density of states $\rho^{(c)}(M)$, the total emission number $\bar{\mathcal{N}}$ in (5.2.1) (or higher spectral moment) is ultraviolet convergent so long as linear dilaton has a nonzero spatial component, $\mathbf{V} \neq 0$, first observed in [135]. Notice also that temporal component of the linear dilaton does not alter the ultraviolet behavior. This is most readily seen for small \mathbf{V} by expanding the density of states. To study anatomy of the ultraviolet behavior, we shall now perform Fourier transformation and re-express $\bar{\mathcal{N}}$ in the open string channel.

5.2.2 open string channel viewpoint

Physical observables such as $\bar{\mathcal{N}}$ ought to be well-defined under the Fourier transform from the closed string channel to the open string one because

1. We start with defining expression of $\bar{\mathcal{N}}$, consistent with the optical theorem in the closed string channel.
2. The expression is closed in the Euclidean signature. Hence we are free from any subtlety that may arise from analytic continuations between Euclidean and Lorentzian signature of the space-time.

As in [135], we expand the transition probability $\mathcal{P}(\omega)$ in convergent power series, whose terms can be interpreted as D-instantons arrayed along imaginary time coordinate:

$$\mathcal{P}(\omega) = \frac{4\pi^2}{\beta^2} \sum_{n,m=0}^{\infty} e^{-2\pi\alpha'\omega W(m,n)} \quad (5.16)$$

where the location of the D-instantons is denoted as

$$\alpha'W(m,n) = \sqrt{\alpha'} \left[\left(n + \frac{1}{2}\right)\beta + \left(m + \frac{1}{2}\right)\frac{1}{\beta} \right] \geq \sqrt{\alpha'} . \quad (5.17)$$

Thus, we take

$$\bar{\mathcal{N}} = \left(\frac{2\pi N_p}{\beta}\right)^2 V_p \sum_M \int_{-\infty}^{\infty} \frac{d^{D-1-p}\mathbf{k}}{(2\pi)^{D-1-p}} \sum_{m,n=0}^{\infty} \frac{1}{2\omega} e^{-2\pi\alpha'\omega W(m,n)} \quad (5.18)$$

and rewrite each D-instanton contribution parametrically via the closed string channel modulus t_c as

$$\frac{1}{2\omega} e^{-2\pi\alpha'\omega W(m,n)} = \frac{\pi\alpha'}{2} \int_{-\infty}^{\infty} \frac{dk_0}{2\pi} \int_0^{\infty} dt_c e^{-2\pi t_c \cdot \frac{1}{4}\alpha'(k_0^2 + \mathbf{k}^2 + M^2)} e^{2\pi i\alpha' k_0 W(m,n)} , \quad (5.19)$$

which gives

$$\begin{aligned} \overline{\mathcal{N}} = & \left(\frac{2\pi N_p}{\beta}\right)^2 V_p \frac{\pi\alpha'}{2} \sum_{m,n=0}^{\infty} \int_0^{\infty} dt_c \int_{-\infty}^{\infty} \frac{dk_0}{2\pi} \int_{-\infty}^{\infty} \frac{d^{D-1-p}\mathbf{k}}{(2\pi)^{D-1-p}} e^{-2\pi t_c \cdot \frac{1}{4}\alpha'(k_0^2 + \mathbf{k}^2)} e^{2\pi i\alpha' k_0 W(m,n)} \\ & \times \sum_M \sqrt{\rho^{(c)}(M)} e^{-2\pi t_c \cdot \frac{1}{4}\alpha' M^2}. \end{aligned} \quad (5.20)$$

Here, we exchanged order of summations and integrations, and first performed integrals over off-shell momenta (k_0, \mathbf{k}) and sum over mass level M . The sum over M yields modular covariant partition function $Z^{(c)}(q_c)$ in terms of the Dedekind eta function:

$$\begin{aligned} Z^{(c)}(q_c) &\equiv \sum_M \sqrt{\rho^{(c)}(M)} q_c^{\frac{1}{4}\alpha' M^2} \quad \text{where} \quad q_c \equiv e^{-2\pi t_c} \\ &= \eta^{-(D-2)}(q_c). \end{aligned} \quad (5.21)$$

Integrations over the $(D-p)$ -dimensional momenta (k_0, \mathbf{k}) yield $(2\pi^4\alpha't_c)^{-(D-p)/2}$ times Gaussian damping factor $e^{-2\pi\alpha'W^2(m,n)/t_c}$. We now perform modular transformation to the open string channel $t_c = 1/t_o$, where t_o is modulus of the open string channel and $q_o \equiv e^{-2\pi t_o}$. Putting all these together, we finally have

$$\overline{\mathcal{N}} = C_p V_p \sum_{m,n=0}^{\infty} \int_0^{\infty} \frac{dt_o}{t_o} t_o^{-p/2} e^{-2\pi t_o \alpha' W^2(m,n)} \eta^{-(D-2)}(q_o), \quad (5.22)$$

with $C_p = \left(\frac{2\pi N_p}{\beta}\right)^2 \frac{\pi\alpha'}{2} (2\alpha'\pi^4)^{-\frac{D-p}{2}}$, reproducing the result reported in [135]. As it stands, the final expression (5.22) is at odd to the intuition based on, for example, the Schwinger pair production in (time-dependent) electric field, since the integral over the open string modulus t_o is still intact. If the total emission number can be interpreted as arising from on-shell two-particle branch cut in the open string channel, the modulus integral ought to be absent! Therefore, To understand underlying physics better, we shall now compute the cylinder amplitude directly and then extract the imaginary part via the optical theorem.

5.2.3 Lorentzian cylinder amplitude

Unitarity and optical theorem thereof, combined with the open-closed string channel duality, should enable us to extract the emission number $\overline{\mathcal{N}}$ of closed strings from decaying Dp -brane as the imaginary part of the cylinder amplitude. In the closed string channel diagram, the computation reduces to (5.2.1), as in quantum field theory. It is, however, somewhat nontrivial to evaluate the imaginary part of the cylinder amplitude directly from the open string channel. Here we present the *ab initio* derivation, refining that in the text of [135], by starting with manifestly well-defined Lorentzian cylinder amplitude.

We begin with the cylinder amplitude in the closed string channel in which both the world-sheet and the target space-time signatures are taken Lorentzian. Omitting overall

numerical factors for the moment, the amplitude is given by

$$Z_{\text{cylinder}} = i\pi\alpha'V_p \int_{s_c^{\text{IR}}}^{s_c^{\text{UV}}} ds_c \int_{-\infty}^{\infty} \frac{d\omega_L}{2\pi} \frac{\pi^2/\beta^2 \cdot q_c^{-(1-i\hat{\epsilon})^2 \frac{1}{4}\alpha'\omega_L^2}}{\sinh(\pi\beta\omega_L\sqrt{\alpha'}) \sinh(\pi\omega_L\sqrt{\alpha'}/\beta)} Z_{\mathcal{M}}^{(c)}(q_c), \quad (5.23)$$

where $q_c = e^{2\pi i\tau_c}$ with $\tau_c = s_c + i\epsilon$, and $Z_{\mathcal{M}}(q_c)$ represents the contribution from the closed string zero-modes and oscillator parts.⁶¹ The Lorentzian world-sheet is regularized by $i\epsilon$ prescription, while the Lorentzian space-time is regularized by $-i\hat{\epsilon}$ -prescription. s_c^{UV} (s_c^{IR}) is an ultraviolet (infrared) regulator of the closed string channel modulus. With these prescriptions, the integral over ω_L is convergent so long as $2\hat{\epsilon}s_c^{\text{UV}} > \epsilon > 0$ is retained.

Defining the open string modular parameter as $q_o = e^{-2\pi i\tau_o}$ where $\tau_o = s_o - i\epsilon$ with $s_o = 1/s_c$, one can rewrite (5.23) in terms of open string channel energy ω'_L as

$$Z_{\text{cylinder}} = V_p \int_{s_o^{\text{UV}}}^{s_o^{\text{IR}}} ds_o \int_{-\infty}^{\infty} d\omega'_L \left(i\pi\alpha' \int_{-\infty}^{\infty} d\omega_L \frac{\cos(\pi\alpha'\omega_L\omega'_L)}{\sinh(\pi\beta\omega_L\sqrt{\alpha'}) \sinh(\pi\omega_L\sqrt{\alpha'}/\beta)} \right) \times q_o^{-(1+i\hat{\epsilon}')^2 \frac{1}{4}\alpha'\omega'_L{}^2} Z_{\mathcal{M}}^{(o)}(q_o), \quad (5.24)$$

where $s_o^{\text{IR}} \equiv 1/s_c^{\text{UV}}$, $s_o^{\text{UV}} \equiv 1/s_c^{\text{IR}}$ are the cut-off's in the open string modulus. As opposed to the closed string channel, we have to adopt the $+i\hat{\epsilon}'$ -prescription for the Lorentzian space-time, and the above integral is well-defined as long as $2\hat{\epsilon}'s_o^{\text{UV}} > \epsilon$. The expression in the large parenthesis yields the open string density of states, $\rho^{(o)}(\omega'_L)$. It is infrared divergent at $\omega_L = 0$. To regularize it, we subtract minimally the double pole⁶² so that

$$\begin{aligned} \rho^{(o)}(\omega'_L)_{\text{reg}} &= i\pi\alpha' \int_{-\infty}^{\infty} d\omega_L \left(\frac{\cos(\pi\alpha'\omega_L\omega'_L)}{\sinh(\pi\beta\omega_L\sqrt{\alpha'}) \sinh(\pi\omega_L\sqrt{\alpha'}/\beta)} - \frac{1}{\pi^2\alpha'\omega_L^2} \right) \\ &= -2\partial_{\omega'_L} \log S_{\beta} \left(Q_{\beta} + i\sqrt{\alpha'}\omega'_L \right), \end{aligned} \quad (5.25)$$

where the ‘ q -Gamma function’ $S_{\beta}(x)$ is defined by⁶³

$$-\partial_x \log S_{\beta}(x) = \int_{-\infty}^{\infty} dt \left(\frac{\cosh((x - Q_{\beta})t)}{2 \sinh(\beta t) \sinh(t/\beta)} - \frac{1}{2t^2} \right) \quad (5.26)$$

for $\text{Re}(x) < 2Q_{\beta}$ and analytically continued to the whole complex plane.⁶⁴ See, for example, [92, 93].

Now we perform the Wick-rotation both in the target space and on the world-sheet. First, Wick rotate the open string channel energy as $\omega'_L \rightarrow e^{i(\frac{\pi}{2}-0)}\omega'_L$ and set $\omega'_L = i\omega'$ ($\omega' \in \mathbb{R}$). Then, we can safely Wick rotate the world-sheet Schwinger parameter as $s_o \rightarrow -it_o$ ($t > 0$). Notice that we will need to perform the Euclidean rotation in opposite direction for the

⁶¹We are using different normalization for modulus parameters from [135]: $t(\text{KLMS}) = (\pi/4)t(\text{here})$. In addition, they adopted $\alpha' = 1$ convention.

⁶²This subtraction does not affect the imaginary part of the partition function we are primarily interested in.

⁶³Here the normalization of variable x differs with factor 2 from the one given in [92].

⁶⁴Notice that the Lorentzian density (5.25) is well-defined without the analytic continuation. We stress that this should be contrasted against the approach of [135].

closed and the open string channels due to the difference of the $i\epsilon$ -prescription. There is no obstruction in such contour deformation because $\partial_x \log S_\beta(x)$ has poles only on the real axis. We will see that this is specific to the decaying D-brane situation and do not hold generally. In fact, in section 8.2 dealing with the rolling D-branes, we shall show that there exist extra contributions from crossing poles in the course of the contour rotation and that their contributions are essential for maintaining the unitarity. After Wick rotating the world-sheet, the cylinder amplitude in the open string sector is given by

$$Z_{\text{cylinder}} = -2V_p \int_0^\infty dt_o \int_{(1-i0)\mathbb{R}} d\omega' \partial_{\omega'} \log S_\beta \left(Q_\beta - \sqrt{\alpha'} \omega' \right) q_o^{\frac{1}{4} \alpha' \omega'^2} Z_M^{(o)}(q_o) . \quad (5.27)$$

Imaginary part of the partition function comes from the simple poles of the q -Gamma function $S_\beta(Q_\beta - \sqrt{\alpha'} \omega')$ at $\frac{1}{2} \omega' = W(m, n)$ for $n, m \in \mathbb{Z}_{\geq 0}$ and simple zeros for $n, m \in \mathbb{Z}_{< 0}$. Therefore, collecting imaginary parts from the contour integration over ω' and applying the optical theorem, we finally obtain

$$\overline{\mathcal{N}} = \text{Im } Z_{\text{cylinder}} = C_p V_p \sum_{n, m=0}^\infty \int_0^\infty \frac{dt_o}{t_o} t_o^{-\frac{p}{2}} e^{-2\pi t_o \alpha' W^2(m, n)} \eta^{-(D-2)}(q_o) , \quad (5.28)$$

where we have evaluated the free oscillator part explicitly and reinstated overall numerical factors. This is in perfect agreement with (5.10), and it may be interpreted as a nontrivial check of unitarity and open-closed duality in the Lorentzian signature.

5.2.4 D-brane decay in two-dimensional string theory

In a similar method, one can compute the spectral observables from the D-brane decay in two-dimensional string theory [136]. The boundary state for the unstable D-brane in two-dimension is given by the ZZ-brane boundary state [137]:

$$\langle e^{(ik+2/\sqrt{\alpha'})\phi} \rangle_{\text{disk}} = \mu^{-\frac{i}{2} \sqrt{\alpha'} k} \frac{2\sqrt{\pi}}{\Gamma(1 - ik\sqrt{\alpha'}) \Gamma(ik\sqrt{\alpha'})} . \quad (5.29)$$

Combining it with the rolling tachyon boundary states, the total emission number of closed string is given by

$$\overline{\mathcal{N}} = N_o^2 \int_0^\infty dk \int_0^\infty \frac{d\omega}{2\omega} \mathcal{P}(\omega, k) \delta(\omega - k) , \quad (5.30)$$

where the on-shell condition $\omega = k$ is imposed, and the transition probability is

$$\mathcal{P}(\omega, k) = \left| \langle e^{-i\omega X^0} e^{(ik+2/\sqrt{\alpha'})\phi} \rangle_{\text{disk}} \right|^2 = \frac{\sinh^2(\pi k \sqrt{\alpha'})}{\sinh^2(\pi \omega \sqrt{\alpha'})} . \quad (5.31)$$

We see that, after performing the k -integration, the resultant total emission number is ultraviolet divergent.

To express $\overline{\mathcal{N}}$ in open string channel, we repeat the analysis of section 5.2.3 and expand the transition probability in arrays of imaginary D-instantons. The result is

$$\begin{aligned}\overline{\mathcal{N}} &= N_o^2 \sum_{m,n=0}^{\infty} \int_0^{\infty} dk \int_0^{\infty} dt_c \int_{-\infty}^{\infty} \frac{dk_0}{2\pi} e^{-2\pi t_c \cdot \frac{1}{4}\alpha'(k_0^2+k^2)} e^{2\pi i\alpha' k_0 W(m,n)} \sinh^2(\pi k\sqrt{\alpha'}) \Big|_{\beta \rightarrow 1} \\ &= N_o^2 \sum_{m,n=0}^{\infty} \int_0^{\infty} \frac{dt_o}{t_o} \left(\frac{1}{q_o} - 1\right) q_o^{\alpha' W^2(m,n)} \Big|_{\beta \rightarrow 1},\end{aligned}\tag{5.32}$$

where we have reinstated $W(m,n)$ for the purpose of regularization.⁶⁵ The expression exhibits ultraviolet divergence as $t_o \rightarrow \infty$.

On the other hand, it is possible to obtain the same radiation rate from the direct evaluation of the imaginary part of the Lorentzian cylinder amplitude in the open-string channel as was done in section 5.2.3:

$$Z_{\text{cylinder}} = iN_o^2 \int_0^{\infty} ds_c \int_{-\infty}^{\infty} \frac{d\omega_L}{2\pi} \int_0^{\infty} \frac{dk}{2\pi} \frac{\sinh(\pi\sqrt{\alpha'}k)^2}{\sinh(\pi\sqrt{\alpha'}\omega_L)^2} q_c^{\frac{1}{4}\alpha'(-\omega_L^2+k^2)}.\tag{5.33}$$

After rewriting the open string density by the q -Gamma function as in section 5.2.3, we obtain open string channel expression of the partition function. We then find the imaginary part from the poles located at $\frac{1}{2}\omega' = W(m,n)$, and reproduce (5.32). This confirms that the partition function is manifestly unitary, obeying the optical theorem. Here again, the regularization $\beta \rightarrow 1$ is implicit.

5.2.5 ZZ brane decay in various dimensions

It is possible to generalize the discussion of section 5.2.4 for ZZ branes in various dimensions by introducing the time-like linear dilaton theory. If we write the dilaton slope of the Liouville and time-like linear dilaton direction as $V_\phi = b + b^{-1}$ and $V_t = \beta - \beta^{-1}$ respectively, the criticality condition is given by

$$26 = D + 6V_\phi^2 - V_t^2.\tag{5.34}$$

We can combine the one-point function for the ZZ brane (with general b) and the decaying D-brane boundary states for the boundary time-like Liouville theory to compute the radiation rate as was studied in [138]. A similar cancellation as we discussed in section 5.2.1 gives the UV power-like structure of the closed string radiation rate.⁶⁶ The result suggests again the universality of the decaying D-brane spectrum.

In this construction, owing to the criticality condition (5.34), the existence of the time-like dilaton is unavoidable. In the following, we study the decay of the ZZ brane in $\mathcal{N} = 2$ Liouville theory (or D0-brane Euclidean $SL(2; \mathbb{R})/U(1)$ coset model. See section 6 for more details) to study more realistic models, where $\beta = 1$ (i.e. flat limit) is feasible (see [139] for a particular case. This subsection is based on a generalization of their results).

⁶⁵Because of the subtraction of singular vector in $(1/q_o - 1)$, the resultant amplitude is *non-unitary*.

⁶⁶Technically speaking, for $D > 26$, we encounter a closed string IR divergence [138].

The absolute square of the boundary wavefunction for the $\mathcal{N} = 2$ ZZ-brane is given by

$$|\Psi(p, m)|^2 = \delta_{m, \bar{m}} \frac{\sinh(2\pi p) \sinh(2\pi p/k)}{\cosh(2\pi p) + \cos(\pi m)}, \quad (5.35)$$

while that for the ($\mathcal{N} = 1$ supersymmetric) rolling D-brane with time-like linear dilaton $V_t = \beta - \beta^{-1}$ is

$$|\Psi(E)^2| = \frac{1}{\sinh(\beta E) \sinh(\beta^{-1} E)}. \quad (5.36)$$

We can evaluate the on-shell ($E^2 = M^2 + \frac{p^2}{2k} + \frac{m^2}{2k}$) emission with fixed transverse mass M as

$$\begin{aligned} N(M) &= \int dp \sum_m |\Psi(p, m)|^2 |\Psi(E(p, m))|^2 \\ &\sim \int dp e^{\frac{\pi}{k} p - \pi(\beta + \beta^{-1}) \sqrt{M^2 + \frac{p^2}{2k}}} \\ &\sim e^{-2\pi M \sqrt{(\frac{\beta + \beta^{-1}}{2})^2 - \frac{1}{2k}}}, \end{aligned} \quad (5.37)$$

where in the last line we have used the saddle point approximation.

On the other hand, the density of states for the emitted closed string for large M is given by

$$\sqrt{\rho^{(c)}} \sim e^{4\pi M \sqrt{\frac{c_{\text{eff}}}{24}}} = e^{2\pi M \sqrt{(\frac{\beta + \beta^{-1}}{2})^2 - \frac{1}{2k}}}. \quad (5.38)$$

Thus, we see an exact cancellation of the exponential part of the closed emission rate, leaving us with a familiar power-like universal closed string emission rate.

We have several comments here

- We can analyse the bosonic case in the same way. The first difference is k in (5.35) should be replaced with $\kappa - 2$. The second difference is E in (5.36) should be replaced with $\sqrt{2}E$. The final closed string emission rate changes, as a consequence, to $N(M) \sim e^{-2\pi \sqrt{(\beta + \beta^{-1})^2/2 - \frac{1}{2(\kappa - 2)}}}$, which will cancel against the bosonic Hagedorn density of states $\sqrt{\rho^{(c)}} \sim e^{4\pi M \sqrt{\frac{c_{\text{eff}}}{24}}} \sim e^{2\pi \sqrt{(\beta + \beta^{-1})^2/2 - \frac{1}{2(\kappa - 2)}}$.
- For simplicity, we studied the emission rate from the closed string perspective. The open string computation like we did in section 5.2.2, 5.2.3 is straightforward, and we will not repeat it here.
- The conclusion here is independent of the level k of the $SL(2; \mathbb{R})/(1)$, which, on one hand, suggests a universality of the D-brane decay. On the other hand, it seems curious to observe that nothing special happens at $k = 1$, where we expect a “black hole - string transition”. As we will see in section 7, 8 in detail, the rolling (or Euclidean hairpin) D-brane captures or probes the “black hole - string transition”. We will return to this question in section 9.

5.2.6 electric field and long string formation

One simple generalization of the rolling D-brane was, as we studied in section 5.1.3, the inclusion of the linear dilaton. Another simple generalization is to introduce constant electric field on the D-brane, i.e. we introduce the fundamental string charge [140, 141].

In order to introduce the constant electric field (say $F^{01} = \epsilon$) on the D-brane, we can use the stringy version of the Lorentz boost. The successive applications of T-duality, Lorentz boost and inverse T-duality, we end up with the boundary states with electric flux. Operationally, the transformation is

$$\begin{aligned} |0\rangle &\rightarrow \gamma|0\rangle, \quad t \rightarrow \gamma^{-1}t, \quad \omega \rightarrow \gamma\omega \\ \begin{pmatrix} \alpha^0 \\ \alpha^1 \end{pmatrix} &\rightarrow \Lambda^{-1} \begin{pmatrix} \alpha^0 \\ \alpha^1 \end{pmatrix}, \quad \begin{pmatrix} \bar{\alpha}^0 \\ \bar{\alpha}^1 \end{pmatrix} \rightarrow \Lambda \begin{pmatrix} \bar{\alpha}^0 \\ \bar{\alpha}^1 \end{pmatrix}, \end{aligned} \quad (5.39)$$

where

$$\Lambda = \gamma \begin{pmatrix} 1 & \epsilon \\ \epsilon & 1 \end{pmatrix}, \quad \gamma = \frac{1}{\sqrt{1-\epsilon^2}}. \quad (5.40)$$

From this transformation law, the energy momentum tensor can be easily read as

$$\begin{aligned} T_{00} &\sim E\gamma \\ T_{01} &\sim -Ee^2\gamma - E\gamma^{-1}\exp(-\gamma^{-1}t) \\ T_{11} &\sim -E\gamma^{-1}\exp(-\gamma^{-1}t), \end{aligned} \quad (5.41)$$

in the $t \rightarrow \infty$ limit. The study of the closed string radiation from the boundary states is straightforward. When x^1 direction is noncompact, the result is

$$\langle N \rangle = \sum_M \int dk \frac{|\Psi(\omega_{k,M})|^2}{2\omega_{k,M}} \simeq \int^\infty dM \sqrt{\rho^{(c)}(M)} e^{-2\pi\gamma M} = \int^\infty dM e^{-2\pi(\gamma-1)M} \quad (5.42)$$

and the total emission rate is exponentially suppressed essentially due to the Lorentz time delay [142, 143].

Now let us suppose that x^1 direction is compactified with the radius R . In this case, we have to sum over the winding mode:

$$N(M) = \sum_w \int dk \frac{|\Psi(\omega_{k,M})|^2}{2\omega_{k,M}} \simeq \sum_w \int dk e^{-2\pi\gamma(\sqrt{(wR)^2+k^2+M^2}-\epsilon R w)}. \quad (5.43)$$

For large M , the summation over w can be evaluated by the saddle point methods, which leads to

$$\langle N \rangle \sim \int^\infty dM \sqrt{\rho^{(c)}(M)} N(M) \sim \int^\infty dM M^\beta \quad (5.44)$$

We recover the power-like behavior of the emission rate [144].⁶⁷ The computation reveals that the winding mode dominates the emission rate in the electrified D-brane decay. Mathematically, this is due to the (T-dualized) Lorentz invariance in the $R \rightarrow 0$ limit. Physically, the decay of the D-brane produces many long macroscopic strings as a final decay product, which has a cosmological significance as we will review in section 5.5.

⁶⁷The power dependence β is determined from the details of the model e.g. dimensionality of the D-brane and the details of the internal CFT etc.

5.3 Classical correspondence

The Dirac-Born-Infeld form of the rolling tachyon effective action (5.1) suggests a possible geometrical interpretation of the open string tachyon condensation. Such a geometrical interpretation of the rolling tachyon process would shed a new light upon our understanding of the nature of the open string tachyon and its condensation. It would also provide a guiding principle for a geometrical interpretation of the closed string tachyon condensation, for qualitative properties of the closed string tachyon condensation are poorly understood compared with the open string tachyon condensation.

In [145], an interesting connection between the D-brane motion in the (near horizon) NS5-brane background and the rolling tachyon dynamics was pointed out. Since the NS5-brane has a tension proportional to $1/g_s^2$, in perturbative string theories, we can regard it as a fixed background, in which the D-brane, whose tension is proportional to $1/g_s$ moves. In other words, in the perturbative string theories, the probe D-brane approximation is good and trustful.

The effective action for the D-brane motion in NSNS-background (i.e. without any R-R fields), is given by the Dirac-Born-Infeld action

$$S = -T_p \int d^{p+1} \sigma e^{-\Phi} \sqrt{-\det(X^*[G + B]_{\mu\nu})} , \quad (5.45)$$

where $X^*[G + B]$ denotes the pullback to the Dp -brane world-volume.

As proposed in [145], let us consider the D0-brane motion in near horizon NS5-brane geometry (2.3).⁶⁸ Let us fix the world-sheet reparametrization invariance by taking the static gauge $\sigma^0 = t$. In this gauge, the DBI action reduces to

$$S = -T_0 \int dt e^{\frac{\rho}{\sqrt{2k}}} \sqrt{1 - \dot{\rho}^2} , \quad (5.46)$$

where dot denotes the derivative with respect to $\sigma_0 = t$, and we have rescaled the radial direction ρ so that we have a canonical kinetic term.

Let us compare the effective action for the radion field ρ (5.46) with the open string tachyon effective action (5.1). It is almost clear in the large (negative) region of ρ , these two expressions essentially coincide with each other.⁶⁹ This is the classical ‘‘tachyon - radion correspondence’’: one can identify the effective action for the rolling tachyon problem with the effective action for the rolling D-brane in the NS5-brane, or linear dilaton, background. The ‘‘radion field’’ ρ plays the role of the tachyon field T here. Note, however, that the radion field is actually not tachyonic, although it has run-away potential, nor has an unstable extremum in the potential because it is a massless field at the tree level.

One can readily solve the classical equation of motion based on the action (5.46) as

$$e^{-\frac{\rho}{\sqrt{2k}}} = c \cosh\left(\frac{t}{\sqrt{2k}}\right) , \quad (5.47)$$

⁶⁸If one considers a homogeneous motion of the D-brane, the net result does not depend on the spacial dimension of the D-brane. We also assume that D-brane sits at a point in the internal space S^3 .

⁶⁹If one take $k = 2$, the coincidence becomes exact including the numerical factor in the tachyon (radion) potential.

which agrees with the late time behavior of the rolling tachyon problem (5.3). The energy momentum tensor can be read as

$$\begin{aligned} T_{00} &= E\delta(\rho - \rho_0(t)) \\ T_{0\rho} &= E \tanh\left(\frac{t}{\sqrt{2k}}\right) \delta(\rho - \rho_0(t)) \\ T_{ij} &= -E \operatorname{sech}^2\left(\frac{t}{\sqrt{2k}}\right) \delta(\rho - \rho_0(t)) \delta_{ij} \quad (i, j = 1, \dots, p), \end{aligned} \quad (5.48)$$

where $\rho_0(t)$ is the classical solution of the radion motion (5.47). As expected, the energy momentum tends to that for a pressure-less dust as $t \rightarrow \infty$. The (0ρ) component has a natural interpretation as the momentum transfer in the ρ direction because the decaying D-brane moves in the ρ direction almost at the speed of light as $t \rightarrow \infty$.

What is the end point of the ‘‘radion condensation’’? In the case of the open string tachyon condensation, Sen’s conjecture states that we end up with the closed string vacuum, where the open string excitation becomes infinitely massive and disappear from the physical spectrum. From the effective field theory approach taken here, it is difficult to establish this statement in a satisfactory manner because in the large ρ regime, the effective string coupling becomes larger due to the linear dilaton gradient. One way to study this might be to uplift the system to M-theory (e.g. by using the interpolating metric proposed in [146]). The subsequent physics, however, is intuitively clear: the D-brane will be absorbed into the NS5-brane and form a non-threshold bound states. The open string spectrum on the D-brane should be modified so that it matches with the excitation on the bound states.⁷⁰

There are several generalizations of the problem. One interesting question is whether we can obtain the effective DBI action having the exactly identical potential with the rolling tachyon not only in the large ρ region. This is possible by considering an array of the NS5-brane on $\mathbb{R}^3 \times \mathbb{S}^1$ rather than the stack of NS5-branes in \mathbb{R}^4 [147]. Because of the oppositely-directed attractive force between two NS5-branes, the potential of the D-brane can have a local extremum:

$$S = -T_0 \int dt \frac{1}{\cosh \frac{\rho}{\sqrt{2k}}} \sqrt{1 - \dot{\rho}^2}, \quad (5.49)$$

which completely agrees with (5.1). Unfortunately, unlike the NS5-branes on \mathbb{R}^4 , the exact quantization of the rolling D-brane in this geometry is unavailable.⁷¹

Another interesting generalization is to consider the D-brane motion in the non-extremal black NS5-brane background. Interestingly, after a simple coordinate transformation, the classical motion of D-brane in the non-extremal NS5-brane (outside of the horizon) is identical to that in the extremal NS5-brane. To see this we note that, by introducing ‘tachyon’ variable $Y \equiv \log \sinh \rho$, DBI Lagrangian of the D0-brane can be cast to that of rolling

⁷⁰It would be an interesting open problem to study the tachyon - radion correspondence from the open string field theory and prove the analogue of Sen’s conjecture.

⁷¹The exact boundary states for *static* (unstable) brane in a similar background has been constructed in [27], which reproduces the mass of the geometrical tachyon (i.e. radion).

tachyon:

$$L_{D0} = -e^{-\Phi} \sqrt{\left(\frac{ds}{dt}\right)^2} = -V(Y) \sqrt{1 - \dot{Y}^2} \quad \text{where} \quad V(Y) = M_0 e^Y, \quad (5.50)$$

if we restricted ourselves to the region outside of the horizon. An important point is that, in sharp contrast to the extremal background (2.3), the dilaton is finite everywhere. Thus, the strong coupling singularity is now capped off by the horizon. The construction of the exact boundary states for the rolling D-brane in the two-dimensional black hole (or non-extremal NS5-brane) is one of the main themes of this thesis.

For another example of exactly solvable deformation, one can introduce constant electric fields as we did in the rolling tachyon example. This has been studied in [148], where we have constructed exact boundary states and have shown the correspondence between the electrified rolling tachyon problem and the electrified rolling radion problem even with $\alpha' \sim 1/k$ corrections. As yet another generalization, the rotating D-brane solution in NS5-brane background has been also studied in [145], which could be regarded as a rotational Lorentz boosted solution as pointed out in [148], but the exact boundary state is yet to be constructed. Other classical studies of D-brane motion in related background include [149, 150, 151, 152, 153, 154, 155, 156, 157, 158, 159, 160, 161, 162, 163, 164, 165].

Before concluding this subsection, we would like to stress again that the correspondence at the level of the effective action is only valid in the large ρ or T regime, where the effective action analysis loses its validity because the effective string coupling grows there. Therefore, the quantum correspondence we will prove in later sections, based on the one-loop string perturbation theory, is actually not so obvious, and we should rather regard it as a highly nontrivial statement of the universality of the properties of decaying D-branes.

5.4 Quantum correspondence

So far, we have mainly discussed the classical correspondence between the rolling tachyon problem and the rolling radion problem at the level of the effective action. Aside from the debate over the effectiveness of the rolling tachyon DBI-like action (5.1), we have one tunable parameter k in the rolling radion problem, so it is important to analyse a possible k dependence of this correspondence.

We know that $1/k$ measures the α' corrections to the background geometry from the discussion in section 2. When k becomes larger, the classical geometry, and hence, the DBI action is more trustful. On the other hand, when k becomes smaller, the geometry shows large α' corrections and the effective action approach may break down. Especially, the exact correspondence at the level of the effective action requires $k = 2$, which is rather in a strongly coupled regime.⁷²

In particular, if one considers the two-dimensional black hole geometry (as the non-extremal NS5-branes background), the appearance of the stretched horizon blurs the geometry. In addition, we expect a “black hole - string transition” at $k = 1$. It is of utmost interest to probe such a phase transition from the rolling D-brane.

⁷²In the bosonic case, we need to set $k = 1$.

In the following sections, we will construct the exact boundary states for such rolling D-branes in NS5-brane background, and reveal the nature of the $1/k \sim \alpha'$ corrections to the tachyon - radion correspondence. After the construction of the exact boundary states, we study the closed string radiation rate as we did in the rolling tachyon case in section 5.2 and compare the results.

For convenience, we summarize our main physical results here [1]:

1. The closed string emission rate from the rolling D-brane (which will be computed in section 8.2) yields exactly the same behavior as that from the rolling tachyon (which was computed in section 5.2). Especially, the power-like behavior of the spectrum density does not depend on k (up to an overall normalization). This is true as long as $k > 1$, and confirms the tachyon - radion correspondence from the exact boundary states.
2. Independence of the extra parameter k , which even governs the world-sheet (stringy) α' correction suggests a universal nature of the decaying D-brane: all the energy of the D-brane will be radiated as a gas of closed strings, whose dominant contribution comes from the highly massive (long) strings. If one introduces the fundamental string charge, as an electric flux, the dominant contributions from the rolling D-brane again comes from the winding strings as we have seen in the rolling tachyon problem in section 5.2.6.
3. The situation changes drastically if one studies the case $k < 1$. The closed string emission rate is exponentially suppressed, and the tachyon - radion correspondence breaks down. This is in accord with the “black hole - string transition” at $k = 1$ discussed in section 4. Our result is the first physical manifestation of the “black hole - string transition” in the two-dimensional black hole probed by the rolling D-brane.

5.5 Cosmological implications

From the early days of its invention, the rolling tachyon system has also been studied in the context of the cosmological applications. In particular, the realization of the inflation in string theory has attracted more and more attention recently with increasing evidence for the existence of such period in the history of our universe (see [166] and references therein). Indeed, one of the simplest proposals for the inflation from the string theory is the tachyon inflation, where the (open string) tachyon plays the role of the inflaton [167, 168, 169, 170, 171]. The tachyon - radion correspondence discussed so far enables us to consider varieties of radion (or geometrical tachyon) inflation. From the classical tachyon - radion correspondence, many features of the tachyon inflation can be translated into that of the radion inflation with more generalities [172].

The starting point of the tachyon (radion) inflation is (minimal) coupling of the DBI-like action (5.1) (5.46) to the gravity:

$$L_{\text{eff}} = \sqrt{-g} \left(\frac{R}{16\pi G} - V(T) \sqrt{1 + g^{\mu\nu} \partial_\mu T \partial_\nu T} \right). \quad (5.51)$$

For our realistic application, we consider the four-dimensional (non-compact) space-time, and $8\pi G = M_p^{-2}$ with the four-dimensional Planck constant M_p . Under the assumption of the Friedman-Robertson-Walker isotropic universe, the four dimensional metric can be written as⁷³

$$ds^2 = -dt^2 + a(t)^2 dx_i^2 \quad (i = 1, 2, 3) . \quad (5.52)$$

We begin with the equation of motion for T :

$$\frac{\ddot{T}}{1 - \dot{T}^2} + 3H\dot{T} + \frac{V'}{V} = 0 , \quad (5.53)$$

where the prime denotes the derivative with respect to T (i.e. $V' = \partial V(T)/\partial T$) and the dot denotes the time derivative. H here denotes the Hubble parameter $H \equiv \dot{a}/a$. In the slow-roll approximation (i.e. $\dot{T} \gg 1$), the Friedman equation reads

$$H^2 = \left(\frac{\dot{a}}{a}\right)^2 = \frac{V(T)}{3M_p^2} , \quad (5.54)$$

and the slow-roll equation reduces to

$$3H\dot{T} = \frac{V'(T)}{V} . \quad (5.55)$$

For the slow-roll parameter $\eta \sim (H')^2/H^4$ to be small enough, we must require

$$H^2 \gg \frac{(V')^2}{V^2} . \quad (5.56)$$

Suppose our (geometrical) tachyon potential has a local extremum as is the case with the rolling tachyon and the geometrical tachyon in the array of NS5-brane backgrounds. Inflation near the local extremum is possible if $H^2 \gg |m^2|$, where m^2 is the mass for the (geometric) tachyon. The condition is equivalent to

$$\frac{g_s}{vl_s} \gg \frac{C}{kl_s} , \quad (5.57)$$

where v is the volume of the compactification,⁷⁴ and if we kept track of every numerical factor, we could find $C \sim 260$. In the original rolling tachyon problem, $k = 2$ and it is difficult to find a consistent solution in the perturbative string theory while maintaining the COBE normalization $H/M_p \sim 10^{-5}$ [167, 168]. In the geometric tachyon, we have one parameter k , and if we choose large enough k , it is possible to satisfy the condition (5.57) consistent with the COBE normalization. We can also satisfy the slow-roll condition in the geometric tachyon. For instance, $\eta \ll 1$ is equivalent to the condition $H \gg |m|$ for $T < O(1)$.

⁷³Since the inflation flattens the space in an exponential manner, we have assumed a flat space universe for simplicity.

⁷⁴We are assuming a direct product type compactification. If we consider the warped compactification, we can relax the condition.

The key point here is that we have an extra tunable parameter k to obtain a sustainable inflation in the case of the geometric tachyon unlike the original rolling tachyon cosmology, where such a tunable parameter is absent.

Nevertheless, we still have a serious drawback of this rolling tachyon (radion) type cosmology as pointed out in [167, 168, 171]. The problem is related to how the inflation will end. Since the effective potential for the rolling tachyon (radion) runs away exponentially as $T \rightarrow \infty$, there is no minimum for the tachyon to oscillate. Therefore, it is allegedly impossible to reheat the universe to produce various matters, i.e. after the tachyon inflation we end up with an empty universe, which is of course unacceptable.

Again in the context of the geometric tachyon (radion), we can avoid this reheating problem by preparing a ring of the NS5-branes and evolution of the D-brane inside the ring [172]. The effective potential has global minima and the oscillation around the minima produces the reheating needed to produce matter and hence our galaxies.

We can continue this line of reasoning and study for instance the spectral index of the cosmic microwave background etc, but this is not the main scope of this thesis. Rather, we would like to point out how inaccurate this kind of effective action analysis for the rolling D-brane is *after coupling to the massive closed string sector*. Especially, the stringy treatment of the decay of the D-brane completely changes the nature of the reheating from such rolling tachyon (or D-brane) systems.

Let us begin with the following illustrative toy example. In the above discussions, couplings of the (decaying or rolling) D-brane to higher massive stringy modes (except for graviton) have been neglected. In the usual field theory, we expect corrections to the effective action of order $\sim M_p^2/M^2$, where M^2 denotes the mass of the fields integrated out. The point is that we have to sum over infinitely many massive fields: e.g. in the Kaluza-Klein theory, $M^2 \propto n^2$, where n denotes the internal momenta, so the summation over n schematically gives

$$\sum_n \frac{1}{M_n^2} \sim \sum_n \frac{1}{n^2} = \frac{\pi^2}{6}, \quad (5.58)$$

which is finite. However, in string theory, the number of massive string modes grows exponentially $\rho(M) \sim \exp(\beta_{\text{Hg}} M)$ as we discussed the Hagedorn temperature in section 4.1. Thus the summation over all the massive modes with the coupling $\sim 1/M_s^2$ clearly diverges.

In reality, the coupling to the massive closed string sectors is much softer and the exponentially suppressed as $\exp(-\beta M)$. The case-by-case computation is needed to see which exponential factor governs, but from our results (summarized in section 5.5) it seems universal that the exponential part cancels out and the closed string backreaction is characterized by a power-like behavior irrespective of the superficial strength of the $\alpha' \sim 1/k$ corrections.⁷⁵

In this way, we can conclude that the reheating of the universe through the rolling tachyon - radion is rather effective than one might expect from the naively truncated effective action. As the direct calculation shows, almost all of the energy is radiated as the closed strings without any need for the oscillation around the extremum.⁷⁶ The actual problem, therefore,

⁷⁵It is also interesting to note that the exponential suppression of the higher massive modes occurs when $k < 1$ in the regime where the supergravity approximation is invalid.

⁷⁶As we have discussed in section, 5.2, the emission rate is power-like finite for higher dimensional branes.

is how we can transmit energy from the radiated (massive) closed string to the standard model sector. This problem is rather model dependent and we will not study it any further in detail here (see e.g. [173, 174, 175, 176] for recent studies).

As we have studied in section 5.2, the final decay product of the rolling tachyon and rolling D-brane is highly probable to be long closed strings. This can be directly seen by assigning fundamental string charges to the unstable D-branes, but without assigning such charges, intuitively it is expected to be so by considering a pair production. This is in good agreement with the usual Kibble mechanism of producing long macroscopic strings in the universe: causally disconnected region creates long strings and they evolve independently. It would be of great interest to study this problem quantitatively from the string theory viewpoint and determine a remaining density of cosmic strings associated with the D-brane decay (see [177] for a review of cosmic strings from the superstring theory). Such studies will verify or even exclude the geometric tachyon inflation. It is also of great importance to revisit the reheating process of various D-brane inflation scenarios to see whether the classical oscillatory contribution is really dominant over the emission of the highly massive string modes.

However, this does not mean an effectiveness of the truncated effective action (DBI+FRW such as (5.51)) to discuss the closed string backreaction. It just means that it is more effective to decay by disconnecting patches of D-brane as D0 particles (assuming it is uncharged). Mathematically, it is just an artefact of the one-point decay and the one-point decay is no more effective than the higher-point decay.

6 D-branes in Two-dimensional Black Hole

We now begin with our studies on D-branes in the two-dimensional black hole background. In this section, we review the D-branes in the Euclidean two-dimensional black hole. The organization of the section is as follows. In section 6.1, we classically analyze the D-branes in the two-dimensional black hole and derive the mini-superspace boundary wavefunction. In section 6.2, we review the exact boundary states describing the D-branes in the two-dimensional black hole system.

6.1 Classical D-branes

6.1.1 DBI analysis

The classification of the D-brane in general curved backgrounds is given by the solution of the Dirac-Born-Infeld action coupled with Chern-Simons action.⁷⁷ The total effective action is

$$S = -\mu_p \int d^{p+1}\xi e^{-\Phi} \sqrt{-\det(G_{ab} + B_{ab} + F_{ab})} + i\mu_p \int e^{F_2+B_2} \wedge \sum_q C_q, \quad (6.1)$$

where the summation over C_q should be taken over all R-R fields in the theory we are considering.

In this section, we study the D-branes in the Euclidean two-dimensional black hole:

$$ds^2 = k\alpha'(\tanh^2 \rho d\theta^2 + d\rho^2), \quad e^{2\Phi} = \frac{k}{\mu \cosh^2 \rho}. \quad (6.2)$$

In the Euclidean two-dimensional black hole background, there exist no Kalb-Ramond $B_{\mu\nu}$ field nor the R-R fields, so the effective action is simply given by the DBI term with possible electro-magnetic flux $F_{\mu\nu}$ on it. Since we are in the Euclidean signature, the DBI action (6.1) should be Wick-rotated in an appropriate manner:⁷⁸

$$S^E = \mu_p \int d^p \xi e^{-\Phi} \sqrt{\det(G_{ab} + B_{ab} + F_{ab})}. \quad (6.3)$$

We begin with the (Euclidean) D0-brane. The D0-brane is a point particle and the DBI action on it is simply given by

$$S_{D0} = \mu_0 e^{-\Phi} \propto \cosh \rho. \quad (6.4)$$

It is clear that the extremum of the action is obtained when $\rho = 0$. Thus we conclude that the D0-brane is localized at the tip of the cigar.

⁷⁷Of course, one could imagine unstable D-branes whose effective action is *not* given by the DBI action + Chern-Simons, but they are outside the scope of our discussion.

⁷⁸Our “Wick rotation” here is nothing but adding a (dummy) extra decoupling time direction and set trivial Neumann boundary condition along the time. In particular, we will assume $F + B$ is real.

Next we study the D1-brane. The DBI action for the D1-brane is given by

$$S_{D1} = \mu_1 \int d\theta \cosh \rho(\theta) \sqrt{\rho'(\theta)^2 + \tanh^2 \rho(\theta)} , \quad (6.5)$$

where we have fixed the reparametrization invariance by using the gauge $\xi = \theta$. The equation of motion is easily solved from the “energy” conservation:

$$\text{const} = \cosh \rho \frac{\tanh^2 \rho}{\sqrt{(\rho')^2 + \tanh^2 \rho}} \quad (6.6)$$

as

$$\sinh(\rho) \cos(\theta - \theta_0) = \sinh \rho_0 . \quad (6.7)$$

For later purposes, we note that if one uses the complex coordinate

$$u = \sinh \rho e^{i\theta} , \quad \bar{u} = \sinh \rho e^{-i\theta} , \quad (6.8)$$

the classical trajectory (6.7) takes the form of a straight line in the complex u plane. This can be also seen from the fact that the DBI action takes the flat form

$$S_{D1} = \mu_1 \int d\xi \sqrt{\frac{du}{d\xi} \frac{d\bar{u}}{d\xi}} \quad (6.9)$$

in this coordinate.

We finally examine the D2-brane. In this case, we can introduce a magnetic flux $F_{\rho\theta} = f(\rho, \theta)$. By fixing the reparametrization invariance as $\xi_1 = \rho$, $\xi_2 = \theta$, the DBI action reads

$$S_{D2} = \mu_2 \int d\theta d\rho \cosh \rho \sqrt{\tanh^2 \rho + f^2(\rho, \theta)} . \quad (6.10)$$

From the Gauss law constraint, we have

$$c = \frac{\cosh \rho f(\rho, \theta)}{\sqrt{\tanh^2 \rho + f^2(\rho, \theta)}} , \quad (6.11)$$

which determines the magnetic flux as

$$f^2(\rho, \theta) = \frac{c^2 \tanh^2 \rho}{c^2 - \cosh^2 \rho} . \quad (6.12)$$

If $c > 1$, the D2-brane partially wraps the cigar and has a boundary at $\rho = \text{arccosh}(c)$ because at that value of ρ , the magnetic field blows up. On the other hand, if $c < 1$, the D2-brane wraps the whole cigar. In the latter case, the magnetic field on the D2-brane induces a D0-brane charge near the tip of the cigar, which should be quantized. Writing $c = \sin \sigma \leq 1$, we obtain the classical quantization condition as

$$\frac{\sigma - \sigma'}{2\pi} k \in \mathbb{Z} . \quad (6.13)$$

In quite a similar fashion, we can also study the classical D-branes in the T-dualized trumpet background:

$$ds^2 = d\rho^2 + \frac{1}{\tanh^2 \rho} d\tilde{\theta}^2, \quad e^\Phi = \frac{k}{\mu \sinh \rho}. \quad (6.14)$$

Since the discussion is completely in parallel, we only present the results.

The D0-brane (probably D1-brane?) could be localized at $\rho = 0$. Since $\rho = 0$ is a singularity in the trumpet geometry, the presence of such D-branes are not obvious at all. Formally, we can regard it as a T-dual of the D0-brane of the cigar geometry.

The D1-brane is given by the solution of the DBI action

$$S_{D1} = \mu_{D1} \int d\tilde{\theta} \sinh \rho \sqrt{\frac{1}{\tanh^2 \rho} + (\rho')^2}, \quad (6.15)$$

in the static gauge. The solution is given by

$$\cosh \rho \cos(\tilde{\theta} - \tilde{\theta}_0) = \gamma. \quad (6.16)$$

when $\gamma > 1$, the D1-brane is connected, while when $\gamma < 1$, the D1-branes go through the singularity and possibly they become disconnected. Naturally, the D1-brane in the trumpet geometry is regarded as a T-dual of the D2-brane in the cigar geometry. The parameter γ corresponds to the parameter c in the cigar geometry.⁷⁹

The D2-brane is classified by the solution of the DBI action

$$S_{D2} = \mu_{D2} \int d\rho d\tilde{\theta} \sinh \rho \sqrt{\frac{1}{\tanh^2 \rho} + F^2}. \quad (6.17)$$

The Gauss law constraint gives

$$F^2 = \frac{\beta^2}{\tanh^2 \rho (\sinh^2 \rho - \beta^2)}. \quad (6.18)$$

The D2-brane always has a boundary at $\rho = \operatorname{arcsinh}(\beta)$. The D2-brane in the trumpet geometry naturally corresponds to the T-dual of the D1-brane in the cigar. The parameter identification is obviously given by $\beta = \sinh \rho_0$ appearing in (6.7).

6.1.2 group theoretical viewpoint

In section 6.1.1, we have studied the classical D-brane in the Euclidean two-dimensional black hole from the effective DBI action. Since the two-dimensional black hole system can be realized as the $SL(2; \mathbb{R})/U(1)$ coset model, we can study the classification of the D-brane from the gauged WZNW model [178, 179, 180, 181, 182, 183]. Indeed all the D-branes discussed in section 6.1.1 descend from the branes in the parent $SL(2; \mathbb{R})$ WZNW model.

⁷⁹The parameter $\tilde{\theta}_0$ can be T-dualized to the holonomy of the gauge field A_0 in the cigar. Since the D2-brane has a nontrivial fundamental group $\pi_1 = \mathbb{Z}$, different A_0 gives a different D-brane (for $c > 1$).

The starting point is the D-branes in the parent $SL(2; \mathbb{R})$ WZNW model. We focus on the maximally symmetric D-branes for technical simplicity. As we proceed, we will see that the maximally symmetric D-branes are enough to obtain all the D-branes constructed from the DBI analysis done in section 6.1.1. The maximally symmetric D-branes in the WZNW model are classified by the (twined) conjugacy class of the group G with a possible quantization condition [184, 185, 186, 187, 188]. We call them A-branes (conjugacy class) and B-branes (twined conjugacy class) respectively.

In our $SL(2; \mathbb{R})$ group with the Euler angle parametrization $g = e^{i\sigma_2 \frac{t-\theta}{2}} e^{\rho\sigma_1} e^{i\sigma_2 \frac{t+\theta}{2}}$, the conjugacy class is given by

$$\text{Tr}(g) = 2 \cos t \cosh \rho \equiv 2\kappa, \quad (6.19)$$

and the twined conjugacy class is given by

$$\text{Tr}(\sigma_1 g) = 2 \cos \theta \sinh \rho \equiv 2\kappa' . \quad (6.20)$$

up to conjugation.

The D-branes in the axial coset model is obtained by gauging g by hgh , where $h^a = e^{i\sigma_2 a}$ in our case. For A-brane, we have to sum over the gauge orbit of the parent D-brane parametrized by κ in order to obtain a gauge invariant object. The gauge transformation of the conjugacy class is given by

$$\text{Tr}(h^a g h^a) = 2 \cos(t + a) \cosh \rho, \quad (6.21)$$

so the gauge invariant orbit of the parent D-brane is given by

$$\cosh \rho \geq \kappa . \quad (6.22)$$

Projecting it down on the coset coordinate (in the gauge $t = 0$) is now trivial, and we have obtained the D2-brane wrapped (partially) around the cigar whose world volume is restricted by the condition (6.22). The shapes of the A-branes obtained here are in complete agreement with the ones obtained from the DBI analysis in section 6.1.1. The precise parameter identification is $c = \kappa$ for the D2-brane.⁸⁰ We also note that A-brane is invariant under the isometry of the coset in this construction.

Similarly from the parent B-brane, we can construct the D1-brane of the coset. In this case, since the twined conjugacy class is already gauge invariant, we can directly project (6.20) down onto the coset coordinate. The resulting D1-brane trajectory is given by

$$\sinh \rho \cos \theta = \kappa' , \quad (6.23)$$

which is nothing but the one obtained in (6.7) from the DBI analysis (with $\theta_0 = 0$). The B-brane constructed in this way breaks the isometry of the coset, so it has a Nambu-Goldstone

⁸⁰There are several independent ways to justify this parameter identification. For instance, one can show it directly from the detailed study on the boundary conditions of the gauged WZNW model with boundaries. In [189], they have shown that the parameter κ is indeed the field strength appearing in the effective action of the D-brane at the boundary by using the T-duality technique. Their study of the $SU(2)/U(1)$ model can be translated to our Euclidean $SL(2; \mathbb{R})/U(1)$ model with no essential modifications.

mode along the θ direction. This corresponds to the rotation of σ_1 and σ_3 in the definition of the twined conjugacy class (6.20).

We could repeat the same analysis for the vector coset (\sim trumpet geometry). Since the argument is completely in parallel, we skip the detailed discussion, and simply note that the results agree with the DBI analysis.

6.1.3 mini-superspace boundary wavefunction

In the context of the string theory, D-branes can be described either from the open string viewpoint or from the closed string viewpoint (i.e. channel duality). Technically, this is achieved by the modular transformation of the cylinder amplitudes. The boundary state $|B\rangle$ is defined by

$$Z_{\text{cylinder}} \equiv \int dt_o \text{Tr}_o e^{-\pi H_o t_o} = \int \frac{dt_c}{t_c} \langle B | e^{-\pi H_c t_c} | B \rangle , \quad (6.24)$$

where $H_o = L_0$ is the open string Hamiltonian while $H_c = L_0 + \bar{L}_0$ is the closed string Hamiltonian. The boundary state $|B\rangle$ satisfies the gluing condition

$$(L_n - \bar{L}_{-n})|B\rangle = 0, \quad (6.25)$$

for the energy-momentum tensor (and similar gluing conditions for any other conserved currents if any: see section 6.2 for further details).

At the level of the minisuperspace approximation, the boundary states can be seen as the coupling of the D-brane to the closed string zero mode:

$$\langle B |_{\text{mini}} = \int_0^\infty \frac{dp}{2\pi} \Psi_0(p, n) \langle \langle p, n | , \quad (6.26)$$

where $|p, n\rangle\rangle$ is the so-called Ishibashi state [190] associated with the primary states $|p, n\rangle$ (see section 6.2 for details), but in the mini-superspace approximation, there is no difference between the two $|p, n\rangle\rangle \sim |p, n\rangle$ because they are different only in the non-zero mode sector. The semiclassical boundary wavefunction $\Psi_0(p, n)$ is obtained from the overlap between the D-brane and the primary state $|p, n\rangle$ as

$$\Psi_0(p, n) = \langle B | p, n \rangle . \quad (6.27)$$

The explicit form of the primary state $|p, n\rangle$ and the classical trajectory have been given in the form of the minisuperspace approximation as we have studied in section 3.2.3 and section 6.1.1.

In the following, we compute the minisuperspace boundary wavefunction Ψ_0 for each D-branes studied in section 6.1.1. The results will be compared with the proposed exact boundary states in section 6.2. We expect that they will agree with each other in the semiclassical limit ($k \rightarrow \infty$), and indeed they do as we will see.

Let us begin with the D0-brane. Classically, the D0-brane is localized at the tip of the cigar $\rho = 0$, and the boundary wavefunction is simply given by the minisuperspace

wavefunction for $|p, n\rangle$ evaluated at $\rho = 0$. From the explicit minisuperspace wavefunction (3.48), we can easily derive

$$\Psi_0^{\text{D0}}(p, n) = -\delta_{n,0} \frac{\Gamma^2(-j)}{\Gamma(-2j-1)} = -\delta_{n,0} \frac{\Gamma^2(\frac{1}{2} - \frac{ip}{2})}{\Gamma(-ip)}. \quad (6.28)$$

We note that D0-brane does not couple to the momentum mode along θ , which is consistent with the interpretation that the D0-brane is an A-brane (see section 6.1.2). The exact analysis shows that it couples to the winding mode and the discrete states localized near the tip of the cigar, but the minisuperspace analysis cannot capture them.

Next let us consider the D1-brane. Classically, the D1-brane has the shape of the hairpin. A semiclassical D-brane boundary wavefunction is the weighted sum of the wavefunction of closed string states restricted to the location of the D-brane. In the mini-superspace approximation, as is implicit in [79], the weighted sum equals to the overlap between the mini-superspace wavefunction and the delta function constraint enforcing (ρ, θ) coordinates over the hairpin trajectory (6.7) (with respect to the volume element (3.47)). The result is

$$\begin{aligned} & \int_0^\infty \sinh \rho \, d \sinh \rho \int_{-\frac{\pi}{2} + \theta_0}^{\frac{\pi}{2} + \theta_0} d\theta \, \delta\left(\cos(\theta - \theta_0) \sinh \rho - \sinh \rho_0\right) \phi_n^p(\rho, \theta) \\ &= \int_{-\frac{\pi}{2}}^{\frac{\pi}{2}} d\theta' \frac{\sinh \rho_0}{\cos^2 \theta'} \phi_n^p(\hat{\rho}(\rho_0, \theta'), \theta') e^{in\theta_0}, \end{aligned} \quad (6.29)$$

where $\theta' = (\theta - \theta_0)$ and $\hat{\rho}(\rho_0, \theta')$ refers to the solution of $\cos \theta' \sinh \rho = \sinh \rho_0$. Using the decomposition (3.54), we are then to evaluate integrals:

$$\begin{aligned} & \int_{-\frac{\pi}{2}}^{\frac{\pi}{2}} d\theta \frac{\sinh \rho_0}{\cos^2 \theta} \phi_{L,n}^p(\hat{\rho}(\rho_0, \theta), \theta) = \frac{2\pi\Gamma(ip)}{\Gamma(\frac{1}{2} + \frac{ip+n}{2}) \Gamma(\frac{1}{2} + \frac{ip-n}{2})} e^{-ip\rho_0}, \\ & \int_{-\frac{\pi}{2}}^{\frac{\pi}{2}} d\theta \frac{\sinh \rho_0}{\cos^2 \theta} \phi_{R,n}^p(\hat{\rho}(\rho_0, \theta), \theta) = \frac{2\pi\Gamma(-ip)}{\Gamma(\frac{1}{2} - \frac{ip+n}{2}) \Gamma(\frac{1}{2} - \frac{ip-n}{2})} e^{+ip\rho_0}. \end{aligned} \quad (6.30)$$

Details of the computation are relegated in Appendix A.5. Using the mini-superspace reflection amplitude (3.51), we then obtain

$$\Psi_{\text{D1}}^{(0)}(\rho_0, \theta_0; p, n) = \frac{2\pi\Gamma(ip)}{\Gamma(\frac{1}{2} + \frac{ip+n}{2}) \Gamma(\frac{1}{2} + \frac{ip-n}{2})} e^{in\theta_0} (e^{-ip\rho_0} + (-1)^n e^{+ip\rho_0}). \quad (6.31)$$

The D1-brane couples to the momentum mode as is clear from the geometry, which is consistent with the interpretation that the D1-brane is a B-brane (see section 6.1.2).

Finally, we study the D2-brane. The D2-brane is parametrized by the parameter c appearing in the amount of the magnetic flux (6.12). Since the qualitative features of the D2-brane seem to be different for $c > 1$, and $c < 1$, it is natural to study them separately. Since the mini-superspace analysis for the D2-brane has not been available in the literature, we would like to present it slightly in detail here.⁸¹

⁸¹The author would like to thank S. Ribault for stimulating discussions on this problem.

Let us begin with the case when $c > 1$. The D2-brane only partially wraps the cigar because at $\rho = \text{arccosh}(c)$, the field strength diverges. We parametrize $c = \cosh r_0$.

Since the D2-brane couples to the winding states, the minisuperspace analysis is only possible for the zero winding sector.⁸² The (zero momentum/winding) minisuperspace wavefunction is given by

$$\begin{aligned}\phi_{p,m=0}(\rho) &= -\frac{\Gamma^2(-j)}{\Gamma(-2j-1)}F(j+1, -j; 1; -\sinh^2 \rho) \\ &= (\sinh \rho)^{-1-ip}F\left(\frac{1}{2} + \frac{ip}{2}, \frac{1}{2} + \frac{ip}{2}; 1+ip; -\frac{1}{\sinh^2 \rho}\right) \\ &\quad + \frac{\Gamma(ip)\Gamma^2(\frac{1}{2} - \frac{ip}{2})}{\Gamma(-ip)\Gamma^2(\frac{1}{2} + \frac{ip}{2})}(\sinh \rho)^{-1+ip}F\left(\frac{1}{2} - \frac{ip}{2}, \frac{1}{2} - \frac{ip}{2}; 1-ip; -\frac{1}{\sinh^2 \rho}\right)\end{aligned}\quad (6.32)$$

where $j = -\frac{1}{2} + \frac{ip}{2}$.

The boundary wavefunction in the minisuperspace approximation is given by

$$\Psi_2(r_0)^{\text{mini}} = \int_{r_0}^{\infty} d\rho \cosh \rho \frac{\sinh \rho}{\sqrt{\cosh^2 \rho - \cosh^2 r_0}} \phi_p(\rho). \quad (6.33)$$

Now we can perform the integration as follows

$$\begin{aligned}&\int_{r_0}^{\infty} d\rho \cosh \rho \frac{\sinh \rho}{\sqrt{\cosh^2 \rho - \cosh^2 r_0}} (\sinh \rho)^{-1-ip}F\left(\frac{1}{2} + \frac{ip}{2}, \frac{1}{2} + \frac{ip}{2}; 1+ip; -\frac{1}{\sinh^2 \rho}\right) \\ &= \frac{\Gamma(ip+1)}{\Gamma(\frac{1}{2} + \frac{ip}{2})^2} \sum_{n=0}^{\infty} (-1)^n (\sinh^2 r_0)^{-n-\frac{ip}{2}} \frac{\sqrt{\pi} \Gamma(n + \frac{ip}{2}) \Gamma(\frac{1}{2} + \frac{ip}{2} + n)}{2 \Gamma(ip+1+n)n!} \\ &= \frac{\Gamma(\frac{ip}{2})}{\Gamma(\frac{1}{2} + \frac{ip}{2})} (\sinh^2 r_0)^{-\frac{ip}{2}} \frac{\sqrt{\pi}}{2} F\left(\frac{ip}{2}, \frac{1}{2} + \frac{ip}{2}; ip+1, -\frac{1}{\sinh^2 r_0}\right) \\ &= \frac{\pi \Gamma(ip)}{\Gamma(\frac{1}{2} + \frac{ip}{2})^2} e^{-ipr_0}.\end{aligned}\quad (6.34)$$

We refer to the appendix A.5 for the last equality (see also [1]). Combining it with the second integration that can be treated in the same manner, we obtain

$$\Psi_2(r_0)^{\text{mini}} = \frac{\pi \Gamma(ip)}{\Gamma(\frac{1}{2} + \frac{ip}{2})^2} \cos(pr_0). \quad (6.35)$$

We can see that the boundary wavefunction for the partially wrapped D2-brane is consistent with the class 2 boundary wavefunction proposed in [191] at least for the zero winding sector (see section 6.2 for details).

We can repeat our analysis when $\beta \leq 1$ and reproduces the minisuperspace limit of the class 3 boundary states in the zero-winding sector. In the T-dual picture, (partially

⁸²We could avoid this problem in the T-dual picture, which will be discussed later.

wrapped) D2-brane in the cigar geometry is supposed to be given by the D1-brane in the trumpet geometry.⁸³

Let us now move on to the minisuperspace wavefunction for the D1-brane in the trumpet geometry. From the semiclassical DBI action

$$L = \sinh \rho \sqrt{\dot{\rho}^2 + k^{-2} \coth^2 \rho} , \quad (6.36)$$

the equation of motion is easily integrated with the help of the energy conservation:

$$L - \dot{\rho} \frac{\partial L}{\partial \dot{\rho}} = \text{const} , \quad (6.37)$$

and one can see that the classical D1-brane is described by the trajectory

$$\cosh \rho = \frac{\cosh r_0}{\cos \left[(\tilde{\theta} - \tilde{\theta}_0)/k \right]} . \quad (6.38)$$

The appearance of the $1/k$ in the argument of the cosine is important. If k is an even integer, the asymptotic form of the D-brane trajectory is given by the coincident two-branes, while for an odd integer k , it is given by the parallel two-branes placed at the anti-podal points in \mathbb{S}^1 .⁸⁴

The semiclassical boundary wavefunction is obtained by integrating the classical closed string wavefunction over the classical D-brane trajectory as

$$\begin{aligned} \Psi_2(\tilde{\theta}_0, r_0)^{\text{mini}} &= e^{i w \tilde{\theta}_0} \int_1^\infty \cosh \rho d(\cosh \rho) \int_{-\frac{k\pi}{2}}^{\frac{k\pi}{2}} d\tilde{\theta} \delta(\cos(\tilde{\theta}/k) \cosh \rho - \cosh r_0) \phi_{p,w}(\rho, \tilde{\theta}) \\ &= \int_{-\frac{k\pi}{2}}^{\frac{k\pi}{2}} d\tilde{\theta} \frac{\cosh r_0}{\cos^2(\tilde{\theta}/k)} \phi_{p,w}(\hat{\rho}(r_0, \tilde{\theta}), \tilde{\theta}) , \end{aligned} \quad (6.39)$$

where $\hat{\rho}(r_0, \tilde{\theta})$ is the solution of $\cos(\tilde{\theta}/k) \cosh \rho = \cosh r_0$. The integration is feasible due to the formula

$$\begin{aligned} \int_{-\frac{k\pi}{2}}^{\frac{k\pi}{2}} d\tilde{\theta} \frac{\cosh r_0}{\cos^2(\tilde{\theta}/k)} e^{i w \tilde{\theta}} (\cosh \rho)^{-1-ip} F \left(\frac{1}{2} - \frac{k w}{2} + \frac{i p}{2}, \frac{1}{2} + \frac{k w}{2} + \frac{i p}{2}; 1 + i p; \frac{\cos^2(\tilde{\theta}/k)}{\cosh^2 r_0} \right) \\ = \frac{2\pi \Gamma(ip)}{\Gamma(\frac{1}{2} + \frac{i p}{2} + \frac{k w}{2}) \Gamma(\frac{1}{2} + \frac{i p}{2} - \frac{k w}{2})} e^{-i p r_0} , \end{aligned} \quad (6.40)$$

whose derivation is relegated to the appendix B (see also [1]).

⁸³One subtle point of the trumpet geometry is that the semiclassical limit is unclear. We regard $k \rightarrow \infty$ as the semiclassical limit for ρ direction, but θ direction is apparently not. We will neglect this subtlety for a moment.

⁸⁴For general k , asymptotic position of the two branes breaks the (discrete) periodic symmetry.

In this way, we derive the minisuperspace limit of the boundary wavefunction that describes the D1-brane in the trumpet geometry:

$$\Psi_2(\tilde{\theta}_0, r_0)^{\text{mini}} = N(b) \frac{\Gamma(2j+1)}{\Gamma(1+j+\frac{kw}{2})\Gamma(1+j-\frac{kw}{2})} e^{iw\tilde{\theta}_0} \cos(r_0(2j+1)) , \quad (6.41)$$

where $j = -\frac{1}{2} + \frac{ip}{2}$. This should be identified with the boundary wavefunction for the partially wrapped D2-brane via the T-duality. Note that for zero winding sector $w = 0$, the wavefunction agrees with the direct evaluation (6.35).

In a similar manner, the classical boundary wavefunction for the totally wrapped D2-brane is given by

$$\Psi_3(\sigma, \theta_0) = \Gamma(2j+1) e^{i\theta_0\omega} \left[\frac{\Gamma(-j+\frac{kw}{2})}{\Gamma(j+1+\frac{kw}{2})} e^{i\sigma(2j+1)} + \frac{\Gamma(-j-\frac{kw}{2})}{\Gamma(j+1-\frac{kw}{2})} e^{-i\sigma(2j+1)} \right] . \quad (6.42)$$

The parameters r_0 and σ are supposedly related to the magnetic flux on the D2-brane:

$$F = \frac{\beta^2 \tanh^2 \rho}{\cosh^2 \rho - \beta^2} d\theta d\rho , \quad (6.43)$$

where $\beta = \sin \sigma$ for $\beta \leq 1$ and $\beta = \cosh r_0$ for $\beta \geq 1$. We expect that these two classes of branes coincide in the limit $\beta = 1$ (i.e. $\sigma = \pm \frac{\pi}{2}$ and $r_0 = 0$).

From the geometry of the semiclassical D-brane, we expect that if one takes a suitable limit of the boundary states, the class 2 D-brane (partially wrapped D-brane) will coincide with the class 3 D-brane (totally wrapped D-brane). To compare these two branes, we can directly show that

$$\Psi_3(\pi/2, -k\pi/2) + \Psi_3(\pi/2, k\pi/2) = \Psi_2(0, 0) . \quad (6.44)$$

This result also shows that the boundary wavefunction (6.42) describes the half cut D2-brane.

6.1.4 embedding into NS5-branes

We have obtained the classical D-brane solutions in the (Euclidean) two-dimensional black hole background. As we have reviewed in section 2, we can embed the two-dimensional black hole into the superstring theory as NS5-branes (or more generally little string theories on singular Calabi-Yau spaces). Here we would like to summarize some of the D-brane solutions in the NS5-brane background to see how one can construct them from those in the two-dimensional black hole system [192, 25, 193, 194, 37, 27, 195].

Let us first concentrate on the D1-brane solution in the ring-likely separated NS5-brane solution (2.13) corresponding to

$$\frac{\left[\frac{SL(2;\mathbb{R})_k}{U(1)} \times \frac{SU(2)_k}{U(1)} \right]_{\perp}}{\mathbb{Z}_k} . \quad (6.45)$$

Naturally, we can combine various D-branes in the $SL(2;\mathbb{R})/U(1)$ coset and $SU(2)/U(1)$ coset to construct D-branes in this background. We further focus on the two-plane $x^8 = x^9 = 0$, setting $\theta = 0$.

The first combination is the D0-brane in the cigar and the D1-brane in the bell. The result is the D1-brane stretching between NS5-branes as in figure 7. In the context of the LST, we interpret them as W-bosons. The second combination is the (uncut) D1-brane in the trumpet and D0-brane in the bell. The resulting geometry is the straight line on the $x^8 = x^9 = 0$ plane as in figure 7. The third combination is the cut D1-brane in the trumpet and D0-brane in the bell. It corresponds to the semi-infinite D-brane attached to the NS5-branes as in figure 7.

The geometries of the D3-brane are much more complicated. We would like to refer to [196, 195] for detailed study of the D3-brane geometries in the NS5-brane background.

Recently, a static D-brane configuration in the black hole background has attracted much attention for a possible application to the phase transition of the fundamental matters in QCD [197]. In our two-dimensional black hole setup, it amounts to the study of the D-brane in the black NS5-brane background. In the Rindler limit studied in [197], the difference between the black NS5-brane and the black D-brane does not exist. It would be interesting to study the exact boundary states for the D-branes in the black NS5-brane background to probe the α' corrections to the phase transition discussed there.

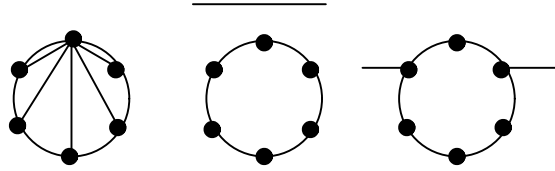


Figure 7: The left figure shows W-bosons in LST. The central figure shows an uncut D1-brane. The right figure shows cut D1-branes attached to the NS5-branes.

6.2 Exact boundary states

6.2.1 Ishibashi states

To construct the exact Cardy boundary states for the D-branes in the two-dimensional black hole background, we begin with the Ishibashi states. For definiteness, we first concentrate on the bosonic axial coset, which is given by the Euclidean cigar.

The coset Ishibashi states naturally descend from those for the parent current algebra. The Ishibashi state satisfies the boundary condition

$$\begin{aligned} (L_n - \bar{L}_{-n})|A\rangle &= 0 \\ (J_n - \bar{J}_{-n})|A\rangle &= 0, \end{aligned} \tag{6.46}$$

for A-brane and

$$\begin{aligned} (L_n - \bar{L}_{-n})|B\rangle &= 0 \\ (J_n + \bar{J}_{-n})|B\rangle &= 0, \end{aligned} \tag{6.47}$$

for B-brane. In terms of the primary states of the coset, A-boundary condition means $m = \bar{m} = \frac{k\omega}{2}$, and B-boundary condition means $m = -\bar{m} = \frac{n}{2}$. Physically, the A-branes couple to the winding states while B-brane couple to the momentum states in the coset.

The Ishibashi state is naturally endowed with the classification via the character of the coset model. For continuous series, we have the following normalization

$$\begin{aligned} {}_B\langle\langle p', n' | e^{-\pi t(L_0 + \bar{L}_0)} | p, n \rangle\rangle_B &= [\delta(p - p') + R(p, n)\delta(p + p')] \delta_{n, n'} \frac{q^{-\frac{p^2}{4(\kappa-2)} + \frac{n^2}{4\kappa}}}{\eta(\tau)^2} \\ {}_A\langle\langle p', \omega' | e^{-\pi t(L_0 + \bar{L}_0)} | p, \omega \rangle\rangle_A &= [\delta(p - p') + R(p, \omega)\delta(p + p')] \delta_{\omega, \omega'} \frac{q^{-\frac{p^2}{4(\kappa-2)} + \frac{\omega^2}{4}}}{\eta(\tau)^2}, \end{aligned} \quad (6.48)$$

where the subscript denote the boundary condition (either A-type or B-type), and $R(p, n)$ (or $R(p, \omega)$) denote the reflection amplitude. The Ishibashi state is parametrized by the radial momentum p and the angular momentum n (or the winding number ω).

For the supersymmetric coset, we impose the following boundary condition for the Ishibashi states:

$$\begin{aligned} (L_n - \bar{L}_{-n})|A\rangle\rangle &= 0 \\ (G_r^\pm - i\bar{G}_{-r}^\mp)|A\rangle\rangle &= 0 \\ (J_n - \bar{J}_{-n})|A\rangle\rangle &= 0, \end{aligned} \quad (6.49)$$

for A-type boundary conditions, and

$$\begin{aligned} (L_n - \bar{L}_{-n})|B\rangle\rangle &= 0 \\ (G_r^\pm - i\bar{G}_{-r}^\pm)|B\rangle\rangle &= 0 \\ (J_n + \bar{J}_{-n})|B\rangle\rangle &= 0, \end{aligned} \quad (6.50)$$

for B-type boundary conditions. Both types of the boundary conditions are compatible with the diagonal $\mathcal{N} = 1$ superconformal symmetry

$$(G_r - i\bar{G}_{-r})|A \text{ or } B\rangle\rangle, \quad (6.51)$$

where $G_r = G_r^+ + G_r^-$ that should be gauged in the fermionic string theory. Physically, A-type boundary condition corresponds to Dirichlet boundary condition along the cigar angular direction, and B-type boundary condition corresponds to Neumann boundary condition.

The Ishibashi states for the supersymmetric coset for continuous series is parametrized by three quantum number (p, m, s) . Our normalization is

$$\begin{aligned} &{}_A\langle\langle p', \omega', s' | e^{-\pi\tau_c(L_0 + \bar{L}_0)} e^{i\pi y(J_0 + \bar{J}_0)} | p, \omega, s \rangle\rangle_A \\ &= \delta_{\omega', \omega} (\delta(p - p') + \delta(p + p') R(j, \frac{k\omega}{2}, \frac{k\omega}{2})) \text{ch}_{j, \frac{k\omega}{2}, s}(i\tau_c, y), \end{aligned} \quad (6.52)$$

for the A-brane, and

$$\begin{aligned} &{}_B\langle\langle p', n', s' | e^{-\pi\tau_c(L_0 + \bar{L}_0)} e^{i\pi y(J_0 + \bar{J}_0)} | p, n, s \rangle\rangle_B \\ &= \delta_{n', n} (\delta(p - p') + \delta(p + p') R(j, \frac{n}{2}, -\frac{n}{2})) \text{ch}_{j, \frac{n}{2}, s}(i\tau_c, y), \end{aligned} \quad (6.53)$$

for the B-brane. Here s denotes the spectral flow parameter. Note that the boundary condition demands $m = \bar{m} = \frac{k\omega}{2}$ for the A-brane and $m = -\bar{m} = \frac{n}{2}$ for the B-brane. The $\mathcal{N} = 2$ character $\text{ch}_{j,m,s}$ is defined as

$$\text{ch}_{j,m,s}(\tau, y) = q^{\frac{p^2}{4k} + \frac{(m+s)^2}{k} + \frac{s^2}{2}} z^{\frac{2m}{k} + s} \frac{\theta_3(\tau, y)}{\eta(\tau)^3}, \quad (6.54)$$

for NS sector ($z = e^{2\pi iy}$).

6.2.2 exact boundary wavefunction

Let us first summarize the exact boundary wavefunction for the D-branes whose classical properties we discussed in section 6.1. We relegate a (partial) derivation of the exact boundary wavefunctions based on the modular bootstrap to section 6.2.3.

For the bosonic two-dimensional black hole, we expand the Cardy boundary states as

$$\langle B| = \int dp \sum_m \Psi(p, m) \langle\langle p, m| + (\text{discrete}) . \quad (6.55)$$

Compared with the minisuperspace approximation (6.26), we have allowed the winding states (for B-brane) and a possible discrete state contribution. In the following, we focus on the continuous part. The discrete part can be read from the analytic continuation of the boundary wavefunction $\Psi(p, m)$ with respect to the parameters of the continuous series restricted to the value corresponding to the discrete series (i.e. $\Psi(j = m, m)$).

The exact boundary wavefunction for the D0-brane (class 1 A-type brane) is given by

$$\Psi_{\text{D0}}(j, \omega) = \nu_b^{2j+1} \frac{\Gamma(-j + \frac{k\omega}{2})\Gamma(-j - \frac{k\omega}{2})}{\Gamma(-2j - 1)\Gamma(1 - b^2(2j + 1))}, \quad (6.56)$$

where $b = (k-2)^{-1/2}$, and $\nu_b = \frac{\Gamma(1-b^2)}{\Gamma(1+b^2)}$. It is easy to see that the exact boundary wavefunction (6.56) reduces to the mini-superspace result (6.28) in the large k limit by setting $\omega = 0$ up to a p independent overall normalization factor. The exact boundary state for the D0-brane couples to winding states. It also couples to the discrete series localized near the tip of the cigar.

The exact boundary wavefunction for the D1-brane (class 2' B-type brane) is given by

$$\Psi_{\text{D1}}(j, n)^{r, \theta_0} = \nu_b^{2j+1} e^{in\theta_0} \frac{\Gamma(2j+1)\Gamma(1+b^2(2j+1))}{\Gamma(1+j+\frac{n}{2})\Gamma(1+j-\frac{n}{2})} (e^{-r(2j+1)} + (-1)^n e^{r(2j+1)}). \quad (6.57)$$

The D1-brane only couples to the momentum states. In particular, it does not couple to any discrete states. In the classical limit $k \rightarrow \infty$, the boundary wavefunction reproduces that of the minisuperspace approximation (6.31).

The exact boundary wavefunction for the partially wrapped D2-brane (class 2 A-type brane) is given by

$$\Psi_{\text{D2}}(j, \omega)^{r_0, \bar{\theta}_0} = \nu_b^{2j+1} \frac{\Gamma(2j+1)\Gamma(1+b^2(2j+1))}{\Gamma(1+j+\frac{k\omega}{2})\Gamma(1+j-\frac{k\omega}{2})} e^{i\omega\bar{\theta}_0} \cos(r_0(2j+1)). \quad (6.58)$$

It does not couple to the discrete states localized at the tip of the cigar as is expected from the geometry. We can readily see that the classical limit ($k \rightarrow \infty$) of (6.58) reduces to the minisuperspace wavefunction (6.41).

Finally, the exact boundary wavefunction of the totally wrapped D2-brane (class 3 A-type brane) is given by

$$\begin{aligned} \Psi_{\text{D2}'}(j, \omega)^{\sigma, \theta_0} &= \nu_b^{2j+1} \Gamma(1 + b^2(2j + 1)) \Gamma(2j + 1) e^{i\theta_0 \omega} \times \\ &\times \left[\frac{\Gamma(-j + \frac{k\omega}{2})}{\Gamma(j + 1 + \frac{k\omega}{2})} e^{i\sigma(2j+1)} + \frac{\Gamma(-j - \frac{k\omega}{2})}{\Gamma(j + 1 - \frac{k\omega}{2})} e^{-i\sigma(2j+1)} \right], \end{aligned} \quad (6.59)$$

with the relative quantization condition $\sigma - \sigma' = 2\pi \frac{m}{k-2}$, $m \in \mathbb{Z}$.

The other possible exact boundary states for the two-dimensional black hole have been proposed in the literatures [198, 199, 200]. However, they do not possess sensible open string spectra⁸⁵ nor corresponding semiclassical limits, so we will not discuss them in detail here. Their properties are in many sense similar to the generalized ZZ branes proposed in [137]. As such they could be important so as to understand the nonperturbative contributions to the partition function of the two-dimensional Euclidean black hole.

The boundary wavefunctions for the supersymmetric two-dimensional black hole are essentially the same as those for the bosonic one. In the NS sector, the only difference is to replace $b^2 = \frac{1}{k-2}$ with $\frac{1}{k}$. The boundary wavefunction for the other sector is obtained by the spectral flow.

6.2.3 Cardy condition and modular bootstrap

There are several different ways to derive the boundary wavefunctions for the D-branes in the $SL(2; \mathbb{R})/U(1)$ coset model. One of the simplest ways to obtain them is to descend them from the branes in the parent $SL(2; \mathbb{R})$ WZNW model (or \mathbb{H}_+^3 model). This method has a small drawback for our purposes because we should derive the boundary states for $SL(2; \mathbb{R})$ WZNW model (or \mathbb{H}_3^+ model) first [201]. In this section, we take another root, which uses the so-called ‘‘modular bootstrap’’ method to derive all the A-branes in the Euclidean two-dimensional black hole.⁸⁶

The modular bootstrap method is intimately related to the Cardy condition for boundary states [202]. The Cardy condition is the physical constraint on the open string spectra between two different D-branes. Let us denote the boundary states for any pair of these two branes as $|a\rangle$ and $|b\rangle$. The Cardy condition says that the open string spectra between these two D-branes should have open string characters with positive multiplicities:

$$Z_{a,b} = \text{Tr}_{a,b} q^{L_0} = \sum_i n_{a,b}^i \chi_i(q), \quad (6.60)$$

⁸⁵Most of them contain tachyon in their spectra. Furthermore, they often have imaginary conformal weights when we study overlaps with class 2 (class 2') branes.

⁸⁶As we will see, we cannot derive the boundary wavefunctions for B-branes in this approach. We need a more technically involved strategy such as the conformal bootstrap to derive them.

where $\chi_i(q)$ is the open string character, and $n_{a,b}^i$ should be positive integers from the unitarity of the theory.⁸⁷ Now we modular transform the open string character $\tau \rightarrow -1/\tau$ in order to obtain the closed string description:

$$\langle a|e^{i\tau\pi H_c}|b\rangle = Z_{ab}(q) = \sum_{i,j} n_{a,b}^i S_{ij} \chi_j(\tilde{q}) , \quad (6.61)$$

with $\tilde{q} \equiv e^{-2\pi i/\tau}$, where S_{ij} is the modular S -matrix for characters χ_i .

At this point, it is not immediately obvious whether the multiplicities $n_{a,b}^i$ are all positive integers if one introduces an arbitrary set of boundary states $|a\rangle$. This integrality condition is the Cardy condition for boundary states. The Cardy condition guarantees a physical interpretation of the open string spectra from the open-closed duality.

Actually, there is a canonical solution of the Cardy condition based on the Verlinde formula [203]. We assume that the boundary state is a superposition of the Ishibashi states with normalization

$$\langle\langle i|e^{i\tau\pi H_c}|j\rangle\rangle = \delta_{ij} \chi_i(q) . \quad (6.62)$$

We then assume the existence of the simplest boundary states (identity brane) $|\hat{0}\rangle$ whose self overlap gives an identity representation in the open string sector: $n_{\hat{0},\hat{0}}^i = \delta_0^i$. Since the fusion of the identity operator is itself, we have a relation

$$|\langle\hat{0}|j\rangle|^2 = S_{0,j} . \quad (6.63)$$

As a consequence, the state $|\hat{0}\rangle$ can be written as

$$|\hat{0}\rangle = \sum_j \sqrt{S_{0,j}} |j\rangle , \quad (6.64)$$

up to an overall phase factor (possibly dependent on j).

Now we *define* Cardy boundary states as

$$|a\rangle = \sum_j \frac{S_{aj}}{\sqrt{S_{0j}}} |j\rangle \quad (6.65)$$

which contains the open string spectrum $n_{\hat{0}a}^i = \delta_a^i$ in the overlap with the identity brane. These Cardy states satisfy the Cardy condition (6.60)

$$\langle a|j\rangle\langle j|b\rangle = \frac{S_{aj}S_{jb}}{S_{0j}} = \sum_i S_{ij} n_{ab}^i , \quad (6.66)$$

where n_{ab}^i is given by the Fusion coefficient \mathcal{N}_{ab}^i that is a positive integral matrix. The last equality is due to a remarkable identity under the name of the Verlinde formula. The Verlinde

⁸⁷Implicitly here we are assuming that the open string between $|a\rangle$ and $|b\rangle$ are bosonic. Otherwise the negative multiplicity is allowed as fermions. For NS-NS overlap, we expect that the overlap should contain bosonic excitations.

formula can be shown for unitary compact CFTs by studying the monodromy constraint for the torus amplitudes.

Let us move on to the boundary wavefunction for A-branes in the two-dimensional black hole. Our first assumption is the existence of the identity brane, which will be identified as the D0-brane at the tip of the cigar. We assume that the self-overlap of this identity brane yields the identity representation summed over the spectral flow in the open string spectrum. Summation over the spectral flow is needed in order to guarantee the quantization of the $U(1)_R$ charge in the closed string spectrum.⁸⁸

For definiteness, we study the NS-sector of the supersymmetric $SL(2; \mathbb{R})/U(1)$ coset. Our assumption mentioned above is

$$Z_{00} = \langle 0 | e^{-\pi\tau_c(L_0 + \bar{L}_0 - \frac{c}{12}) + iy(J_0 + \bar{J}_0)} | 0 \rangle = \sum_n \frac{\text{ch}_{0,n,n}(\tau_o)(1 - q_o)}{(1 + yq_o^{\frac{1}{2}+n})(1 + y^{-1}q_o^{\frac{1}{2}-n})} . \quad (6.67)$$

The modular S-transformation of the extended character of the identity representation (the identity character summed over the spectral flow) is given by [194]:

$$Z_{00} = \int_{-\frac{1}{2} + i\mathbb{R}_+} dj \sum_{m \in \frac{k}{2}\mathbb{Z}} \frac{i \sin(\pi(2j+1)) \sin \frac{\pi}{k}(2j+1)}{2 \sin(j+m)\pi \sin(j-m)\pi} \text{ch}_{j,m,0}(\tau_c) + (\text{discrete}) . \quad (6.68)$$

The discrete terms are a little bit trickier to obtain, and we refer the complete form to original papers [194].

The boundary wavefunction is essentially obtained by taking the square root of the modular S-matrix in analogy with (6.64). Expanding the identity boundary state as

$$\langle 0 | = \int_{-\frac{1}{2} + i\mathbb{R}_+} dj \sum_m \Psi(j, m)_0 \langle \langle j, m | , \quad (6.69)$$

we obtain

$$\Psi(j, m)_0 = \nu_b^{2j+1} \frac{\Gamma(-j + \frac{k\omega}{2})\Gamma(-j - \frac{k\omega}{2})}{\Gamma(-2j-1)\Gamma(1 - b^2(2j+1))} . \quad (6.70)$$

We should note that the condition does not determine the (j, m) dependent phase factor of the boundary wavefunction. The ambiguity of the phase, however, is completely fixed by the reflection relation

$$\Psi(-p, m) = R(p, m)\Psi(p, m) , \quad (6.71)$$

together with the Hermiticity condition $\Psi(p, m)^\dagger = \Psi(-p, -m)$.

The next assumption is the overlap between the identity brane $|0\rangle$ and the general brane $|a\rangle$ labeled by the character of the $SL(2; \mathbb{R})/U(1)$ coset model in analogy with (6.65):

$$\langle 0 | e^{-\pi\tau_c(L_0 + \bar{L}_0 - \frac{c}{12}) + iy(J_0 + \bar{J}_0)} | a \rangle = \chi_a(i\tau_o, y) . \quad (6.72)$$

⁸⁸Otherwise, we obtain the D-brane in the decompactified theory, which has been studied in [204, 198], in the context of the $\mathcal{N} = 2$ Liouville theory. We also note that our summation over the spectral flow is different from [194], where the summation is taken over $n \in k\mathbb{Z}$ for integral k . For A-brane, the latter summation leads to the integral $U(1)_R$ charge (i.e. fractional ω quantum number).

We assume that the open string character appearing in the right hand side is given by the continuous series summed over the spectral flow (class 2 brane) and the discrete series summed over the spectral flow (class 3 brane).

The S-modular transformation of the extended character for the continuous series (parametrized by J and M) is particularly easy:

$$\sum_{n \in \mathbb{Z}} \text{ch}_{J,M+n,n}(\tau_o, y) = -i \sum_{m \in \frac{k}{2}\mathbb{Z}} \int_{-\frac{1}{2} + i\mathbb{R}_+} dj \text{ch}_{j,m,0}(\tau_c, y) e^{-\frac{4\pi i M m}{k}} \cos\left[\frac{\pi}{k}(2j+1)(2J+1)\right]. \quad (6.73)$$

From the modular bootstrap ansatz (6.72), we obtain the boundary wavefunction corresponding to the continuous series as

$$\begin{aligned} \Psi(p, m)_{J,M} &= \Psi(-p, -m)_0^{-1} e^{-\frac{4\pi i M m}{k}} \cos\left[\frac{\pi}{k}(2j+1)(2J+1)\right] \\ &= \nu_b^{2j+1} \frac{\Gamma(2j+1)\Gamma(1+b^2(2j+1))}{\Gamma(1+j+\frac{k\omega}{2})\Gamma(1+j-\frac{k\omega}{2})} e^{-\frac{4\pi i M m}{k}} \cos\left[\frac{\pi}{k}(2j+1)(2J+1)\right]. \end{aligned} \quad (6.74)$$

With the parameter identification $r_0 = \frac{\pi}{k}(2J+1)$, $\theta_0 = -2\pi M$, we have obtained the boundary wavefunction for the partially wrapped D2-brane.

The S-modular transformation of the extended character for the discrete series are more involved:

$$\begin{aligned} &\sum_{n \in \mathbb{Z}} \frac{y^{-\frac{2}{k}(M+n)} \text{ch}_{J,M+n,n}(\tau_o, y)}{1 + y^{-1} q_o^{\frac{1}{2} + J - M - n}} \\ &= -i \sum_{m \in \frac{k}{2}\mathbb{Z}} \int_{-\frac{1}{2} + \mathbb{R}_+} dj \text{ch}_{j,m}(\tau_c, y) e^{2\pi i M \omega} \left[\frac{e^{i(2J+1)(2j+1)}}{\sin \pi(j - \frac{k\omega}{2})} - \frac{e^{-(2J+1)(2j+1)}}{\sin(\pi(j + \frac{k\omega}{2}))} \right] \\ &+ (\text{discrete}). \end{aligned} \quad (6.75)$$

From the modular bootstrap ansatz (6.72), we obtain the boundary wavefunction corresponding to the discrete series as

$$\begin{aligned} &\Psi(p, m)_{J,M} \\ &= \nu_b^{2j+1} \Gamma(1+b^2(2j+1)) \Gamma(2j+1) e^{2\pi i M \omega} \times \\ &\times \left[\frac{\Gamma(-j + \frac{k\omega}{2})}{\Gamma(j+1 + \frac{k\omega}{2})} e^{i\pi(m-j) + i(2J+1)(2j+1)} - \frac{\Gamma(-j - \frac{k\omega}{2})}{\Gamma(j+1 - \frac{k\omega}{2})} e^{i\pi(m+j) - i(2J+1)(2j+1)} \right], \end{aligned} \quad (6.76)$$

where the parameter identification with the class 3 brane is $\theta_0 = 2\pi M + \frac{k\pi}{2}$, and $\sigma = -\frac{\pi}{2} + \frac{\pi}{k}(2J+1)$.

So far, we have obtained as many branes as the extended character of the $\mathcal{N} = 2$ supersymmetry (or $SL(2; \mathbb{R})/U(1)$ coset). We, however, have to check whether the obtained D-branes satisfy the Cardy condition among themselves. Namely, we have to compute the cylinder amplitudes and decompose them into the open string characters and verify the

positive definiteness of the density of states for continuous series and the positive integral multiplications for the discrete series. This was automatically guaranteed for the compact unitary CFTs thanks to the Verlinde formula. In our noncompact case, it is not a trivial problem. Indeed, although, almost all overlaps are consistent with the Cardy condition, the self-overlaps between class 3 branes for irrational value of k , we encounter negative multiplicities of discrete series in their spectra [79].⁸⁹

One might wonder what goes wrong with the modular bootstrap for the B-branes. The gist is that there is no identity brane for the B-boundary conditions. One can formally write down the modular bootstrap equations like (6.68), but there does not exist any analytic solution compatible with the reflection amplitudes for B boundary conditions. Due to this lack of the identity B-brane, the whole construction of the modular bootstrap breaks down. The coset construction from the descent of branes in \mathbb{H}_3^+ model was given in [79]. The conformal bootstrap for the dual $\mathcal{N} = 2$ Liouville theory can be found in [204, 199]

⁸⁹For integral value of k , this subtlety is avoided [195]. For general fractional value of k , the situation is more involved and the results depend on the combination of the other sectors embedded in the full string theory and the appropriate GSO condition we impose. The case by case study of these cases can be found in [194].

7 Rolling D-brane in Two-dimensional Black Hole

In this section, we study the D-branes in Lorentzian two-dimensional black hole. The organization of the section is as follows. In section 7.1, we study the classical D-branes in the Lorentzian two-dimensional black hole. In section 7.2, we construct the boundary states for the rolling D-brane from the Wick rotation of the class 2 brane in the Euclidean two-dimensional black hole system.⁹⁰ In section 7.3, we study some properties of our boundary wavefunction focusing on $1/k$ corrections.

7.1 Classical D-branes

7.1.1 DBI analysis

The classical D-branes in Lorentzian two-dimensional black hole is classified by the solution of the equation of motion coming from the DBI action

$$S^L = \mu_{p+1} \int d^{p+1}\xi e^{-\Phi} \sqrt{-\det(G_{ab} + B_{ab} + F_{ab})} . \quad (7.1)$$

The classical background is given by

$$ds^2 = k\alpha'(-\tanh^2 \rho dt^2 + d\rho^2), \quad e^{2\Phi} = \frac{k}{\mu \cosh^2 \rho} , \quad (7.2)$$

or when we are interested in the global structure of the solution, we use the Kruscal coordinate

$$ds^2 = -2k \frac{dudv}{1-uv} , \quad e^{2\Phi} = \frac{k}{\mu(1-uv)} . \quad (7.3)$$

by the coordinate transformation: $u = \sinh \rho e^t$, $v = -\sinh \rho e^{-t}$.

We begin with the D(-1) instanton. A physical meaning of such D-brane is a little bit unclear in the Lorentzian signature, but the “effective action”

$$S_{-1} \propto e^{-\phi} = \sqrt{1-uv} \quad (7.4)$$

could be extremized at $u = v = 0$ or $\rho = 0$.

Next we study the D0-brane. In the local coordinate outside the horizon, we can write down the DBI action as

$$S_0 = \mu_0 \int dt \cosh \rho(t) \sqrt{-\dot{\rho}(t)^2 + \tanh^2 \rho(t)} , \quad (7.5)$$

where we have fixed the reparametrization invariance by taking the temporal gauge $\xi_0 = t$. From the energy conservation, we obtain

$$\text{const} = \cosh \rho \frac{\tanh^2 \rho}{\sqrt{-\dot{\rho}^2 + \tanh^2 \rho}} , \quad (7.6)$$

⁹⁰This part of the thesis is based on [1].

which can be integrated to

$$\sinh(\rho) \cosh(t - t_0) = \text{const} . \quad (7.7)$$

The D0-brane motion (7.7) also follows from the Wick rotation $\theta \rightarrow it$ to the hairpin brane (6.7) in the Euclidean two-dimensional black hole. As we mentioned in section 5.3, The action (7.5) can be rewritten in the same form as the rolling D-brane in the linear dilaton background by introducing ‘tachyon’ variable $Y \equiv \log \sinh \rho$:

$$L_{\text{D0}} = -V(Y) \sqrt{1 - \dot{Y}^2} \quad \text{where} \quad V(Y) = M_0 e^Y , \quad (7.8)$$

which leads us to the ‘tachyon - radion correspondence’ discussed in section 5.

To study the global structure, we use the Kruscal coordinate (7.3). In this coordinate system, the DBI action takes the flat form

$$S = \mu_0 \int d\xi \sqrt{\frac{du dv}{d\xi d\xi}} . \quad (7.9)$$

The equation of motion is solved by a straight line in the (u, v) plane. It is interesting to note that the D0-brane does not feel the existence of the singularity at $uv = 1$. The classical trajectory is analytically continued inside the singularity in a trivial way. This is because the curvature singularity is cancelled against the dilaton singularity, which appears in the DBI action in the opposite way. The coupling to the dilaton is a crucial difference between the D-brane and a usual particle (such as a point like F-string or folded string solution discussed in section 3.3.2) in the two-dimensional black hole background.

Let us finally consider the D1-brane. The DBI action in the Kruscal coordinate is

$$S_1 = \mu_1 \int dudv \sqrt{1 - uv} \sqrt{\frac{1}{(1 - uv)^2} - F_{uv}^2} \quad (7.10)$$

in the gauge $\xi_0 = u$, $\xi_1 = v$. The Gauss law constraint

$$f = \frac{\sqrt{1 - uv} F_{uv}}{\sqrt{\frac{1}{(1-uv)^2} - F_{uv}^2}} \quad (7.11)$$

is solved by

$$F_{uv}^2 = \frac{f^2}{(1 - uv + f^2)(1 - uv)^2} . \quad (7.12)$$

When $f^2 > 0$, the world-sheet of the D1-string covers the whole physical region of the two-dimensional black hole, and possibly it has a boundary inside the singularity at $uv = 1 + f^2$. When $f^2 = -\kappa^2 < 0$, the D1-string has a boundary at $uv = 1 - \kappa^2$, and describes a long folded string. However, the DBI action for the long folded string becomes imaginary, so the solution is overcritical and unphysical.⁹¹

⁹¹This is a general feature of the Lorentzian solution for the D-brane with the boundary coming from the blow-up of the field strength. In the Lorentzian signature, the terms inside the square root of the DBI action is bounded, or in other words the field strength has a critical value. Thus any D-brane that has a boundary due to the divergence of the field strength is overcritical and hence unphysical unlike the case in the Euclidean signature.

7.1.2 group theoretical viewpoint

As we have done in section 6.1.2, we can also study the classical D-brane in the Lorentzian two-dimensional black hole from the coset construction. We parametrize the parent $SL(2; \mathbb{R})$ element g as

$$g = \begin{pmatrix} a & u \\ -v & b \end{pmatrix}, \quad uv + ab = 1. \quad (7.13)$$

Under the axial gauge transformation $\delta g = \epsilon(\sigma_3 g + g \sigma_3)$, the (u, v) is invariant, and serves as a gauge invariant coordinate describing the two-dimensional black hole (i.e. we can identify them as (u, v) in the Kruscal coordinate (7.3)).

The maximally symmetric D-brane in the parent $SL(2; \mathbb{R})$ WZNW model is classified by the (twined) conjugacy class of the group. The conjugacy class is given by

$$\text{Tr}(g) = a + b \quad (7.14)$$

and the twined conjugacy class is given by

$$\text{Tr}(\sigma_1 g) = u - v, \quad (7.15)$$

up to a conjugation (i.e. Lorentz boost between σ_1 and σ_2). To derive the D-branes in the coset model, we have to project the twined conjugacy class to the coset variables for A-branes. For B-branes, we first take a superposition of the gauge orbit of the conjugacy class so that we obtain a gauge invariant object as a D-brane.

Let us begin with the A-branes. The twined conjugacy class (7.15) is invariant under the axial gauge transformation, so the D-brane (D0-brane) is classified by the equation

$$2\kappa = \text{Tr}(\sigma_1 g) = u - v, \quad (7.16)$$

which gives a straight line in the Kruscal coordinate of the two-dimensional black hole as we observed in section 7.1.1 from the DBI analysis. More general branes are obtained by the Lorentz boost:

$$ue^{t_0} - ve^{-t_0} = 2\kappa. \quad (7.17)$$

The existence of such boosted D-branes are consistent with the fact that the existence of the Nambu-Goldstone modes associated with the symmetry breaking due to the A-brane as we have reviewed in section 6.1.2.

Let us move on to the B-branes. In this case, the conjugacy class is not invariant under the axial gauge transformation. In order to obtain an invariant object that can be projected down to the coset, we need to sum over the gauge orbit. With fixing the trace as $a + b = 2\kappa$, the determinant constraint reads

$$uv = 1 - \kappa^2 + (a - \kappa)^2 \geq 1 - \kappa^2. \quad (7.18)$$

It is not difficult to see that the gauge orbit of the conjugacy class precisely agrees with the domain bounded by the last inequality. The string configuration reproduces the folded D1-string obtained from the DBI analysis in section 7.1.1. We note, however, that the solution is

overcritical and unphysical as we have seen in section 7.1.1.⁹² We also see that the D-string that covers the whole physical region of the two-dimensional black hole cannot be obtained from a simple descent from the D-branes in the $SL(2; \mathbb{R})$ WZNW model without an analytic continuation.

7.2 Boundary states from Wick rotation

7.2.1 analytic continuation of boundary states

In this section, we shall construct the exact boundary state describing the D0-brane moving in the Lorentzian two-dimensional black hole background. Recall that the Lorentzian two-dimensional black hole ('Lorentzian cigar') background is obtainable by the Wick rotation $\theta = it$ of the Euclidean one (3.45)

$$ds^2 = 2k(d\rho^2 - \tanh^2 \rho dt^2) \quad \text{and} \quad e^\Phi = \frac{e^{\Phi_0}}{\cosh \rho} . \quad (7.19)$$

Wick-rotating the geodesic of the Euclidean D1-brane, we found the geodesic of the Lorentzian D0-brane in (7.7) as

$$\cosh(t - t_0) \sinh \rho = \sinh \rho_0 , \quad (7.20)$$

where t_0, ρ_0 are free parameters. Notice that the D0-brane reaches the horizon $\rho = 0$ at $t \rightarrow \pm\infty$ irrespective of the values of ρ_0 and t_0 . Thus, formally, the Lorentzian D0-brane boundary state is obtainable by Wick rotation of the Euclidean D1-brane boundary state (6.57) if we are interested in the physics outside the event horizon.⁹³

Reconstructing boundary states of the Lorentzian D-brane from those of the Euclidean D-brane is generically not unique. Rather, the following potential subtleties need to be faced:

- The Euclidean momentum n along the asymptotic circle of cigar is quantized, while the corresponding quantum number in the Lorentzian theory (*i.e.* the energy) takes a continuous value.
- The Wick rotations of primary states are not necessarily unique. Often, appropriate boundary conditions should be specified.

As for the first point, which has to do with Matsubara formulation, we can formally avoid the difficulty of quantized momentum by the following heuristic consideration. Suppose the boundary wave function $\hat{f}(n, \alpha)$ ($n \in \mathbb{Z}$ is the quantized Euclidean energy, and α denotes

⁹²It is not uncommon that the group theoretical classification of the D-branes in the Lorentzian coset gives unphysical D-branes (see e.g. [205]). Our identification of the parameter is different from the one given in [183], which solves a small puzzle raised there. The extra i comes from a (hypothetical) time-like T-duality [206] which we need to perform to obtain the parameter identification according to the discussion given in [189].

⁹³Some classical analysis of D-brane dynamics was attempted in [183] within the Dirac-Born-Infeld approach.

the remaining quantum numbers not touched here) is given by the Fourier transform of a periodic function $f(x + 2\pi, \alpha) = f(x, \alpha)$. We then obtain

$$\begin{aligned} \langle B | &= \sum_{\alpha} \sum_{n \in \mathbb{Z}} \tilde{f}(n, \alpha) \langle \langle n, \alpha | = \sum_{\alpha} \sum_{n \in \mathbb{Z}} \frac{1}{2\pi} \int_{-\pi}^{\pi} dx f(x, \alpha) e^{inx} \langle \langle n, \alpha | \\ &= \sum_{\alpha} \int_{-\infty}^{\infty} \frac{dq}{2\pi} \int_{-\infty}^{\infty} dx f(x, \alpha) e^{iqx} \langle \langle q, \alpha | , \end{aligned} \quad (7.21)$$

where we used the identity $\sum_{n \in \mathbb{Z}} \delta(q - n) = \sum_{m \in \mathbb{Z}} e^{2\pi imq}$ in obtaining the last expression. Assuming that $f(x, \alpha)$ is analytic along the entire real x axis, the Wick rotation can be performed. Often, $f(x, \alpha)$ is non-analytic over the real x axis, and the integral in the last expression is ill-defined. This turns out to be the case for the boundary wave function of the Euclidean D1-brane (6.57): in the coordinate space, the wave function has branch cuts and singularities along the real x -axis. In such cases, the best we can do is to adopt the slightly deformed integration contour \mathcal{C} in x -space⁹⁴ to render the Fourier integral well-defined:

$$\langle B' | \Big|_{\text{Euclidean}} := \sum_{\alpha} \int_{-\infty}^{\infty} \frac{dq}{2\pi} \int_{\mathcal{C}} dx f(x, \alpha) e^{iqx} \langle \langle q, \alpha | . \quad (7.22)$$

Likewise, disk one-point function of vertex operator $\Phi_{q, \alpha}^{\text{Euclidean}}$ (associated with the Ishibashi state $\langle \langle q, \alpha |$) is evaluated as the deformed contour integral:

$$\left\langle \Phi_{q, \alpha}^{\text{Euclidean}} \right\rangle_{\text{disk}} = \mathbb{E} \langle B' | q, \alpha \rangle = \int_{\mathcal{C}} dx f(x, \alpha) e^{iqx} . \quad (7.23)$$

Assuming sufficient analyticity, one then defines Wick rotation of the states (7.22) by the contour deformation of \mathcal{C} accompanied by the continuation $q \rightarrow i\omega, x \rightarrow it$;

$$\langle B' | \Big|_{\text{Lorentzian}} := \sum_{\alpha} \int_{-\infty}^{\infty} \frac{id\omega}{2\pi} \int_{-\infty}^{\infty} idt f(it, \alpha) e^{-i\omega t} \langle \langle i\omega, \alpha | . \quad (7.24)$$

This is essentially the procedure taken in [207]. Of course, we potentially have an ambiguity in the choice of the contour \mathcal{C} , and the correct choice should be determined by the physics under study.

In the present case $\langle B |$ corresponds to (6.57) and $\langle B' |$ is given by

$${}_{\text{D1}} \langle B' ; \rho_0, \theta_0 | = \int_0^{\infty} \frac{dp}{2\pi} \int_{-\infty}^{\infty} \frac{dq}{2\pi} \Psi'_{\text{D1}}(\rho_0, \theta_0; p, q) \langle \langle p, q | , \quad (7.25)$$

⁹⁴To be more precise, we should allow to use some decomposition

$$f(x, \alpha) = f_1(x, \alpha) + f_2(x, \alpha) + \dots ,$$

and to take the different contours for each piece $f_i(x, \alpha)$.

where

$$\begin{aligned}
& \Psi'_{\text{D1}}(\rho_0, \theta_0; p, q) \\
&= \frac{\sinh(\pi p)}{\left| \cosh\left(\pi \frac{p+iq}{2}\right) \right|^2} \frac{\pi \Gamma(ip) \Gamma\left(1 + \frac{ip}{k}\right)}{\Gamma\left(\frac{1}{2} + \frac{ip+q}{2}\right) \Gamma\left(\frac{1}{2} + \frac{ip-q}{2}\right)} e^{iq\theta_0} \left[e^{-ip\rho_0} + \frac{\cosh\left(\pi \frac{p-i|q|}{2}\right)}{\cosh\left(\pi \frac{p+i|q|}{2}\right)} e^{ip\rho_0} \right] \\
&\equiv B\left(\frac{1}{2} - \frac{ip-q}{2}, \frac{1}{2} - \frac{ip+q}{2}\right) \Gamma\left(1 + \frac{ip}{k}\right) e^{iq\theta_0} \left[e^{-ip\rho_0} + \frac{\cosh\left(\pi \frac{p-i|q|}{2}\right)}{\cosh\left(\pi \frac{p+i|q|}{2}\right)} e^{ip\rho_0} \right]. \quad (7.26)
\end{aligned}$$

Here $B(p, q) \equiv \Gamma(p)\Gamma(q)/\Gamma(p+q)$ denotes Euler's beta function. The integration contour

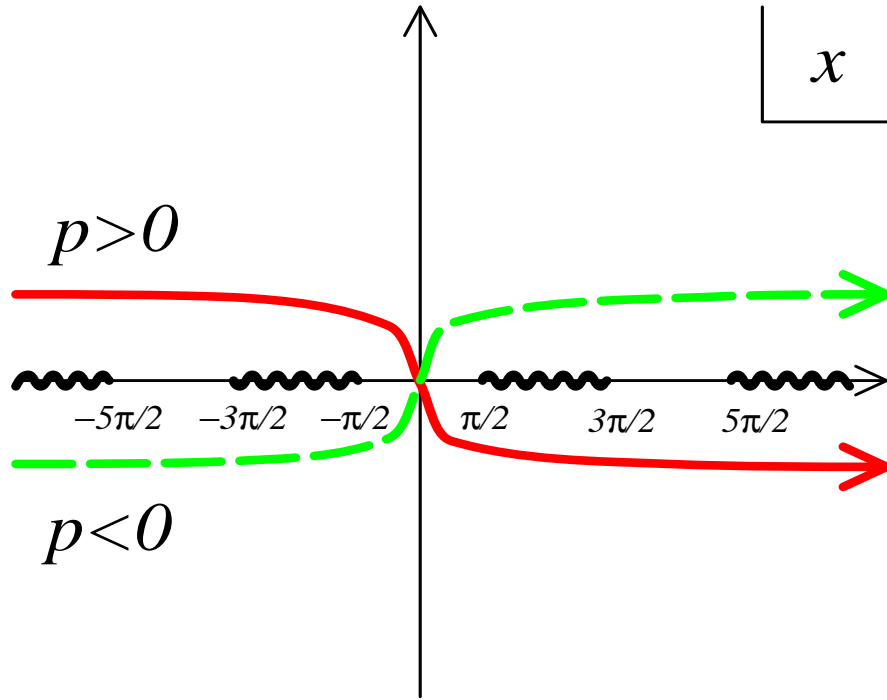


Figure 8: The red (green broken) line is the contour \mathcal{C}^+ for $p > 0$ to the Lorentzian time. Notice that an infinite number of branch cuts repeats in the Euclidean time: $\frac{\pi}{2} + 2n\pi < x < \frac{3\pi}{2} + 2n\pi$, ($n \in \mathbb{Z}$) along the real x -axis.

\mathcal{C} we choose is shown in Figure 8 [207]. As in (6.30), we separately evaluated the integrals of $\phi_{L,q}^p$ and $\phi_{R,q}^p$ based on the decomposition (3.54). For the convergence of integrals, we choose the contour \mathcal{C}^+ for $\phi_{L,q}^p$ ($p > 0$ sector) and \mathcal{C}^- for $\phi_{R,q}^p$ ($p < 0$ sector). Such choice of integration contours rendered an extra damping factor $\sinh(\pi p)/|\cosh(\pi \frac{p+iq}{2})|^2$, which improves the ultraviolet behavior of the wavefunction and makes it possible to take the Wick rotation sensibly. The non-trivial phase factor $\cosh(\pi \frac{p-i|q|}{2})/\cosh(\pi \frac{p+i|q|}{2})$ in the second term originates from the reflection amplitude, and it reduces to $(-1)^n$ when $q = n \in \mathbb{Z}$.

The second subtlety implies that $\langle\langle i\omega, \alpha |$ is not uniquely defined in (7.24). This is the issue that arises in a background with horizon, equivalently, non-existence of globally definable timelike Killing vector. As such, this subtlety did not arise for the extremal NS5-brane geometry (described asymptotically by free linear dilaton theory) considered in [207]. In section 7.2.4, within the mini-superspace analysis for the Lorentzian two-dimensional black hole, we shall clarify this subtlety.

An alternative, sensible prescription of the analytic continuation is to define the disk one-point correlator *directly* via the Lorentzian Fourier transform:

$$\left\langle \Phi_{\omega, \alpha}^{\text{Lorentzian}} \right\rangle_{\text{disk}} = \int_{-\infty}^{\infty} dt f(it, \alpha) e^{-i\omega t} . \quad (7.27)$$

This is *not* always equivalent to the the former method elaborated above. In fact, the latter method does not necessarily assert that the boundary state constructed so is expandable in terms of the Lorentzian Ishibashi states that are analytically continued from the Euclidean ones.⁹⁵

In section 3.3.4, we have reviewed the primary states for the Lorentzian two-dimensional black hole. Having obtained the Lorentzian primary states, we shall now construct several interesting class of boundary states for a D0-brane propagating in the black hole background. We have seen that the D0-brane propagates along the trajectory (7.20). The two-dimensional black hole is eternal, so, in addition to the past and the future asymptotic infinities, the causal propagation region has the past horizon \mathcal{H}^- surrounding the white hole singularity and the future horizon \mathcal{H}^+ surrounding the black hole singularity. As such, by taking variety of possible boundary conditions, we can construct interesting class of boundary states.

7.2.2 boundary state of D0-brane absorbed to future horizon

Consider first the boundary state obeying the boundary condition $\psi(\rho, t) \rightarrow 0$ at the past horizon \mathcal{H}^- , viz. the primary states $|U_\omega^p\rangle$. This boundary condition is relevant for scattering of a D0-brane off the black hole, since the condition represents absorption only and no emission of the D0-brane by the black hole. D0-brane boundary state obeying such absorbing boundary condition is then expanded solely by the Ishibashi states $\widehat{U}\langle\langle p, \omega |, |p, \omega \rangle\rangle^U$ that are associated with the primary states $\widehat{\langle U_\omega^p |, |U_\omega^p\rangle}$:

$$\begin{aligned} \text{absorb}\langle B; \rho_0, t_0 | &= \int_0^\infty \frac{dp}{2\pi} \int_{-\infty}^\infty \frac{d\omega}{2\pi} \Psi_{\text{absorb}}(\rho_0, t_0; p, \omega) \widehat{U}\langle\langle p, \omega | , \\ |B; \rho_0, t_0\rangle_{\text{absorb}} &= \int_0^\infty \frac{dp}{2\pi} \int_{-\infty}^\infty \frac{d\omega}{2\pi} \Psi_{\text{absorb}}^*(\rho_0, t_0; p, \omega) |p, \omega\rangle\rangle^U . \end{aligned} \quad (7.28)$$

The boundary wavefunction $\Psi_{\text{absorb}}(\rho_0, t_0; p, \omega)$ is then interpreted as the disk one-point correlators:

$$\Psi_{\text{absorb}}(\rho_0, t_0; p, \omega) = \langle U_\omega^p \rangle_{\text{disk}} \equiv \text{absorb}\langle B; \rho_0, t_0 | U_\omega^p \rangle , \quad (7.29)$$

⁹⁵Recently, we have succeeded the direct evaluation of the overlap integral. See appendix B.5 for details.

The boundary wavefunction (7.29) is then obtained by taking the Wick rotation $q \rightarrow i\omega$ ($q \rightarrow -i\omega$) for $q < 0$ ($q > 0$) in (7.26) (recall (3.100)):⁹⁶

$$\Psi_{\text{absorb}}(\rho_0, t_0; p, \omega) = B(\nu_+, \nu_-) \Gamma\left(1 + \frac{ip}{k}\right) e^{-i\omega t_0} \left[e^{-ip\rho_0} - \frac{\cosh\left(\pi \frac{p-\omega}{2}\right)}{\cosh\left(\pi \frac{p+\omega}{2}\right)} e^{ip\rho_0} \right], \quad (7.30)$$

The relative minus sign in the second term of $\Psi_{\text{absorb}}(\rho_0, t_0; p, \omega)$ originates from the fact that the contour rotation defining the Wick rotation has opposite directions for \mathcal{C}^+ (suitable for $p > 0$) and \mathcal{C}^- (suitable for $p < 0$). See figure 8. This boundary wavefunction (7.30) satisfies the exact reflection relation

$$\Psi_{\text{absorb}}(\rho_0, t_0; -p, \omega) = \mathcal{R}(-p, \omega) \Psi_{\text{absorb}}(\rho_0, t_0; p, \omega). \quad (7.31)$$

With such boundary condition, the boundary wavefunction (7.30) would have no overlap with D0-brane's trajectory (7.20) in the far past region $t \ll t_0$. In fact, the trajectory (7.20) starts from the past horizon \mathcal{H}^- at $t = -\infty$, reaches the time-symmetric point $\rho = \rho_0$ at $t = t_0$, and then falls back the future horizon \mathcal{H}^+ at $t = +\infty$, while the wavefunction U_ω^p does not have any component outgoing from \mathcal{H}^- . We thus interpret that the boundary state (7.30) describes the future half of the classical trajectory (7.20). We shall hence call it the 'absorbed D-brane'.

By utilizing the radion-tachyon correspondence, the rolling radion (as described by the boundary state (7.30)) can be also interpreted as the rolling tachyon. In the latter interpretation, the D0-brane absorbed to the future horizon is the counterpart of the future-half S-brane [208, 209, 210], in which the tachyon rolls down the potential hill at asymptotic future $t \rightarrow +\infty$ and emits radiation.

7.2.3 boundary state of D0-brane emitted from past horizon

Consider next the boundary condition: $\psi(\rho, t) \rightarrow 0$ at \mathcal{H}^+ , viz. use the basis $|p, \omega\rangle\rangle^V$, $\widehat{V}\langle\langle p, \omega|$ instead of $|p, \omega\rangle\rangle^U$, $\widehat{U}\langle\langle p, \omega|$. Utilizing the reflection relation, we can first rewrite (7.26) as the form which only includes the $p < 0$ Ishibashi states by means of the reflection relation. Then, we can analytically continue the states $|\phi_q^{-p}\rangle$ ($p > 0$) into $|V_\omega^p\rangle$. The resultant boundary state is obtained by simply replacing $p \rightarrow -p$, $\omega \rightarrow -\omega$ in (7.30);

$$\begin{aligned} \text{emitted}\langle B; \rho_0, t_0 | &= \int_0^\infty \frac{dp}{2\pi} \int_{-\infty}^\infty \frac{d\omega}{2\pi} \Psi_{\text{emitted}}(\rho_0, t_0; p, \omega) \widehat{V}\langle\langle p, \omega | . \\ |B; \rho_0, t_0\rangle_{\text{emitted}} &= \int_0^\infty \frac{dp}{2\pi} \int_{-\infty}^\infty \frac{d\omega}{2\pi} \Psi_{\text{emitted}}^*(\rho_0, t_0; p, \omega) |p, \omega\rangle\rangle^V . \end{aligned} \quad (7.32)$$

where

$$\Psi_{\text{emitted}}(\rho_0, t_0; p, \omega) = B(\nu_+^*, \nu_-^*) \Gamma\left(1 - \frac{ip}{k}\right) e^{-i\omega t_0} \left[e^{ip\rho_0} - \frac{\cosh\left(\pi \frac{p-\omega}{2}\right)}{\cosh\left(\pi \frac{p+\omega}{2}\right)} e^{-ip\rho_0} \right].$$

⁹⁶In reality, there is a further overall factor i , but, for notational simplicity, we will absorb it to the definition of the Ishibashi states.

Obviously, the emitted D0-brane wavefunction is the time-reversal of the absorbed D0-brane wavefunction (7.30):

$$\Psi_{\text{emitted}}(\rho_0, t_0; p, \omega) = \Psi_{\text{absorb}}^*(\rho_0, -t_0; p, \omega) .$$

Namely, it describes the D0-brane emitted from the past horizon at asymptotic past $t = -\infty$. By the choice of the boundary condition, this boundary state (7.32) describes only the past half of the classical D0-brane trajectory (7.20).

The exact reflection relation has the form

$$\Psi_{\text{emitted}}(\rho_0, t_0; -p, \omega) = \mathcal{R}^*(-p, \omega) \Psi_{\text{emitted}}(\rho_0, t_0; p, \omega) . \quad (7.33)$$

Again, in light of the radion-tachyon correspondence, the D0-brane emitted from the past horizon is the counterpart of the past-half S-brane in tachyon rolling. The radiation creeps up the tachyon potential hill from past infinity and forms an unstable D-brane.

7.2.4 boundary state of time-symmetric D0-brane

The third possible boundary state is obtainable by *directly* taking the analytic continuation in the disk one-point amplitudes, as we already mentioned. Recalling (3.100), we shall analytically continue the disk amplitudes as (assume $p > 0$)

$$\langle \phi_q^{+p} \rangle_{\text{disk}} \longrightarrow \langle U_\omega^p \rangle_{\text{disk}} \quad \text{and} \quad \langle \phi_q^{-p} \rangle_{\text{disk}} \longrightarrow \langle V_\omega^p \rangle_{\text{disk}} . \quad (7.34)$$

The Euclidean one-point amplitudes $\langle \phi_q^{\pm p} \rangle_{\text{disk}}$ are given in (7.26), and can be expressed in contour integrals as in (7.23). Recall that $\langle \phi_{L,q}^p \rangle_{\text{disk}}$, $\langle \phi_{R,q}^p \rangle_{\text{disk}}$ are prescribed by the contour integrals over \mathcal{C}^+ , \mathcal{C}^- in figure 8. We shall thus analytically continue them to the real time axis (imaginary x -axis). In this way, we extract the Lorentzian disk one-point amplitudes as

$$\langle U_\omega^p \rangle_{\text{disk}} = \langle U_\omega^p \rangle_{\text{disk}}^{(\text{absorb})} \quad \text{and} \quad \langle V_\omega^p \rangle_{\text{disk}} = \langle V_\omega^p \rangle_{\text{disc}}^{(\text{emitted})} , \quad (7.35)$$

where the right-hand sides are simply the amplitudes associated with the ‘absorbed’ and ‘emitted’ D0-branes considered in the previous subsections and explicitly given in (7.30) and (7.32). Since U_ω^p and V_ω^p constitute the complete set of basis for Lorentzian primary fields, the amplitudes (7.35) would yield yet another Lorentzian D0-brane boundary states. As is obvious from the above construction, this state keeps the time-reversal symmetry manifest and reproduces the entire classical trajectory (7.20), that is, it describes a D0-brane emitted from the past horizon and reabsorbed to the future horizon. From the viewpoint of the boundary conformal theory, this would be considered the most natural one since it captures the entire classical trajectory of the D0-brane. In the radion-tachyon correspondence, this state is the counterpart of the full S-brane [208, 130, 131, 132].

Explicitly, the time-symmetric boundary states are given by

$$\begin{aligned}
& \text{symm}\langle B; \rho_0, t_0 | \\
&= \text{absorb}\langle B; \rho_0, t_0 | + \text{emitted}\langle B; \rho_0, t_0 | \\
&= \int_0^\infty \frac{dp}{2\pi} \int_{-\infty}^\infty \frac{d\omega}{2\pi} \left[2\Psi_{\text{symm}}(\rho_0, t_0; p, \omega) {}^L\langle p, \omega | + 2\Psi_{\text{symm}}^*(\rho_0, -t_0; p, \omega) {}^R\langle p, \omega | \right] \\
& |B; \rho_0, t_0\rangle_{\text{symm}} \\
&= |B; \rho_0, t_0\rangle_{\text{absorb}} + |B; \rho_0, t_0\rangle_{\text{emitted}} \\
&= \int_0^\infty \frac{dp}{2\pi} \int_{-\infty}^\infty \frac{d\omega}{2\pi} \left[2\Psi_{\text{symm}}^*(\rho_0, t_0; p, \omega) |p, \omega\rangle\right]^L + 2\Psi_{\text{symm}}(\rho_0, -t_0; p, \omega) |p, \omega\rangle\right]^R \quad (7.36)
\end{aligned}$$

where

$$\Psi_{\text{symm}}(\rho_0, t_0; p, \omega) = B(\nu_+, \nu_-) \Gamma\left(1 + \frac{ip}{k}\right) e^{-ip\rho_0 - i\omega t_0} \quad (7.37)$$

and ${}^L\langle p, \omega |, |p, \omega\rangle^L, {}^R\langle p, \omega |, |p, \omega\rangle^R$ are the Ishibashi states constructed over the primary states $\langle L_\omega^p |, |L_\omega^p\rangle, \langle R_\omega^p |, |R_\omega^p\rangle$,⁹⁷ respectively. One can readily check that the second lines in (7.36) are indeed correct by evaluating the disk one-point amplitudes from them. For instance, using (3.108), we obtain

$$\begin{aligned}
\langle U_\omega^p \rangle_{\text{disk}}^{(\text{symm})} &= \text{symm}\langle B; \rho_0, t_0 | U_\omega^p \rangle \\
&= \Psi_{\text{symm}}(\rho_0, t_0; p, \omega) + \mathcal{R}(p, \omega) \Psi_{\text{symm}}^*(\rho_0, -t_0; p, \omega) \\
&= B(\nu_+, \nu_-) \Gamma\left(1 + \frac{ip}{k}\right) e^{-i\omega t_0} \left[e^{-ip\rho_0} - \frac{\cosh\left(\pi \frac{p-\omega}{2}\right)}{\cosh\left(\pi \frac{p+\omega}{2}\right)} e^{ip\rho_0} \right] \\
&= \langle U_\omega^p \rangle_{\text{disk}}^{(\text{absorb})} \equiv \text{absorb}\langle B; \rho_0, t_0 | U_\omega^p \rangle. \quad (7.38)
\end{aligned}$$

Other one-point amplitudes can be checked analogously.

Two remarks are in order. First, notice that, though the disk one-point amplitudes are, the symmetric boundary states (7.36) by themselves are *not* analytically continuable to the Euclidean boundary state (7.26). This should not be surprising as the Lorentzian Hilbert space is generated by *twice* as many generators as the Euclidean theory. In other words, the Lorentzian bases $|U_\omega^p\rangle, |V_\omega^p\rangle$ correspond to $|\phi_n^p\rangle, |\phi_n^{-p}\rangle$ in the Euclidean theory, which were however linearly dependent due to the reflection relation. Nevertheless, the boundary state (7.36) is a consistent one and yields disk one-point amplitudes that can be correctly continued to the Euclidean ones. Second, the full Lorentzian Hilbert space is decomposed as

$$\mathcal{H} = \mathcal{H}^U \oplus \mathcal{H}^V \quad \text{and} \quad \widehat{\mathcal{H}} = \widehat{\mathcal{H}}^U \oplus \widehat{\mathcal{H}}^V, \quad (7.39)$$

where \mathcal{H}^U (\mathcal{H}^V) is spanned by $|U_\omega^p\rangle, (|V_\omega^p\rangle)$ and their descendants. The dual space $\widehat{\mathcal{H}}^U$ ($\widehat{\mathcal{H}}^V$) is similarly spanned by $\langle U_\omega^p |, (\langle V_\omega^p |)$. Here, the Hilbert subspaces $\mathcal{H}^U, \widehat{\mathcal{H}}^U$ ($\mathcal{H}^V, \widehat{\mathcal{H}}^V$) correspond to the boundary condition $\psi(\rho, t) \rightarrow 0$ at \mathcal{H}^- (\mathcal{H}^+). The ‘absorbed’ and ‘emitted’

⁹⁷The extra factor of ‘2’ was introduced for convenience. Recall (3.108).

D0-brane boundary states (7.30), (7.32) are consistent *only* in the subspaces \mathcal{H}^U , \mathcal{H}^V ($\widehat{\mathcal{H}}^U$, $\widehat{\mathcal{H}}^V$), while the ‘symmetric’ D0-brane boundary state (7.36) is well-defined in the entire Hilbert space \mathcal{H} ($\widehat{\mathcal{H}}$). We thus have simple relations

$$\begin{aligned} |B; \rho_0, t_0\rangle_{\text{absorb}} &= P_U |B; \rho_0, t_0\rangle_{\text{symm}} & \text{and} & \quad \text{absorb}\langle B; \rho_0, t_0| = \text{symm}\langle B; \rho_0, t_0| \widehat{P}_U, \\ |B; \rho_0, t_0\rangle_{\text{emitted}} &= P_V |B; \rho_0, t_0\rangle_{\text{symm}} & \text{and} & \quad \text{emitted}\langle B; \rho_0, t_0| = \text{symm}\langle B; \rho_0, t_0| \widehat{P}_V, \end{aligned} \quad (7.40)$$

where $P_{U,V}$ ($\widehat{P}_{U,V}$) denotes projection of the Hilbert space \mathcal{H} to $\mathcal{H}^{U,V}$ ($\widehat{\mathcal{H}}^{U,V}$).

7.3 Rolling D-brane gathers moss

As we have discussed in section 4, it is of critical importance to study the $1/k$ corrections to the boundary states in order to understand the ‘‘black hole - string transition’’ probed by our rolling D-brane. We first note that the boundary wavefunction itself is an analytic function with respect to k ,⁹⁸ so the boundary wavefunction itself is a well-defined quantity even for $k < 1$. An alternative way to confirm this is to note that, at least in the Euclidean signature, the boundary wavefunction satisfies the conformal bootstrap equation for the dual $\mathcal{N} = 2$ Liouville theory whose description is more reliable for $k < 1$.

To see the effect of the $1/k$ corrections clearly, it is convenient to go to the coordinate space representation rather than the momentum space representation. For simplicity, we take the linear dilaton (extremal) limit of the boundary wavefunction (see section 8.5 for details of this limit). In the momentum space we have,

$$\Psi(\rho_0, t_0; p, \omega) = \frac{1}{2} B(\nu_+, \nu_-) \Gamma\left(1 + i\frac{p}{k}\right) e^{-ip\rho_0 - i\omega t_0}, \quad \text{where} \quad \nu_{\pm} \equiv \frac{1}{2} - i\frac{p \pm \omega}{2}. \quad (7.41)$$

We can Fourier transform this boundary wavefunction to obtain the boundary wavefunction in the coordinate space:

$$\Psi(\rho, t) = \frac{\sqrt{k}}{\pi(2 \cosh t)^{k+1}} \exp\left[-k\rho - \frac{e^{-k\rho}}{(2 \cosh t)^k}\right]. \quad (7.42)$$

It will be localized along the classical trajectory:

$$\rho_0(t) = -\log(2 \cosh t) \quad (7.43)$$

in the semiclassical limit (i.e. $k \rightarrow \infty$). For finite k , the classical trajectory is smeared.

To go further, we study the energy momentum distribution for finite k . Expanding the boundary states and reading the coupling to the gravity, we obtain (see [148] for details of the computation)

$$T_{00} = \left(\frac{e^{-\rho}}{2 \cosh t}\right)^{k-1} \exp\left[-\left(\frac{e^{-\rho}}{2 \cosh t}\right)^k\right]. \quad (7.44)$$

⁹⁸A possible exception is the factor ν_b^{2j+1} . However, this factor can be absorbed (renormalized) into the cosmological constant operator of the $\mathcal{N} = 2$ Liouville theory, or the mass of the two-dimensional black hole, so we will neglect this small subtlety.

The distribution of the energy is Poisson type and the maximum of the energy density is now located at

$$\frac{e^{-\rho}}{2 \cosh t} = 1 - \frac{1}{k} . \quad (7.45)$$

The variance of the distribution is computed as

$$\Delta\rho \simeq \sqrt{\frac{1}{2(k-1)}} , \quad (7.46)$$

which can be regarded as the smearing factor for the classical trajectory due to the α' corrections. One might say that the rolling D-brane gathers moss in the α' corrected black hole background. The moss could be identified with the analytic continuation of the winding tachyon [100]. Indeed the similar smearing factor in the Euclidean hairpin brane can be understood from the open string winding tachyon condensation near the tip of the Euclidean hairpin.

We again emphasize that the coordinate space wavefunction itself is an analytic function with respect to k . However, below $k = 1$, the variance of the smeared D-brane trajectory (7.46) diverges, which means that the boundary wavefunction does not have a sensible interpretation as a rolling D-brane in the classical two-dimensional black hole any more. The transition point exactly coincides with the “black hole - string transition” point we discussed in section 4. The classical black hole appears no more black hole at this point, and the D-brane cannot roll down into the hole as a probe. In section 8, we compute the closed string radiation rate from the rolling D-brane, and see explicitly that the radiation rate also reveals such a phase transition as expected. As a consequence, we will see that the “tachyon - radion correspondence” and the universality of the decaying D-brane breaks down.

As a generalization of the construction, we can introduce the fundamental string charge (electric flux) along the rolling D-brane boundary states. The construction is based on the Lorenz boost technique reviewed in section 5.2.6. The corresponding boundary states have been studied in [148, 155].

8 Black Hole - String Transition from Probe Rolling D-brane

In this section we compute the closed string radiation rate from the rolling D-brane. The organization of this section is as follows. In section 8.1, we compute the closed string radiation rate from the closed string perspective. In section 8.2, we study the same closed string radiation rate from the open string perspective, establishing the consistency between unitarity and channel duality. In section 8.3, we discuss the black hole - string transition from the probe rolling D-brane. In section 8.4, the boundary states and radiation in R-R sector are discussed. In section 8.5, we study the extremal NS5-brane limit. Finally in section 8.6, we present the physical interpretations of Hartle-Hawking states for rolling D-branes.⁹⁹

8.1 Radiation out of rolling D-brane from closed string viewpoint

In the background of the black hole, the D0-brane moves along the geodesic and we have constructed a variety of boundary states describing the geodesic motion, specified by appropriate boundary conditions.

Both by gravity and by strong string coupling gradient, the Dp -brane is pulled in and finds its minimum energy and mass at the location of the NS5-brane. The Dp -brane is supersymmetric in flat space-time, but preserves no supersymmetry in black NS5-brane background. Even in extremal NS5-brane background, until the Dp -brane dissociates into the NS5-brane and form a non-threshold bound-state, the space-time supersymmetry is completely broken. In these respects, the Dp -brane propagating in the NS5-brane background is much like excited Dp -brane (many excited open strings attached on it) in flat space-time. Decay of the latter via closed string emission was studied extensively for $p = 1$ [211, 212]: the decay spectrum was found to match exactly with the Hawking radiation of the non-extremal black hole made out of these excited D-branes, and the effective temperature of excited open string modes agrees exactly with the Hawking temperature. In this section, we shall find certain analogous results for the closed string radiation off the rolling D0-brane, though special features also arise.

As the D0-brane is pulled in, acceleration would grow and radiates off the binding energy into closed string modes. Details of the radiation spectra would differ for different choice of the boundary conditions, viz. for different boundary states of the D0-brane. In this section, as a probe of the black hole geometry and D-brane dynamics therein, we shall analyze spectral distribution of the closed string radiation off the rolling D0-particle.

By applying the optical theorem, the radiation rate during the radion-rolling process is obtainable as the imaginary part of the annulus amplitude in the closed string channel.¹⁰⁰ Denote the differential number density $d\mathcal{N}(p, M)$ of the radiation at a fixed value of the radial momentum p and the mass-level M . By the definition of the D-brane boundary state,

⁹⁹This section is based on [1, 2].

¹⁰⁰For the tachyon rolling process in flat space-time background, the amplitude was evaluated first in [213, 135].

the radiation number density $d\mathcal{N}$ is then given in terms of the boundary wave functions:

$$\begin{aligned} d\mathcal{N}(p, M) &:= \frac{dp}{2\pi} \frac{dM}{(2\pi)^d} \int d\omega \left\langle \Psi(\omega, p, M) \left| \delta(L_0 + \bar{L}_0) \right| \Psi(\omega, p, M) \right\rangle \\ &= \frac{dp}{2\pi} \frac{dM}{(2\pi)^d} \frac{1}{2\omega(p, M)} \left| \Psi(p, \omega(p, M)) \right|^2. \end{aligned} \quad (8.1)$$

Here, ω, p are the energy and the radial momentum in two-dimensional Lorentzian background, M is the total mass (conformal weight) of the remaining subspaces of dimension d (including mass gap), $\Psi(\omega, p, M)$ is the boundary wave function (including that of the remaining subspace), and $\omega(p, M) (> 0)$ is the on-shell energy of the radiated closed string state determined by the on-shell condition $L_0 + \bar{L}_0 = 0$ including the ghost contribution. From the kinematical consideration, it is obvious that the differential number density (8.1) is nonzero only when the D-brane is rolling. Of particular physical interest is the spectral distribution in the phase-space, as measured by the independent moments, *e.g.*

$$\left\langle \omega^m M^n \right\rangle = \int \frac{dp}{2\pi} \frac{dM}{(2\pi)^d} \omega^m(p, M) M^n \frac{1}{2\omega(p, M)} \left| \Psi(p, \omega(p, M)) \right|^2$$

for $m, n = 0, 1, 2, \dots$. We shall evaluate these spectral observables by first evaluating the integral over the radial momentum p by saddle-point approximation. In doing so, we pay particular attention to the asymptotic behavior as the mass-level M becomes asymptotically large. We shall then evaluate the integral over the mass-level (conformal weight) M , and extract the spectral observables.

Consider the boundary state (7.30) describing a D0-brane absorbed by the future horizon. The radiation emitted by the D0-brane is decomposable into ‘incoming’ (toward the horizon) and ‘outgoing’ (toward the null infinity) components in the far future. The positive energy sector is expanded by the wavefunction U_ω^p , and has the following asymptotic behavior at $t \rightarrow +\infty$:

$$U_\omega^p(\rho, t) \sim e^{-i\omega \ln \rho - i\omega t} + d(p, \omega) e^{-\rho} e^{+ip\rho - i\omega t} \quad \text{where} \quad |d(p, \omega)| \sim e^{-\pi p}. \quad (8.2)$$

Here, we assumed $\omega \sim M \gg 0$. The first and the second terms correspond to the incoming wave supported around $\rho = 0$ and the outgoing wave supported in the region $\rho \sim +\infty$, respectively. The damping factor $d(p)$ originates from the exact reflection amplitude $\mathcal{R}(p, \omega)$. (See (3.102), (3.103).) To obtain the radiation number density, we need to evaluate $|\Psi(p, \omega)|^2 \times |U_\omega^p(\rho, t)|^2$. At far future infinity, the interference term in $|U_\omega^p|^2$ drops off upon taking the p -integral. Therefore, after integrating over the radial momentum p , the partial radiation distribution is seen to consist of the ‘incoming’ and ‘outgoing’ parts:

$$\begin{aligned} \mathcal{N}(M)_{\text{in}} &\equiv \int_0^M dM \frac{d\mathcal{N}_{\text{in}}}{dM} = \int_0^\infty \frac{dp}{2\pi} \frac{1}{2\omega(p, M)} \left| \Psi(p, \omega(p, M)) \right|^2 \\ \mathcal{N}(M)_{\text{out}} &\equiv \int_0^M dM \frac{d\mathcal{N}_{\text{out}}}{dM} = \int_0^\infty \frac{dp}{2\pi} \frac{1}{2\omega(p, M)} \left| d(p) \right|^2 \left| \Psi(p, \omega(p, M)) \right|^2. \end{aligned} \quad (8.3)$$

We shall now evaluate the branching ratio between the two radiation rates (8.3) with emphasis on possible string world-sheet effects. To this end, consider the conformal field theory

defined by $SL(2; \mathbb{R})/U(1) \times \mathcal{M}$, where $SL(2; \mathbb{R})/U(1)$ denotes the (super)coset model and \mathcal{M} denotes a unitary (super)conformal field theory of central charge $c_{\mathcal{M}}$. Such (super)conformal field theory covers a variety of interesting string theory backgrounds. For the fermionic string, superconformal invariance asserts that the central charge ought to be critical:

$$3\left(1 + \frac{2}{k}\right) + c_{\mathcal{M}} = 15 ,$$

where k denotes the level of the super $SL(2; \mathbb{R})$ current algebra. If the background describes a stack of black NS5-branes, $\mathcal{M} = SU(2)_k \times \mathbb{R}^5$ where k equals to the NS5-brane charge. Likewise, for the bosonic string case, conformal invariance asserts that the central charge should take the critical value:

$$2 + \frac{6}{\kappa - 2} + c_{\mathcal{M}} = 26 , \quad (8.4)$$

where now κ refers to the level of the bosonic $SL(2; \mathbb{R})$ current algebra. For the background describing the black hole in two-dimensional string theory, \mathcal{M} is empty and κ should be set to $9/4$.

It would be illuminating to analyze the branching ratio for the ‘rolling closed string’, viz. a closed string state of fixed transverse mass M and radial momentum p propagating in black hole geometry. The branching ratio is simply given by the reflection amplitude (see (3.111)):

$$\left. \frac{\mathcal{N}_{\text{out}}(p, \omega)}{\mathcal{N}_{\text{in}}(p, \omega)} \right|_{\text{closed string}} = |\mathcal{R}(p, \omega)|^2 = \frac{\cosh^2 \pi \left(\frac{\omega-p}{2}\right)}{\cosh^2 \pi \left(\frac{\omega+p}{2}\right)} . \quad (8.5)$$

As emphasized below (3.111), string world-sheet effects are present for the reflection amplitude \mathcal{R} itself but, being an overall phase, it drops out of (8.5). The k -dependence enters in the branching ratio (8.5) only through the on-shell dispersion relation $\omega = \sqrt{p^2 + 2kM^2}$. For two-dimensional case, first studied in [75] and [214], $k = 1/2$, $M = 0$ and $\omega = p$, so the scattering probability is exponentially suppressed as the energy increases.

For a fixed transverse mass M and the forward radial momentum p , the reflection probability of the infalling D0-brane is given precisely by the same result as (8.5):

$$\left. \frac{\mathcal{N}_{\text{out}}(p, \omega)}{\mathcal{N}_{\text{in}}(p, \omega)} \right|_{\text{D0-brane}} = |\mathcal{R}(p, \omega)|^2 = \frac{\cosh^2 \pi \left(\frac{\omega-p}{2}\right)}{\cosh^2 \pi \left(\frac{\omega+p}{2}\right)} . \quad (8.6)$$

This is simply because back-scattering of the boundary wave function originates from that of the closed string wave function: roughly speaking, the boundary wave function is defined by overlap of the closed string wave function with the classical trajectory of the D0-brane.

Radiation out of the falling D0-brane is coherent, so we integrate over the radial momentum p as in (8.3) in extracting the branching ratio. We shall first analyze the partial radiation distribution at large mass-level, $M \rightarrow \infty$. More precisely, we shall examine asymptotic behavior of $\mathcal{N}(M)$ multiplied by the phase-space ‘degeneracy factor’ $\rho(M) \sim e^{\frac{1}{2}M\beta_{\text{Hg}}}$, where β_{Hg} denotes inverse of the Hagedorn temperature. The closed string states that couple to the boundary states are left-right symmetric, so we need to take the square root of the usual

degeneracy factor in the closed string sector. Here, inverse of the Hagedorn temperature is given by

$$\beta_{\text{Hg}} = 4\pi \sqrt{1 - \frac{1}{2k}} , \quad (8.7)$$

for the superstring theory, and

$$\beta_{\text{Hg}} = 4\pi \sqrt{2 - \frac{1}{2(\kappa - 2)}} , \quad (8.8)$$

for the bosonic string theory, where the $1/k$ ($1/\kappa$)-correction is interpreted as the string world-sheet effects of the two-dimensional background. These results are derivable from the Cardy formula with the ‘effective central charge’ $c_{\text{eff}} = c - 24h_{\text{min}}$ [122], where h_{min} refers to the lowest conformal weight of normalizable primary states.

8.1.1 radiation distribution in superstring theory

Let us begin with the spectral distribution in superstring theories. We shall focus exclusively on the NS-NS sector of the radiation and defer the analysis of the R-R sector to section 8.4. The on-shell condition of closed string state in NS-NS sector is given by

$$-\frac{\omega^2}{4k} + \frac{p^2}{4k} + \frac{1}{4k} + \Delta_{\mathcal{M}} = \frac{1}{2} , \quad (8.9)$$

where $\Delta_{\mathcal{M}}$ denotes the conformal weight of the \mathcal{M} -part. The on-shell energy is given by

$$\omega \equiv \omega(p, M) = \sqrt{p^2 + 2kM^2} \quad \text{where} \quad M^2 \equiv 2 \left(\Delta_{\mathcal{M}} + \frac{1}{4k} - \frac{1}{2} \right) .$$

Consider now a D0-brane propagating outside the black hole and absorbed into the future horizon. The relevant boundary wave function was constructed in (7.30) and, from them, the differential radiation number distributions (8.3) can be computed. At large ω and p , using Stirling’s approximation, we find that

$$\begin{aligned} \mathcal{N}(M)_{\text{in}} &= \int_0^\infty \frac{dp}{2\pi} \frac{1}{2\omega(p, M)} \left| \Psi_{\text{absorb}}(\rho_0, t_0; p, \omega(p, M)) \right|^2 \\ &\sim \frac{1}{M} \int_0^\infty dp e^{+\pi(1-\frac{1}{k})p - \pi\sqrt{p^2+2kM^2}} \end{aligned} \quad (8.10)$$

$$\begin{aligned} \mathcal{N}(M)_{\text{out}} &= \int_0^\infty \frac{dp}{2\pi} \left| d(p, \omega(p, M)) \right|^2 \frac{1}{2\omega(p, M)} \left| \Psi_{\text{absorb}}(\rho_0, t_0; p, \omega(p, M)) \right|^2 \\ &\sim \frac{1}{M} \int_0^\infty dp e^{-\pi(1+\frac{1}{k})p - \pi\sqrt{p^2+2kM^2}} . \end{aligned} \quad (8.11)$$

In the second lines, we have taken M large, viz. $\omega \gg p \gg 1$, and keep the leading terms only. Thus, for each fixed but large M , the partial number distributions take the forms:

$$\mathcal{N}(M)_{\text{in}} \sim \int_0^\infty dp \sigma_{\text{in}}(p) e^{-\frac{1}{2}\beta_{\text{Hw}}M} \quad \text{and} \quad \mathcal{N}(M)_{\text{out}} \sim \int_0^\infty dp \sigma_{\text{out}}(p) e^{-\frac{1}{2}\beta_{\text{Hw}}M} , \quad (8.12)$$

where

$$\beta_{\text{Hw}} = 2\pi\sqrt{2k} , \quad (8.13)$$

is the inverse Hawking temperature of the fermionic two-dimensional black hole. As discussed above, the radiation off the D-brane in NS5-brane background is analogous to the decay of excited D-brane in flat ambient space-time. Indeed, asymptotic expression (8.12) suggests that open string excitations of energy M on the rolling D0-brane are populated as the distribution function $\exp(-\frac{1}{2}\beta_{\text{Hw}}M)$ and decay into closed string radiation. In this interpretation, the distribution function encodes change of available states for open string excitations on the D0-brane after emitting radiations of energy M . Curiously, ‘effective temperature’ of the excited closed strings is set by the Hawking temperature of the nonextremal NS5-brane, not that of a black hole that would have been made of the D0-brane. It is tempting to interpret this as indicating that the D0-brane represents a class of possible excitation modes of the black NS5-brane. The closed string states of energy M emitted by the D0-brane are certainly coherent, but according to this interpretation, they still can be recasted in effective thermal distribution set by the Hawking temperature of the two-dimensional black hole. We will later discuss again the origin of such effective thermal behavior of the rolling D0-brane from the viewpoints of Euclidean cylinder amplitudes, extending the argument of [75] about the Hawking radiation in the purely closed string background.

The functions σ_{in} and σ_{out} are interpretable as the black hole ‘greybody’ factors for incoming and outgoing parts of the radiation. The factor $1/2$ in the exponent of the Boltzmann distribution function reflects the fact that only left-right symmetric closed string states can appear in the boundary states and the radiated closed string modes.

The ‘greybody factors’ $\sigma_*(p)$ depend on the radial momentum p exponentially, so the radiation distribution would be modified *once* the radial momentum p is integrated out. Below, we shall show this explicitly. We are primarily interested in keeping track of string world-sheet effects set by the value of the level k . We shall consider different ranges of the level k separately, and focus on the asymptotic behaviors at large M via the saddle point methods.

(i) $k > 1$:

This is the case for the black NS5-brane background. Consider first the incoming part. Since $1 - \frac{1}{k} > 0$, the dominant contribution in the p -integral arises from the saddle point:

$$p \sim p_* = \frac{k-1}{\sqrt{1-\frac{1}{2k}}} M .$$

Substituting this to (8.10), we obtain

$$\mathcal{N}(M)_{\text{in}} \sim e^{-2\pi M \sqrt{1-\frac{1}{2k}}} = e^{-\frac{1}{2}M\beta_{\text{Hg}}} , \quad (8.14)$$

up to pre-exponential powers of M . Taking account of the density of states $\rho(M) \sim e^{\frac{1}{2}M\beta_{\text{Hg}}}$, we find that $\rho(M)\mathcal{N}(M)_{\text{in}}$ scales with powers of M , and is independent of k .

More explicitly, for the black NS5-brane $\mathcal{M} = SU(2)_k \times \mathbb{R}^5$, the incoming radiation distribution of the D p -brane parallel to the NS5-brane yields

$$\begin{aligned} \mathcal{N}(M)_{\text{in}} &\sim \frac{1}{M} \int \frac{d^{5-p} \mathbf{k}_\perp}{(2\pi)^{5-p}} \int_0^\infty dp e^{\pi(1-\frac{1}{k})p - \pi\sqrt{p^2 + 2k(M^2 + \mathbf{k}_\perp^2)}} \\ &\sim M^{2-\frac{p}{2}} e^{-2\pi M \sqrt{1-\frac{1}{2k}}} . \end{aligned}$$

Taking account of the density of states $\rho(M) \sim M^{-3} e^{2\pi M \sqrt{1-\frac{1}{2k}}}$, the average radiation number distribution is given by

$$\frac{\overline{\mathcal{N}}_{\text{in}}}{V_p} \sim \int^{M_D} \frac{dM}{M} M^{-\frac{p}{2}} \quad \text{where} \quad M_D \sim \mathcal{O}\left(\frac{1}{g_{\text{st}}}\right) . \quad (8.15)$$

This result coincides with the computations of [213, 135], and corroborates with the radion-tachyon correspondence. Interestingly, the incoming part of the radiation number distribution in the nonextremal NS5-brane background is exactly the same as the distribution in the extremal NS5-brane background. Later, we shall examine carefully taking the extremal limit and its consequence in section 8.6. As in the extremal case, (8.15) implies that nearly all the D0-brane potential energy is released into closed string radiations before it falls into the black hole.

On the other hand, for the outgoing radiation, the far infrared $p \sim 0$ dominates the momentum integral. We thus obtain

$$\mathcal{N}(M)_{\text{out}} \sim e^{-2\pi M \sqrt{\frac{k}{2}}} = e^{-\frac{1}{2} M \beta_{\text{Hw}}} ,$$

displaying effective thermal distribution set by the Hawking temperature. Taking account of the density of states,

$$\rho(M) \mathcal{N}(M)_{\text{out}} \sim e^{\frac{1}{2} M (\beta_{\text{Hg}} - \beta_{\text{Hw}})} = e^{2\pi M \left(\sqrt{1-\frac{1}{2k}} - \sqrt{\frac{k}{2}} \right)} .$$

This is ultraviolet finite for any k since

$$\left(1 - \frac{1}{2k} \right) - \frac{k}{2} = -\frac{1}{2k} (k-1)^2 < 0 . \quad (8.16)$$

We thus conclude that the radiation number distribution is mostly in the incoming part:

$$\left. \frac{\mathcal{N}_{\text{out}}(M) \rho(M)}{\mathcal{N}_{\text{in}}(M) \rho(M)} \right|_{\text{falling D0}} \sim \frac{e^{-\frac{1}{2} \beta_{\text{Hg}} M}}{e^{-\frac{1}{2} \beta_{\text{Hw}} M}} = e^{2\pi M \left(\sqrt{1-\frac{1}{2k}} - \sqrt{\frac{k}{2}} \right)} \ll 1 .$$

Intuitively, this may be understood as follows: for the absorbed boundary state, the boundary condition is such that the D0-brane flux is directed from past null infinity to the future horizon. This also corroborates the observation that $T_{t\rho}$ -component of D0-brane's energy-momentum tensor is nonzero and increases monotonically as the D0-brane approaches the future horizon. The outgoing part of the distribution is

exponentially small compared to the incoming part and exhibits effective thermal distribution at the Hawking temperature. Notice that, despite being so, this outgoing part has nothing to do with the Hawking radiation of the black hole. The latter is the feature of the background by itself. A priori, the outgoing radiation could be in a distribution characterized by a temperature different from the Hawking temperature. As mentioned above, it is tempting to interpret coincidence of the two temperatures as a consequence of maintaining equilibrium between the black NS5-brane and the D0-brane.

(ii) $\frac{1}{2} < k \leq 1$:

This is the regime which includes the conifold geometry at $k = 1$. Since $1 - \frac{1}{k} \leq 0$, the dominant contribution to the momentum integral is from $p \sim 0$, not only for the outgoing radiation but also for the incoming one. We thus obtain

$$\mathcal{N}(M)_{\text{in}} \sim \mathcal{N}(M)_{\text{out}} \sim e^{-2\pi M \sqrt{\frac{k}{2}}} \equiv e^{-\frac{1}{2} M \beta_{\text{Hw}}} , \quad (8.17)$$

viz. both are in effective thermal distribution set by the Hawking temperature. All spectral moments are manifestly ultraviolet finite since, at large M , exponential growth of the density of the final closed string states is insufficient to overcome the suppression by the distribution. Thus,

$$\left. \frac{\mathcal{N}_{\text{out}}(M)\rho(M)}{\mathcal{N}_{\text{in}}(M)\rho(M)} \right|_{\text{falling D0}} \sim 1.$$

We interpret this as indicating that the D0-brane does not radiate off most of its energy before falling into the horizon.

(iii) $k = \frac{1}{2}$:

This special case corresponds to empty \mathcal{M} . The two-dimensional background permits no transverse degrees of freedom of the string. The physical spectrum includes massless tachyon only, with $M = 0$ and $\rho(M) = 1$. We now have a crucial difference from the previous cases for the on-shell configurations. The radial momentum p is fixed by the on-shell condition as $\omega = \pm p$, so it should not be integrated over for the final states. Consequently, we cannot decompose the radiation distribution into incoming and outgoing radiations, and only the total distribution is physically relevant.

We thus obtain the following large ω behavior of the radiation distribution:

$$\mathcal{N}(\omega) \sim e^{-2\pi\omega} \equiv e^{-\omega\beta_{\text{Hw}}} . \quad (8.18)$$

Again, we have found effective thermal distribution at the Hawking temperature! Notice the absence of extra 1/2-factor in contrast to the previous regimes. This is not a contradiction. In the present case, the transverse oscillators are absent and the string behaves as a point particle. Again, the D0-brane does not radiate off most of its energy before falling across the black hole horizon. In the linear dilaton regime, the boundary

states and possible connection with the matrix model for the two-dimensional type 0A/0B string theory have been discussed in [157]. Given the phase transition we observed, however, the classical intuition of such “rolling D-brane” in the two-dimensional noncritical string theory is rather questionable. It would be interesting to give an interpretation from the dual matrix models.

8.1.2 radiation distribution in bosonic string theory

The analysis for the bosonic string case proceeds quite the same route. The boundary state for the infalling D0-brane includes the string world-sheet correction factor $\Gamma\left(1 + i\frac{p}{\kappa-2}\right)$, where again κ refers to the level of bosonic $SL(2; \mathbb{R})/U(1)$ coset model. The on-shell condition now reads

$$-\frac{\omega^2}{4\kappa} + \frac{p^2}{4(\kappa-2)} + \frac{1}{4(\kappa-2)} + \Delta_{\mathcal{M}} = 1, \quad (8.19)$$

where $\Delta_{\mathcal{M}}$ denotes the conformal weight in the \mathcal{M} -sector. This is solved by

$$\omega \equiv \omega(p, M) = \sqrt{\frac{\kappa}{\kappa-2}p^2 + 2\kappa M^2} \quad \text{where} \quad M^2 \equiv 2\left(\Delta_{\mathcal{M}} + \frac{1}{4(\kappa-2)} - 1\right). \quad (8.20)$$

The partial radiation number distribution at large M limit is given by:

$$\mathcal{N}(M)_{\text{in}} \sim \frac{1}{M} \int_0^\infty dp e^{+\pi\left(1-\frac{1}{\kappa-2}\right)p - \pi\sqrt{\frac{\kappa}{\kappa-2}p^2 + 2\kappa M^2}}. \quad (8.21)$$

$$\mathcal{N}(M)_{\text{out}} \sim \frac{1}{M} \int_0^\infty dp e^{-\pi\left(1+\frac{1}{\kappa-2}\right)p - \pi\sqrt{\frac{\kappa}{\kappa-2}p^2 + 2\kappa M^2}}. \quad (8.22)$$

Thus, as in the superstring case, there can arise several distinct behaviors depending on how stringy the background is.

(i) $\kappa > 3$:

Consider first the incoming radiation part. Since $1 - \frac{1}{\kappa-2} > 0$, the dominant contribution to the momentum integral in (8.21) is from the saddle point

$$p \sim p_* = \frac{\kappa - 3}{\sqrt{2 - \frac{1}{2(\kappa-2)}}} M.$$

We thus obtain, up to pre-exponential powers of M ,

$$\mathcal{N}(M)_{\text{in}} \sim e^{-2\pi M \sqrt{2 - \frac{1}{2(\kappa-2)}}} = e^{-\frac{1}{2}M\beta_{\text{Hg}}},$$

where β_{Hg} denotes the Hagedorn temperature of the bosonic string theory (8.8). In this way, we again find the power-law behavior of $\rho(M)\mathcal{N}(M)_{\text{in}}$ at large M , independent of the level κ .

For the outgoing radiation part, again the $p \sim 0$ dominates the momentum integral in (8.22). The result is

$$\mathcal{N}(M)_{\text{out}} \sim e^{-2\pi M \sqrt{\frac{\kappa}{2}}} = e^{-\frac{1}{2}M\beta_{\text{Hw}}}.$$

Here,

$$\beta_{\text{Hw}} \equiv 2\pi\sqrt{2\kappa}$$

is the Hawking temperature of the bosonic two-dimensional black hole. We then obtain

$$\rho(M)\mathcal{N}(M)_{\text{out}} \sim e^{\frac{1}{2}(\beta_{\text{Hg}}-\beta_{\text{Hw}})M} = e^{2\pi M\left[\sqrt{2-\frac{1}{2(\kappa-2)}}-\sqrt{\frac{\kappa}{2}}\right]} .$$

As in the superstring case, the exponent is always negative definite:

$$\left(2 - \frac{1}{2(\kappa-2)}\right) - \frac{\kappa}{2} = -\frac{(\kappa-3)^2}{2(\kappa-2)} \leq 0 .$$

so the outgoing radiation distribution (as well as spectral moments) is manifestly ultraviolet finite.

Physical interpretation of the above results is the same as the superstring case: The D0-brane falling into the black hole has nonzero component $T_{t\rho}$ of the energy-momentum tensor, and entails that dominant part of the closed string radiation is incoming toward the future horizon. The outgoing part of the radiation is exponentially suppressed, and is in effective thermal distribution set by the Hawking temperature. Again, this distribution is distinct from the Hawking radiation of the two-dimensional black hole. As for the fermionic string, the branching ratio is exponentially suppressed.

(ii) $\frac{9}{4} < \kappa \leq 3$:

In this regime, $1 - \frac{1}{\kappa-2} < 0$ and the momentum integrals for both incoming and outgoing radiation distributions are dominated by $p \sim 0$:

$$\mathcal{N}(M)_{\text{in}} \sim \mathcal{N}(M)_{\text{out}} \sim e^{-2\pi M\sqrt{\frac{\kappa}{2}}} \equiv e^{-\frac{1}{2}M\beta_{\text{Hw}}} .$$

Both are in effective thermal distribution at the Hawking temperature, and all spectral moments are manifestly ultraviolet finite since, at large M , the growth of the density of state does not overcome the suppression by the distribution. The branching ratio remains order unity.

(iii) $\kappa = \frac{9}{4}$:

This is the most familiar situation: black hole in two-dimensional bosonic string theory, originally studied in [71, 72, 73, 215]. The physical spectrum of closed string consists only of the massless tachyon, so we again need to set $M = 0$ and $\rho(M) = 1$. The calculation is slightly more complicated than the supersymmetric case: The canonically normalized energy is

$$E = \frac{\sqrt{2}}{3}\omega = \sqrt{2}p ,$$

so we obtain

$$\mathcal{N}(E) \sim e^{\pi\left(1-\frac{1}{4}\right)p-\pi\sqrt{\frac{9/4}{1/4}}p} = e^{-3\sqrt{2}\pi E} \equiv e^{-E\beta_{\text{Hw}}} .$$

It again shows effective thermal distribution of the radiated closed string modes at the Hawking temperature: $\beta_{\text{Hw}} = 2\pi\sqrt{2\kappa} = 3\pi\sqrt{2}$.

8.1.3 radiation distribution for emitted or time-symmetric boundary states

The closed string radiations for the other types boundary states, viz. the ‘emitted’ (7.32) or the ‘symmetric’ (7.36) D0-branes, can be studied analogously.

For the emitted D0-brane boundary state (7.32), by the time-reversal, we should observe the radiation distribution at the far past: $t \sim -\infty$. The relevant decomposition corresponding to (8.2) is given by (assuming $\omega > 0$, $p > 0$)

$$V_\omega^p(\rho, t) \sim e^{i\omega \ln \rho - i\omega t} + d^*(p, \omega) e^{-\rho} e^{-ip\rho - i\omega t}, \quad (8.23)$$

where the first term is supported near the past horizon and the second term corresponds to the incoming wave from the null infinity. Obviously we find precisely the same behavior of the radiation distribution as the absorbed D0-brane once the role of ‘in’ and ‘out’ states are reversed. So, for $k > 1$, $\mathcal{N}(M)_{\text{in}} \sim \exp(-\frac{1}{2}\beta_{\text{Hw}}M)$ while $\mathcal{N}(M)_{\text{out}} \sim \exp(-\frac{1}{2}\beta_{\text{Hg}}M)$ and, for $1 \geq k > 1/2$, $\mathcal{N}(M)_{\text{in}}, \mathcal{N}(M)_{\text{out}} \sim \exp(-\frac{1}{2}\beta_{\text{Hw}}M)$.

Consider next the boundary state describing D0-brane in symmetric boundary condition (7.36). Recalling the relations (7.35), one finds that the radiation rates are simply obtained by adding contributions from ‘absorbed’ and ‘emitted’ D0-brane boundary states. Thus, the radiation distributions behave as $\mathcal{N}(M)_{\text{in}}, \mathcal{N}(M)_{\text{out}} \sim \exp(-\frac{1}{2}\beta_{\text{Hg}}M)$ for $k > 1$ and the dependence on Hawking temperature disappeared.¹⁰¹ We then find that the ‘detailed balance’ $\mathcal{N}(M)_{\text{in}} = \mathcal{N}(M)_{\text{out}}$ is obeyed. This is as expected since the boundary state (7.36) is defined so that it keeps the time-reversal symmetry and the one-particle state unitarity manifest.

8.1.4 revisit to the radiation distribution from thermal sting propagator

To close this section we discuss the radiation distribution from a different angle. Although the argument given here would be somewhat heuristic, it is quite helpful to grasp physical intuition and to understand where the thermal-like behavior of closed string radiation comes from. This argument is much like the one given in [75], where the Hawking radiation of 2-dimensional black-hole is discussed by the closed string thermal propagator. In a sense, our discussion is an extension of it to the open string sector.

We start with the (thermal) cylinder amplitude for the D1-brane on the Euclidean cigar

¹⁰¹Dependence on the Hawking temperature exponentially suppressed, so completely negligible compared to other power-suppressed subleading terms.

(6.57)¹⁰². This is approximately evaluated as (we omit the parameters ρ_0, θ_0 for simplicity)

$$\begin{aligned} \mathcal{A}_{\text{cylinder}}^{(E)} &= \int_0^\infty dT {}_{D1}\langle B | e^{-\pi T H^{(c)}} | B \rangle_{D1} \approx \sum_M \sum_{n \in \mathbb{Z}} \int dp \frac{1}{p^2 + \left(\frac{2\pi n}{\beta_{\text{Hw}}}\right)^2 + M^2} \sqrt{\rho(M)} |\Psi_{D1}(p, n)|^2 \\ &= \frac{\beta_{\text{Hw}}}{2\pi} \sum_M \int dp dq \sqrt{\rho(M)} \frac{|\Psi_{D1}\left(p, \frac{\beta_{\text{Hw}} q}{2\pi}\right)|^2}{p^2 + q^2 + M^2} \left(1 + \sum_{m \in \mathbb{Z}_{>0}} e^{i\beta_{\text{Hw}} m q} + \sum_{m \in \mathbb{Z}_{>0}} e^{-i\beta_{\text{Hw}} m q}\right) \end{aligned} \quad (8.24)$$

Here p is the radial momentum and n is the KK momentum along the asymptotic circle of cigar (thermal circle). M is again the transverse mass in the \mathcal{M} -sector and $\rho(M)$ is the density of closed string states. $\beta_{\text{Hw}} \equiv 2\pi\sqrt{2k}$ again denotes the inverse Hawking temperature. Let us try to Wick rotate it by the contour deformation of q -integration in the similar manner to [75]. Setting $q = i\omega$ ¹⁰³, $\mathcal{A}_{\text{cylinder}}^{(L)} = -i\mathcal{A}_{\text{cylinder}}^{(E)}$, we formally obtain

$$\begin{aligned} \mathcal{A}_{\text{cylinder}}^{(L)} &\approx \frac{\beta_{\text{Hw}}}{2\pi} \sum_M \int dp \sqrt{\rho(M)} \left[\int d\omega \frac{|\Psi_{D1}\left(p, \frac{i\beta_{\text{Hw}}\omega}{2\pi}\right)|^2}{p^2 + M^2 - \omega^2 + i\epsilon} - \frac{2\pi i}{\omega_{p,M}} \frac{|\Psi_{D1}\left(p, \frac{i\beta_{\text{Hw}}\omega_{p,M}}{2\pi}\right)|^2}{e^{\beta_{\text{Hw}}\omega_{p,M}} - 1} \right] \end{aligned} \quad (8.25)$$

where $\omega_{p,M} \equiv \sqrt{p^2 + M^2}$ is the on-shell energy and we here used

$$\left| \Psi_{D1}\left(p, -\frac{i\beta_{\text{Hw}}\omega_{p,M}}{2\pi}\right) \right|^2 = \left| \Psi_{D1}\left(p, \frac{i\beta_{\text{Hw}}\omega_{p,M}}{2\pi}\right) \right|^2.$$

Because we have $\left| \Psi_{D1}\left(p, \frac{i\beta_{\text{Hw}}\omega}{2\pi}\right) \right|^2 \propto e^{\frac{1}{2}\beta_{\text{Hw}}|\omega|}$, the first term (including the Feynman propagator) gives a UV divergent contribution. This is not surprising and shows the reason why the naive Wick-rotation of (6.57) does not work. The second term shows a ‘thermal-like’ form and actually contributes to the imaginary part of cylinder amplitude we are interested in. It gives the expected behavior;

$$\begin{aligned} \text{Im } \mathcal{A}_{\text{thermal}}^{(L)} &\propto \frac{1}{\omega_{p,M}} \frac{1}{e^{\beta_{\text{Hw}}\omega_{p,M}} - 1} \sqrt{\rho(M)} \left| \Psi_{D1}\left(p, \frac{i\beta_{\text{Hw}}\omega}{2\pi}\right) \right|^2 \\ &\sim \frac{\sqrt{\rho(M)}\sigma(p)}{\omega_{p,M}} e^{-\frac{1}{2}\beta_{\text{Hw}}\omega_{p,M}}, \end{aligned} \quad (8.26)$$

which reproduces the previous results (8.12), including the correct grey body factor $\sigma(p)$. Recall that, in our construction of Lorentzian boundary states, the presence of the damping

¹⁰²To be more precise, we consider the fermionic black-hole of level k and focus on the space-time bosons. If considering the space-time fermions, the thermal KK momentum should be half integer $n \in 1/2 + \mathbb{Z}$, rather than $n \in \mathbb{Z}$, which leads to the fermionic distribution $1/(e^{\beta_{\text{Hw}}\omega_{p,M}} + 1)$ instead of $1/(e^{\beta_{\text{Hw}}\omega_{p,M}} - 1)$ in the following argument.

¹⁰³Here, ω, p are normalized as $L_0 = -\frac{1}{2}\omega^2 + \frac{1}{2}p^2 + \dots$, rather than $L_0 = -\frac{1}{4k}\omega^2 + \frac{1}{4k}p^2 + \dots$.

factor was crucial, which reads as $\frac{\sinh \pi \sqrt{2k} p}{\cosh \left[\pi \sqrt{\frac{k}{2}} (p+\omega) \right] \cosh \left[\pi \sqrt{\frac{k}{2}} (p-\omega) \right]}$ in the convention here. This factor shows the same asymptotic behavior in the large ω or large p region as the Boltzmann distribution functions $1/(e^{\beta_{\text{Hw}} \omega} \pm 1)$. In this sense, our Wick-rotation of boundary states would be roughly identified with the procedure which keeps only the second term in (8.25), suggesting the origin of the thermal-like distribution derived from our Lorentzian boundary states.

Another helpful argument is achieved by starting with the open string channel of thermal cylinder amplitude (8.24). Let us focus on the asymptotic region $\rho \gg 0$ for simplicity, in which the hairpin D1-brane (6.57) appears just as two halves of $D1-\bar{D}1$ system, which are Dirichlet along the thermal circle, (so, identified as the ‘ $sD-s\bar{D}$ system’ [209]) as pointed out in [207]. In this set up, by a simple kinematical reason, we find *on-shell* closed string states in the cylinder amplitude, while only *off-shell* states in the open string channel. As discussed *e.g.* in [216, 217], using the modular transformation, we can show the thermal distribution of *physical* closed string states emitted/absorbed by the $sD-s\bar{D}$ system is captured by the *unphysical* open string winding modes along the thermal circle¹⁰⁴. Especially, the unit of winding energy should determine the temperature of thermal distribution of closed string states coupled with the $sD-s\bar{D}$ system. In the present case it is identified with the interval of the hairpin ($= \frac{1}{2}\beta_{\text{Hw}}$), which is just associated to the $D1-\bar{D}1$ open string. (Note that, taking suitably the GSO projection into account, we can find the zero winding modes, *i.e.* the $D1-D1$ or $\bar{D}1-\bar{D}1$ strings, are canceled out. See [207].) This is the simplest explanation of why we get the thermal-like distribution $\propto e^{-\frac{1}{2}\beta_{\text{Hw}} \omega_{p,M}}$ from the cylinder amplitude (8.24).

Curiously, all the *regular* solutions of $D0$ -brane motion are just straight lines in the Kruscal coordinates, and thus Wick-rotated to the hairpin profiles with the *same* interval; $\frac{1}{2}\beta_{\text{Hw}}$. This fact leads us to the same thermal-like behaviors (8.12) characterized by the Hawking temperature (before integrating p out)¹⁰⁵, as is already pointed out.

8.2 Radiation out of rolling D-brane from open string viewpoint

8.2.1 open string channel viewpoint

What is the nature of the ultraviolet behavior of the emission number $\bar{\mathcal{N}}$ and how is it compared to the decay of rolling D-brane? To answer these, we shall now recast (8.27) in the open string channel, following technical procedures considered in section 5.2 and appendix of [135].

In the closed string channel, the closed string radiation has been computed as (see section

¹⁰⁴This is a simple extension of the standard argument of the thermal toroidal partition functions [110, 111, 112, 113, 114]. For instance, the Hagedorn behavior is interpretable as the tachyonic instability due to the *unphysical* winding modes along the thermal circle.

¹⁰⁵One might ask why the $D0$ -brane motion with different ‘temperature’ is not considered. However, such $D0$ -branes correspond to singular hairpin profiles and thus do to singular Lorentzian trajectories. These cannot be the solutions of DBI action of $D0$ -branes by the divergence of the velocity at the singular points. Quite interestingly, this feature is similar to the original Hawking’s idea : requiring the smooth Euclidean geometry, we can fix the particular asymptotic periodicity of Euclidean time, which yields the temperature characterizing the radiation from black-hole.

8.1)

$$\bar{\mathcal{N}} = N_{\text{NS}}^2 \sum_M \sqrt{\rho^{(c)}(M)} \int_0^\infty \frac{dp}{2\pi} \frac{1}{2\omega} \mathcal{P}(p, \omega), \quad (8.27)$$

where N_{NS} is an appropriate numerical factor, $\omega = \sqrt{p^2 + 2kM^2}$ is the on-shell energy of the emitted closed string, and

$$\mathcal{P}(p, \omega) \equiv |\Psi(p, \omega)|^2 = \frac{\sinh \pi \sqrt{\frac{\alpha'}{2}} p}{\left(\cosh \pi \sqrt{\frac{\alpha'}{2}} p + \cosh \pi \sqrt{\frac{\alpha'}{2}} \omega \right) \sinh \frac{\pi}{k} \sqrt{\frac{\alpha'}{2}} p} \quad (8.28)$$

is the transition probability.

We begin with expanding the transition probability $\mathcal{P}(p, \omega)$ of the D0-brane (8.28) in power series of contribution of imaginary branes:

$$\mathcal{P}(p, \omega) = \sum_{n=1}^{\infty} a_n(p) e^{-\pi n \omega \sqrt{\frac{\alpha'}{2}}}, \quad (8.29)$$

$$a_n(p) = 2(-1)^{n+1} \frac{\sinh \left(\pi n \sqrt{\frac{\alpha'}{2}} p \right)}{\sinh \left(\frac{\pi}{k} \sqrt{\frac{\alpha'}{2}} p \right)}. \quad (8.30)$$

As before, we parametrically rewrite (8.27) as

$$\begin{aligned} \bar{\mathcal{N}} &= N_{\text{NS}}^2 \sum_M \sqrt{\rho^{(c)}(M)} \\ &\times \int_0^\infty \frac{dp}{2\pi\sqrt{2k}} \sum_{n=1}^{\infty} \int_{-\infty}^{\infty} \frac{dk_0}{2\pi\sqrt{2k}} \int_0^\infty \frac{\alpha'}{2} dt_c a_n(p) e^{\pi i n \sqrt{\frac{\alpha'}{2}} k_0} e^{-2\pi t_c \frac{1}{4} \alpha' \left(\frac{k_0^2 + p^2}{2k} + M^2 \right)}, \end{aligned} \quad (8.31)$$

by introducing the Schwinger parameter t_c in the closed string channel.¹⁰⁶

We now evaluate each contribution separately. Begin with the sum over the transverse mass M . By definition, the sum gives modular invariant cylinder amplitude of the \mathcal{M} -sector:

$$\begin{aligned} \sum_M \sqrt{\rho^{(c)}(M)} e^{-2\pi t_c \frac{\alpha'}{4} M^2} &= Z_{\mathcal{M}}^{(c)}(q_c) \quad \text{where} \quad q_c = e^{-2\pi t_c} \\ &= Z_{\mathcal{M}}^{(o)}(q_o) \quad \text{where} \quad q_o = e^{-2\pi t_o} \quad (t_o \equiv 1/t_c) \end{aligned} \quad (8.32)$$

by applying the standard open-closed duality and expressing the result in terms of the open string Schwinger parameter t_o .

¹⁰⁶Strictly speaking, we could have the closed string tachyon $M^2 < 0$, and the rewriting (8.31) would not be completely correct due to the infrared divergence. We can avoid this difficulty by considering the GSO projected amplitude. We are concerned with the large M asymptotics, so shall go on ignoring it to avoid unessential complexity.

The amplitude $Z_{\mathcal{M}}^{(o)}(t_o)$ asymptotes at large t to (corresponding to the ultraviolet behavior in the closed string channel):

$$Z_{\mathcal{M}}^{(o)}(t_o) \sim t_o^\gamma e^{2\pi t_o \cdot \frac{\mathcal{M}}{24}} = t_o^\gamma e^{\pi t_o (1 - \frac{1}{2k})} \quad \text{for} \quad t_o \rightarrow +\infty. \quad (8.33)$$

Here, the exponent γ is determined by the number of non-compact Neumann directions in the \mathcal{M} -sector. Such details, however, are not relevant for our discussions.

The Gaussian integral over k_0 is readily evaluated, resulting in

$$\overline{\mathcal{N}} = N_{\text{NS}}^2 \sqrt{\frac{\alpha'}{2}} \int_0^\infty \frac{dp}{2\pi\sqrt{2k}} \sum_{n=1}^\infty \int_0^\infty \frac{dt_o}{t_o^2} \sqrt{t_o} a_n(p) e^{-\pi t_o \frac{n^2 k}{2} - \frac{2\pi}{t_o} \frac{\alpha'}{4} \frac{p^2}{2k}} \cdot Z_{\mathcal{M}}^{(o)}(t_o). \quad (8.34)$$

The k_0 -integral yields the Boltzmann factor with the temperature determined by the Euclidean periodicity ($1/Q$ in our case) for the ‘hairpin brane’ [79, 194, 204, 98], which is the Euclidean rotation of the rolling D-brane, as clarified in [1, 100]. This is essentially the same as the standard argument for thermal tachyon in the thermal string theory [110, 111, 112, 113, 114].

Our goal is to re-express the rate (8.27) in the open string channel, so we shall Fourier transform the closed string momentum p to the open string momentum p' . This requires a careful treatment, because the momentum-dependent coefficients $a_n(p)$ in (8.30) could be exponentially growing functions. In such cases, the Fourier transform may not exist in a naive sense. We start with the identity:

$$e^{-2\pi t_o \cdot \frac{1}{4} \alpha' \frac{p^2}{2k}} = \sqrt{t_o} \int_{\mathbb{R}+i\xi} \sqrt{\frac{\alpha'}{2}} \frac{dp'}{\sqrt{2k}} e^{-2\pi t_o \cdot \frac{1}{4} \alpha' \frac{p'^2}{2k} + 2\pi i \cdot \frac{1}{2} \alpha' \frac{pp'}{2k}} \quad \text{for} \quad \xi \in \mathbb{R}. \quad (8.35)$$

In the p -integral, the function $e^{2\pi i \frac{1}{2} \alpha' \frac{pp'}{2k}}$ works as a damping factor and renders the integral finite if the parameter ξ is chosen suitably. For later convenience, we shall decompose $a_n(p)$ as

$$a_n(p) = a_n^+(p) - a_n^-(p),$$

$$a_n^\pm(p) \equiv (-1)^{n+1} \frac{e^{\pm \pi n \sqrt{\frac{\alpha'}{2}} p}}{\sinh\left(\pi \frac{\pi}{k} \sqrt{\frac{\alpha'}{2}}\right)}. \quad (8.36)$$

Observing the asymptotic behavior of the coefficients $a_n^+(p)$, we readily find that the closed string channel momentum integral $\int dp a_n^+(p) e^{2\pi i \cdot \frac{1}{2} \alpha' \frac{pp'}{2k}}$ is well-defined as long as ξ_n^+ is chosen within the range $(nk - 1) < \sqrt{\frac{\alpha'}{2}} \xi_n^+ < (nk + 1)$. We can then safely exchange the order of the integrals. Carrying out the p -integral first, we find ¹⁰⁷

$$\int_{\mathbb{R}-i0} \frac{dp}{\sqrt{2k}} a_n^+(p) e^{-2\pi t_o \frac{\alpha'}{4} \frac{p^2}{2k}} = (-1)^{n+1} \frac{i\sqrt{tk}}{\sqrt{2}} \int_{\mathbb{R}+i\xi_n^+} \frac{dp'}{\sqrt{2k}} \frac{e^{\pi \left(\sqrt{\frac{\alpha'}{2}} \frac{p'}{2} - i \frac{nk}{2}\right) - 2\pi t_o \frac{\alpha'}{4} \frac{p'^2}{2k}}}{\cosh \pi \left(\sqrt{\frac{\alpha'}{2}} \frac{p'}{2} - i \frac{nk}{2}\right)}. \quad (8.37)$$

¹⁰⁷Here, we are temporarily shifting the contour as $\mathbb{R} \rightarrow \mathbb{R} - i0$ to avoid the pole $p = 0$. We eventually restore it back to \mathbb{R} after taking the difference $a_n(p) \equiv a_n^+(p) - a_n^-(p)$. The final result (8.42) remains intact, even if another contour shift $\mathbb{R} + i0$ is taken, as is easily checked.

Finally, we shift the contour back: $\mathbb{R} + i\xi_n^+ \rightarrow \mathbb{R}$ so that the open string momentum p' is real-valued. In this step, we cross the poles so need to take care of pole contributions. (See Figure 1.)

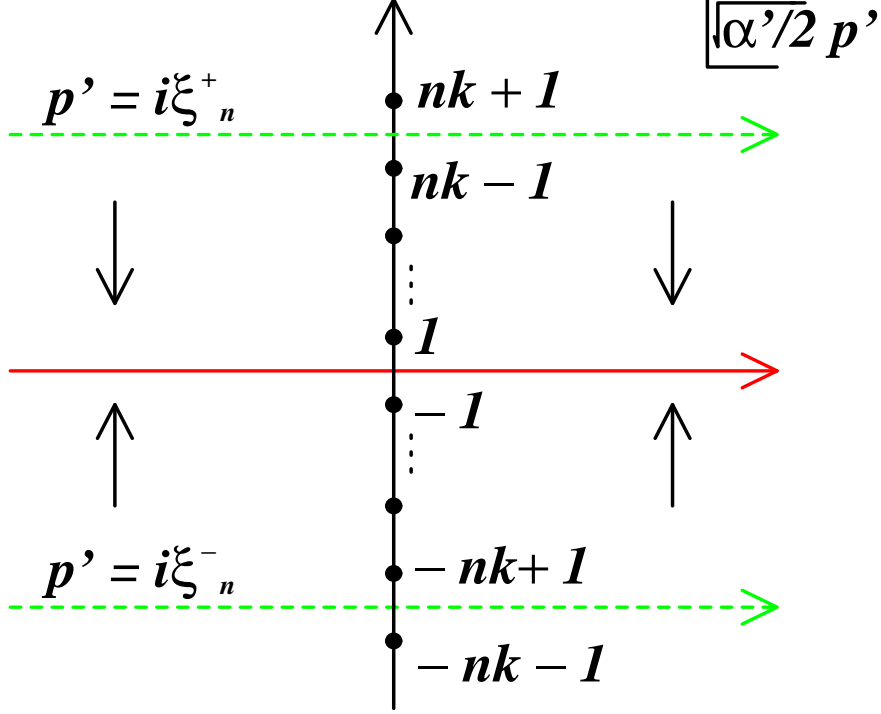


Figure 9: Deformation of the contour from the broken line to the solid line picks up pole contributions.

The relevant poles are located at

$$\sqrt{\frac{\alpha'}{2}} p' = i\alpha_m, \quad \alpha_m \equiv nk - 2 \left(m + \frac{1}{2} \right) \quad \text{where } m = 0, 1, \dots, \left[\frac{nk}{2} - \frac{1}{2} \right], \quad (8.38)$$

where $[\]$ denotes the Gauss symbol, and their residues are evaluated as $(-1)^{n+1} \frac{i}{\pi} e^{\pi t_o \frac{\alpha_n^2}{2k}}$. We thus obtain

$$\begin{aligned} \int_{\mathbb{R}-i0} \sqrt{\frac{\alpha'}{2}} \frac{dp}{\sqrt{2k}} a_n^+(p) e^{-2\pi t_c \frac{\alpha' p^2}{4} \frac{p^2}{2k}} &= (-1)^{n+1} \frac{i\sqrt{kt_o}}{\sqrt{2}} \int_{-\infty}^{\infty} \sqrt{\frac{\alpha'}{2}} \frac{dp'}{2k} \frac{e^{\pi \left(\sqrt{\frac{\alpha'}{2}} \frac{p'}{2} - i \frac{nk}{2} \right) - 2\pi t_o \frac{\alpha' p'^2}{4} \frac{p'^2}{2k}}}{\cosh \pi \left(\sqrt{\frac{\alpha'}{2}} \frac{p'}{2} - i \frac{nk}{2} \right)} \\ &+ 2(-1)^{n+1} \sqrt{t_o} \sum_{m=0}^{\left[\frac{nk}{2} - \frac{1}{2} \right]} e^{\frac{\pi t_o k}{2} \left[n - \frac{2}{k} \left(m + \frac{1}{2} \right) \right]^2}. \end{aligned} \quad (8.39)$$

The integral of $a_n^-(p)$ is calculated in a similar way. This time, we should start with the contour $\mathbb{R} + i\xi_n^-$ with $(-nk - 1) < \sqrt{\frac{\alpha'}{2}} \xi_n^- < (-nk + 1)$ and, after performing the p -integral

first, again shift it back to $\mathbb{R} + i\xi_n^- \rightarrow \mathbb{R}$. The relevant pole contributions come from $\sqrt{\frac{\alpha'}{2}}p' = -i\alpha_m$ ($m = 0, 1, \dots, [\frac{nk}{2} - \frac{1}{2}]$), and we obtain

$$\begin{aligned} \int_{\mathbb{R}-i0} \sqrt{\frac{\alpha'}{2}} \frac{dp}{\sqrt{2k}} a_n^-(p) e^{-\pi t_c \alpha' \frac{p^2}{2k}} &= (-1)^{n+1} \frac{i\sqrt{t_o k}}{\sqrt{k}} \int_{-\infty}^{\infty} \sqrt{\frac{\alpha'}{2}} \frac{dp'}{\sqrt{2k}} \frac{e^{\pi \left(\sqrt{\frac{\alpha'}{2}} \frac{p'}{2} + i \frac{nk}{2} \right) - 2\pi t_o \frac{\alpha'}{4} \frac{p'^2}{2k}}}{\cosh \pi \left(\sqrt{\frac{\alpha'}{2}} \frac{p'}{2} + i \frac{nk}{2} \right)} \\ &\quad - 2(-1)^{n+1} \sqrt{t_o} \sum_{m=0}^{[\frac{nk}{2} - \frac{1}{2}]} e^{\frac{\pi t_o k}{2} \left[n - \frac{2}{k} \left(m + \frac{1}{2} \right) \right]^2}. \end{aligned} \quad (8.40)$$

Notice that the relative sign change in the pole term compared to $a_n^+(p)$ integral originates from the orientation of integration contour surrounding each pole. Therefore, we find

$$\begin{aligned} \int_0^{\infty} \sqrt{\frac{\alpha'}{2}} \frac{dp}{\sqrt{2k}} a_n(p) e^{-2\pi t_c \frac{\alpha'}{4} \frac{p^2}{2k}} &= \frac{1}{2} \int_{-\infty}^{\infty} \sqrt{\frac{\alpha'}{2}} \frac{dp}{\sqrt{2k}} (a_n^+(p) - a_n^-(p)) e^{-2\pi \alpha' \frac{t_c}{4} \frac{p^2}{2k}} \\ &= (-1)^{n+1} \frac{\sqrt{t_o k}}{\sqrt{2}} \int_{-\infty}^{\infty} \sqrt{\frac{\alpha'}{2}} \frac{dp'}{\sqrt{2k}} \frac{\sin(\pi nk) e^{-2\pi t_o \frac{\alpha'}{4} \frac{p'^2}{2k}}}{\cosh \left(\pi \sqrt{\frac{\alpha'}{2}} p' \right) + \cos(\pi nk)} \\ &\quad + 2(-1)^{n+1} \sqrt{t_o} \sum_{m=0}^{[\frac{nk}{2} - \frac{1}{2}]} e^{\frac{\pi t_o k}{2} \left[n - \frac{2}{k} \left(m + \frac{1}{2} \right) \right]^2}. \end{aligned} \quad (8.41)$$

In this way, we derive the desired open string channel expression of the total radiation rate;

$$\begin{aligned} \bar{\mathcal{N}} &= N_{\text{NS}}^2 \int_0^{\infty} \frac{dt_o}{t_o} \left(F_{\text{naive}}(t_o) + F_{\text{pole}}(t_o) \right), \\ F_{\text{naive}}(t_o) &= \sqrt{\frac{k}{2}} \int_{-\infty}^{\infty} \sqrt{\frac{\alpha'}{2}} \frac{dp'}{\sqrt{2k}} \sum_{n=1}^{\infty} (-1)^{n+1} \frac{\sin(\pi nk) e^{-\pi t_o \left(\frac{\alpha'}{2} \frac{p'^2}{2k} + \frac{2n^2}{k} \right)}}{\cosh \left(\pi \sqrt{\frac{\alpha'}{2}} p' \right) + \cos(\pi nk)} Z_{\mathcal{M}}^{(o)}(t_o) \\ F_{\text{pole}}(t_o) &= 2 \sum_{n=1}^{\infty} (-1)^{n+1} \sum_{m=0}^{[\frac{nk}{2} - \frac{1}{2}]} e^{\pi t_o \left[\frac{2}{k} \left(m + \frac{1}{2} \right) \right]^2 - 2n \left(m + \frac{1}{2} \right)} Z_{\mathcal{M}}^{(o)}(t_o). \end{aligned} \quad (8.42)$$

The first term in (8.42) coincides with the total radiation claimed by [164] modulo inessential numerical factor¹⁰⁸. It remains finite as $t_o \rightarrow +\infty$. The second term, which the analysis of [164] missed altogether, is of crucial importance. It is evident that the $m = 0$ term is the leading contribution for each n .¹⁰⁹ Recalling $Z_{\mathcal{M}}^{(o)}(t_o) \sim e^{\pi t_o \left(1 - \frac{1}{2k} \right)}$ asymptotically (up to pre-exponential power corrections), each $m = 0$ term behaves as

$$\sim e^{\pi t_o \left(\frac{1}{2k} - n \right) + \pi t_o \left(1 - \frac{1}{2k} \right)} = e^{\pi t_o (1-n)} \quad \text{as} \quad t_o \rightarrow +\infty. \quad (8.43)$$

¹⁰⁸It differs slightly from the one given in [164] in that we study the fermionic string, while [164] studies the bosonic string.

¹⁰⁹Here we have assumed that $k > 1$.

Therefore, we get the leading contribution from the $n = 1$ term, which shows a massless behavior. Hence, we have reproduced the Hagedorn-growth behavior expected in [207, 152, 148, 1]. Notice that all the $n > 1$ contributions are massive, and thus are not relevant in the ultraviolet regime of closed string radiations.

8.2.2 Lorentzian cylinder amplitude

In the previous section, we recasted the total emission number $\overline{\mathcal{N}}$ of the rolling D0-brane, defined as the sum over the on-shell states of emitted closed string (8.27), in the open string channel. Now, by the optical theorem and the channel duality, we ought to be able to obtain $\overline{\mathcal{N}}$ equally well from the cylinder amplitude evaluated in the open channel. In this section, we shall compute explicitly the cylinder amplitude in the open string channel and show that its imaginary part reproduces precisely the result (8.42). This would serve as a non-trivial check-point of our previous analysis for the consistency with unitarity and the open-closed channel duality. Notice in particular that the channel duality is far from being obvious in the world-sheet in Lorentzian signature. For definiteness, we continue to focus on the NS sector.

We start with the cylinder amplitude with Lorentzian world-sheet ¹¹⁰ Z_{cylinder} :

$$\begin{aligned}
Z_{\text{cylinder}} &= i \frac{\alpha'}{2} \int_{s_c^{\text{UV}}}^{s_c^{\text{IR}}} ds_c \int_0^\infty \frac{dp}{\sqrt{2k}} \int_{-\infty}^\infty \frac{d\omega_L}{\sqrt{2k}} \frac{\sinh\left(\pi\sqrt{\frac{\alpha'}{2}}p\right)}{\left[\cosh\left(\pi\sqrt{\frac{\alpha'}{2}}\omega_L\right) + \cosh\left(\pi\sqrt{\frac{\alpha'}{2}}p\right)\right] \sinh\left(\frac{\pi}{k}\sqrt{\frac{\alpha'}{2}}p\right)} \\
&\quad \times \frac{q_c^{\frac{1}{4}\alpha'(\frac{p^2}{2k} - (1-i\hat{\epsilon})\frac{\omega_L^2}{2k})}}{\eta(q_c)^2} \frac{\theta_3(q_c)}{\eta(q_c)} \cdot Z_{\mathcal{M}}^{(c)}(q_c) \cdot \eta(q_c)^2 \frac{\eta(q_c)}{\theta_3(q_c)}. \tag{8.44}
\end{aligned}$$

Here, we again adopt the $i\epsilon$ -prescription for the Lorentzian world-sheet, while the $-i\hat{\epsilon}$ -prescription for the Lorentzian space-time. The integration is well-defined so long as $2\hat{\epsilon}s_c^{\text{UV}} > \epsilon > 0$ is retained.

The second line in (8.44) combines contributions of the $\text{SL}(2)_k/\text{U}(1)$, \mathcal{M} , and the world-sheet ghosts. The ghost contribution $\eta(q_c)^2 \frac{\eta(q_c)}{\theta_3(q_c)}$ is seen to cancel out the contribution of longitudinal oscillators. Thus, the amplitude simplifies to

$$\begin{aligned}
Z_{\text{cylinder}} &= i \frac{\alpha'}{2} \int_{s_c^{\text{UV}}}^{s_c^{\text{IR}}} ds_c \int_0^\infty \frac{dp}{\sqrt{2k}} \int_{-\infty}^\infty \frac{d\omega_L}{\sqrt{2k}} \frac{\sinh\left(\pi\sqrt{\frac{\alpha'}{2}}p\right) q_c^{\frac{1}{4}\alpha'(\frac{p^2}{2k} - (1-i\hat{\epsilon})\frac{\omega_L^2}{2k})} \cdot Z_{\mathcal{M}}^{(c)}(q_c)}{\left[\cosh\left(\pi\sqrt{\frac{\alpha'}{2}}\omega_L\right) + \cosh\left(\pi\sqrt{\frac{\alpha'}{2}}p\right)\right] \sinh\left(\frac{\pi}{k}\sqrt{\frac{\alpha'}{2}}p\right)}. \tag{8.45}
\end{aligned}$$

We now modular transform (8.45) to the open string channel. Define again the open string modulus as $q_o = e^{-2\pi i\tau_o}$, where $\tau_o = s_o - i\epsilon$ and $s_o = 1/s_c$. Using the Fourier transform

¹¹⁰Here, we stress the importance of taking the world-sheet Lorentzian. The Fourier transformation from the closed to open channel is well-defined only for the Lorentzian ω_L in space-time. Accordingly, we need to take the Lorentzian world-sheet so that the cylinder amplitude becomes well-defined.

identity:

$$\int_{-\infty}^{\infty} dx \frac{\sin(\pi ax)}{\sinh(\pi x)} e^{-2\pi i k x} = \frac{\sinh(\pi a)}{\cosh(2\pi k) + \cosh(\pi a)}, \quad (|\operatorname{Im} a| < 1) \quad (8.46)$$

we then obtain

$$Z_{\text{cylinder}} = \frac{i\alpha'}{4} \int_{s_o^{\text{UV}}}^{s_o^{\text{IR}}} \frac{ds_o}{s_o} \int_{-\infty}^{\infty} \frac{dp'}{\sqrt{2k}} \int_{-\infty}^{\infty} d\frac{\omega'_L}{\sqrt{2k}} \frac{\sinh\left(\pi\sqrt{\frac{\alpha'}{2}}\omega'_L\right) q_o^{\frac{1}{4}\alpha'\left(\frac{p'^2}{2k} - (1+i\epsilon')^2\frac{\omega'^2}{2k}\right)} \cdot Z_{\mathcal{M}}^{(o)}(q_o)}{\left[\cosh\left(\pi\sqrt{\frac{\alpha'}{2}}\omega'_L\right) + \cosh\left(\pi\sqrt{\frac{\alpha'}{2}}p'\right)\right] \sinh\left(\frac{\pi}{k}\sqrt{\frac{\alpha'}{2}}\omega'_L\right)}. \quad (8.47)$$

Again $s_o^{\text{UV}} \equiv 1/s_c^{\text{IR}}$, $s_o^{\text{IR}} \equiv 1/s_c^{\text{UV}}$ are the cut-off's and the expression (8.47) is well-defined so long as $2\epsilon' s_o^{\text{UV}} > \epsilon$.

8.2.3 analytic continuation

We shall now analytically continue both the space-time and the world-sheet to the Euclidean signature. We have to carefully make the continuation so that keeping the original amplitude (8.47) unchanged (up to cut-off's). As in the previous section, we should first Wick rotate in space-time $\omega'_L \rightarrow e^{i(\frac{\pi}{2}-0)}\omega'_L$ with $\omega'_L = i\omega'$ ($\omega' \in \mathbb{R}$), and then rotate the world-sheet $s_o \rightarrow -it_o$ ($t > 0$). We shall omit the cutoff's from now on. We reach the expression

$$Z_{\text{cylinder}} = Z_{\text{naive}} + Z_{\text{pole}}, \quad (8.48)$$

where the first part is the contribution from naive continuation, while the second parts originates from the poles passed over by the rotated contour: $\omega'_L \rightarrow e^{i(\frac{\pi}{2}-0)}\omega'_L$. See Figure 2. The first part Z_{naive} is given by

$$Z_{\text{naive}} = \int_0^{\infty} \frac{dt_o}{t_o} \int_{-\infty}^{\infty} \frac{dp'}{\sqrt{2k}} \int_{(1-i0)\mathbb{R}} \frac{d\omega'}{\sqrt{2k}} \frac{-\frac{1}{4}\alpha' \sin\left(\pi\sqrt{\frac{\alpha'}{2}}\omega'\right) q_o^{\frac{1}{4}\alpha'\left(\frac{p'^2}{2k} + \frac{\omega'^2}{2k}\right)} \cdot Z_{\mathcal{M}}^{(o)}(q_o)}{\left[\cos\left(\pi\sqrt{\frac{\alpha'}{2}}\omega'\right) + \cosh\left(\pi\sqrt{\frac{\alpha'}{2}}p'\right)\right] \sin\left(\frac{\pi}{k}\sqrt{\frac{\alpha'}{2}}\omega'\right)}. \quad (8.49)$$

The second part Z_{pole} arises from the poles located at

$$\sqrt{\frac{\alpha'}{2}}\omega'_L = \begin{cases} \sqrt{\frac{\alpha'}{2}}|p'| + i(2m+1) & m \in \mathbb{Z}_{\geq 0} \\ -\sqrt{\frac{\alpha'}{2}}|p'| + i(2m+1) & m \in \mathbb{Z}_{< 0} \end{cases} \quad (8.50)$$

whose residues are (after taking the open string channel modulus Euclidean, $q_o = e^{-2\pi t}$)

$$\frac{i}{2} \sqrt{\frac{2}{\alpha'}} \cdot \frac{\sqrt{2}}{2\pi\sqrt{k}} \frac{e^{\pm \frac{i\pi}{k}t(2m+1)} \sqrt{\frac{\alpha'}{2}}|p'| - \pi t \frac{2}{k}(m+\frac{1}{2})^2}{\sinh \frac{\pi}{k} \left(\pm \sqrt{\frac{\alpha'}{2}}|p'| + i(2m+1) \right)}. \quad (8.51)$$

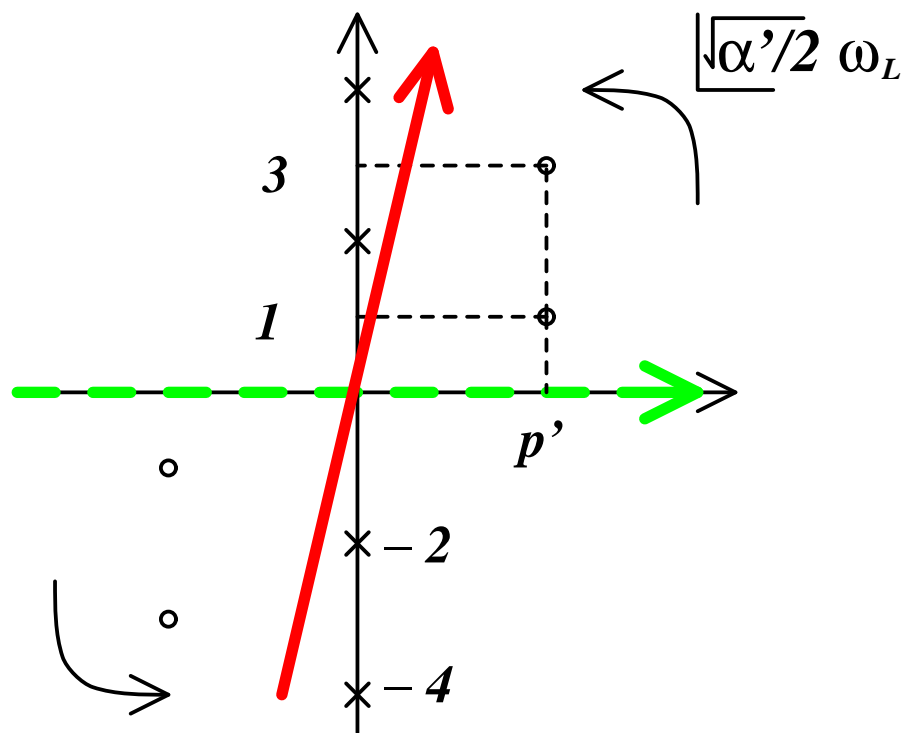


Figure 10: The ω_L -integral with Lorentzian contour (broken line) and the Euclidean contour (solid line).

We thus obtain

$$\begin{aligned}
Z_{\text{pole}} &= \int_0^\infty \frac{dt_o}{t_o} \left[\sum_{m \geq 0} \int_0^\infty \sqrt{\frac{\alpha'}{2}} \frac{dp'}{\sqrt{2k}} - \sum_{m < 0} \int_{-\infty}^0 \sqrt{\frac{\alpha'}{2}} \frac{dp'}{\sqrt{2k}} \right] e^{\frac{i\pi}{k} t(2m+1) \sqrt{\frac{\alpha'}{2}} p' - \pi t \frac{2}{k} (m+\frac{1}{2})^2} \\
&\quad \times 2\pi i \cdot \frac{i\sqrt{2}}{4\pi\sqrt{k}} \left[\frac{1}{\sinh \frac{\pi}{k} \left(\sqrt{\frac{\alpha'}{2}} p' + i(2m+1) \right)} + (p' \leftrightarrow -p') \right] Z_{\mathcal{M}}^{(o)}(q_o) \\
&= -2\sqrt{\frac{2}{k}} \int_0^\infty \frac{dt_o}{t_o} \sum_{m=0}^\infty \int_0^\infty \sqrt{\frac{\alpha'}{2}} \frac{dp'}{\sqrt{2k}} \frac{e^{\frac{i\pi}{k} t(2m+1) \sqrt{\frac{\alpha'}{2}} p' - \pi t \frac{2}{k} (m+\frac{1}{2})^2}}{\sinh \frac{\pi}{k} \left(\sqrt{\frac{\alpha'}{2}} p' + i(2m+1) \right)} \cdot Z_{\mathcal{M}}^{(o)}(q_o) .
\end{aligned} \tag{8.52}$$

We thus obtained manifestly convergent open string channel expressions (8.49), (8.52) for the cylinder amplitude in Lorentzian signature of the space-time.

8.2.4 optical theorem at work

With the Lorentzian (in space-time) cylinder amplitude (8.49), (8.52) available, we now apply the unitarity and obtain total emission number $\overline{\mathcal{N}}$ via imaginary part of Z_{cylinder} . In the analysis of [164] only the naive contribution Z_{naive} was considered. Taking the imaginary part picks up infinite poles located at the real ω' -axis (the imaginary ω'_L -axis), depicted in Figure 2. Their contributions yield

$$\begin{aligned}
&\text{Im } Z_{\text{naive}} \\
&= -\frac{1}{2} \int_0^\infty \frac{dt_o}{t_o} \int_{-\infty}^\infty \sqrt{\frac{\alpha'}{2}} \frac{dp'}{\sqrt{2k}} \sum_{\substack{n \neq 0 \\ n \in \mathbb{Z}}} \pi \text{sgn}(n) \frac{(-1)^n \sqrt{k} \sin(\pi nk) e^{-\pi t_o \left(\frac{\alpha'}{2} \frac{p'^2}{2k} + \frac{n^2 k}{2} \right)}}{\pi \sqrt{2} \cos(\pi nk) + \cosh \left(\pi \sqrt{\frac{\alpha'}{2}} p' \right)} \cdot Z_{\mathcal{M}}^{(o)}(q_o) \\
&= -\sum_{n=1}^\infty \int_0^\infty \frac{dt_o}{t_o} \int_{-\infty}^\infty \sqrt{\frac{\alpha'}{2}} \frac{dp'}{\sqrt{2k}} \frac{(-1)^n \sqrt{k} \sin(\pi nk) e^{-\pi t_o \left(\frac{\alpha'}{2} \frac{p'^2}{2k} + \frac{n^2 k}{2} \right)}}{\sqrt{2} \cos(\pi nk) + \cosh \left(\pi \sqrt{\frac{\alpha'}{2}} p' \right)} \cdot Z_{\mathcal{M}}^{(o)}(q_o) ,
\end{aligned} \tag{8.53}$$

reproducing the first term in (8.42).

We next evaluate the contribution from the pole contribution Z_{pole} (8.52). As is easily seen, taking the imaginary part just amounts to extending the integration region of p' in (8.52) to the whole real axis $(-\infty, \infty)$. By closing the p' -contour in the upper half plane, we

thus obtain

$$\begin{aligned}
& \text{Im } Z_{\text{pole}} \\
&= i\sqrt{\frac{2}{k}} \int_0^\infty \frac{dt_o}{t_o} \sum_{m=0}^\infty \int_{-\infty}^\infty \sqrt{\frac{\alpha'}{2}} \frac{dp'}{\sqrt{2k}} \frac{e^{\frac{i\pi}{k}t_o(2m+1)\sqrt{\frac{\alpha'}{2}}p' - \pi t_o \frac{2}{k}(m+\frac{1}{2})^2}}{\sinh \frac{\pi}{k} \left(\sqrt{\frac{\alpha'}{2}}p' + i(2m+1) \right)} \cdot Z_{\mathcal{M}}^{(o)}(q_o) \\
&= 2\pi i \cdot i\sqrt{\frac{2}{k}} \int_0^\infty \frac{dt_o}{t_o} \sum_{m=0}^\infty \sum_{\substack{n > \frac{1}{k}(2m+1) \\ n \in \mathbb{Z}_{>0}}} \frac{(-1)^n \sqrt{k}}{\pi \sqrt{2}} e^{-\pi t_o n(2m+1) + \pi t_o \frac{2}{k}(m+\frac{1}{2})^2} \cdot Z_{\mathcal{M}}^{(o)}(q_o) \\
&= -2 \int_0^\infty \frac{dt_o}{t_o} \sum_{n=1}^\infty \sum_{m=0}^{\lfloor \frac{nk}{2} - \frac{1}{2} \rfloor} (-1)^n e^{-\pi t_o n(2m+1) + \pi t_o \frac{2}{k}(m+\frac{1}{2})^2} \cdot Z_{\mathcal{M}}^{(o)}(q_o) . \tag{8.54}
\end{aligned}$$

In the last line, we exchanged order of the double summations. The final result agrees perfectly with the total emission number $\overline{\mathcal{N}}$ in (8.42) evaluated via direct computation of the transition amplitudes in Euclidean world-sheet.

8.2.5 imaginary D-instantons: decaying versus rolling

In the previous sections, we studied spectral observables in causal processes involving decay of unstable D-brane and rolling of accelerated D-brane. The main result of this work is that transformation of the total emission number $\overline{\mathcal{N}}$ and the cylinder amplitude Z_{cylinder} from the closed string channel to the open string channel require careful analytic continuation on the world-sheet and that, unlike other results claimed in the literatures, the analytic continuation we adopt gives results consistent with the unitarity via the optical theorem $\overline{\mathcal{N}} = \text{Im } Z_{\text{cylinder}}$. In particular, we found that the cylinder amplitude consists in general of two parts $Z_{\text{cylinder}} = Z_{\text{naive}} + Z_{\text{pole}}$, and the second part is crucial for ensuring the unitarity through its imaginary part. While we dealt with decaying or rolling process of the D-brane, the rules we developed ought to extend to other real-time processes such as open string and D-brane dynamics in electric field or plane-wave field background.

In this section, we highlights several important steps we noted in establishing consistency between the channel duality and the unitarity.

Throughout this work, the strategy for recasting the closed string emission spectra in open string channel was to expand the transition probability $\mathcal{P}(\omega, \mathbf{p})$ in power series of ‘imaginary D-instantons’ [218, 213, 219], viz. contributions of localized states at time $2\pi i \alpha' W(m, n)$ for decaying D-branes and at time $(2\pi i \sqrt{\frac{k}{2}})n \sqrt{\frac{\alpha'}{2}}$ for rolling D-branes, respectively.

A crucial difference we noted for the rolling D-brane in NS5-brane background, $k > 1$, that weight of the n -th imaginary D-instanton, $a_n(p)$, is a non-trivial function of p . We emphasized above that the momentum dependence came about because accelerated D-brane rolls in the two-dimensional subspace $\mathbb{R}_t \times \mathbb{R}_\phi$. Being process dependent, it could be that, in general, *the weights are exponentially growing functions of momentum, and their Fourier transformations are not necessarily well-defined*. This was indeed the case for the rolling D-brane case. We thus prescribed the Fourier transform of the D-instanton weight by analytic continuation via a deformed integration contour. The prescription then yielded in the open

string channel the contribution Z_{pole} beyond the naive one Z_{naive} . Moreover, whereas the naive contribution is always ultraviolet finite, the pole contribution exhibited ultraviolet divergence. Since $\overline{\mathcal{N}}$ (or higher spectral moment) is ultraviolet divergent, we concluded that the presence of ultraviolet divergent Z_{pole} is crucial for consistency with the unitarity and the channel duality.

From mathematical viewpoint, we found that the pole contribution Z_{pole} in (8.42) is present in so far as we adopt mathematically well-posed prescription of the Fourier transform. From physics viewpoint, we can also argue that the first term Z_{naive} by itself cannot be the correct answer and the second term Z_{pole} ought to dominate over the first one.

In the range $k > 1$, it is easy to see that $\text{Im} Z_{\text{naive}}$ can take a negative value if we tune the value k suitably within this range. If Z_{naive} is all there is for the cylinder amplitude, the negative value of its imaginary part contradicts with the fact that the total emission number $\overline{\mathcal{N}}$ is positive by definition. Moreover, for integral value of k , which corresponds to rolling D-branes in k coincident NS5 backgrounds, we observe that the first term Z_{naive} vanishes identically since the integrand vanishes. The above observations indicate that extra contribution ought to be present to the cylinder amplitude beyond the naive contribution, Z_{naive} .

On other other hand, we do not have any contradiction of the cylinder amplitude with the unitarity once the contribution Z_{pole} is taken into account. This is because Z_{pole} is dominant (generically divergent) over Z_{naive} and always positive. We conclude that our prescription for the cylinder amplitude renders the total emission number, as extracted from the optical theorem as $\overline{\mathcal{N}} = \text{Im} Z$ always positive and well-defined.

The situation is in sharp contrast to that for decaying D-brane case. There, as recapitulated in section 2, the D-instanton weights were constant ($a_{n,m} = 1$), so the issue of Fourier transform was void from the outset. Again, as explained in section 2, the momentum independence came about because unstable D-brane decays at rest (or trivially Lorentz boosted). The situation in NS5-brane phase $k > 1$ is also in contrast to that in extreme string phase [124], $1/2 \leq k \leq 1$, or in ‘out-going’ radiation in nonextremal NS5-brane background (which involves two-dimensional black hole geometry) [1]. For these, the leading weight $a_1(p)$ is a bounded function and have well-defined Fourier transformation. Thus, there does not arise any extra contribution beyond Z_{naive} . We thus obtain via optical theorem an ultraviolet finite total emission number.¹¹¹

In the previous work [1], we also noted that the first D-instanton weight $a_1(p)$ is identifiable with the ‘grey body factor’ $\sigma(p)$ in the total emission number $\overline{\mathcal{N}}$. There, the identification was based on saddle-point analysis valid at large mass $M \rightarrow \infty$ in the closed string channel. The present result in the open string channel, where the leading ultraviolet divergence arises from the weight $a_1(p)$, then supports the identification.¹¹²

¹¹¹Even in the deep stringy phase $1/2 \leq k \leq 1$, $a_n(p)$ is exponentially divergent for sufficiently large n . Therefore, the formula given in [164] have to be still corrected. However, only the $n = 1$ term could cause the Hagedorn divergence as noted above. Hence, this correction does not modify ultraviolet behavior of the emission number density.

¹¹²Footnote 3 of [164] claims the saddle-point approximation used in our earlier works is invalid. We disagree with their claim: the relevant integral is of the type

$$\int^{\infty} dp \exp \left[-Mf\left(\frac{p}{M}\right) \right].$$

8.2.6 comparisons

From our analysis, it became clear the reason why [135] obtained the correct result for the decay of unstable D-brane is because the contour rotation in Fourier transform did not encounter any pole (since the D-instanton weights $a_n(p)$ were p -independent constants), and the naive manipulation yielded the correct result. In [164], the prescription of [135] was taken literally also for the rolling of accelerated D-brane. It was then concluded that Z_{naive} refers to the total cylinder amplitude. We showed throughout this work that this is incorrect since it overlooked the pole contribution Z_{pole} . After all, only after taking this extra contribution into account, we showed that the cylinder amplitude is consistent with the channel duality and the unitarity.

Finally, we find it illuminating to understand why $\overline{\mathcal{N}}$ exhibited Hagedorn divergence in the two-dimensional string theory studied in [136], whereas it is ultraviolet finite in the linear dilaton background studied in [135] in two-dimensional space-time (that is, $c_{\text{eff}} = 0$). The reason is because the boundary wave function (D-brane transition amplitude) of the former has non-trivial p -dependence that exponentially diverges, whereas the latter does not.

We finish this subsection with a comment on the origin of the “black hole - string transition” from the open string viewpoint. Operationally, the transition occurs because in the double summation of (8.54), the lightest contribution ($m = 0, n = 1$) is outside the range of summation for $k < 1$. In other words, the lightest open string exchange mode, contributing to the power-like divergence of the imaginary part is projected out. This suggests that the long range interaction between the brane is drastically different between $k < 1$, and $k > 1$. It would be of great interest to uncover this phenomenon and explain the intuitive reason for the breaking of the tachyon - radion correspondence from the open string viewpoint.

8.3 Black hole - string transition

It has been a recurrent theme [103, 104, 106, 105, 107] that an elementary particle or a string is a black hole: a configuration consisting of (multiple) strings with high enough total mass is equivalent to a black hole of the same mass and other conserved charges as we have reviewed in section 4. This brings a question whether a given configuration is most effectively described in terms of strings or black holes. By the black hole - string transition, we will refer to such change of the effective description for a configuration involving massive string excitations. Roughly speaking, the string is dual to the black hole and vice versa.

An immediate, interesting question is whether the two-dimensional black hole geometries is also subject to the black hole - string transition and if so what precisely the dual of the geometries would be. In this section, we shall investigate this transition by studying rolling dynamics of a D0-brane placed on the background. If the background undergoes the transition between the black hole and the string configurations, propagation of a probe D0-brane would be affected accordingly. The transition is triggered by k or κ , which measures characteristic curvature scale of the background measured in string unit and hence string world-sheet

As $M \rightarrow \infty$, the saddle point approximation is well justified in so far as

$$f(p_*/M) \sim \mathcal{O}(1), \quad f''(p_*/M) > 0, \quad f^{(2n)}(p_*/M) \sim \mathcal{O}(1), \quad (n \geq 2), \quad (p_* : \text{saddle}),$$

and this is indeed our case.

effects. We shall explore a signal of the transition by examining spectral distribution of the closed string radiation out of the rolling D0-brane. Other physical observables associated with D0-brane would certainly be equally viable probes. Though straightforward to analyze, in this work, we shall not consider them.

8.3.1 probing black hole - string transition via D-brane

In section 8.2, we observed that $\mathcal{N}(M)_{\text{in}} \gg \mathcal{N}(M)_{\text{out}}$ for both the supersymmetric and bosonic string theories in case the string world-sheet effects are weak enough, viz. $k > 1$ and $\kappa > 3$, respectively. Obviously, such behavior can be interpreted as indicating that the background on which the radiative process takes place is indeed a black-hole: D0-brane falls into the horizon and subsequent radiation is mostly absorbed by the black hole. On the other hand, the behavior that $\mathcal{N}(M)_{\text{in}} \sim \mathcal{N}(M)_{\text{out}} \gg \rho(M)^{-1}$ for $k < 1$ or $\kappa < 3$ does not seem to bear features present in the black hole background: while D0-brane falls inward, subsequent radiation is not mostly absorbed by the black hole but disperse away. Since this is the regime where the string world-sheet effects are significant, the background may be described most effectively in terms of strings. We are thus led to conclude that the background, whose stringy effects are controlled by the parameter k or κ , would make a phase-transition between the black hole and the string across $k = 1$ or $\kappa = 3$. In a different physical context, this so-called “black hole - string transition” was studied recently [96, 124]. What distinguishes our consideration and result from [96, 124] is that we are probing possible phase-transition of the (closed string) background by introducing a D0-brane in it and studying open string dynamics.

Possible existence of such a phase transition was first hinted in [122] in the closed string sector, where they observed that the $\mathcal{N} = 2$ Liouville superpotential becomes normalizable once $k > 1$ and it violates the Seiberg bound. Recall that the marginal interaction term is

$$S^\pm = \psi^\mp e^{-\frac{1}{\mathcal{Q}}(\phi \pm iY)}, \quad (\mathcal{Q} = \sqrt{2/k}) \quad (8.55)$$

for the $\mathcal{N} = 2$ Liouville theory, and

$$S^\pm = e^{-\frac{1}{\mathcal{Q}}(\phi \pm \sqrt{1+\mathcal{Q}^2}iY)} \equiv e^{-\sqrt{\frac{\kappa-2}{2}}\phi \mp \sqrt{\frac{\kappa}{2}}iY}, \quad (\mathcal{Q} = \sqrt{2/(\kappa-2)}), \quad (8.56)$$

for the bosonic sine-Liouville theory, respectively. Both interactions are normalizable (exponentially falling off in the asymptotic far region) if the curvature is sufficiently small that $k > 1$ or $\kappa > 3$ is satisfied. As is well-known, $\mathcal{N} = 2$ Liouville or sine-Liouville theory is T-dual to the $SL(2; \mathbb{R})/U(1)$ coset theory [92, 82, 83, 94], so the condition on the level k or κ ought naturally to descend to the two-dimensional black hole description. Indeed, such aspect was discussed in [96] purely in the language of the $SL(2; \mathbb{R})/U(1)$ coset theory (see also [94]). Their reasoning is closely related to the non-formation of the black hole in two-dimensional string theory (see also [220] for the discussion concerning this issue from the matrix model viewpoint). In the strong curvature regime, $k < 1$, the background is described more effectively in terms of the $\mathcal{N} = 2$ Liouville theory as it is weakly coupled. Evidently, the black hole interpretation of the $SL(2; \mathbb{R})/U(1)$ theory is less clear in this region, because the classical $\mathcal{N} = 2$ Liouville theory does not admit an interpretation in terms of black hole geometry in any obvious way.

We emphasize that such black hole - string transition is not likely to arise perturbatively and could arise only from nonperturbative string world-sheet effects as we have reviewed in section 3 and 4. For instance, tree-level closed string amplitudes are manifestly analytic with respect to the level k . These amplitudes exhibit a finite absorption rate (thus displaying the non-unitarity of the reflection amplitudes) regardless of the value of k . In fact, finite- k correction to the amplitudes yield an irrelevant phase-factor [75, 214].

However, as was first observed in [148], situation changes drastically if we consider the closed string radiation from the rolling D-brane in such a background. In [148], it was shown that the distribution of radiation off D0-brane in extremal NS5-brane background becomes ultraviolet finite for $k < 1$. In the previous section, extending the analysis of [148], we have shown that the $k = 1$ transition shows up manifestly in the open string sector in the sense that branching ratio between the incoming and the outgoing radiation distribution (as well as spectral moments) behaves very differently across $k = 1$. Remarkably, retaining finite $1/k$ -correction, which originated from consistency with the exact reflection relations, was crucial in obtaining physically sensible results *even for* $k \gg 1$. Cancellation between the radiation distribution and the exponential growth of the density of states at large M is quite nontrivial, and relied crucially on precise functional dependence on k .

An ‘order-parameter’ of the transition is thus provided by the radiation distribution of rolling D-brane. The phase transition across $k = 1$ is that while the radiation distribution from the falling D-brane exhibits powerlike ultraviolet divergence for $k > 1$, it becomes finite for $k < 1$. Thus, the rolling D-brane in the $k < 1$ regime does *not* yield a large back-reaction unlike the $k > 1$ case. This is also consistent with the assertion that black hole cannot be formed in the two-dimensional string theory: It seems difficult to construct two-dimensional black hole by injecting D-branes to the linear dilaton (or usual Liouville) theory.¹¹³

It is also worth mentioning that the radion-tachyon correspondence is likely to fail in the two-dimensional string theory ($k = 1/2$). In fact, had we have such a correspondence, the rolling radion of the D0-brane could be identified with the rolling tachyon of the ZZ-brane in the Liouville theory. On the other hand, it is known that the radiation distribution of the ZZ brane exhibits a powerlike ultraviolet divergence [136] at leading order in string perturbation theory, while that of the falling D0-brane does not.

8.3.2 holographic viewpoint

The black hole - string transition across $k = 1$ also has a natural interpretation in terms of the holographic principle, as recently discussed in [124]. Adding Q_1 fundamental strings to k NS5-branes, one obtains the familiar bulk geometry of the AdS_3/CFT_2 -duality. In this context, the density of states of the dual conformal field theory is given by the naive Cardy formula $S = 2\pi\sqrt{\frac{cL_0}{6}} + 2\pi\sqrt{\frac{\bar{c}\bar{L}_0}{6}}$ with $c = 6kQ_1$ for $k > 1$, but not for $k < 1$. Rather, the central charge that should be used in the Cardy formula is replaced by an effective one $c_{\text{eff}} = 6Q_1(2 - \frac{1}{k})$ [122]. The similar effects also showed up in the double scaling limit of the ‘little string theory’(LST) [82, 83].¹¹⁴ We shall now show that such change of the central

¹¹³Such a possibility was proposed in [96].

¹¹⁴Even though the original ‘little string theory’ is the theory of NS5-brane, so k should be positive integer-valued, one can also consider models with fractional value of the level k , which is less than 1 generically.

charge is also imperative for reproducing the closed string radiation distribution correctly from the dual holographic picture.

It is an interesting attempt to reproduce the phase transition in the radiation distribution of rolling D-brane across $k = 1$ from the holographic viewpoint. In [152], it was proposed that the rolling D-brane should correspond to the decay of a certain defect in the dual LST. We shall now extend that analysis to the $k < 1$ case and explore the phase-transition. The relevant holographic description is based on the following two assumptions.

1. fixed radiation number distribution: The radiation distribution for a fixed mass M is determined by large k behavior of the pressure in the far future (past). This is equivalent to the statement that the decay of the radion is described by a ‘holographic tachyon condensation’. We assume that there is no phase transition at $k = 1$ for a fixed mass M .¹¹⁵ In our convention, the distribution is given by

$$\mathcal{N}(M)_{\text{LST}} \sim e^{-2\pi M \sqrt{\frac{k}{2}}} . \quad (8.57)$$

2. change of density of states: The final density of closed little string states in the ‘holographic tachyon condensation’ is given by the square root of the full nonperturbative density of states in LST. As is discussed in [124], the full nonperturbative density of states of the LST is believed to exhibit a phase transition at $k = 1$: for $k > 1$, the density of states is related to the Hawking temperature as

$$n(M)_{\text{LST}} \sim e^{4\pi M \sqrt{\frac{k}{2}}} . \quad (8.58)$$

In other words, the Hagedorn temperature in LST should be equated with the Hawking temperature [146] (see also, *e.g.* [222, 223, 12]).

On the other hand, for $k < 1$, because of the non-normalizability of the black hole excitation, the nonperturbative density of states of the LST is equivalent to the density of states of the (dual) perturbative string theory [124]:

$$n(M)_{\text{LST}} \sim e^{4\pi M \sqrt{1 - \frac{1}{2k}}} . \quad (8.59)$$

With these assumptions, we can estimate the average radiation number of the ‘holographic tachyon condensation’ to be

$$\overline{\mathcal{N}}_{\text{LST}} = \int_0^\infty dM \mathcal{N}(M) \sqrt{n(M)_{\text{LST}}} .$$

This is achieved by considering the *wrapped* NS5-brane backgrounds, or compactifications on a Calabi-Yau threefold having rational singularity [24]. From the regularized torus partition function, one can prove that there is no normalizable massless states (corresponding to the ‘Lehmann-Symanzik-Zimmerman-poles’ [221]) in such string vacua if $k < 1$, as was discussed in *e.g.* [27, 37].

¹¹⁵Theoretically, there is no reason to exclude a finite $1/k$ correction here. We only need this assumption phenomenologically in order to reproduce the ten-dimensional calculation even for $k > 1$. A priori, the tachyon condensation (in the critical bosonic string) itself may receive large string world-sheet corrections. In the Dirac-Born-Infeld action analysis, such potential corrections were completely dropped out.

Note that, in contrast to the bulk string theory calculation, we have no integration over the radial momentum. Substituting (8.57) and (8.58) or (8.59) according to the value of k , we obtain

$$\overline{\mathcal{N}}_{\text{LST}} \sim \int^{\infty} dM e^{-2\pi M \sqrt{\frac{k}{2}} + 2\pi M \sqrt{\frac{k}{2}}}$$

for $k > 1$, showing powerlike ultraviolet divergent behavior because of the complete cancellation in the exponent, and

$$\overline{\mathcal{N}}_{\text{LST}} \sim \int^{\infty} dM e^{-2\pi M \sqrt{\frac{k}{2}} + 2\pi M \sqrt{1 - \frac{1}{2k}}},$$

for $k < 1$, showing exponential suppression in the ultraviolet. It is easy to see that this holographic dual computation reproduces the bulk computation presented in section 8.1.1 up to a subleading power dependence (8.14), (8.16).¹¹⁶

It should be noted, however, that the cancellation between the radiation distribution and the density of states has a different origin in the dual holographic description as compared to the bulk side. In the holographic description, the origin of the phase transition is the nonperturbative density of the states in LST while the radiation distribution at a fixed mass-level M keeps its functional form unchanged. On the other hand, in the bulk theory, origin of the cancellation was that the radiation distribution changes at $k = 1$ due to the disappearance of the non-trivial saddle point in the integration of the radial momentum p , while the density of states is always given by the same formula. Thus the agreement between the two descriptions is quite non-trivial and we believe that our results provide yet another evidence of the holographic duality for the NS5-brane and black hole physics.

Though we presented the dual description based on some assumptions, we can turn the logic around and regard our results as a support for such assumptions. In particular the quantum gravity phase transition at $k = 1$ in the dual theory proposed in [124] is crucial for understanding the radiation distribution out of a defect decay in the dual LST. We thus propose our discussion in this section as a strong support for black hole - string transition.

8.4 Boundary states and radiation in Ramond-Ramond sector

In the case of fermionic black hole background, the rolling D0-brane would also radiate off closed string states in the Ramond-Ramond (R-R) sector. In this section, we shall construct R-R boundary state of the D0-brane and compute radiation rates. Since the world-sheet theory corresponds to $\mathcal{N} = 2$ superconformal field theory, correlation functions of the R-R sector and boundary states are readily obtainable by performing the standard $\mathcal{N} = 2$ spectral flow.

We shall begin with discussion regarding properties of reflection amplitudes for the R-R sector (see [214] in the context of two-dimensional black hole). Recall that the reflection relation was given in the NS-NS sector as

$$U_{\omega}^{-p}(\rho, t)^{\text{NS}} = \mathcal{R}^{\text{NS}}(-p, \omega) U_{\omega}^p(\rho, t)^{\text{NS}} \quad \text{and} \quad V_{\omega}^{-p}(\rho, t)^{\text{NS}} = \mathcal{R}^{\text{NS}*}(-p, \omega) V_{\omega}^p(\rho, t)^{\text{NS}},$$

¹¹⁶The exact determination of the pre-exponential power part is beyond the scope of the rough estimate presented here. It requires the full computational ability in the LST.

where the exact reflection amplitude $\mathcal{R}^{\text{NS}}(-p, \omega)$ was defined by

$$\mathcal{R}^{\text{NS}}(p, \omega) = \frac{\Gamma(1 + \frac{ip}{k})\Gamma(+ip)\Gamma^2(\frac{1}{2} - i\frac{p+\omega}{2})}{\Gamma(1 - \frac{ip}{k})\Gamma(-ip)\Gamma^2(\frac{1}{2} + i\frac{p-\omega}{2})}.$$

To obtain the reflection relation of the R-R sector, we shall perform the spectral flow by half unit of the $\mathcal{N} = 2$ $U(1)$ current.

In sharp contrast to the $\mathcal{N} = 2$ Liouville theory, the reflection amplitude now depends on the spin structure of the R-R sector.¹¹⁷ Explicitly, the spectral flow is defined as $\omega \rightarrow \omega \pm i$, where the $+$ sign corresponds to spin $(+, -)$ states and $-$ sign corresponds to spin $(-, +)$ states (in the $(\frac{1}{2}, \frac{1}{2})$ picture): in the $\rho \rightarrow \infty$ limit, they are described by $S^\pm e^{-\rho} e^{-ip\rho - i\omega t}$ and the conformal weight is given by $h = \frac{p^2 - \omega^2 + 1}{4k} + \frac{1}{8}$.

Therefore, for the R-R states with spin $(+, -)$, the exact reflection amplitudes become

$$\mathcal{R}^{\text{R}+}(p, \omega) = \frac{\Gamma(1 + \frac{ip}{k})\Gamma(+ip)\Gamma^2(1 - i\frac{p+\omega}{2})}{\Gamma(1 - \frac{ip}{k})\Gamma(-ip)\Gamma^2(1 + i\frac{p-\omega}{2})}. \quad (8.60)$$

Equivalently, if we take spin $(-, +)$ R-R states, the exact reflection amplitudes become

$$\mathcal{R}^{\text{R}-}(p, \omega) = \frac{\Gamma(1 + \frac{ip}{k})\Gamma(+ip)\Gamma^2(-i\frac{p+\omega}{2})}{\Gamma(1 - \frac{ip}{k})\Gamma(-ip)\Gamma^2(+i\frac{p-\omega}{2})}. \quad (8.61)$$

It is important to notice that the latter amplitudes have a second order zero in the light-cone direction $p = \omega > 0$ (recall that $p > 0$ in our convention). Similarly, we could derive the reflection relation for (\pm, \pm) spin structure, but the resultant amplitudes are compatible only with the analytic continuation to the ‘winding time’ (in the interior of the singularity), so we would not delve into details anymore.

Consider next the boundary wave function of the R-R sector. For definiteness, we shall take the absorbed D0-brane (7.30) (We focus on the $t_0 = 0$ case for simplicity.)

$$\text{absorb}\langle B, \text{NS}; \rho_0 | = \int_0^\infty \frac{dp}{2\pi} \int_{-\infty}^\infty \frac{d\omega}{2\pi} \Psi_{\text{absorb:NS}}(\rho_0; p, \omega) \hat{v} \langle \langle p, \omega |$$

where

$$\Psi_{\text{absorb:NS}}(\rho_0; p, \omega) = \frac{\Gamma(\frac{1}{2} - i\frac{p+\omega}{2})\Gamma(\frac{1}{2} - i\frac{p-\omega}{2})}{\Gamma(1 - ip)} \Gamma\left(1 + \frac{ip}{k}\right) \left[e^{-ip\rho_0} - \frac{\cosh\left(\pi\frac{p-\omega}{2}\right)}{\cosh\left(\pi\frac{p+\omega}{2}\right)} e^{+ip\rho_0} \right].$$

The boundary wave functions of the R-R sector are then derived by applying the $\mathcal{N} = 2$ spectral flow $\omega \rightarrow \omega \pm i$:

$$\Psi_{\text{absorb:R}+}(\rho_0; p, \omega) \frac{\Gamma(-i\frac{p+\omega}{2})\Gamma(1 - i\frac{p-\omega}{2})}{\Gamma(1 - ip)} \Gamma\left(1 + \frac{ip}{k}\right) \left[e^{-ip\rho_0} + \frac{\sinh\left(\pi\frac{p-\omega}{2}\right)}{\sinh\left(\pi\frac{p+\omega}{2}\right)} e^{+ip\rho_0} \right],$$

¹¹⁷This is because, in the $\mathcal{N} = 2$ Liouville theory, the reflection amplitudes for the momentum modes have a symmetry under $\omega \rightarrow -\omega$.

and

$$\Psi_{\text{absorb:R-}}(\rho_0; p, \omega) = \frac{\Gamma(1 - i\frac{p+\omega}{2})\Gamma(-i\frac{p-\omega}{2})}{\Gamma(1 - ip)} \Gamma\left(1 + \frac{ip}{k}\right) \left[e^{-ip\rho_0} + \frac{\sinh\left(\pi\frac{p-\omega}{2}\right)}{\sinh\left(\pi\frac{p+\omega}{2}\right)} e^{+ip\rho_0} \right],$$

for the two opposite spin structures. These boundary wave functions are of course consistent with the exact reflection amplitudes (8.60),(8.61).

From these boundary wave functions, we can deduce some physical properties of the boundary states in the R-R sector:

- For $k > \frac{1}{2}$, in the saddle point approximation of the radial momentum integral, radiation distribution of the R-R sector behaves the same as that of the NS-NS sector. In particular, the absolute value of the reflection amplitudes behave in the similar manner. Thus, the radiation distribution of the R-R sector is the same as that of the NS-NS sector.
- For $k = \frac{1}{2}$, viz. the two-dimensional black hole, considerable differences arise. Both boundary wave function and reflection amplitudes show singularity (or zero) when we take particular spin structure. It is not clear what the origin of these singularities of lightlike on-shell states $p = \omega$ would be. We note that some related discussions were given in [214].
- In the mini-superspace limit $k \rightarrow \infty$, the mass gap in the R-R sector vanishes. Therefore, it is well-posed to question radiation of the massless R-R states off the R-R charge. From the boundary states given above, we observe that, assuming $p, \omega > 0$, there is no lightlike pole in $R+$ state while there is a pole at $p = +\omega$ in the $R-$ state. It is also interesting to note that, in the subleading contribution proportional to $e^{+ip\rho_0}$, the pole from the gamma function is cancelled by the zero in the $\sinh(\pi\frac{p-\omega}{2})$ factor.

A possible interpretation is that, roughly speaking, R-R charge is localized on the incoming light-cone $p = \omega$.¹¹⁸

8.5 Back to extremal NS5-brane background

By tuning off $\mu \rightarrow 0$, we are back to the extremal NS5-brane background. Roughly speaking, the extremal background is described by the free linear dilaton theory, but crucial differences from the non-extremal counterpart studied in this work are the followings:

- We have no reflection relation, and the $p > 0$ and $p < 0$ states should be treated as independent states.¹¹⁹

¹¹⁸This is true only in the asymptotic region $\rho \rightarrow \infty$ since the distribution near $\rho = 0$ is further related to the basis of Ishibashi states used in the expansion. In the case of ‘absorbed’ basis, there is no contribution from the past horizon. In addition, because the reflection amplitude vanishes in the $R-$ sector, an observer at $\rho \rightarrow \infty$ do not detect any outgoing wave.

¹¹⁹In this sense, the arguments given in [207] are not completely precise, although the main part of physical results, say, the closed string radiation rates, are not altered.

- The conformal field theory description is not effective in the entire space-time: the string coupling diverges at the location of the NS5-brane. We cannot completely trace the classical trajectory of the D0-brane (7.20) without facing strong coupling problem.

We thus have to keep it in mind that the validity of the conformal field theory description of extremal NS5-brane is limited to the sufficiently weak string coupling region.

For the extremal NS5-brane, since the relevant conformal field theory involves linear dilaton and hence is a free theory, we can introduce the basis of the Ishibashi states as $|p, \omega\rangle\rangle$, ($p, \omega \in \mathbb{R}$) associated with the wave function $\psi_\omega^p(\rho, t) \propto e^{-\rho} e^{-ip\rho - i\omega t}$. Another non-trivial difference from the non-extremal case is the volume form of the space-time. Since we have the linear dilaton $\Phi = \text{const} - \rho$ and a flat metric $G_{ij} = \eta_{ij}$, the relevant volume form becomes

$$d\text{Vol} = e^{-2\Phi} \sqrt{G} d\rho dt = e^{2\rho} d\rho dt . \quad (8.62)$$

Now, the classical trajectory of D0-brane in the extremal NS5-brane is given by [145]:

$$2 \cosh(t - t_0) e^\rho = e^{\rho_0} . \quad (8.63)$$

The boundary state describing the D0-brane moving along (8.63) ought to have the following form:

$$\langle B; \rho_0, t_0 | = \int_{-\infty}^{\infty} \frac{dp}{2\pi} \int_{-\infty}^{\infty} \frac{d\omega}{2\pi} \Psi(\rho_0, t_0; p, \omega) \langle\langle p, \omega | . \quad (8.64)$$

The boundary wave function is evaluated as

$$\begin{aligned} \Psi(\rho_0, t_0; p, \omega) &\sim \int dv \delta\left(2 \cosh(t - t_0) e^\rho - e^{\rho_0}\right) e^{-\rho - ip\rho - i\omega t} \\ &= \int_{-\infty}^{\infty} dt e^{-ip\rho_0} e^{-i\omega t} \left[2 \cosh(t - t_0)\right]^{ip-1} \\ &= \frac{1}{2} B \left(\frac{1}{2} - i\frac{p+\omega}{2}, \frac{1}{2} - i\frac{p-\omega}{2}\right) e^{-ip\rho_0 - i\omega t_0} . \end{aligned} \quad (8.65)$$

In the last expression, we used the formula (A.40). This is essentially the calculation given in [207]. Finally, by restoring the important ‘world-sheet correction factor’ $\Gamma\left(1 + i\frac{p}{k}\right)$,¹²⁰ we obtain the boundary wave function

$$\Psi(\rho_0, t_0; p, \omega) = \frac{1}{2} B(\nu_+, \nu_-) \Gamma\left(1 + i\frac{p}{k}\right) e^{-ip\rho_0 - i\omega t_0} . \quad \text{where} \quad \nu_\pm \equiv \frac{1}{2} - i\frac{p \pm \omega}{2} ,$$

This is the extremal counterpart of the ‘symmetric D0-brane’ in the non-extremal NS5-brane background (7.36).

¹²⁰Since in this case we do not have the reflection relation, the inclusion of the factor $\Gamma\left(1 + i\frac{p}{k}\right)$ may sound less affirmative than the nonextremal NS5-brane background. We argue that the procedure is actually justified by considering the limit from the non-extremal case.

We can also consider the ‘half S-brane’ counterpart by taking the Hartle-Hawking contours depicted in the Figures 11 and 12. Namely, for the ‘absorbed brane’, we obtain

$$\text{absorb} \langle B; \rho_0, t_0 | = \left(\int_0^\infty \frac{dp}{2\pi} \int_0^\infty \frac{d\omega}{2\pi} + \int_{-\infty}^0 \frac{dp}{2\pi} \int_{-\infty}^0 \frac{d\omega}{2\pi} \right) \Psi(\rho_0, t_0; p, \omega) \langle \langle p, \omega | , \quad (8.66)$$

and for the ‘emitted brane’,

$$\text{emitted} \langle B; \rho_0, t_0 | = \left(\int_0^\infty \frac{dp}{2\pi} \int_{-\infty}^0 \frac{d\omega}{2\pi} + \int_{-\infty}^0 \frac{dp}{2\pi} \int_0^\infty \frac{d\omega}{2\pi} \right) \Psi(\rho_0, t_0; p, \omega) \langle \langle p, \omega | . \quad (8.67)$$

They are regarded as the counterparts of (8.71) and (8.72).

The radiation rates were already evaluated in [207, 152].¹²¹ Crucial differences from the non-extremal case are the followings: We have the ‘forward radiations’ (*e.g.*, the incoming radiation for the absorbed D-brane (8.66)) only and no ‘backward radiations’ (*e.g.*, the outgoing radiation for the absorbed D-brane). This is because there is no reflection relation in the extremal case. The forward radiations behave in the completely same way as the non-extremal case (that is, in a fermionic two-dimensional black hole with $k > 1$), giving rise to the Hagedorn-like ultraviolet divergence again. At fixed but large M before integrating over p , the partial radiation number distribution takes again exactly the same asymptotic form as in (8.12) except that now the coefficient $2\pi\sqrt{2k}$ is *not* interpretable as the inverse Hawking temperature of the black hole.¹²² Again, this has to do with the peculiarity that the Hawking temperature of the two-dimensional black hole is set by the level k , not by the nonextremality μ . On the other hand, the absence of the backward radiation matches with the extremality of the background; there is no Hawking radiation.

8.6 More on physical interpretations : Hartle-Hawking states

We shall now revisit the boundary states we constructed in this work and elaborate further on their physical interpretations with particular emphasis on analogy with the rolling tachyon problem via the radion-tachyon correspondence. We also elaborate on the fate of R-R charge carried by the D0-brane. To be concrete, we shall focus on the cases $k \geq 2$ admitting interpretation in terms of near horizon geometry of black NS5 branes.

The boundary state (7.30) describes the late-time rolling ($t \gg t_0$) of the D0-brane rolling into the black NS5 branes. The relevant D0-brane has the initial condition $\rho = \rho_0$, $\frac{d\rho}{dt} = 0$ at $t = t_0$ and starts to roll down toward the black hole. After sufficiently long coordinate time elapsed, the D0-brane gets close to the future horizon (\mathcal{H}^+). As examined in section 4, almost all energy of the D0-brane is absorbed by the black hole in the form of incoming radiation. The incoming radiation is dominated by very massive, and hence highly non-relativistic closed string excitations. Via the radion-tachyon correspondence, these states are identifiable with the ‘tachyon matter’ in the rolling tachyon problem in flat space-time. On the other hand, we have seen that a small part of energy escapes to the spatial infinity (\mathcal{I}^+)

¹²¹ In this paper, we scaled energy and momentum differently from [207]. In light of normalization as in (8.9), ω, p in this work should be read as $2\sqrt{k}$ times ω, p in [207].

¹²² An obvious alternative interpretation could be that, even for extremal background, the falling D0-brane excites the NS5-brane above the extremality.

as the outgoing radiation. We have seen that the spectral distribution is characterized by the Hawking temperature, and is necessarily dominated by light modes. This interpretation is quite natural from the viewpoint of the radion-tachyon correspondence for the extremal NS5-brane background [145]. Since we are now working with the non-extremal NS5-brane background, our analysis may be considered as an evidence that the correspondence is valid even at finite temperature.

What about evolution in the far past $t < t_0$? Here, we face a subtlety. Recall that the boundary condition defining (7.30) does not allow contributions from the past horizon (\mathcal{H}^-), namely, the basis of Ishibashi states $|p, \omega\rangle\rangle^U$ does not reproduce the past half of the classical trajectory (7.20). Rather, the NS-NS sector of the D0-brane boundary wave function appears widely distributed in the space-time in the far past. This may be interpreted as radiations imploding to $\rho = \rho_0$ from spatial infinity, but then it is subtle to trace the R-R charge carried by the D0-brane, created out of the imploding radiation. Classically, the D0-brane charge density ought to be localized along the classical trajectory (7.20) and hence emanates from the past horizon. Once stringy effects are taken into account, the charge appears to originate from asymptotic infinity along the light-cone coordinate. Complete understanding of this curious feature is highly desirable but we shall relegate it to future study. Here, instead, we present a simple prescription of avoiding this subtlety: a version of ‘Hartle-Hawking’ boundary condition.

We shall first focus on the absorbed D0-brane boundary state (7.30). Formally, by construction, we can regard the boundary wave function specified by the time-integration over the ‘real contour’ $\mathcal{C} = \mathbb{R}$ as in (7.24). Now, let us discuss what happens if we choose the ‘Hartle-Hawking’ type contour instead of the real contour, which connect the Euclidean time with the future or past half of real time axis at $t = t_0$:

$$\mathcal{C}_{\text{future}}^{\pm} = (t_0 + i\mathbb{R}_{\mp}) \cup (t_0 + \mathbb{R}_{+}) \quad , \quad \mathcal{C}_{\text{past}}^{\pm} = (t_0 + i\mathbb{R}_{\mp}) \cup (t_0 + \mathbb{R}_{-}) \quad . \quad (8.68)$$

More precisely, we should avoid suitably the branch cuts on $t_0 + i\mathbb{R}$ to render the integral convergent. See Figures 11 and 12 for details. The superscript $+$ ($-$) is associated with the positive (negative) energy sector. Note that the phase-factor $e^{-i\omega t}$ behaves well on the lower (upper) half of complex t -plane if ω is positive (negative). Let us pick up $\mathcal{C}_{\text{future}}$. Following the traditional interpretation of the Hartle-Hawking type wave function, we may suppose that both the D0-brane and black NS5-brane are created from ‘nothing’ at $t = t_0$, and then the D0-brane starts to fall down toward the future horizon along the classical trajectory (7.20). In this prescription, the subtlety we mentioned above is completely circumvented.

One may paraphrase the prescription as follows: choosing the Hartle-Hawking contour $\mathcal{C}_{\text{future}}$, we explicitly obtain

$$\begin{aligned} & {}_{HH+, \text{absorb}}\langle B; \rho_0, t_0 | \\ & = \int_0^{\infty} \frac{dp}{2\pi} \left[\int_0^{\infty} \frac{d\omega}{2\pi} \Psi_{\text{symm}}(\rho_0, t_0; p, \omega) + \int_{-\infty}^0 \frac{d\omega}{2\pi} \mathcal{R}(p, \omega) \Psi_{\text{symm}}^*(\rho_0, -t_0; p, \omega) \right] \hat{u} \langle \langle p, \omega | \quad , \end{aligned} \quad (8.69)$$

where $\Psi_{\text{symm}}(\rho_0, t_0; p, \omega)$ is defined in (7.36). In fact, by taking $\mathcal{C}_{\text{future}}$, we are only left with the L_{ω}^p (R_{ω}^p)-part of the one-point function for the $\omega > 0$ ($\omega < 0$) sector. See figure 11.

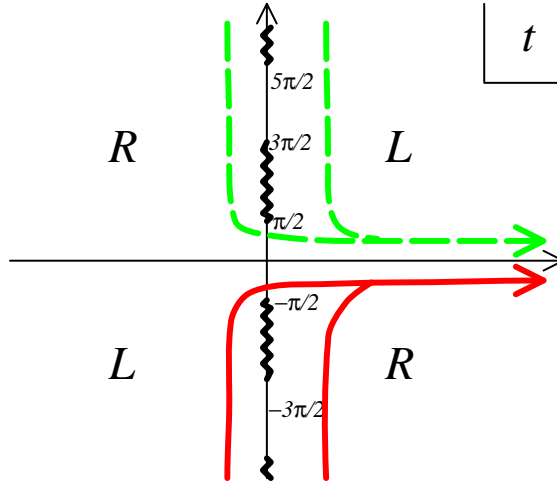


Figure 11: ‘future Hartle-Hawking contour’: the red (green broken) line is the contour $\mathcal{C}_{\text{future}}^+$ for $\omega > 0$ ($\mathcal{C}_{\text{future}}^-$ for $\omega < 0$). The ‘L’ (‘R’) contour should be used if calculating the overlap with $L_{\omega}^p(\rho, t)$ ($R_{\omega}^p(\rho, t)$) for the convergence of integral.

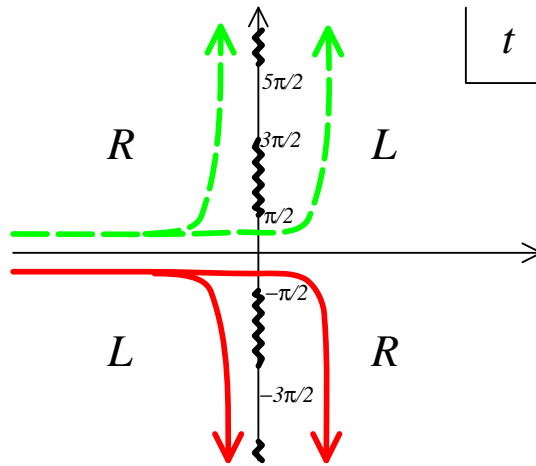


Figure 12: ‘past Hartle-Hawking contour’: the red (green broken) line is the contour $\mathcal{C}_{\text{past}}^+$ for $\omega > 0$ ($\mathcal{C}_{\text{past}}^-$ for $\omega < 0$).

This boundary wave function is formally regarded as the limit of (7.30) under $t_0 \rightarrow -\infty$, $\rho_0 \rightarrow +\infty$ while keeping $|\rho_0|/|t_0|$ finite. Note that the second (first) term $\propto e^{ip\rho_0 - i\omega t_0}$ ($\propto e^{-ip\rho_0 - i\omega t_0}$) in (7.30) oscillates very rapidly in this limit for $\omega > 0$ ($\omega < 0$) and hence drops off.¹²³ The limit just means that the D0-brane moving along the trajectory (7.20) is coming from the past infinity (\mathcal{I}^-), and falling into the future horizon (\mathcal{H}^+). Everything is supposed to be localized over the classical trajectory in this case.

Adopting the past Hartle-Hawking contour $\mathcal{C}_{\text{past}}$ for the boundary state of emitted D0-brane (7.32) is completely parallel. We take the time-reversal of the above:

$$\begin{aligned} & {}_{HH-, \text{emit}}\langle B; \rho_0, t_0 | \\ &= \int_0^\infty \frac{dp}{2\pi} \left[\int_0^\infty \frac{d\omega}{2\pi} \Psi_{\text{symm}}^*(\rho_0, -t_0; p, \omega) + \int_{-\infty}^0 \frac{d\omega}{2\pi} \mathcal{R}^*(p, \omega) \Psi_{\text{symm}}(\rho_0, t_0; p, \omega) \right] \widehat{V} \langle p, \omega |, \end{aligned} \quad (8.70)$$

which is regarded as the $t_0 \rightarrow +\infty$, $\rho_0 \rightarrow +\infty$ limit of (7.32). It describes the trajectory of D0-brane emitted from the past horizon \mathcal{H}^- and escaping to the future infinity \mathcal{I}^+ .

Let us turn to the ‘symmetric’ D0-brane (7.36). Naively, it appears that the prescription is that

$$\begin{aligned} & {}_{HH+, \text{symm}}\langle B; \rho_0, t_0 |' \\ &= \int_0^\infty \frac{dp}{2\pi} \left[\int_0^\infty \frac{d\omega}{2\pi} 2\Psi_{\text{symm}}(\rho_0, t_0; p, \omega) {}^L\langle p, \omega | + \int_{-\infty}^0 \frac{d\omega}{2\pi} 2\Psi_{\text{symm}}^*(\rho_0, -t_0; p, \omega) {}^R\langle p, \omega | \right] \end{aligned} \quad (8.71)$$

for the future Hartle-Hawking contour $\mathcal{C}_{\text{future}}$, and

$$\begin{aligned} & {}_{HH-, \text{symm}}\langle B; \rho_0, t_0 |' \\ &= \int_0^\infty \frac{dp}{2\pi} \left[\int_0^\infty \frac{d\omega}{2\pi} 2\Psi_{\text{symm}}^*(\rho_0, -t_0; p, \omega) {}^R\langle p, \omega | + \int_{-\infty}^0 \frac{d\omega}{2\pi} 2\Psi_{\text{symm}}(\rho_0, t_0; p, \omega) {}^L\langle p, \omega | \right] \end{aligned} \quad (8.72)$$

for the past Hartle-Hawking contour $\mathcal{C}_{\text{past}}$. However, this cannot be the whole story. The existence of Euclidean part of the Hartle-Hawking path-integral enforces the boundary states to be expanded by the basis smoothly connected to the Euclidean ones, while $|L_\omega^p\rangle$, $|R_\omega^p\rangle$ do not possess such a property. Consequently, to achieve the correct Hartle-Hawking states, we ought to make further the projection to \mathcal{H}^U , ($\widehat{\mathcal{H}}^U$) for the contour $\mathcal{C}_{\text{future}}$, and to \mathcal{H}^V , ($\widehat{\mathcal{H}}^V$)

¹²³More precise argument would be as follows: The disk amplitude for a wave packet *e.g.* $\int \frac{dp}{2\pi} \int \frac{d\omega}{2\pi} f(p, \omega) |L_\omega^p\rangle$ is evaluated as $\lim_{\rho_0 \rightarrow +\infty, t_0 \rightarrow -\infty} \int \frac{dp}{2\pi} \int \frac{d\omega}{2\pi} f(p, \omega) \Psi(\rho_0, t_0; p, \omega)$. Then, the rapidly oscillating term in the boundary wave function $\Psi(\rho_0, t_0; p, \omega)$ cannot contribute for any L^2 -normalizable wave packet $f(p, \omega)$ due to the Riemann-Lebesgue theorem.

for $\mathcal{C}_{\text{past}}$. We thus obtain as the correct Hartle-Hawking states:

$$\begin{aligned} {}_{HH+, \text{symm}}\langle B; \rho_0, t_0 | &= {}_{HH+, \text{symm}}\langle B; \rho_0, t_0 |' \widehat{P}_U \equiv {}_{HH+, \text{absorb}}\langle B; \rho_0, t_0 | , \\ {}_{HH-, \text{symm}}\langle B; \rho_0, t_0 | &= {}_{HH-, \text{symm}}\langle B; \rho_0, t_0 |' \widehat{P}_V \equiv {}_{HH-, \text{emitted}}\langle B; \rho_0, t_0 | , \end{aligned} \quad (8.73)$$

where the right-hand sides are already given in (8.69), (8.70).

Remarkably, this feature resembles much that of the S-branes discussed in [213]. Namely, it was shown there that

$$\text{half S-brane} \cong \text{full S-brane with the Hartle-Hawking contour} . \quad (8.74)$$

In our case, (7.36) corresponds to the full S-brane, while the Hartle-Hawking state (8.69) ((8.70)) is identifiable as the analogue of the half S-brane describing unstable D-brane decay (creation) process. The equalities (8.73) suggest that we have roughly identical relation to (8.74).

Notice that the parameters ρ_0, t_0 appear just as phase factors of boundary wave functions in (8.69), (8.70) contrary to (7.30), (7.32). Namely, the choice of parameters ρ_0, t_0 does not cause any physical difference for the Hartle-Hawking type states : They all can be regarded as describing the D0-brane moving from \mathcal{I}^- to \mathcal{H}^+ (from \mathcal{H}^- to \mathcal{I}^+) for (8.69) (for (8.70)) irrespective of ρ_0, t_0 . These two parameters merely parameterize displacing the trajectory in two-dimensional black hole background. Similar feature comes about for the full S-brane with Hartle-Hawking contour as well: It is equivalent to the half S-brane not depending on any shift of the origin (the point connecting the real and imaginary times).

Finally, we remark a comment from the viewpoints of boundary conformal field theory: in contrast to the original ones (7.30), (7.32) and (7.36), the Hartle-Hawking boundary states (8.73) (or equivalently (8.69), (8.70)) are not compatible with the reflection relations. One may regard the boundary states (7.30) and (7.32) as the ‘completions’ of the Hartle-Hawking states (8.73) so that they satisfy the reflection relations.

9 Conclusion and Discussions

In this thesis, we have examined the exact boundary states describing the rolling D-brane in the two-dimensional black hole system. In this final section, we would like to summarize our main results and discuss their physical relevance.

In the introduction, we asked three fundamental questions about the nature of the quantum gravity, or string theory as a candidate for the theory of everything:

- Small charge black hole v.s. large charge black hole.
- Analyticity v.s. non-analyticity in physical amplitudes.
- Unitarity v.s. open closed duality.

It would be natural to conclude this thesis by asking how far we can answer these questions after our studies on the rolling D-brane in two-dimensional black hole system. To answer these three fundamental questions, in this paper, we have constructed the exact boundary states describing the rolling D-brane in the two-dimensional black hole system (section 7) to probe the quantum geometry. Our main results are

- The tachyon - radion correspondence is proved for $k > 1$ by studying the closed string radiation rate from the α' exact rolling D-brane solution (section 8.1).
- The black hole - string transition is observed at $k = 1$ in the closed string radiation rate as a physical order parameter (section 8.3).
- The consistency between the unitarity and open closed duality is shown to be recovered after a careful treatment of the Wick rotation (section 8.2).

Although our model is rather a specific one, we can naturally extend our results to draw many universal features of the quantum gravity. In the rest of this section, we recapitulate our arguments and present some discussions with possible future directions to pursue.

First of all, we have shown in section 8 that the total emission rate of the rolling D-brane into the two-dimensional black hole system behaves exactly same as that for the rolling tachyon in flat Minkowski space studied in section 5. This result strongly suggests universal features of the physics associated with the D-brane decay.

The universality is an important concept in any physical system. In our decaying D-brane system, we have shown that the closed string radiation rate is independent of the free parameter k representing the level of the current algebra. Since $1/k$ correction governs the α' correction to the geometry, the physical quantity observed in the decaying D-brane process is independent of the stringy corrections. The classical tachyon - radion correspondence still holds even after introducing the stringy corrections independent of its strength (as long as $k > 1$).

Indeed, the universal behavior of the closed string radiation should be true from the following simple argument. The D-brane energy that should be released during the decay is always proportional to $1/g_s$, so in the perturbative string computation, we expect a divergence in the radiation rate: otherwise we have to face the missing energy problem.¹²⁴

¹²⁴At first sight, this viewpoint contradicts our computation that the higher dimensional D-brane shows a power-like *finite* emission rate (energy), but this is an artefact of the one-particle decay.

Furthermore the universality holds under almost every exactly solvable deformations of the model such as an inclusion of the time-like linear dilaton, electric field etc (see section 5,8). In [139], a similar computation has been performed in the AdS_3 space, supporting the universality of the decaying D-brane systems in yet another solvable background. We would like to emphasize again that our results do not depend on the level k which governs the strength of the world-sheet α' corrections *as long as* $k > 1$. This indeed provides a strong support for the tachyon-radion correspondence even at the quantum level.

At this point, it is worthwhile mentioning Sen's open-string completeness conjecture [224, 225, 127]: *There is a quantum open string theory (OSFT) that describes the full dynamics of an unstable Dp-brane without an explicit coupling to closed strings. Furthermore, Ehrenfest theorem holds in the weakly coupled OSFT; the classical results correctly describes the time evolution of the quantum expectation values.* The tachyon-radion correspondence directly results in the same conjecture for the rolling D-brane system. The smeared trajectory (or “moss” around the rolling D-brane) we observed in our rolling D-brane system with exact α' correction is an interesting twist to this conjecture.

Secondly, we have shown that the interplay between the analyticity and non-analyticity of the physical amplitudes are crucial to discuss the black hole - string phase transition. The integration over the radial momenta, which at the same time is crucial to prove the tachyon - radion correspondence, introduces the non-analyticity in the physical observables, resulting in the phase transition.

More precisely, we have directly observed the black hole - string phase transition from the exact boundary states for the probe rolling D-brane in the two-dimensional black hole background. The phase transition occurs exactly when the Hawking temperature of the two-dimensional black hole coincides with the Hagedorn temperature of the string background as we decrease the charge of the two-dimensional black hole (level of the current algebra). Below the phase transition point, the physical interpretations of the $SL(2; \mathbb{R})/U(1)$ coset model as a black hole geometry break down and become obscure. Our results show that the tachyon - radion correspondence fails at the phase transition point, and the physics associated with the D-brane decay changes drastically.

Indeed, as we have shown in section 8, a drastic change occurs when we study the dynamics of rolling D-branes in the two-dimensional black hole with $k < 1$. From the arguments given in section 4, we expect “black hole - string transition”. This transition is subtle even from the exact CFT analysis because in deriving every formulae in the closed string scattering amplitudes, we assume an analyticity in k . How can we probe the “black hole - string transition” with respect to k when the amplitude is analytic in k ? In the open string channel, k dependence is also analytic in the amplitudes as well. However, if we compute the physical quantities such as closed string emission rate, the non-analyticity with respect to k emerges. In this way, we have succeeded in probing the “black hole - string transition”, as an emergent phase transition, by studying the rolling D-brane dynamics in the background.

It would be interesting to note that not every D-brane can probe the “black hole - string transition”. As we have seen in section (5.2.5), the decay of the unstable D0-brane in the Euclidean two-dimensional black hole does *not* show any “black hole - string transition” at $k = 1$. The decay rate of unstable D-branes shows a universal property irrespective of the value of k . We do not have a good physical explanation of this phenomenon at this moment,

but it would be interesting to give a further study and determine which objects can probe the phase transition.

In the Euclidean signature target-space theory after the analytic continuation, the phase transition is induced from the non-perturbative α' corrections related to the winding-tachyon condensation. In the original Lorentzian signature target-space, one might understand it as a thermal (winding) tachyon condensation, or in the real time picture at the phase transition point, we would encounter associated (local) Hagedorn divergence of the black hole thermodynamics.

It is natural to expect that our results on the string - black hole phase transition is rather robust and universal. Indeed, the transition is barely affected under various marginal deformations of the solvable model such as incorporation of the linear dilaton or the electric field. It would be interesting to extend our analysis to more realistic higher dimensional black hole systems realized in superstring theory.¹²⁵

Philosophically, the concept of the phase in the quantum gravity is rather obscure. We know that in smaller dimensional field theories or in finite size theories, there is no notion of the phase transition. What happens, then, if the dimensionality or size of the universe fluctuate as is supposed to be the case with the quantum gravity?¹²⁶ Our study only touches a possible hidden nature of the phase transition as non-analytic behaviors of the physical quantities (not amplitudes themselves). It would be worth studying further the potential origins of the non-analyticity in physical quantities in more general situations.

So far, we have restricted ourselves to $g_s \rightarrow 0$ limit throughout this thesis, but finite g_s effects cannot be neglected in any realistic string theory. It is natural to assume that the finite g_s effect sets a cut-off for the emitted closed string energy because it cannot emit energy greater than the tension of the decaying D-brane $\sim 1/g_s$. Therefore, the emission rate roughly behaves as

$$\mathcal{N} \sim \int^{1/g_s} ddMN(M) \sqrt{\rho^{(c)}(M)} \quad (9.1)$$

with an explicit cut-off at $1/g_s$. This also means that the radial momentum p/\sqrt{k} should be less than $1/g_s$. Does this constraint smoothen out the phase transition? The saddle point approximation is not accurate as M becomes smaller, so we expect that the phase transition becomes smooth as we introduces g_s corrections. This is consistent with the statement that the “black hole - string transition” is actually a “black hole - string crossover”.

We have constructed several boundary states for the rolling D-branes in the two-dimensional black hole system. The failure of the uniqueness is physically relevant because in the time-dependent problems in string theory, the boundary conditions should be always imposed in accordance with the physics we are interested in. Mathematically, the different choices of the contour integration give rise to different physics. The tachyon - radion correspondence beautifully connects different solutions (contours) of the rolling tachyon with those for the rolling radion.

¹²⁵Recently, the black hole - string transition has been studied in the context of AdS_5/CFT_4 correspondence in [226].

¹²⁶A good example is the de-Sitter space, where the quantum gravity is supposed to consist of finite degrees of freedom.

For the absorbed D-brane boundary condition studied in section 7.2.2, the dominant infalling closed string radiation (at the Hagedorn temperature) accompanies the outgoing closed string radiation (at the Hawking temperature). The existence of the anomalously small outgoing radiation originates from the boundary condition imposed at the horizon. This reminds us of the closed string Hawking radiation discussed in section 2.4. Combining the discussion given in section 8.1.4, we can see that the origin of the thermal-like behaviour of the rolling D-brane radiation is closely related to the boundary condition imposed on the wavefunction (Ishibashi states). It would be interesting to make more precise the relation between the boundary conditions imposed on the string theory and the apparent anomaly as Hawking-like radiation.

Finally, we have discussed the consistency between the unitarity and the open-closed duality in the radiative process for the decay of unstable D-brane and rolling of accelerated D-brane dynamics in section 5.2 and 8.2 respectively. From “ab initio” derivation in the open string channel, both in Euclidean and Lorentzian world-sheet approaches, we have found heretofore overlooked contribution to the spectral amplitudes and observables. The contribution is fortuitously absent for decay of unstable D-brane, but is present for rolling of accelerated D-brane. We have shown that the contribution is imperative for ensuring unitarity and optical theorem.

Our notion of the unitarity is rather specific, so we have not discussed more fundamental questions e.g. about the unitarity of the quantum black hole systems associated with Hawking evaporation. The information paradox of the black hole system should be resolved within the context of the string theory if it is really a fundamental theory of everything.

These three questions raised in this thesis are basic but profound ones that people might first come up with when they would like to discuss the fundamental properties of the quantum gravity. We have attacked them from the concrete examples of the exactly solvable string black hole background. At this moment, we do not have complete answers to these questions in the tremendously huge string landscape, but we believe that our little step in the small corner will ultimately lead to their final answers.

Acknowledgements

The author would like to thank all my friends, my family, and my teachers for supporting him to write up this thesis. In particular the author would like to express his sincere thanks to his supervisor Tohru Eguchi for continuous encouragement and advice. Also he would like to express his special thanks to Soo-Jong Rey and Yuji Sugawara for the fruitful collaborations. The most of the main results in this thesis is based on the collaborations with them. He also acknowledges Sylvain Ribault and Yuji Tachikawa for stimulating discussions on the type 2 boundary states and a-theorem violation for generalized conifolds. This research is supported in part by JSPS Research Fellowships for Young Scientists.

A Appendices I: Conventions and Useful Formulae

A.1 conventions

world-sheet

In this thesis, we use $(-, +, +, \dots, +)$ conventions for target-space metric signature. For the world-sheet coordinate with Lorentzian signature, we use $-\infty < \tau < \infty$ and $0 \leq \sigma \leq 2\pi$ ($\sigma + 2\pi \simeq \sigma$). The light cone coordinate is defined as

$$\begin{cases} \sigma_+ = \sigma + \tau \\ \sigma_- = \sigma - \tau \end{cases} . \quad (\text{A.1})$$

We abbreviate their derivatives as $\partial_+ = \frac{\partial}{\partial \sigma_+}$ and $\partial_- = \frac{\partial}{\partial \sigma_-}$.

On the other hand, the complex coordinate on the complex plane is defined as

$$\begin{cases} z = x_1 + ix_2 \\ \bar{z} = x_1 - ix_2 \end{cases} \quad (\text{A.2})$$

We abbreviate their derivatives as $\partial = \frac{\partial}{\partial z}$ and $\bar{\partial} = \frac{\partial}{\partial \bar{z}}$. The integration measure is given by $dz^2 \equiv dx_1 dx_2$.

Throughout this thesis, we use the convention $\alpha' = l_s^2 = 2$ as long as otherwise stated. However, in several places, we explicitly write down α' for reader's convenience to compare our results with those in literatures, where different conventions are sometimes used.

theta functions with characteristic

$$\begin{aligned} \theta_0(\tau, v) &= \theta_4(\tau, v) = \prod_{m=1}^{\infty} (1 - q^m)(1 - zq^{m-1/2})(1 - z^{-1}q^{m-1/2}) \\ \theta_1(\tau, v) &= -2q^{1/4} \sin \pi v \prod_{m=1}^{\infty} (1 - q^m)(1 - zq^m)(1 - z^{-1}q^m) \\ \theta_2(\tau, v) &= 2q^{1/4} \cos \pi v \prod_{m=1}^{\infty} (1 - q^m)(1 + zq^m)(1 + z^{-1}q^m) \\ \theta_3(\tau, v) &= \prod_{m=1}^{\infty} (1 - q^m)(1 + zq^{m-1/2})(1 + z^{-1}q^{m-1/2}) \\ \eta(\tau) &= q^{1/24} \prod_{m=1}^{\infty} (1 - q^m) , \end{aligned} \quad (\text{A.3})$$

where $q = \exp(2\pi i\tau)$ and $z = \exp(2\pi iv)$. Their S -modular transformations are

$$\begin{aligned} \theta_0(-1/\tau, v/\tau) &= (-i\tau)^{1/2} \exp(\pi iv^2/\tau) \theta_2(\tau, v) \\ \theta_1(-1/\tau, v/\tau) &= -(-i\tau)^{1/2} \exp(\pi iv^2/\tau) \theta_1(\tau, v) \\ \theta_2(-1/\tau, v/\tau) &= (-i\tau)^{1/2} \exp(\pi iv^2/\tau) \theta_0(\tau, v) \\ \theta_3(-1/\tau, v/\tau) &= (-i\tau)^{1/2} \exp(\pi iv^2/\tau) \theta_3(\tau, v) \\ \eta(-1/\tau) &= (-i\tau)^{1/2} \eta(\tau) . \end{aligned} \quad (\text{A.4})$$

The theta functions satisfy the following Riemann quartic identity:

$$2 \prod_{a=1}^4 \theta_1(\tau, v'_a) = \prod_{a=1}^4 \theta_3(\tau, v_a) - \prod_{a=1}^4 \theta_2(\tau, v_a) - \prod_{a=1}^4 \theta_0(\tau, v_a) + \prod_{a=1}^4 \theta_1(\tau, v_a) , \quad (\text{A.5})$$

where

$$\begin{aligned} 2v'_1 &= v_1 + v_2 + v_3 + v_4 , & 2v'_2 &= v_1 + v_2 - v_3 - v_4 , \\ 2v'_3 &= v_1 - v_2 + v_3 - v_4 , & 2v'_4 &= v_1 - v_2 - v_3 + v_4 . \end{aligned} \quad (\text{A.6})$$

As a corollary, we obtain the abstruse identity of Jacobi:

$$\theta_0^4(\tau, v) + \theta_2^2(\tau, v) = \theta_1^2(\tau, v) + \theta_3^4(\tau, v) . \quad (\text{A.7})$$

Hypergeometric functions

Gauss's hypergeometric function is defined as

$$F(a_1, a_2; b; z) = {}_2F_1(a_1, a_2; b; z) = \sum_{l=0}^{\infty} \frac{(a_1)_l (a_2)_l}{(b)_l} \frac{z^l}{l!} , \quad (\text{A.8})$$

where

$$(a)_l \equiv \frac{\Gamma(a+l)}{\Gamma(a)} . \quad (\text{A.9})$$

The analytic continuation of the hypergeometric function is defined by

$$\begin{aligned} F(\alpha, \beta; \gamma; z) &= \frac{\Gamma(\gamma)\Gamma(\beta-\alpha)}{\Gamma(\beta)\Gamma(\gamma-\alpha)} (-z)^{-\alpha} F(\alpha, \alpha+1-\gamma; \alpha+1-\beta; 1/z) \\ &+ \frac{\Gamma(\gamma)\Gamma(\alpha-\beta)}{\Gamma(\alpha)\Gamma(\gamma-\beta)} (-z)^{-\beta} F(\beta, \beta+1-\gamma; \beta+1-\alpha; 1/z) , \end{aligned} \quad (\text{A.10})$$

$$\begin{aligned} F(\alpha, \beta; \gamma; z) &= \frac{\Gamma(\gamma)\Gamma(\gamma-\beta-\alpha)}{\Gamma(\gamma-\beta)\Gamma(\gamma-\alpha)} F(\alpha, \beta; \alpha+\beta+1-\gamma; 1-z) \\ &+ \frac{\Gamma(\gamma)\Gamma(\alpha+\beta-\gamma)}{\Gamma(\alpha)\Gamma(\beta)} (1-z)^{\gamma-\alpha-\beta} F(\gamma-\alpha, \gamma-\beta; 1+\gamma-\alpha-\beta; 1-z) \end{aligned} \quad (\text{A.11})$$

If $\gamma = \alpha + \beta + m$ with a certain integer m , the above formula should be modified due to the logarithmic singularity at $z = 1$. In a particular case ($m = 0$), which is interesting to us, the modified formula [227] reads

$$F(\alpha, \beta; \alpha + \beta; z) = \frac{\Gamma(\alpha + \beta)}{\Gamma(\alpha)\Gamma(\beta)} \sum_{n=0}^{\infty} \frac{a_{(n)} b_{(n)}}{(n!)^2} [h_n'' - \log(1-z)] (1-z)^n , \quad (\text{A.12})$$

where $h_n'' = 2\psi(n+1) - \psi(\alpha+n) - \psi(\beta+n)$ with $\psi(z) \equiv \frac{\Gamma'(z)}{\Gamma(z)}$.

We also introduce the generalized hypergeometric function

$${}_3F_2(a_1, a_2, a_3; b_1, b_2; z) = \sum_{l=0}^{\infty} \frac{(a_1)_l (a_2)_l (a_3)_l}{(b_1)_l (b_2)_l} \frac{z^l}{l!}, \quad (\text{A.13})$$

whose asymptotic expansion (as $z \rightarrow \infty$) is given by

$$\begin{aligned} & {}_3F_2(a_1, a_2, a_3; b_1, b_2; z) \\ &= \frac{\Gamma(b_1)\Gamma(b_2)}{\Gamma(a_1)\Gamma(a_2)\Gamma(a_3)} \sum_{k=1}^3 \frac{\Gamma(a_k) \prod_{j=1; j \neq k}^3 (a_j - a_k)}{\prod_{j=1}^2 \Gamma(b_j - a_k)} (-z)^{-a_k} [1 + O(z^{-1})]. \end{aligned} \quad (\text{A.14})$$

A.2 $SL(2; \mathbb{R})$ current algebra

We will collect useful facts about the $SL(2; \mathbb{R})$ current algebra and fix our notations. We begin with the zero mode. Our conventions for the commutation relations of the $SL(2; \mathbb{R})$ algebra are

$$[J^1, J^2] = -iJ^3, [J^2, J^3] = iJ^1, [J^3, J^1] = iJ^2. \quad (\text{A.15})$$

We will also introduce

$$J^{\pm} = J^1 \pm iJ^2, \quad (\text{A.16})$$

which gives

$$[J^3, J^{\pm}] = \pm J^{\pm}, [J^+, J^-] = -2J^3. \quad (\text{A.17})$$

The quadratic Casimir is defined as

$$C_2 = (J^1)^2 + (J^2)^2 - (J^3)^2 \equiv -j(j-1). \quad (\text{A.18})$$

We summarize the unitary (irreducible) representations of the $SL(2; \mathbb{R})$ algebra parametrized by j

1. Principal discrete representations (highest or lowest weight states): they contain the state that is annihilated by J^+ or J^- respectively. Their modules are generated as

$$D^+ = \{|j; m\rangle : m = -j, -j+1, -j+2, \dots\}, \quad (\text{A.19})$$

and

$$D^- = \{|j; m\rangle : m = j, j-1, j-2, \dots\}, \quad (\text{A.20})$$

obtained by acting J^- or J^+ on the highest or lowest weight state. The representation is unitary when $j \leq -\frac{1}{2}$.

2. Principal continuous series: they are realized by

$$C_j^\alpha = \{|j, \alpha; m\rangle : m = \alpha, \alpha \pm 1, \alpha \pm 2, \dots\} \quad (\text{A.21})$$

where $J^3|j, \alpha; m\rangle = m|j, \alpha; m\rangle$. Without loss of generality, we take $0 \leq \alpha < 1$. The representation is unitary when $j = -1/2 + is$ with $s \in \mathbb{R}^+$.

3. Complementary representations: similar to the continuous series but with real j . They are unitary when $-1 < j < -1/2$ and $-j - 1/2 < |\alpha - 1/2|$.

4. Identity representation: this is the trivial representation with $j = -1$.

Let us move to the affine current algebra $\widehat{SL}(2; \mathbb{R})$. The relevant OPEs are

$$\begin{cases} j^3(z)j^3(0) \sim -\frac{\kappa}{2z^2} \\ j^3(z)j^\pm(0) \sim \pm\frac{1}{z}j^\pm(0) \\ j^+(z)j^-(0) \sim \frac{\kappa}{z^2} - \frac{2}{z}j^3(0) \end{cases} . \quad (\text{A.22})$$

Corresponding affine Lie algebra is given by

$$\begin{aligned} [J_n^3, J_m^3] &= -\frac{k}{2}n\delta_{m,-n} , \\ [J_n^3, J_m^\pm] &= \pm J_{n+m}^\pm , \\ [J_n^+, J_m^-] &= -2J_{n+m}^3 + kn\delta_{m,-n} . \end{aligned} \quad (\text{A.23})$$

The energy momentum tensor is given by the Sugawara form:

$$T(z) = \frac{1}{\kappa - 2}(j^1j^1 + j^2j^2 - j^3j^3)(z) \quad (\text{A.24})$$

with the central charge $c = 3 + \frac{6}{\kappa - 2}$.

We summarize the characters of the unitary representations of $\widehat{SL}(2; \mathbb{R})$ current algebra. The character is defined as $\text{Tr} q^{L_0} y^{J_0^3}$ with $q \equiv e^{2\pi i\tau}$, $y \equiv e^{2\pi iu}$.

1. Principal discrete representations (highest or lowest weight states): the characters can be written as

$$\chi_j^\pm(\tau, u) = \pm i \frac{q^{-\frac{1}{\kappa-2}(j-\frac{1}{2})^2} y^{\pm(j-\frac{1}{2})}}{\theta_1(\tau, u)} . \quad (\text{A.25})$$

2. Principal continuous series: the character is given by

$$\chi_{s,\alpha}(\tau, u) = \frac{q^{\frac{s^2}{\kappa-2}}}{\eta(\tau)^3} \sum_{n \in \mathbb{Z}} y^{n+\alpha} . \quad (\text{A.26})$$

3. Complementary representations: the character is given by

$$\chi_{j,\alpha}(\tau, u) = \frac{q^{\frac{(j-\frac{1}{2})^2}{\kappa-2}}}{\eta(\tau)^3} \sum_{n \in \mathbb{Z}} y^{n+\alpha} . \quad (\text{A.27})$$

4. Identity representation: the character is given by

$$\chi_0(\tau, u) = i \frac{q^{-\frac{1}{4(\kappa-2)}} y^{-1/2} (1-y)}{\theta_1(\tau, u)} . \quad (\text{A.28})$$

It is possible to construct more general representations of the current algebra by using (n -units of) the spectral flows

$$j_m^3 \rightarrow j_m^3 - \frac{\kappa}{2} n \delta_{m,0} , \quad j_m^\pm \rightarrow j_{m \pm n}^\pm , \quad L_m \rightarrow L_m + n j_m^3 - \frac{\kappa}{4} n^2 \delta_{m,0} . \quad (\text{A.29})$$

Unlike in the case of the compact group, we actually obtain new representations, but their conformal dimensions are typically unbounded below.

A.3 Coordinate on $SL(2; \mathbb{R})$

The Euler angle parametrization $g(r, t, \phi) \in SL(2; \mathbb{R})$ suitable for the Euclidean coset is given by

$$e^{i\sigma_1 \frac{t-\phi}{2}} e^{r\sigma_2} e^{i\sigma_1 \frac{t+\phi}{2}} = \begin{pmatrix} \cos t \cosh r - \sin \phi \sinh r & \cosh r \sin t + \cos \phi \sinh r \\ -\cosh r \sin t + \cos \phi \sinh r & \cos t \cosh r + \sin \phi \sinh r \end{pmatrix} , \quad (\text{A.30})$$

where $0 < t \leq 2\pi$, $0 \leq r$ and $0 < \phi \leq 2\pi$ for the single cover of $SL(2; \mathbb{R})$.

On the other hand, for the Lorentzian coset, a useful Euler angle parametrization $g(r, t_L, t_R)$ is given by

$$e^{\sigma_3 t_L} e^{r\sigma_2} e^{\sigma_3 t_R} = \begin{pmatrix} e^{t_L+t_R} \cosh r & e^{t_L-t_R} \sinh r \\ e^{-t_L+t_R} \sinh r & e^{-t_L-t_R} \cosh r \end{pmatrix} , \quad (\text{A.31})$$

where t_L and t_R are noncompact.¹²⁷

To connect it with the AdS_3 space, it is customary to introduce the parametrization

$$g = \begin{pmatrix} x^0 + x^2 & x^1 + x^3 \\ x^1 - x^3 & x^0 - x^2 \end{pmatrix} \quad (\text{A.32})$$

so that we can see the $SL(2; \mathbb{R})$ group as a hyperbola

$$(x^0)^2 - (x^1)^2 - (x^2)^2 + (x^3)^2 = 0 \quad (\text{A.33})$$

embedded in Minkowski space (x^0, x^1, x^2, x^3) with signature $(-, +, +, -)$.

¹²⁷The parametrization does *not* cover the whole $SL(2; \mathbb{R})$ manifold.

A.4 Frequently used formulae

$$\Gamma(z+1) = z\Gamma(z) . \quad (\text{A.34})$$

$$\Gamma(z)\Gamma(1-z) = \frac{\pi}{\sin \pi z} . \quad (\text{A.35})$$

$$\Gamma\left(\frac{1}{2} + z\right)\Gamma\left(\frac{1}{2} - z\right) = \frac{\pi}{\cos \pi z} . \quad (\text{A.36})$$

$$\Gamma(2z) = (2\pi)^{-1/2} 2^{2z-1/2} \Gamma(z)\Gamma(z+1/2) . \quad (\text{A.37})$$

$$\int_0^\infty dx \frac{x^c}{\sqrt{x^2+a^2}} = \frac{a^c \Gamma(-\frac{c}{2}) \Gamma(\frac{1+c}{2})}{2\sqrt{\pi}} . \quad (\text{A.38})$$

$$\int_{-\frac{\pi}{2}}^{\frac{\pi}{2}} (2 \cos \theta)^{a-1} e^{ib\theta} d\theta = \pi \frac{\Gamma(a)}{\Gamma\left(\frac{1}{2} + \frac{a+b}{2}\right) \Gamma\left(\frac{1}{2} + \frac{a-b}{2}\right)} , \quad (\text{Re } a > 0 , \quad |\text{Re } b| < \text{Re } a + 1) , \quad (\text{A.39})$$

$$\int_{-\infty}^{\infty} (2 \cosh t)^{a-1} e^{ibt} dt = \frac{1}{2} B\left(\frac{1}{2} - \frac{a+ib}{2}, \frac{1}{2} - \frac{a-ib}{2}\right) \equiv \frac{1}{2} \frac{\Gamma\left(\frac{1}{2} - \frac{a+ib}{2}\right) \Gamma\left(\frac{1}{2} - \frac{a-ib}{2}\right)}{\Gamma(1-a)} ,$$

$$(\text{Re } a < 1 , \quad |\text{Im } b| < 1 - \text{Re } a) . \quad (\text{A.40})$$

The integral (A.40) follows from the more general formula:

$$\int_0^\infty \frac{\cosh(2at)}{\cosh^{2\beta}(pt)} dt = 4^{\beta-1} p^{-1} B\left(\beta + \frac{a}{p}, \beta - \frac{a}{p}\right) , \quad (p > 0, \quad \text{Re}\left(\beta \pm \frac{a}{p}\right) > 0) , \quad (\text{A.41})$$

given in [227].

A.5 Proof of (6.30) and (6.40)

Here we would like to evaluate explicitly the integral (6.30) for any ρ_0 (strictly speaking, we need to assume $\sinh \rho_0 > 1$). We begin with series expansion of the hypergeometric function in $\phi_n^p(\rho, \theta)$:

$$F\left(\frac{1}{2} + \frac{ip+n}{2}, \frac{1}{2} + \frac{ip-n}{2}; ip+1; -\frac{\cos^2 \theta}{\sinh^2 \rho_0}\right)$$

$$= \sum_{\ell=0}^{\infty} \frac{\Gamma(ip+1)}{\Gamma\left(\frac{1}{2} + \frac{ip+n}{2}\right) \Gamma\left(\frac{1}{2} + \frac{ip-n}{2}\right)} \frac{\Gamma\left(\frac{1}{2} + \frac{ip+n}{2} + \ell\right) \Gamma\left(\frac{1}{2} + \frac{ip-n}{2} + \ell\right)}{\Gamma(ip+1+\ell)} \frac{(-1)^\ell}{\ell!} \left(\frac{\cos \theta}{\sinh \rho_0}\right)^{2\ell} . \quad (\text{A.42})$$

Using the formula (A.39), we can perform, in the ℓ -th sector, the integral (6.30) as

$$\Psi_\ell = g(\ell) \int_{-\frac{\pi}{2}}^{\frac{\pi}{2}} d\theta e^{in\theta} (\cos \theta)^{ip-1+2\ell} = \frac{g(\ell)}{2^{ip-1+2\ell}} \cdot \frac{\pi \Gamma(ip-1+2\ell+1)}{\Gamma\left(\frac{1}{2} + \ell + \frac{ip+n}{2}\right) \Gamma\left(\frac{1}{2} + \ell + \frac{ip-n}{2}\right)} ,$$

where $g(\ell)$ refers to

$$g(\ell) = \frac{(-1)^\ell}{\ell!} (\sinh \rho_0)^{-ip-2\ell} \frac{\Gamma(ip+1)}{\Gamma(\frac{1}{2} + \frac{ip+n}{2})\Gamma(\frac{1}{2} + \frac{ip-n}{2})} \frac{\Gamma(\frac{1}{2} + \frac{ip+n}{2} + \ell)\Gamma(\frac{1}{2} + \frac{ip-n}{2} + \ell)}{\Gamma(ip+1+\ell)}. \quad (\text{A.43})$$

Then the total integral (6.30) is

$$\sum_{\ell=0}^{\infty} \Psi_\ell = \frac{\pi}{2^{ip-1} (\sinh \rho_0)^{ip}} \frac{\Gamma(ip+1)}{\Gamma(\frac{1}{2} + \frac{ip+n}{2})\Gamma(\frac{1}{2} + \frac{ip-n}{2})} \sum_{\ell=0}^{\infty} \frac{(-1)^\ell}{\ell!} \frac{1}{2^{2\ell} (\sinh \rho_0)^{2\ell}} \frac{\Gamma(ip+2\ell)}{\Gamma(ip+1+\ell)}. \quad (\text{A.44})$$

We can rewrite the summation into a hypergeometric function by using

$$\Gamma(ip+2\ell) = \frac{2^{ip-1+2\ell}}{\sqrt{\pi}} \Gamma\left(\frac{ip}{2} + \ell\right) \Gamma\left(\frac{1}{2} + \frac{ip}{2} + \ell\right). \quad (\text{A.45})$$

and then obtain

$$\sum_{\ell=0}^{\infty} \Psi_\ell = \frac{\sqrt{\pi}}{(\sinh \rho_0)^{ip}} \frac{\Gamma(\frac{ip}{2})\Gamma(\frac{1}{2} + \frac{ip}{2})}{\Gamma(\frac{1}{2} + \frac{ip+n}{2})\Gamma(\frac{1}{2} + \frac{ip-n}{2})} F\left(\frac{ip}{2}, \frac{1}{2} + \frac{ip}{2}; ip+1; -\frac{1}{\sinh^2 \rho_0}\right). \quad (\text{A.46})$$

Making use of the formula

$$F\left(2\alpha, 2\beta; \alpha + \beta + \frac{1}{2}; z\right) = F\left(\alpha, \beta; \alpha + \beta + \frac{1}{2}; 4z(1-z)\right). \quad (\text{A.47})$$

$$|z| < \frac{1}{2}, \quad |z(1-z)| < \frac{1}{4}$$

we find that

$$\sum_{\ell=0}^{\infty} \Psi_\ell = \frac{\sqrt{\pi}}{(\sinh \rho_0)^{ip}} \frac{\Gamma(\frac{ip}{2})\Gamma(\frac{1}{2} + \frac{ip}{2})}{\Gamma(\frac{1}{2} + \frac{ip+n}{2})\Gamma(\frac{1}{2} + \frac{ip-n}{2})} F\left(ip, ip+1, ip+1; \frac{1}{2} - \frac{\cosh \rho_0}{2 \sinh \rho_0}\right). \quad (\text{A.48})$$

Note that the second and third arguments of the hypergeometric function are the same. The function is thus simplified as

$$F\left(ip, ip+1, ip+1; \frac{1}{2} - \frac{\cosh \rho_0}{2 \sinh \rho_0}\right) = \left(\frac{\sinh \rho_0 + \cosh \rho_0}{2 \sinh \rho_0}\right)^{-ip} = (2e^{-\rho_0} \sinh \rho_0)^{ip}, \quad (\text{A.49})$$

because of the relation

$$(1-z)^\alpha = F(-\alpha, \beta; \beta; z). \quad (\text{A.50})$$

In this way, we finally obtain

$$\sum_{\ell=0}^{\infty} \Psi_\ell = \sqrt{\pi} e^{-ip\rho_0} 2^{ip} \frac{\Gamma(\frac{ip}{2})\Gamma(\frac{1}{2} + \frac{ip}{2})}{\Gamma(\frac{1}{2} + \frac{ip+n}{2})\Gamma(\frac{1}{2} + \frac{ip-n}{2})} = \frac{2\pi \Gamma(ip)}{\Gamma(\frac{1}{2} + \frac{ip+n}{2})\Gamma(\frac{1}{2} + \frac{ip-n}{2})} e^{-ip\rho_0}, \quad (\text{A.51})$$

and this is the desired formula.

In a quite similar manner, we can prove (6.40). We begin with series expansion of the hypergeometric function in $\phi_{pw}(\rho, \theta)$:

$$\begin{aligned} & F\left(\frac{1}{2} + \frac{ip+kw}{2}, \frac{1}{2} + \frac{ip-kw}{2}; ip+1; \frac{\cos^2 \theta}{\cosh^2 r_0}\right) \\ &= \sum_{\ell=0}^{\infty} \frac{\Gamma(ip+1)}{\Gamma(\frac{1}{2} + \frac{ip+kw}{2})\Gamma(\frac{1}{2} + \frac{ip-kw}{2})} \frac{\Gamma(\frac{1}{2} + \frac{ip+kw}{2} + \ell)\Gamma(\frac{1}{2} + \frac{ip-kw}{2} + \ell)}{\Gamma(ip+1+\ell)} \frac{1}{\ell!} \left(\frac{\cos \theta}{\cosh r_0}\right)^{2\ell}. \end{aligned} \quad (\text{A.52})$$

Using the formula (A.39), we can perform, in the ℓ -th sector, the integral (6.30) as

$$\Psi_{\ell} = g(\ell) \int_{-\frac{\pi}{2}}^{\frac{\pi}{2}} d\theta e^{ikw\theta} (\cos \theta)^{ip-1+2\ell} = \frac{g(\ell)}{2^{ip-1+2\ell}} \cdot \frac{\pi \Gamma(ip-1+2\ell+1)}{\Gamma(\frac{1}{2} + \ell + \frac{ip+kw}{2})\Gamma(\frac{1}{2} + \ell + \frac{ip-kw}{2})},$$

where $g(\ell)$ refers to

$$g(\ell) = \frac{1}{\ell!} (\cosh r_0)^{-ip-2\ell} \frac{\Gamma(ip+1)}{\Gamma(\frac{1}{2} + \frac{ip+kw}{2})\Gamma(\frac{1}{2} + \frac{ip-kw}{2})} \frac{\Gamma(\frac{1}{2} + \frac{ip+kw}{2} + \ell)\Gamma(\frac{1}{2} + \frac{ip-kw}{2} + \ell)}{\Gamma(ip+1+\ell)}. \quad (\text{A.53})$$

Then the total integral (6.30) is

$$\sum_{\ell=0}^{\infty} \Psi_{\ell} = \frac{\pi}{2^{ip-1} (\cosh r_0)^{ip}} \frac{\Gamma(ip+1)}{\Gamma(\frac{1}{2} + \frac{ip+kw}{2})\Gamma(\frac{1}{2} + \frac{ip-kw}{2})} \sum_{\ell=0}^{\infty} \frac{1}{\ell!} \frac{1}{2^{2\ell} (\cosh r_0)^{2\ell}} \frac{\Gamma(ip+2\ell)}{\Gamma(ip+1+\ell)}. \quad (\text{A.54})$$

We can rewrite the summation into a hypergeometric function by using

$$\Gamma(ip+2\ell) = \frac{2^{ip-1+2\ell}}{\sqrt{\pi}} \Gamma\left(\frac{ip}{2} + \ell\right) \Gamma\left(\frac{1}{2} + \frac{ip}{2} + \ell\right). \quad (\text{A.55})$$

and then obtain

$$\sum_{\ell=0}^{\infty} \Psi_{\ell} = \frac{\sqrt{\pi}}{(\cosh r_0)^{ip}} \frac{\Gamma(\frac{ip}{2})\Gamma(\frac{1}{2} + \frac{ip}{2})}{\Gamma(\frac{1}{2} + \frac{ip+kw}{2})\Gamma(\frac{1}{2} + \frac{ip-kw}{2})} F\left(\frac{ip}{2}, \frac{1}{2} + \frac{ip}{2}; ip+1; \frac{1}{\cosh^2 r_0}\right). \quad (\text{A.56})$$

Making use of the formula

$$\begin{aligned} F\left(2\alpha, 2\beta; \alpha + \beta + \frac{1}{2}; z\right) &= F\left(\alpha, \beta; \alpha + \beta + \frac{1}{2}; 4z(1-z)\right). \\ &|z| < \frac{1}{2}, \quad |z(1-z)| < \frac{1}{4} \end{aligned} \quad (\text{A.57})$$

we find that

$$\sum_{\ell=0}^{\infty} \Psi_{\ell} = \frac{\sqrt{\pi}}{(\sinh r_0)^{ip}} \frac{\Gamma(\frac{ip}{2})\Gamma(\frac{1}{2} + \frac{ip}{2})}{\Gamma(\frac{1}{2} + \frac{ip+n}{2})\Gamma(\frac{1}{2} + \frac{ip-n}{2})} F\left(ip, ip+1, ip+1; \frac{1}{2}(1 - \tanh r_0)\right). \quad (\text{A.58})$$

Note that the second and third arguments of the hypergeometric function are the same. The function is thus simplified as

$$F\left(ip, ip+1, ip+1; \frac{1}{2}(1 - \tanh r_0)\right) = (2e^{-r_0} \cosh r_0)^{ip}, \quad (\text{A.59})$$

because of the relation

$$(1-z)^\alpha = F(-\alpha, \beta; \beta; z) . \quad (\text{A.60})$$

In this way, we finally obtain

$$\sum_{\ell=0}^{\infty} \Psi_\ell = \sqrt{\pi} e^{-ipr_0} 2^{ip} \frac{\Gamma(\frac{ip}{2}) \Gamma(\frac{1}{2} + \frac{ip}{2})}{\Gamma(\frac{1}{2} + \frac{ip+kw}{2}) \Gamma(\frac{1}{2} + \frac{ip-kw}{2})} = \frac{2\pi \Gamma(ip)}{\Gamma(\frac{1}{2} + \frac{ip+kw}{2}) \Gamma(\frac{1}{2} + \frac{ip-kw}{2})} e^{-ipr_0} , \quad (\text{A.61})$$

and this is the desired formula.

B Appendix II: Miscellaneous Topics

B.1 Partition functions

The modular invariant torus partition function is of critical importance in closed string theory to read the spectrum of a given background. In this appendix, we collect partition functions of several CFTs that are relevant for our discussions.

Our main focus is the partition function for the Lorentzian two-dimensional black hole. The partition function for the two-dimensional black hole, however, suffers some subtleties because of the Lorentzian signature of the target space and the divergence coming from the non-compact target space.

With these subtleties in mind, our starting point is the (twisted) partition function for the \mathbb{H}_3^+ model. For a time-being, we restrict ourselves to the bosonic CFT. Since the Euclidean action is bounded, the direct path integral computation is possible [228, 229]. For the vector gauging

$$Z_{(V)}^{\mathbb{H}_3^+}(\tau, u) \equiv \int dg e^{-kS_{(V)}^{\mathbb{H}_3^+}(g, h^u, h^{u^\dagger})} = \frac{e^{\frac{u_2^2}{\tau_2}}}{\sqrt{\tau_2} |\theta_1(\tau, u)|^2} . \quad (\text{B.62})$$

For the axial gauging

$$Z_{(A)}^{\mathbb{H}_3^+}(\tau, u) \equiv \int dg e^{-kS_{(A)}^{\mathbb{H}_3^+}(g, h^u, h^{u^\dagger})} = \frac{e^{\frac{u_2^2}{\tau_2} - \pi k \frac{|u|^2}{\tau_2}}}{\sqrt{\tau_2} |\theta_1(\tau, u)|^2} . \quad (\text{B.63})$$

In the $u \rightarrow 0$ limit, both expressions coincide and (formally) modular invariant.¹²⁸

The partition function for the Euclidean two-dimensional black hole from the axial coset of the \mathbb{H}_+^3 model (denoted by $\mathbb{H}_+^{3(A)}/\mathbb{R}$) is

$$Z_{\mathbb{H}_+^{3(A)}/\mathbb{R}} = \int_{\Sigma} \frac{du^2}{\tau_2} \frac{e^{\frac{u_2^2}{\tau_2}}}{\sqrt{\tau_2} |\theta_1(\tau, u)|^2} \sqrt{\tau_2} |\eta(\tau)|^2 \sum_{m, \omega \in \mathbb{Z}} e^{-\frac{\pi k}{\tau_2} |\omega\tau - m + u|^2} , \quad (\text{B.64})$$

¹²⁸Because of the divergence as $u \rightarrow 0$, these expressions contain rather poor information to read the spectrum (e.g. the partition function is k independent). Actually, the resurrection of the k dependence is one of the key issues to extract contributions from the discrete states and give the improved unitarity bound. In order to do this, we should actually know the central charge of the model independently since the torus partition function does not know *a priori* the shift of the central charge coming from the linear dilaton coupled to the curvature of the world-sheet.

where the integration is over the Jacobian torus $\int_0^1 ds_1 \int_0^1 ds_2$ with $u = s_1\tau - s_2$. The appearance of the (twisted) partition of the compactified boson (with radius $R^2 = k$)

$$Z_{\sqrt{k}}(\tau, u) = \sqrt{\tau_2} |\eta(\tau)|^2 \sum_{m, \omega \in \mathbb{Z}} e^{-\frac{\pi k}{\tau_2} |\omega\tau - m + u|^2} \quad (\text{B.65})$$

suggests an asymptotic geometry of the cigar (with the same radius). Note that the summation over m, ω can be combined into

$$Z_{\mathbb{H}_+^{3(A)}/\mathbb{R}} = \int_{\mathbb{R}^2} \frac{du^2}{\tau_2} \frac{e^{\frac{u^2}{\tau_2} - \frac{\pi k}{\tau_2} |u|^2}}{\sqrt{\tau_2} |\theta_1(\tau, u)|^2} \sqrt{\tau_2} |\eta(\tau)|^2. \quad (\text{B.66})$$

Due to the fact that $\mathbb{H}_+^{3(A)}/\mathbb{R} = SL(2; \mathbb{R})^{(A)}/U(1)$, one can interpret (B.64) as the partition function of the $SL(2; \mathbb{R})^{(A)}/U(1)$ axial coset model.¹²⁹

The partition function for the Lorentzian coset is rather subtle, and we should resort to analytic continuations. Instead of gauging compact subgroup generated by J^3 , we gauge the noncompact subgroup generated by J^2 . Effectively, we can Wick rotate $J^3 \rightarrow iJ^3$. The axially J^2 twisted partition function for (the universal cover of) $SL(2; \mathbb{R})_{(\infty)}^{(A)}$ could be obtained from the analytic continuation ($u \rightarrow iv$) as

$$Z_{(A)}^{SL(2; \mathbb{R})}(\tau, v) \equiv \int dg e^{-k S_{(V)}^{H_3^+}(g, h^v, h^{v\dagger})} = \frac{e^{\frac{v^2}{\tau_2}}}{\sqrt{\tau_2} |\theta_1(\tau, v)|^2}. \quad (\text{B.67})$$

The partition function for the Lorentzian two-dimensional black hole (after an analytic continuation) could be written as

$$Z_{\mathbb{H}_+^{3(A)}/\mathbb{R}} = \int_{\mathbb{R}^2} \frac{dv^2}{\tau_2} \frac{e^{\frac{v^2}{\tau_2} - \frac{\pi k}{\tau_2} |v|^2}}{\sqrt{\tau_2} |\theta_1(\tau, iv)|^2} \sqrt{\tau_2} |\eta(\tau)|^2, \quad (\text{B.68})$$

which agrees with the proposal made in [230] from a different perspective.

¹²⁹In the Euclidean axial coset model, there is no distinction between the single cover of $SL(2; \mathbb{R})$ and the universal cover of the $SL(2; \mathbb{R})$.

B.2 T-duality and Buscher's rule

We summarize Buscher's rule [231, 232] for T-duality:

$$\begin{aligned}
\tilde{G}_{00} &= \frac{1}{G_{00}} \\
\tilde{G}_{0i} &= \frac{B_{0i}}{G_{00}} \\
\tilde{B}_{0i} &= \frac{G_{0i}}{G_{00}} \\
\tilde{G}_{ij} &= G_{ij} - \frac{G_{0i}G_{0j} - B_{0i}B_{0j}}{G_{00}} \\
\tilde{B}_{ij} &= B_{ij} - \frac{G_{0i}B_{0j} - B_{0i}G_{0j}}{G_{00}} \\
\tilde{\Phi} &= \Phi - \frac{1}{4} \log \left(\frac{G_{00}}{\tilde{G}_{00}} \right) ,
\end{aligned} \tag{B.69}$$

where 0 is the direction to be T-dualized.

B.3 $\mathcal{N} = 2$ superconformal algebra and spectral flow

OPEs for the $\mathcal{N} = 2$ SCA are summarized as

$$\begin{aligned}
T(z)T(0) &\sim \frac{c}{2z^4} + \frac{2}{z^2}T(0) + \frac{1}{z}\partial T(0) \\
T(z)G^\pm(0) &\sim \frac{3}{2z^2}G^\pm(0) + \frac{1}{z}\partial G^\pm(0) \\
T(z)J(0) &\sim \frac{1}{z^2}J(0) + \frac{1}{z}\partial J(0) \\
G^+(z)G^-(0) &\sim \frac{2c}{3z^3} + \frac{2}{z^2}J(0) + \frac{2}{z}T(0) + \frac{1}{z}\partial J(0) \\
G^\pm(z)G^\pm(0) &\sim 0 \\
J(z)G^\pm(0) &\sim \pm G^\pm(0) \\
J(z)J(0) &\sim \frac{c}{3z^2} .
\end{aligned} \tag{B.70}$$

Correspondingly the mode expansion yields

$$\begin{aligned}
[L_m, L_n] &= (m-n)L_{m+n} + \frac{c}{12}(m^3 - m)\delta_{m,-n} \\
[L_m, G_r^\pm] &= \left(\frac{m}{2} - r\right) G_{m+r}^\pm \\
[L_m, J_n] &= -nJ_{m+n} \\
\{G_r^+, G_s^-\} &= 2L_{r+s} + (r-s)J_{r+s} + \frac{c}{3}\left(r^2 - \frac{1}{4}\right)\delta_{r,-s} \\
\{G_r^\pm, G_s^\pm\} &= 0 \\
[J_n, G_r^\pm] &= \pm G_{r+n}^\pm \\
[J_m, J_n] &= \frac{c}{3}m\delta_{m,-n} \ ,
\end{aligned} \tag{B.71}$$

where r, s are integers for the R-sector and half-integers for the NS-sector. The $\mathcal{N} = 2$ superconformal algebra admits an isomorphism known as spectral flow:

$$\begin{aligned}
U_\eta L_m U_\eta^{-1} &\rightarrow L_m + \eta J_m + \frac{\eta^2 c}{6} \delta_{m,0} \\
U_\eta G_m^\pm U_\eta^{-1} &\rightarrow G_{m \pm \eta}^\pm \\
U_\eta J_m U_\eta^{-1} &\rightarrow J_m + \frac{\eta}{3} \delta_{m,0} \ .
\end{aligned} \tag{B.72}$$

The explicit form of the unitary operator U_η can be obtained by

$$U_\eta = e^{-i\sqrt{\frac{c}{3}}\eta\phi} \ , \tag{B.73}$$

where

$$J = i\sqrt{\frac{c}{3}}\partial\phi \ . \tag{B.74}$$

B.4 Lichnerowicz obstruction and a -theorem

In this appendix, we show that an apparent violation of the a -theorem for the gauge theory living on the D3-brane at the tip of the Brieskorn-Pham singularities are avoided by the Lichnerowicz obstruction we reviewed in section 2.2.3. Let us consider the Brieskorn-Pham type generalized conifolds

$$x_1^{k_1} + x_2^{k_2} + k_3^{k_3} + k_4^{k_4} = 0 \ . \tag{B.75}$$

Assuming that the Reeb vector (conformal $U(1)_R$ charge) is given by the natural \mathbb{C}^* action induced by the charge vector $(1/k_1, 1/k_2, 1/k_3, 1/k_4)$ on (x_1, x_2, x_3, x_4) , the volume of the associated Sasaki-Einstein manifold can be computed as

$$V = \frac{\pi^3 k_1 k_2 k_3 k_4 \left(\frac{1}{k_1} + \frac{1}{k_2} + \frac{1}{k_3} + \frac{1}{k_4} - 1\right)^3}{27} \ . \tag{B.76}$$

The conjectured a -theorem states that a , which is inversely proportional to V via $AdS-CFT$ correspondence, should be an decreasing function as we decrease k_i as a relevant deformation. The condition is equivalent to

$$-\frac{2}{k_1} + \frac{1}{k_2} + \frac{1}{k_3} + \frac{1}{k_4} \leq 1, \quad (\text{B.77})$$

for k_1 , and similarly for k_2 , k_3 and k_4 .

On the other hand, the Lichnerowicz obstruction applied for the generalized conifold is

$$\sum_i \frac{1}{k_i} \leq 1 + 3\omega_m, \quad (\text{B.78})$$

where ω_m is a charge of holomorphic functions on (B.4). As a holomorphic function, we choose a monomial x_i that has a charge $1/k_i$. Then the Lichnerowicz obstruction (B.78) directly yields the necessary and sufficient condition for the conjectured a -theorem (B.77). Physically speaking, this suggests that the unitarity of the SCFT is crucial for the establishment of the a -theorem as is the case with the two-dimensional c -theorem, where the unitarity is imperative for its proof.

B.5 Boundary wavefunction from direct integration

We would like to compute the boundary wavefunction for the rolling D-brane in the Lorentzian two-dimensional black hole from the direct integration, which was not carried out in [1].

We focus on the overlap between the minisuperspace wavefunction

$$U_\omega^p(\rho, t) = -\frac{\Gamma^2(\nu_+)}{\Gamma(1-i\omega)\Gamma(-ip)} e^{-i\omega t} (\sinh \rho)^{-i\omega} F(\nu_+, \nu_-^*; 1-i\omega; -\sinh^2 \rho), \quad (\text{B.79})$$

and the classical trajectory

$$\cosh(t) \sinh(\rho) = \sinh(\rho_0). \quad (\text{B.80})$$

Explicitly, we would like to evaluate the integral

$$\begin{aligned} \Psi(p, \omega) &= \int_0^\infty \sinh \rho d \sinh \rho \int_{-\infty}^\infty dt \delta(\cosh(t) \sinh(\rho) - \sinh(\rho_0)) U_\omega^p(\rho, \theta) \\ &= \int_{-\infty}^\infty dt \frac{\sinh \rho_0}{\cosh^2 t} U_\omega^p(\rho(\rho_0, t), t). \end{aligned} \quad (\text{B.81})$$

After expanding the hypergeometric function as

$$\begin{aligned} &F\left(\frac{1}{2} - \frac{ip}{2} - \frac{i\omega}{2}, \frac{1}{2} + \frac{ip}{2} - \frac{i\omega}{2}; 1-i\omega, -\frac{\sinh^2 \rho_0}{\cosh^2 t}\right) \\ &= \sum_{l=0} \frac{\Gamma(\frac{1}{2} - \frac{ip}{2} - \frac{i\omega}{2} + l) \Gamma(\frac{1}{2} + \frac{ip}{2} - \frac{i\omega}{2} + l)}{\Gamma(1-i\omega + l)} \times \\ &\times \frac{\Gamma(-i\omega)}{\Gamma(\frac{1}{2} - \frac{ip}{2} - \frac{i\omega}{2}) \Gamma(\frac{1}{2} + \frac{ip}{2} - \frac{i\omega}{2})} \frac{(-)^l \sinh^{2l} \rho_0}{l! \cosh^{2l} t}. \end{aligned} \quad (\text{B.82})$$

the integration over t is possible by the formula

$$\int_{-\infty}^{\infty} (2 \cosh t)^{a-1} e^{ibt} dt = \frac{1}{2} B \left(\frac{1}{2} - \frac{a+ib}{2}, \frac{1}{2} - \frac{a-ib}{2} \right) \equiv \frac{1}{2} \frac{\Gamma \left(\frac{1}{2} - \frac{a+ib}{2} \right) \Gamma \left(\frac{1}{2} - \frac{a-ib}{2} \right)}{\Gamma(1-a)},$$

After collecting terms by using the duplication formula

$$\sqrt{\pi} \Gamma(2l+2-i\omega) = 2^{2l+1-i\omega} \Gamma(2l+1-\frac{i\omega}{2}) \Gamma(2l+\frac{3}{2}-\frac{i\omega}{2}), \quad (\text{B.84})$$

we obtain¹³⁰

$$\begin{aligned} \Psi(p, \omega) &= \left(\frac{\sinh \rho_0}{2} \right)^{1-i\omega} \frac{\Gamma^2 \left(\frac{1}{2} - \frac{ip}{2} - \frac{i\omega}{2} \right) \Gamma \left(\frac{1}{2} + \frac{ip}{2} - \frac{i\omega}{2} \right)}{\Gamma(-ip) \Gamma(1-\frac{i\omega}{2}) \Gamma(\frac{3}{2}-\frac{i\omega}{2})} \\ &\times {}_3F_2 \left(1, \frac{1}{2} - \frac{ip}{2} - \frac{i\omega}{2}, \frac{1}{2} - \frac{ip}{2} - \frac{i\omega}{2}; 1 - \frac{i\omega}{2}, \frac{3}{2} - \frac{i\omega}{2}; -\frac{\sinh^2 \rho_0}{2} \right). \end{aligned} \quad (\text{B.85})$$

Here we have introduced the generalized hypergeometric function

$${}_3F_2(a_1, a_2, a_3; b_1, b_2; z) = \sum_{l=0}^{\infty} \frac{(a_1)_l (a_2)_l (a_3)_l}{(b_1)_l (b_2)_l} \frac{z^l}{l!}, \quad (\text{B.86})$$

where

$$(a)_l \equiv \frac{\Gamma(a+l)}{\Gamma(a)}. \quad (\text{B.87})$$

Let us discuss a particular limit of our boundary wavefunction (B.85). We take the limit $\rho_0 \rightarrow \infty$ to see the connection to our previous results [1]. To see this, we use the asymptotic expansion formula

$$\begin{aligned} &{}_3F_2(a_1, a_2, a_3; b_1, b_2; z) \\ &= \frac{\Gamma(b_1) \Gamma(b_2)}{\Gamma(a_1) \Gamma(a_2) \Gamma(a_3)} \sum_{k=1}^3 \frac{\Gamma(a_k) \prod_{j=1; j \neq k}^3 (a_j - a_k)}{\prod_{j=1}^2 \Gamma(b_j - a_k)} (-z)^{-a_k} [1 + O(z^{-1})]. \end{aligned} \quad (\text{B.88})$$

In this limit, we see that it asymptotically approaches to our previous results

$$\lim_{\rho_0 \rightarrow \infty} \Psi(p, \omega) = B(\nu_+, \nu_-) \Gamma \left(1 + \frac{ip}{k} \right) \left[e^{-ip\rho_0} - \frac{\cosh \left(\pi \frac{p-\omega}{2} \right)}{\cosh \left(\pi \frac{p+\omega}{2} \right)} e^{ip\rho_0} \right] + O(e^{-\rho_0}). \quad (\text{B.89})$$

So importantly, our previous results coincide with the direct evaluation of the overlap only in the limit $\rho_0 \rightarrow \infty$.

Another interesting limit is to take $\rho_0 \rightarrow 0$. If we further specialize in the zero energy overlap (i.e. $\omega = 0$), we have

$$\lim_{\rho_0 \rightarrow 0} \Psi(p, 0) = -\sinh \rho_0 \frac{\Gamma^2 \left(\frac{1}{2} - \frac{ip}{2} \right)}{\Gamma(-ip)}, \quad (\text{B.90})$$

which coincides with the zero-winding sector of the D0-brane in the cigar (up to $\sinh \rho_0$), which is quite expected, given the origin of the minisuperspace calculation. It would be interesting but seem very difficult to compute the emission rate for general ρ_0 .

¹³⁰Presumably up to a numerical factor.

References

- [1] Y. Nakayama, S.-J. Rey, and Y. Sugawara, “D-brane propagation in two-dimensional black hole geometries,” *JHEP* **09** (2005) 020, [hep-th/0507040](#).
- [2] Y. Nakayama, S.-J. Rey, and Y. Sugawara, “Unitarity meets channel-duality for rolling / decaying D- branes,” *JHEP* **08** (2006) 014, [hep-th/0605013](#).
- [3] S. Weinberg and E. Witten, “LIMITS ON MASSLESS PARTICLES,” *Phys. Lett.* **B96** (1980) 59.
- [4] J. M. Maldacena, “The large N limit of superconformal field theories and supergravity,” *Adv. Theor. Math. Phys.* **2** (1998) 231–252, [hep-th/9711200](#).
- [5] O. Aharony, S. S. Gubser, J. M. Maldacena, H. Ooguri, and Y. Oz, “Large N field theories, string theory and gravity,” *Phys. Rept.* **323** (2000) 183–386, [hep-th/9905111](#).
- [6] S.-J. Rey, “AXIONIC STRING INSTANTONS AND THEIR LOW-ENERGY IMPLICATIONS,”. Invited talk given at Workshop on Superstrings and Particle Theory, Tuscaloosa, Alabama, Nov 8-11, 1989.
- [7] S.-J. Rey, “THE CONFINING PHASE OF SUPERSTRINGS AND AXIONIC STRINGS,” *Phys. Rev.* **D43** (1991) 526–538.
- [8] S.-J. Rey, “On string theory and axionic strings and instantons,”. Presented at Particle and Fields '91 Conf., Vancouver, Canada, Aug 18-22, 1991.
- [9] C. G. J. Callan, J. A. Harvey, and A. Strominger, “World sheet approach to heterotic instantons and solitons,” *Nucl. Phys.* **B359** (1991) 611–634.
- [10] C. G. J. Callan, J. A. Harvey, and A. Strominger, “Supersymmetric string solitons,” [hep-th/9112030](#).
- [11] J. M. Maldacena and A. Strominger, “Semiclassical decay of near-extremal fivebranes,” *JHEP* **12** (1997) 008, [hep-th/9710014](#).
- [12] D. Kutasov and D. A. Sahakyan, “Comments on the thermodynamics of little string theory,” *JHEP* **02** (2001) 021, [hep-th/0012258](#).
- [13] K. Sfetsos, “Branes for Higgs phases and exact conformal field theories,” *JHEP* **01** (1999) 015, [hep-th/9811167](#).
- [14] D. Israel, C. Kounnas, A. Pakman, and J. Troost, “The partition function of the supersymmetric two- dimensional black hole and little string theory,” *JHEP* **06** (2004) 033, [hep-th/0403237](#).
- [15] N. Itzhaki, D. Kutasov, and N. Seiberg, “Non-supersymmetric deformations of non-critical superstrings,” *JHEP* **12** (2005) 035, [hep-th/0510087](#).

- [16] F. Gliozzi, J. Scherk, and D. I. Olive, “SUPERSYMMETRY, SUPERGRAVITY THEORIES AND THE DUAL SPINOR MODEL,” *Nucl. Phys.* **B122** (1977) 253–290.
- [17] I. Bakas, “Space-time interpretation of s duality and supersymmetry violations of t duality,” *Phys. Lett.* **B343** (1995) 103–112, [hep-th/9410104](#).
- [18] E. Bergshoeff, R. Kallosh, and T. Ortin, “Duality versus supersymmetry and compactification,” *Phys. Rev.* **D51** (1995) 3009–3016, [hep-th/9410230](#).
- [19] I. Bakas and K. Sfetsos, “T duality and world sheet supersymmetry,” *Phys. Lett.* **B349** (1995) 448–457, [hep-th/9502065](#).
- [20] D. Gepner, “EXACTLY SOLVABLE STRING COMPACTIFICATIONS ON MANIFOLDS OF SU(N) HOLONOMY,” *Phys. Lett.* **B199** (1987) 380–388.
- [21] D. Gepner, “SPACE-TIME SUPERSYMMETRY IN COMPACTIFIED STRING THEORY AND SUPERCONFORMAL MODELS,” *Nucl. Phys.* **B296** (1988) 757.
- [22] D. Ghoshal and C. Vafa, “C = 1 string as the topological theory of the conifold,” *Nucl. Phys.* **B453** (1995) 121–128, [hep-th/9506122](#).
- [23] H. Ooguri and C. Vafa, “Two-Dimensional Black Hole and Singularities of CY Manifolds,” *Nucl. Phys.* **B463** (1996) 55–72, [hep-th/9511164](#).
- [24] A. Giveon, D. Kutasov, and O. Pele, “Holography for non-critical superstrings,” *JHEP* **10** (1999) 035, [hep-th/9907178](#).
- [25] W. Lerche, “On a boundary CFT description of nonperturbative N = 2 Yang-Mills theory,” [hep-th/0006100](#).
- [26] K. Hori and A. Kapustin, “Worldsheet descriptions of wrapped NS five-branes,” *JHEP* **11** (2002) 038, [hep-th/0203147](#).
- [27] T. Eguchi and Y. Sugawara, “Conifold type singularities, N = 2 Liouville and SL(2,R)/U(1) theories,” *JHEP* **01** (2005) 027, [hep-th/0411041](#).
- [28] C. Vafa and N. P. Warner, “CATASTROPHES AND THE CLASSIFICATION OF CONFORMAL THEORIES,” *Phys. Lett.* **B218** (1989) 51.
- [29] W. Lerche, C. Vafa, and N. P. Warner, “CHIRAL RINGS IN N=2 SUPERCONFORMAL THEORIES,” *Nucl. Phys.* **B324** (1989) 427.
- [30] E. J. Martinec, “ALGEBRAIC GEOMETRY AND EFFECTIVE LAGRANGIANS,” *Phys. Lett.* **B217** (1989) 431.
- [31] E. Witten, “Phases of N = 2 theories in two dimensions,” *Nucl. Phys.* **B403** (1993) 159–222, [hep-th/9301042](#).
- [32] K. Hori and C. Vafa, “Mirror symmetry,” [hep-th/0002222](#).

- [33] B. R. Greene, C. Vafa, and N. P. Warner, “CALABI-YAU MANIFOLDS AND RENORMALIZATION GROUP FLOWS,” *Nucl. Phys.* **B324** (1989) 371.
- [34] Y. Kazama and H. Suzuki, “CHARACTERIZATION OF N=2 SUPERCONFORMAL MODELS GENERATED BY COSET SPACE METHOD,” *Phys. Lett.* **B216** (1989) 112.
- [35] Y. Kazama and H. Suzuki, “NEW N=2 SUPERCONFORMAL FIELD THEORIES AND SUPERSTRING COMPACTIFICATION,” *Nucl. Phys.* **B321** (1989) 232.
- [36] Y. Kazama and H. Suzuki, “BOSONIC CONSTRUCTION OF CONFORMAL FIELD THEORIES WITH EXTENDED SUPERSYMMETRY,” *Mod. Phys. Lett.* **A4** (1989) 235.
- [37] T. Eguchi and Y. Sugawara, “SL(2,R)/U(1) supercoset and elliptic genera of non-compact Calabi-Yau manifolds,” *JHEP* **05** (2004) 014, [hep-th/0403193](#).
- [38] T. Eguchi, Y. Sugawara, and A. Taormina, “Liouville field, modular forms and elliptic genera,” [hep-th/0611338](#).
- [39] P. Candelas and X. de la Ossa, “MODULI SPACE OF CALABI-YAU MANIFOLDS,” *Nucl. Phys.* **B355** (1991) 455–481.
- [40] S. Gukov, C. Vafa, and E. Witten, “CFT’s from Calabi-Yau four-folds,” *Nucl. Phys.* **B584** (2000) 69–108, [hep-th/9906070](#).
- [41] P. C. Argyres and M. R. Douglas, “New phenomena in SU(3) supersymmetric gauge theory,” *Nucl. Phys.* **B448** (1995) 93–126, [hep-th/9505062](#).
- [42] P. C. Argyres, M. Ronen Plesser, N. Seiberg, and E. Witten, “New N=2 Superconformal Field Theories in Four Dimensions,” *Nucl. Phys.* **B461** (1996) 71–84, [hep-th/9511154](#).
- [43] T. Eguchi, K. Hori, K. Ito, and S.-K. Yang, “Study of $N = 2$ Superconformal Field Theories in 4 Dimensions,” *Nucl. Phys.* **B471** (1996) 430–444, [hep-th/9603002](#).
- [44] A. Losev, G. W. Moore, and S. L. Shatashvili, “M and m’s,” *Nucl. Phys.* **B522** (1998) 105–124, [hep-th/9707250](#).
- [45] O. Aharony, “A brief review of ‘little string theories’,” *Class. Quant. Grav.* **17** (2000) 929–938, [hep-th/9911147](#).
- [46] N. Seiberg, “Notes on theories with 16 supercharges,” *Nucl. Phys. Proc. Suppl.* **67** (1998) 158–171, [hep-th/9705117](#).
- [47] G. K. Boyerm, P. Charles, “Sasakian Geometry, Hypersurface Singularities, and Einstein Metrics,” *Supplemento ai Rendiconti del Circolo Matematico di Palermo Serie II Suppl* **75** (2005) 57–87.

- [48] J. P. Gauntlett, D. Martelli, J. Sparks, and D. Waldram, “Sasaki-Einstein metrics on $S(2) \times S(3)$,” *Adv. Theor. Math. Phys.* **8** (2004) 711–734, [hep-th/0403002](#).
- [49] M. Cvetič, H. Lu, D. N. Page, and C. N. Pope, “New Einstein-Sasaki spaces in five and higher dimensions,” *Phys. Rev. Lett.* **95** (2005) 071101, [hep-th/0504225](#).
- [50] M. Cvetič, H. Lu, D. N. Page, and C. N. Pope, “New Einstein-Sasaki and Einstein spaces from Kerr-de Sitter,” [hep-th/0505223](#).
- [51] A. Bergman and C. P. Herzog, “The volume of some non-spherical horizons and the AdS/CFT correspondence,” *JHEP* **01** (2002) 030, [hep-th/0108020](#).
- [52] D. Martelli, J. Sparks, and S.-T. Yau, “The geometric dual of a-maximisation for toric Sasaki-Einstein manifolds,” [hep-th/0503183](#).
- [53] D. Martelli, J. Sparks, and S.-T. Yau, “Sasaki-Einstein manifolds and volume minimisation,” [hep-th/0603021](#).
- [54] K. Intriligator and B. Wecht, “The exact superconformal R-symmetry maximizes a,” *Nucl. Phys.* **B667** (2003) 183–200, [hep-th/0304128](#).
- [55] S. S. Gubser, “Einstein manifolds and conformal field theories,” *Phys. Rev.* **D59** (1999) 025006, [hep-th/9807164](#).
- [56] D. Z. Freedman, S. S. Gubser, K. Pilch, and N. P. Warner, “Renormalization group flows from holography supersymmetry and a c-theorem,” *Adv. Theor. Math. Phys.* **3** (1999) 363–417, [hep-th/9904017](#).
- [57] J. P. Gauntlett, D. Martelli, J. Sparks, and S.-T. Yau, “Obstructions to the existence of Sasaki-Einstein metrics,” [hep-th/0607080](#).
- [58] A. A. Tseytlin, “Effective action of gauged WZW model and exact string solutions,” *Nucl. Phys.* **B399** (1993) 601–622, [hep-th/9301015](#).
- [59] V. G. Knizhnik, A. M. Polyakov, and A. B. Zamolodchikov, “Fractal structure of 2d-quantum gravity,” *Mod. Phys. Lett.* **A3** (1988) 819.
- [60] J. D. Bekenstein, “Black holes and entropy,” *Phys. Rev.* **D7** (1973) 2333–2346.
- [61] J. M. Bardeen, B. Carter, and S. W. Hawking, “The Four laws of black hole mechanics,” *Commun. Math. Phys.* **31** (1973) 161–170.
- [62] S. W. Hawking, “Particle creation by black holes,” *Commun. Math. Phys.* **43** (1975) 199–220.
- [63] G. W. Gibbons and S. W. Hawking, “ACTION INTEGRALS AND PARTITION FUNCTIONS IN QUANTUM GRAVITY,” *Phys. Rev.* **D15** (1977) 2752–2756.
- [64] S. P. Robinson and F. Wilczek, “A relationship between Hawking radiation and gravitational anomalies,” *Phys. Rev. Lett.* **95** (2005) 011303, [gr-qc/0502074](#).

- [65] S. Iso, H. Umetsu, and F. Wilczek, “Hawking radiation from charged black holes via gauge and gravitational anomalies,” *Phys. Rev. Lett.* **96** (2006) 151302, [hep-th/0602146](#).
- [66] S. M. Christensen and S. A. Fulling, “TRACE ANOMALIES AND THE HAWKING EFFECT,” *Phys. Rev.* **D15** (1977) 2088–2104.
- [67] S. Iso, H. Umetsu, and F. Wilczek, “Anomalies, Hawking radiations and regularity in rotating black holes,” *Phys. Rev.* **D74** (2006) 044017, [hep-th/0606018](#).
- [68] K. Murata and J. Soda, “Hawking radiation from rotating black holes and gravitational anomalies,” *Phys. Rev.* **D74** (2006) 044018, [hep-th/0606069](#).
- [69] E. C. Vagenas and S. Das, “Gravitational anomalies, Hawking radiation, and spherically symmetric black holes,” [hep-th/0606077](#).
- [70] M. R. Setare, “Gauge and gravitational anomalies and Hawking radiation of rotating BTZ black holes,” [hep-th/0608080](#).
- [71] E. Witten, “On string theory and black holes,” *Phys. Rev.* **D44** (1991) 314–324.
- [72] S. Elitzur, A. Forge, and E. Rabinovici, “Some global aspects of string compactifications,” *Nucl. Phys.* **B359** (1991) 581–610.
- [73] G. Mandal, A. M. Sengupta, and S. R. Wadia, “Classical solutions of two-dimensional string theory,” *Mod. Phys. Lett.* **A6** (1991) 1685–1692.
- [74] A. Hanany, N. Prezas, and J. Troost, “The partition function of the two-dimensional black hole conformal field theory,” *JHEP* **04** (2002) 014, [hep-th/0202129](#).
- [75] R. Dijkgraaf, H. Verlinde, and E. Verlinde, “String propagation in a black hole geometry,” *Nucl. Phys.* **B371** (1992) 269–314.
- [76] V. Kazakov, I. K. Kostov, and D. Kutasov, “A matrix model for the two-dimensional black hole,” *Nucl. Phys.* **B622** (2002) 141–188, [hep-th/0101011](#).
- [77] D. Grumiller, “An action for the exact string black hole,” *JHEP* **05** (2005) 028, [hep-th/0501208](#).
- [78] J. M. Maldacena and H. Ooguri, “Strings in AdS(3) and SL(2,R) WZW model. I,” *J. Math. Phys.* **42** (2001) 2929–2960, [hep-th/0001053](#).
- [79] S. Ribault and V. Schomerus, “Branes in the 2-D black hole,” *JHEP* **02** (2004) 019, [hep-th/0310024](#).
- [80] J. Teschner, “On structure constants and fusion rules in the SL(2,C)/SU(2) WZNW model,” *Nucl. Phys.* **B546** (1999) 390–422, [hep-th/9712256](#).
- [81] J. Teschner, “Operator product expansion and factorization in the H-3+ WZNW model,” *Nucl. Phys.* **B571** (2000) 555–582, [hep-th/9906215](#).

- [82] A. Giveon and D. Kutasov, “Little string theory in a double scaling limit,” *JHEP* **10** (1999) 034, [hep-th/9909110](#).
- [83] A. Giveon and D. Kutasov, “Comments on double scaled little string theory,” *JHEP* **01** (2000) 023, [hep-th/9911039](#).
- [84] I. Bars and J. Schulze, “Folded strings falling into a black hole,” *Phys. Rev.* **D51** (1995) 1854–1868, [hep-th/9405156](#).
- [85] W. A. Bardeen, I. Bars, A. J. Hanson, and R. D. Peccei, “A STUDY OF THE LONGITUDINAL KINK MODES OF THE STRING,” *Phys. Rev.* **D13** (1976) 2364–2382.
- [86] J. M. Maldacena, “Long strings in two dimensional string theory and non- singlets in the matrix model,” *JHEP* **09** (2005) 078, [hep-th/0503112](#).
- [87] V. Fateev, A. B. Zamolodchikov, and A. B. Zamolodchikov, “Boundary Liouville field theory. I: Boundary state and boundary two-point function,” [hep-th/0001012](#).
- [88] J. Teschner, “Remarks on Liouville theory with boundary,” [hep-th/0009138](#).
- [89] L. Fidkowski, “Solving the eigenvalue problem arising from the adjoint sector of the $c = 1$ matrix model,” [hep-th/0506132](#).
- [90] I. Kostov, “Long strings and chiral non-singlets in matrix quantum mechanics,” [hep-th/0610084](#).
- [91] H. J. de Vega, J. Ramirez Mittelbrunn, M. Ramon Medrano, and N. G. Sanchez, “The General solution of the 2-D sigma model stringy black hole and the massless complex Sine-Gordon model,” *Phys. Lett.* **B323** (1994) 133–138, [hep-th/9312085](#).
- [92] V. Fateev, A. Zamolodchikov, and A. Zamolodchikov, “unpublished.”
- [93] Y. Nakayama, “Liouville field theory: A decade after the revolution,” *Int. J. Mod. Phys.* **A19** (2004) 2771–2930, [hep-th/0402009](#).
- [94] K. Hori and A. Kapustin, “Duality of the fermionic 2d black hole and $N = 2$ Liouville theory as mirror symmetry,” *JHEP* **08** (2001) 045, [hep-th/0104202](#).
- [95] D. Tong, “Mirror mirror on the wall: On two-dimensional black holes and Liouville theory,” *JHEP* **04** (2003) 031, [hep-th/0303151](#).
- [96] J. L. Karczmarek, J. M. Maldacena, and A. Strominger, “Black hole non-formation in the matrix model,” *JHEP* **01** (2006) 039, [hep-th/0411174](#).
- [97] P. Baseilhac and V. A. Fateev, “Expectation values of local fields for a two-parameter family of integrable models and related perturbed conformal field theories,” *Nucl. Phys.* **B532** (1998) 567–587, [hep-th/9906010](#).

- [98] S. L. Lukyanov, E. S. Vitchev, and A. B. Zamolodchikov, “Integrable model of boundary interaction: The paperclip,” *Nucl. Phys.* **B683** (2004) 423–454, [hep-th/0312168](#).
- [99] Y. Hikida and T. Takayanagi, “On solvable time-dependent model and rolling closed string tachyon,” *Phys. Rev.* **D70** (2004) 126013, [hep-th/0408124](#).
- [100] D. Kutasov, “Accelerating branes and the string / black hole transition,” [hep-th/0509170](#).
- [101] A. Strominger and C. Vafa, “Microscopic Origin of the Bekenstein-Hawking Entropy,” *Phys. Lett.* **B379** (1996) 99–104, [hep-th/9601029](#).
- [102] A. Dabholkar, “Exact counting of black hole microstates,” *Phys. Rev. Lett.* **94** (2005) 241301, [hep-th/0409148](#).
- [103] G. ’t Hooft, “QUANTUM GRAVITY AND BLACK HOLES,”. Lectures given at Cargese Summer Inst. on Nonperturbative Quantum Field Theory, Cargese, France, Jul 16-30, 1987.
- [104] C. F. E. Holzhey and F. Wilczek, “Black holes as elementary particles,” *Nucl. Phys.* **B380** (1992) 447–477, [hep-th/9202014](#).
- [105] L. Susskind, “Some speculations about black hole entropy in string theory,” [hep-th/9309145](#).
- [106] G. T. Horowitz and J. Polchinski, “A correspondence principle for black holes and strings,” *Phys. Rev.* **D55** (1997) 6189–6197, [hep-th/9612146](#).
- [107] A. Sen, “Extremal black holes and elementary string states,” *Mod. Phys. Lett.* **A10** (1995) 2081–2094, [hep-th/9504147](#).
- [108] L. Susskind, “Strings, black holes and Lorentz contraction,” *Phys. Rev.* **D49** (1994) 6606–6611, [hep-th/9308139](#).
- [109] A. Giveon and D. Kutasov, “The charged black hole / string transition,” *JHEP* **01** (2006) 120, [hep-th/0510211](#).
- [110] J. Polchinski, “EVALUATION OF THE ONE LOOP STRING PATH INTEGRAL,” *Commun. Math. Phys.* **104** (1986) 37.
- [111] B. Sathiapalan, “VORTICES ON THE STRING WORLD SHEET AND CONSTRAINTS ON TORAL COMPACTIFICATION,” *Phys. Rev.* **D35** (1987) 3277.
- [112] Y. I. Kogan, “VORTICES ON THE WORLD SHEET AND STRING’S CRITICAL DYNAMICS,” *JETP Lett.* **45** (1987) 709–712.

- [113] K. H. O'Brien and C. I. Tan, "MODULAR INVARIANCE OF THERMOPARTITION FUNCTION AND GLOBAL PHASE STRUCTURE OF HETEROTIC STRING," *Phys. Rev.* **D36** (1987) 1184.
- [114] J. J. Atick and E. Witten, "THE HAGEDORN TRANSITION AND THE NUMBER OF DEGREES OF FREEDOM OF STRING THEORY," *Nucl. Phys.* **B310** (1988) 291–334.
- [115] G. T. Horowitz, "Tachyon condensation and black strings," *JHEP* **08** (2005) 091, [hep-th/0506166](#).
- [116] S. F. Ross, "Winding tachyons in asymptotically supersymmetric black strings," *JHEP* **10** (2005) 112, [hep-th/0509066](#).
- [117] O. Bergman and S. Hirano, "Semi-localized instability of the Kaluza-Klein linear dilaton vacuum," *Nucl. Phys.* **B744** (2006) 136–155, [hep-th/0510076](#).
- [118] G. T. Horowitz and E. Silverstein, "The inside story: Quasilocal tachyons and black holes," *Phys. Rev.* **D73** (2006) 064016, [hep-th/0601032](#).
- [119] M. Dine, A. Shomer, and Z. Sun, "On Witten's instability and winding tachyons," [hep-th/0607003](#).
- [120] J. McGreevy and E. Silverstein, "The tachyon at the end of the universe," *JHEP* **08** (2005) 090, [hep-th/0506130](#).
- [121] Y. Nakayama, S.-J. Rey, and Y. Sugawara, "The nothing at the beginning of the universe made precise," [hep-th/0606127](#).
- [122] D. Kutasov and N. Seiberg, "Noncritical superstrings," *Phys. Lett.* **B251** (1990) 67–72.
- [123] N. Seiberg, "Notes on quantum Liouville theory and quantum gravity," *Prog. Theor. Phys. Suppl.* **102** (1990) 319–349.
- [124] A. Giveon, D. Kutasov, E. Rabinovici, and A. Sever, "Phases of quantum gravity in AdS(3) and linear dilaton backgrounds," *Nucl. Phys.* **B719** (2005) 3–34, [hep-th/0503121](#).
- [125] A. Adams, J. Polchinski, and E. Silverstein, "Don't panic! Closed string tachyons in ALE space-times," *JHEP* **10** (2001) 029, [hep-th/0108075](#).
- [126] A. Adams, X. Liu, J. McGreevy, A. Saltman, and E. Silverstein, "Things fall apart: Topology change from winding tachyons," *JHEP* **10** (2005) 033, [hep-th/0502021](#).
- [127] A. Sen, "Tachyon dynamics in open string theory," *Int. J. Mod. Phys.* **A20** (2005) 5513–5656, [hep-th/0410103](#).
- [128] M. Schnabl, "Analytic solution for tachyon condensation in open string field theory," [hep-th/0511286](#).

- [129] I. Ellwood and M. Schnabl, “Proof of vanishing cohomology at the tachyon vacuum,” [hep-th/0606142](#).
- [130] A. Sen, “Rolling tachyon,” *JHEP* **04** (2002) 048, [hep-th/0203211](#).
- [131] A. Sen, “Tachyon matter,” *JHEP* **07** (2002) 065, [hep-th/0203265](#).
- [132] A. Sen, “Field theory of tachyon matter,” *Mod. Phys. Lett.* **A17** (2002) 1797–1804, [hep-th/0204143](#).
- [133] M. Gutperle and A. Strominger, “Timelike boundary Liouville theory,” *Phys. Rev.* **D67** (2003) 126002, [hep-th/0301038](#).
- [134] A. Sen, “Symmetries, conserved charges and (black) holes in two dimensional string theory,” *JHEP* **12** (2004) 053, [hep-th/0408064](#).
- [135] J. L. Karczmarek, H. Liu, J. M. Maldacena, and A. Strominger, “UV finite brane decay,” *JHEP* **11** (2003) 042, [hep-th/0306132](#).
- [136] I. R. Klebanov, J. M. Maldacena, and N. Seiberg, “D-brane decay in two-dimensional string theory,” *JHEP* **07** (2003) 045, [hep-th/0305159](#).
- [137] A. B. Zamolodchikov and A. B. Zamolodchikov, “Liouville field theory on a pseudosphere,” [hep-th/0101152](#).
- [138] Y.-L. He and P. Zhang, “ZZ brane decay in D dimensions,” *JHEP* **11** (2006) 014, [hep-th/0607188](#).
- [139] D. Israel and E. Rabinovici, “Rolling tachyon in anti-de Sitter space-time,” [hep-th/0609087](#).
- [140] P. Mukhopadhyay and A. Sen, “Decay of unstable D-branes with electric field,” *JHEP* **11** (2002) 047, [hep-th/0208142](#).
- [141] S.-J. Rey and S. Sugimoto, “Rolling tachyon with electric and magnetic fields: T-duality approach,” *Phys. Rev.* **D67** (2003) 086008, [hep-th/0301049](#).
- [142] K. Nagami, “Closed string emission from unstable D-brane with background electric field,” *JHEP* **01** (2004) 005, [hep-th/0309017](#).
- [143] K. Nagami, “Rolling tachyon with electromagnetic field in linear dilaton background,” *Phys. Lett.* **B591** (2004) 187–196, [hep-th/0312149](#).
- [144] M. Gutperle and P. Yi, “Winding strings and decay of D-branes with flux,” *JHEP* **01** (2005) 015, [hep-th/0409050](#).
- [145] D. Kutasov, “D-brane dynamics near NS5-branes,” [hep-th/0405058](#).
- [146] O. Aharony, M. Berkooz, D. Kutasov, and N. Seiberg, “Linear dilatons, NS5-branes and holography,” *JHEP* **10** (1998) 004, [hep-th/9808149](#).

- [147] D. Kutasov, “A geometric interpretation of the open string tachyon,” [hep-th/0408073](#).
- [148] Y. Nakayama, K. L. Panigrahi, S.-J. Rey, and H. Takayanagi, “Rolling down the throat in NS5-brane background: The case of electrified D-brane,” *JHEP* **01** (2005) 052, [hep-th/0412038](#).
- [149] H. Yavartanoo, “Cosmological solution from D-brane motion in NS5-branes background,” *Int. J. Mod. Phys. A* **20** (2005) 7633–7645, [hep-th/0407079](#).
- [150] K. L. Panigrahi, “D-brane dynamics in Dp-brane background,” *Phys. Lett.* **B601** (2004) 64–72, [hep-th/0407134](#).
- [151] A. Ghodsi and A. E. Mosaffa, “D-brane dynamics in RR deformation of NS5-branes background and tachyon cosmology,” *Nucl. Phys.* **B714** (2005) 30–50, [hep-th/0408015](#).
- [152] D. A. Sahakyan, “Comments on D-brane dynamics near NS5-branes,” *JHEP* **10** (2004) 008, [hep-th/0408070](#).
- [153] N. Toumbas and J. Troost, “A time-dependent brane in a cosmological background,” *JHEP* **11** (2004) 032, [hep-th/0410007](#).
- [154] D. Bak, S.-J. Rey, and H.-U. Yee, “Exactly soluble dynamics of (p,q) string near macroscopic fundamental strings,” *JHEP* **12** (2004) 008, [hep-th/0411099](#).
- [155] B. Chen, M. Li, and B. Sun, “Dbrane near NS5-branes: With electromagnetic field,” *JHEP* **12** (2004) 057, [hep-th/0412022](#).
- [156] J. Kluson, “Non-BPS Dp-brane in Dk-brane background,” *JHEP* **03** (2005) 044, [hep-th/0501010](#).
- [157] J. M. Lapan and W. Li, “Falling D0-branes in 2D superstring theory,” [hep-th/0501054](#).
- [158] S. Thomas and J. Ward, “D-brane dynamics near compactified NS5-branes,” *JHEP* **06** (2005) 062, [hep-th/0501192](#).
- [159] S. Thomas and J. Ward, “Geometrical tachyon kinks and NS5 branes,” *JHEP* **10** (2005) 098, [hep-th/0502228](#).
- [160] J. Kluson, “Remark about non-BPS Dp-brane at the tachyon vacuum moving in curved background,” *Phys. Rev.* **D72** (2005) 106005, [hep-th/0504062](#).
- [161] J. Kluson, “Dynamics of D1-brane in I-brane background,” *JHEP* **12** (2005) 016, [hep-th/0510243](#).
- [162] J. Kluson, R. R. Nayak, and K. L. Panigrahi, “D-brane dynamics in a plane wave background,” *Phys. Rev.* **D73** (2006) 066007, [hep-th/0512159](#).

- [163] E. Papantonopoulos, I. Pappa, and V. Zamarias, “Geometrical tachyon dynamics in the background of a bulk tachyon field,” *JHEP* **05** (2006) 038, [hep-th/0601152](#).
- [164] K. Okuyama and M. Rozali, “Hairpin branes and D-branes behind the horizon,” *JHEP* **03** (2006) 071, [hep-th/0602060](#).
- [165] B. Gumjudpai, T. Naskar, and J. Ward, “A quintessentially geometric model,” [hep-ph/0603210](#).
- [166] A. Linde, “Inflation and string cosmology,” *ECONF* **C040802** (2004) L024, [hep-th/0503195](#).
- [167] L. Kofman and A. Linde, “Problems with tachyon inflation,” *JHEP* **07** (2002) 004, [hep-th/0205121](#).
- [168] A. V. Frolov, L. Kofman, and A. A. Starobinsky, “Prospects and problems of tachyon matter cosmology,” *Phys. Lett.* **B545** (2002) 8–16, [hep-th/0204187](#).
- [169] X.-z. Li, D.-j. Liu, and J.-g. Hao, “On the tachyon inflation,” [hep-th/0207146](#).
- [170] M. Fairbairn and M. H. G. Tytgat, “Inflation from a tachyon fluid?,” *Phys. Lett.* **B546** (2002) 1–7, [hep-th/0204070](#).
- [171] G. Shiu and I. Wasserman, “Cosmological constraints on tachyon matter,” *Phys. Lett.* **B541** (2002) 6–15, [hep-th/0205003](#).
- [172] S. Thomas and J. Ward, “Inflation from geometrical tachyons,” *Phys. Rev.* **D72** (2005) 083519, [hep-th/0504226](#).
- [173] L. Kofman and P. Yi, “Reheating the universe after string theory inflation,” *Phys. Rev.* **D72** (2005) 106001, [hep-th/0507257](#).
- [174] A. R. Frey, A. Mazumdar, and R. Myers, “Stringy effects during inflation and reheating,” *Phys. Rev.* **D73** (2006) 026003, [hep-th/0508139](#).
- [175] D. Chialva, G. Shiu, and B. Underwood, “Warped reheating in multi-throat brane inflation,” *JHEP* **01** (2006) 014, [hep-th/0508229](#).
- [176] X. Chen and S. H. H. Tye, “Heating in brane inflation and hidden dark matter,” *JCAP* **0606** (2006) 011, [hep-th/0602136](#).
- [177] J. Polchinski, “Introduction to cosmic F- and D-strings,” [hep-th/0412244](#).
- [178] J. M. Maldacena, G. W. Moore, and N. Seiberg, “Geometrical interpretation of D-branes in gauged WZW models,” *JHEP* **07** (2001) 046, [hep-th/0105038](#).
- [179] K. Gawedzki, “Boundary WZW, G/H, G/G and CS theories,” *Annales Henri Poincaré* **3** (2002) 847–881, [hep-th/0108044](#).
- [180] S. Elitzur and G. Sarkissian, “D-branes on a gauged WZW model,” *Nucl. Phys.* **B625** (2002) 166–178, [hep-th/0108142](#).

- [181] S. Fredenhagen and V. Schomerus, “D-branes in coset models,” *JHEP* **02** (2002) 005, [hep-th/0111189](#).
- [182] H. Ishikawa, “Boundary states in coset conformal field theories,” *Nucl. Phys.* **B629** (2002) 209–232, [hep-th/0111230](#).
- [183] K. P. Yogendran, “D-branes in 2D Lorentzian black hole,” *JHEP* **01** (2005) 036, [hep-th/0408114](#).
- [184] M. Kato and T. Okada, “D-branes on group manifolds,” *Nucl. Phys.* **B499** (1997) 583–595, [hep-th/9612148](#).
- [185] A. Y. Alekseev and V. Schomerus, “D-branes in the WZW model,” *Phys. Rev.* **D60** (1999) 061901, [hep-th/9812193](#).
- [186] L. Birke, J. Fuchs, and C. Schweigert, “Symmetry breaking boundary conditions and WZW orbifolds,” *Adv. Theor. Math. Phys.* **3** (1999) 671–726, [hep-th/9905038](#).
- [187] R. E. Behrend, P. A. Pearce, V. B. Petkova, and J.-B. Zuber, “Boundary conditions in rational conformal field theories,” *Nucl. Phys.* **B570** (2000) 525–589, [hep-th/9908036](#).
- [188] G. Felder, J. Frohlich, J. Fuchs, and C. Schweigert, “The geometry of WZW branes,” *J. Geom. Phys.* **34** (2000) 162–190, [hep-th/9909030](#).
- [189] M. A. Walton and J.-G. Zhou, “D-branes in asymmetrically gauged WZW models and axial- vector duality,” *Nucl. Phys.* **B648** (2003) 523–541, [hep-th/0205161](#).
- [190] N. Ishibashi, “THE BOUNDARY AND CROSSCAP STATES IN CONFORMAL FIELD THEORIES,” *Mod. Phys. Lett.* **A4** (1989) 251.
- [191] A. Fotopoulos, V. Niarchos, and N. Prezas, “D-branes and extended characters in $SL(2, \mathbb{R})/U(1)$,” *Nucl. Phys.* **B710** (2005) 309–370, [hep-th/0406017](#).
- [192] S. Elitzur, A. Giveon, D. Kutasov, E. Rabinovici, and G. Sarkissian, “D-branes in the background of NS fivebranes,” *JHEP* **08** (2000) 046, [hep-th/0005052](#).
- [193] E. Gava, K. S. Narain, and M. H. Sarmadi, “Little string theories in heterotic backgrounds,” *Nucl. Phys.* **B626** (2002) 3–25, [hep-th/0112200](#).
- [194] T. Eguchi and Y. Sugawara, “Modular bootstrap for boundary $N = 2$ Liouville theory,” *JHEP* **01** (2004) 025, [hep-th/0311141](#).
- [195] D. Israel, A. Pakman, and J. Troost, “D-branes in little string theory,” *Nucl. Phys.* **B722** (2005) 3–64, [hep-th/0502073](#).
- [196] S. Ribault, “D3-branes in NS5-branes backgrounds,” *JHEP* **02** (2003) 044, [hep-th/0301092](#).

- [197] D. Mateos, R. C. Myers, and R. M. Thomson, “Holographic phase transitions with fundamental matter,” *Phys. Rev. Lett.* **97** (2006) 091601, [hep-th/0605046](#).
- [198] C. Ahn, M. Stanishkov, and M. Yamamoto, “ZZ-branes of $N = 2$ super-Liouville theory,” *JHEP* **07** (2004) 057, [hep-th/0405274](#).
- [199] K. Hosomichi, “ $N = 2$ Liouville theory with boundary,” [hep-th/0408172](#).
- [200] S. Ribault, “Discrete D-branes in AdS(3) and in the 2d black hole,” *JHEP* **08** (2006) 015, [hep-th/0512238](#).
- [201] B. Ponsot, V. Schomerus, and J. Teschner, “Branes in the Euclidean AdS(3),” *JHEP* **02** (2002) 016, [hep-th/0112198](#).
- [202] J. L. Cardy, “BOUNDARY CONDITIONS, FUSION RULES AND THE VERLINDE FORMULA,” *Nucl. Phys.* **B324** (1989) 581.
- [203] E. P. Verlinde, “FUSION RULES AND MODULAR TRANSFORMATIONS IN 2-D CONFORMAL FIELD THEORY,” *Nucl. Phys.* **B300** (1988) 360.
- [204] C. Ahn, M. Stanishkov, and M. Yamamoto, “One-point functions of $N = 2$ super-Liouville theory with boundary,” *Nucl. Phys.* **B683** (2004) 177–195, [hep-th/0311169](#).
- [205] Y. Hikida, R. R. Nayak, and K. L. Panigrahi, “D-branes in a big bang / big crunch universe: Nappi-Witten gauged WZW model,” *JHEP* **05** (2005) 018, [hep-th/0503148](#).
- [206] C. M. Hull, “Timelike T-duality, de Sitter space, large N gauge theories and topological field theory,” *JHEP* **07** (1998) 021, [hep-th/9806146](#).
- [207] Y. Nakayama, Y. Sugawara, and H. Takayanagi, “Boundary states for the rolling D-branes in NS5 background,” *JHEP* **07** (2004) 020, [hep-th/0406173](#).
- [208] M. Gutperle and A. Strominger, “Spacelike branes,” *JHEP* **04** (2002) 018, [hep-th/0202210](#).
- [209] A. Strominger, “Open string creation by S-branes,” [hep-th/0209090](#).
- [210] F. Larsen, A. Naqvi, and S. Terashima, “Rolling tachyons and decaying branes,” *JHEP* **02** (2003) 039, [hep-th/0212248](#).
- [211] J. Callan, Curtis G. and J. M. Maldacena, “D-brane Approach to Black Hole Quantum Mechanics,” *Nucl. Phys.* **B472** (1996) 591–610, [hep-th/9602043](#).
- [212] S. R. Das and S. D. Mathur, “Comparing decay rates for black holes and D-branes,” *Nucl. Phys.* **B478** (1996) 561–576, [hep-th/9606185](#).
- [213] N. Lambert, H. Liu, and J. M. Maldacena, “Closed strings from decaying D-branes,” [hep-th/0303139](#).

- [214] A. Giveon, A. Konechny, A. Pakman, and A. Sever, “Type 0 strings in a 2-d black hole,” *JHEP* **10** (2003) 025, [hep-th/0309056](#).
- [215] I. Bars and D. Nemeschansky, “STRING PROPAGATION IN BACKGROUNDS WITH CURVED SPACE-TIME,” *Nucl. Phys.* **B348** (1991) 89–107.
- [216] Y. Sugawara, “Thermal amplitudes in DLCQ superstrings on pp-waves,” *Nucl. Phys.* **B650** (2003) 75–113, [hep-th/0209145](#).
- [217] Y. Sugawara, “Thermal partition functions for S-branes,” *JHEP* **08** (2003) 008, [hep-th/0307034](#).
- [218] A. Maloney, A. Strominger, and X. Yin, “S-brane thermodynamics,” *JHEP* **10** (2003) 048, [hep-th/0302146](#).
- [219] D. Gaiotto, N. Itzhaki, and L. Rastelli, “Closed strings as imaginary D-branes,” *Nucl. Phys.* **B688** (2004) 70–100, [hep-th/0304192](#).
- [220] J. J. Friess and H. L. Verlinde, “Hawking effect in 2-D string theory,” [hep-th/0411100](#).
- [221] O. Aharony, A. Giveon, and D. Kutasov, “LSZ in LST,” *Nucl. Phys.* **B691** (2004) 3–78, [hep-th/0404016](#).
- [222] T. Harmark and N. A. Obers, “Hagedorn behaviour of little string theory from string corrections to NS5-branes,” *Phys. Lett.* **B485** (2000) 285–292, [hep-th/0005021](#).
- [223] M. Berkooz and M. Rozali, “Near Hagedorn dynamics of NS fivebranes, or a new universality class of coiled strings,” *JHEP* **05** (2000) 040, [hep-th/0005047](#).
- [224] A. Sen, “Open-closed duality: Lessons from matrix model,” *Mod. Phys. Lett.* **A19** (2004) 841–854, [hep-th/0308068](#).
- [225] A. Sen, “Remarks on tachyon driven cosmology,” *Phys. Scripta* **T117** (2005) 70–75, [hep-th/0312153](#).
- [226] L. Alvarez-Gaume, P. Basu, M. Marino, and S. R. Wadia, “Blackhole / string transition for the small Schwarzschild blackhole of AdS(5) x S**5 and critical unitary matrix models,” [hep-th/0605041](#).
- [227] H. Bateman, “Higher Transcendental Functions Vol. 1,” *McGRAW-Hill BOOK COMPANY, INC* (1953).
- [228] K. Gawedzki and A. Kupiainen, “COSET CONSTRUCTION FROM FUNCTIONAL INTEGRALS,” *Nucl. Phys.* **B320** (1989) 625.
- [229] K. Gawedzki, “Noncompact WZW conformal field theories,” [hep-th/9110076](#).
- [230] D. Israel, C. Kounnas, and M. P. Petropoulos, “Superstrings on NS5 backgrounds, deformed AdS(3) and holography,” *JHEP* **10** (2003) 028, [hep-th/0306053](#).

- [231] T. H. Buscher, "A SYMMETRY OF THE STRING BACKGROUND FIELD EQUATIONS," *Phys. Lett.* **B194** (1987) 59.
- [232] T. H. Buscher, "PATH INTEGRAL DERIVATION OF QUANTUM DUALITY IN NONLINEAR SIGMA MODELS," *Phys. Lett.* **B201** (1988) 466.